CRYSTALLOGRAPHY OF ARSENATES AND VANADATES OF Co AND Mg

CRYSTALLOGRAPHY OF ARSENATES AND VANADATES OF COBALT AND MAGNESIUM

by

NARASIMHAN KRISHNAMACHARI, B.Sc.,M.Sc.

A Thesis
Submitted to the School of Graduate Studies
in Partial Fulfilment of the Requirements
for the Degree
Doctor of Philosophy

McMaster University
May 1971

DOCTOR OF PHILOSOPHY (1971)
(Chemistry)

McMASTER UNIVERSITY
Hamilton, Ontario.

TITLE: Crystallography of arsenates and vanadates of cobalt and magnesium

AUTHOR: Narasimhan Krishnamachari, B.Sc.
(Madras University)
M.Sc.
(McMaster University)

SUPERVISOR: Professor C. Calvo

NUMBER OF PAGES: ix, 250

SCOPE AND CONTENTS:

The crystal structures of $Co_3(AsO_4)_2$, $Co_{24.2}As_9O_{48}$, $Co_2As_2O_7$ and $Co_7As_{3.6}O_{16}$ have been determined by x-ray diffraction methods. The crystal structure of $Mg_3(VO_4)_2$ has been refined using single crystal x-ray diffraction data. General structural relations between $M_3(XO_4)_2$ type compounds where M refers to a divalent cation with radius comparable to that of cobalt, and x = As or V, are discussed. The deviations from ideality in cation polyhedral groups in crystal structures are analysed.

ACKNOWLEDGEMENTS

I would like to express my most sincere gratitude to Professor C. Calvo for his valuable guidance and assistance throughout the course of this work. I would also like to express my thanks to Professor C.J.L.Lock for valuable suggestions and discussions, to Drs. J. S. Stephens and J. S. Rutherford for making available the computer programs used in the least squares refinement and in the computation of Fourier maps respectively, to Mr. J. Ozog for his assistance in the preparation of, and collection of data on, $Co_2As_2O_7$, and to other members of the group, especially to Dr. J. J. Park, for valuable discussions.

I would like to acknowledge receipt of financial support from the department of chemistry during the period of this work.

I wish to express my thanks to Mrs. Kennelly for typing this thesis.

TABLE OF CONTENTS

LIST OF TABLES

LIST OF ILLUSTRATIONS

CHAPTER 1

INTRODUCTION

The radii of divalent ions of nickel, magnesium, copper, cobalt, zinc, iron and manganese in octahedral coordination with oxygen atoms are approximately 0.70, 0.72, 0.73, 0.74, 0.75, 0.77, and 0.82 Å respectively(1). If packing considerations predominantly influence the structures assumed by crystals, one might expect that chemically analogous compounds of any of these cations with the same anion will be isostructural in the solid state. If, in addition the anions are different but of comparable sizes as well, the same packing considerations lead to the expectation that compounds resulting from a combination of any of the cations with any of the anions might lead to isostructures. Arsenic and vanadium form similar anions $(AsO_4)^{-3}$ and $(VO_4)^{-3}$, $(As_2O_7)^{-4}$ and $(V_2O_7)^{-4}$, etc., and have comparable radii (tetrahedral radii of 0.34 and 0.36 Å respectively(1)). Therefore it may be expected that arsenates and vanadates of nickel, magnesium, copper, cobalt, zinc, iron and manganese will be isostructural. Isostructural forms with orthorhombic symmetry have been reported for the orthovandates of nickel, magnesium, cobalt, zinc and manganese(2,3,4,5). In fact the occurrence of isostructures has sometimes been found even when the sizes of the anions are substantially different. Thus many analogous arsenates and phosphates have been found to be isostructural. However, the reported orthoarsenates of cobalt, nickel and magnesium (6,7,8) are not isostructural with the corresponding vanadates. Cobalt and nickel orthoarsenates are both monoclinic, while magnesium orthoarsenate has been reported to be hexagonal.

In reality, compounds are not just a collection of hard spheres representing atoms or ions, as is assumed in packing considerations of the kind implied above. Factors such as the crystal field stabilization effects and electrostatic interactions between the individual ions in the crystal will also influence the structure assumed by the crystal. Therefore violations of the predictions of structure types based on the concept of isomorphism should be anticipated. Present knowledge does not allow one to successfully predict cases in which the concept might hold, and those in which violations of the concept might be expected. One of the ultimate functions of crystallography is to predict successfully crystal structures in cases where they are unknown. Therefore it is of considerable importance to gain an understanding of the relevant factors which determine the particular structure type assumed by a given crystal, and thereby be able to successfully predict the expected structures in cases where structural information is lacking.

With these considerations, and with the objective of rationalizing and relating the structure types assumed by compounds which might be expected to be isostructural on the basis of packing considerations, detailed structural studies of the arsenates and vanadates of some cations of closely comparable radii were undertaken in the present work. The system of arsenates and vanadates was chosen for these studies, since in addition to the closely similar sizes of arsenic and vanadium, there were other interesting aspects of the structural chemistry of arsenates and vanadates which needed investigation. These are described in the following paragraphs.

a) V-O bond distances in $(VO_4)^{-3}$ groups:

At the time the present work was started, no accurate structure determination of any orthovanadate containing discrete $(VO_4)^{-3}$ group had been reported, and most of the information on bonding characteristics of pentavalent vanadium in compounds containing discrete $(VO_4)^{-3}$ groups had been based on the assumption of isostructures of hydrated sodium orthovanadates, phosphates and arsenates(9). Based on powder data, approximate trial structures had been proposed for $Ni_3(VO_4)_2$(2) and $Co_3(VO_4)_2$(4), but neither of these had been fully refined. There was thus a paucity of accurate information on V-O bond lengths in discrete $(VO_4)^{-3}$ groups.

b) The bonding geometry in AsO_6 groups:

A structure has been proposed by Magneli$^{(10)}$ for calcium metaarsenate based on a qualitative estimation of intensities from the photograph of a powder specimen. The arsenic atom has octahedral coordination of oxygen atoms in this model, and the mean As-O bond distance is 1.9 Å. Magneli $^{(10)}$ has also reported that the metaarsenates of Sr, Cd, Hg, Pb and Co are isostructural with that of calcium. However, none of these structures have been fully refined to date. The only other source of information in the literature on the bond lengths and bonding characteristics of pentavalent arsenic in octahedral coordination with oxygen atoms is the structure of $As_2O_5 \cdot (5/3)H_2O^{(11)}$, with an average As-O bond length of 1.85(8) Å. It is of interest to investigate in detail structures containing pentavalent arsenic in octahedral coordination, in order to gain an understanding of the conditions leading to the preference of this coordination for As^{+5} in the metaarsenates reported by Magneli$^{(10)}$, compared to the normally observed tetrahedral coordination for this species.

c) Suggested occurrence of a range of compositional stability for some compounds in the MO-As_2O_5 systems with M=Ca, Co, Ni, Mg.

In attempts to prepare calcium metaarsenate, Guerin$^{(12)}$ found that calcination of calcium diacid orthoarsenate yielded products which contained varying amounts of As_2O_5 depending on the duration of heating and the temperature of calcination. This observation suggests that stable non-stoichiometric compositions may occur commonly in the case of calcium metaarsenate. Guerin and Masson(13) found that the molar ratio of CoO to As_2O_5 in products of reactions in various attempts to prepare cobalt metaarsenate varied between 0.89 and 1.2 depending on the temperature of the reaction and the duration of heating, though the ideal value for this ratio is 1.0 in the expected stoichiometric product $CoO \cdot As_2O_5$.

Taylor and Heyding(6) reported preparation of the compound $6NiO \cdot As_2O_5$, and also the results of chemical analysis on two independently prepared samples of this compound. The Ni:As ratio in the two cases are 2.9:1 and 3.2:1 respectively, compared to the expected value of 3:1 for the stoichiometric composition. These authors attributed the differences in the two determinations to contamination by side products in the preparative reaction. Davis et al.(7) report ratios of 2.87:1 and 2.95:1 for two independently prepared synthetic samples, and 2.71:1 and 2.59:1 for two different samples of the naturally occurring mineral aerugite, whose powder pattern agrees with that of the synthetic samples. In the case of the cobalt analog, of expected stoichiometric composition $6CoO \cdot As_2O_5$, Masson et al.(13) report that the Co:As ratio in the different preparations was not reproducible and varied between 2.8:1 and 2.9:1. These results suggest the possibility of a wide range of compositional stability with the same basic structure but with different degrees of cation site occupancy in this class of compounds. Davis et al.(7) have suggested this possibility and have speculated that the mineral aerugite is probably near the nickel-poor end of the stable range and the synthetic material is near the nickel-rich end.

Robijn(8) attempted to prepare the compound with the stoichiometric composition $3MgO \cdot As_2O_5$, and reported results of four different determinations of the molar ratio of MgO to As_2O_5 in the sample. This ratio was found to be 3.06, 3.11, 3.06, and 3.45 respectively in the four determinations, again suggesting that magnesium orthoarsenate might form a range of stable non-stoichiometric compositions.

These observations on the different arsenates suggest that occurrence of stable non-stoichiometric compositions might be a general feature of the arsenate systems. It will be of interest to seek structural explanations for the cause of stability of the non-stoichiometric compositions in these cases.

d) Reported crystal parameters of $Co_2As_2O_7$ and $Ni_2As_2O_7$

Taylor and Heyding(6) indexed the powder pattern of $Co_2As_2O_7$ and $Ni_2As_2O_7$ on the basis of unit cells with orthorhombic symmetry, and cell dimensions $\underline{a}_1$ = 8.16(1) Å, $\underline{a}_2$ = 8.56(1) Å, and $\underline{a}_3$ = 9.16(1) Å for $Co_2As_2O_7$, and $\underline{a}_1$ = 8.12(1) Å, $\underline{a}_2$ = 8.521(1) Å, and $\underline{a}_3$ = 9.29(2) Å for $Ni_2As_2O_7$. The unit cell volumes of 639.8 Å^3 and 642.7 Å^3 for $Co_2As_2O_7$ and $Ni_2As_2O_7$ respectively, suggest that there are 5 molecules of these species in their respective unit cells, if it is assumed that the packing efficiencies in these structures are comparable to that in $Mg_2As_2O_7$(14), with 2 molecules in a unit cell of volume 257.9 Å^3. The cell content of 5 molecules of $M_2As_2O_7$ (M = Co or Ni), with 35 oxygen atoms in the cell, is inconsistent with packing in a cell of orthorhombic symmetry, since there is no position with odd multiplicity in any space group with this symmetry. This suggested the need for a re-examination of the crystal parameters of these diarsenates. This need is further strengthened by the observation of Taylor et al.(6) that their indexing and assignment of orthorhombic symmetry for the diarsenates was based on 'careful selection of lines from the powder diagrams of the impure samples of the diarsenates' since pure samples of these could not be obtained in their preparative reactions.

The work described in subsequent chapters of this thesis is the result of attempts at investigating some of the above aspects of the crystal chemistry of arsenates and vanadates. Detailed structure investigation of a few compositions in the CoO-As_2O_5 system, the compound $3MgO \cdot As_2O_5$

in the MgO-As_2O_5 system, and the compound $3MgO{\cdot}V_2O_5$ in the MgO-V_2O_5 system, were undertaken. Some of the relevant information on these and related systems available in the literature before the present work, is briefly reviewed in the subsequent section.

CoO-As_2O_5 and NiO-As_2O_5 systems: Taylor and Heyding(6) attempted to characterize those arsenates of cobalt and nickel which occur in the MO-As_2O_5 systems (M = Co or Ni), in the composition range between $MO{\cdot}As_2O_5$ and MO. The stoichiometric products $NiO{\cdot}As_2O_5$, $2NiO{\cdot}As_2O_5$, $3NiO{\cdot}As_2O_5$ and $6NiO{\cdot}As_2O_5$, as well as the corresponding cobalt compounds, were found by these authors to be the only stable compositions in the two systems in the range investigated. Analogous compositions in the cobalt and nickel compounds were found to have powder diagrams essentially independent of the cation, indicating that they were isostructural. Masson et al.(13) confirmed these findings of Taylor and Heyding in the CoO-As_2O_5 system, and in addition found a new phase with the composition $CoO{\cdot}2As_2O_5$. Guerin and Masson(15) studied the NiO-As_2O_5 system and found the analogous compound $NiO{\cdot}2As_2O_5$. Their work also confirmed the existence of the compounds $NiO{\cdot}As_2O_5$, $2NiO{\cdot}As_2O_5$, and $3NiO{\cdot}As_2O_5$ reported by Taylor et al.

Taylor et al.(6) also reported the powder patterns of the compounds $3MO{\cdot}As_2O_5$ and $6MO{\cdot}As_2O_5$ (M = Co or Ni), and interpreted these patterns on the basis of unit cells with orthorhombic symmetry, and cell dimensions $\underline{a}_1$ = 5.693(5) Å, $\underline{a}_2$ = 8.30(1) Å, $\underline{a}_3$ = 11.04(2) Å for $3NiO \cdot As_2O_5$, $\underline{a}_1$ = 5.594(5) Å, $\underline{a}_2$ = 9.27(1) Å, $\underline{a}_3$ = 12.04(1) Å for $6NiO \cdot As_2O_5$, and comparable cells for the isostructural cobalt analogs. Davis, Hey and Kingbury(7) identified the naturally occurring minerals xanthiosite and aerugite as those corresponding roughly to the compositions $3NiO \cdot As_2O_5$ and $6NiO \cdot As_2O_5$ reported by Taylor et al. They also prepared synthetic samples of these two materials and found that their powder diffraction patterns showed good agreement with those of Taylor et al. except for some disagreement in very weak lines. Single crystal photographs were obtained for $3NiO \cdot As_2O_5$, and a polycrystalline fragment was used to obtain rotation and Weissenberg photographs for $6NiO \cdot As_2O_5$, since in this latter case a single crystal could not be selected from the bulk sample. These photographs indicated that the assignment of orthorhombic symmetry for these compounds by Taylor et al. was erroneous. Davis et al. assigned monoclinic symmetry for the two nickel compounds on the basis of these photographs. $3NiO \cdot As_2O_5$ was found to belong to the space group $P2_1/a$ with cell dimensions $\underline{a}_1$ = 10.174(5) Å, $\underline{a}_2$ = 9.548(2) Å, $\underline{a}_3$ = 9.79(2) Å, β = 90° 58½'(1'). The possible space groups for $6NiO \cdot As_2O_5$ were determined on the basis of the observed systematic extinctions to be C2, Cm or C2/m, with cell dimensions $\underline{a}_1$ = 10.29(2) Å, $\underline{a}_2$ = 5.95(1) Å, $\underline{a}_3$ = 9.79(2) Å, β = 110°19'(5'). The authors did not attempt to postulate a trial structure for the compounds, but pointed out that the observed cell dimensions indicated that the structures consist of hexagonal closest packing of oxygen atoms, with nickel atoms occupying octahedral voids and arsenic atoms occupying tetrahedral voids.

The investigations of Taylor et al.(6) on the diarsenates of cobalt and nickel, the analysis results of Davis et al.(7) and Taylor et al.(6) on the compound of approximate composition $6NiO{\cdot}As_2O_5$, and of Masson et al.(13) on $6CoO{\cdot}As_2O_5$, have already been described in an earlier section.

The MgO-As_2O_5 system: The powder diagram of the compound $3MgO{\cdot}As_2O_5$ has been reported by Travnicek et al.(16) in 1952, Ide et al.(17) in 1962, and by Robijn(8) in 1967. Robijn indexed the pattern on the basis of a hexagonal cell with $\underline{a}_1$ = 10.5 Å and $\underline{a}_3$ = 19.1 Å. No attempt was made in any of the above studies to postulate a trial structure for this compound.

The analytical results of Robijn on this compound have already been discussed in an earlier section.

The MO-V_2O_5 system (M = Mg, Co, Ni, Zn, Mn): Isostructural orthorhombic forms of the orthovanadates of all these cations have been reported(2,3,4,5). Based on powder data, approximate trial structures have been proposed for these(2,4), but none of these had been fully refined at the start of the present work. In addition to the orthorhombic form, two low temperature cubic forms with spinel-like unit cells have been reported in the case of $Co_3(VO_4)_2$(4). No isostructural forms of these low temperature phases have been reported for any of the other cations.

Present work: The detailed structure investigations based on single crystal data are described for the following: $Co_3(AsO_4)_2$ (Ch. 3), the compound of approximate composition $6CoO{\cdot}As_2O_5$ (Ch.4), $Mg_3(AsO_4)_2$ (Ch.5), and $Co_2As_2O_7$ (Ch. 6). An accurate refinement of the structure of $Mg_3(VO_4)_2$ using data collected with an automatic diffractometer has been completed, and is described in Ch. 7. The mean V-O bond length in the $(VO_4)^{-3}$ group in this compound has been determined to an estimated accuracy of 0.002 Å. This work also reports probably the first structure, that of tetragonal $Co_3(AsO_4)_2$ (isostructural with $Mg_3(AsO_4)_2$ (Ch. 5)), in which divalent cobalt occurs in 8-fold coordination. One of the attempts at preparing cobalt metaarsenate, $CoO{\cdot}As_2O_5$, has yielded crystals for which the present x-ray analysis suggests the approximate composition $4CoO{\cdot}As_2O_5$. The detailed structure investigation of this compound is described in Ch. 9. The structural relations between the structures described in this thesis are discussed in the concluding chapter.

CHAPTER 2

METHODS AND TECHNIQUES

In this chapter a brief introduction to the common methods and nomenclature of x-ray crystallography that will be extensively used in subsequent chapters is presented. In addition, a brief introduction to the common features of close-packed structures has been included, since most crystals studied in the present work were found to have the common feature that these could be described in terms of a close-packed arrangement of oxygen ions with the smaller ions in the structures occupying octahedral and tetrahedral voids of this arrangement.

A crystal may be defined as a medium where all the physical properties are invariant under translations $L_1\underline{a}_1 + L_2\underline{a}_2 + L_3\underline{a}_3$, L_1, L_2, L_3 being any three integers and $\underline{a}_1$, $\underline{a}_2$, $\underline{a}_3$ three noncoplanar vectors characteristic of the medium. Thus any physical property of $\Omega(\underline{r})$ of the medium fulfills the condition

$$\Omega(\underline{r}) = \Omega(\underline{r}+L_1\underline{a}_1+L_2\underline{a}_2+L_3\underline{a}_3) \qquad (2.1)$$

for any $\underline{r}$ and for any set of three integers L_1, L_2, L_3. This condition is called the lattice postulate. All physical properties are, in other words, periodic functions of position, with periods $\underline{a}_1$, $\underline{a}_2$, and $\underline{a}_3$. The position vector $\underline{r}$ may be expressed in terms of the components along the vectors $\underline{a}_j$ $(j = 1,2,3)$, i.e. $\underline{r} = x\underline{a}_1 + y\underline{a}_2 + z\underline{a}_3$, and it follows from equation (2.1) that the components x, y, z may be restricted to $0 \leq (x,y,z) < 1$. The assembly of all points $\underline{r} = x\underline{a}_1 + y\underline{a}_2 + z\underline{a}_3$ with $0 \leq (x,y,z) < 1$ is called a unit cell, and is a parallepiped with edges $\underline{a}_1$, $\underline{a}_2$, $\underline{a}_3$ and volume $V = \underline{a}_1 \cdot (\underline{a}_2 \times \underline{a}_3)$. Two points $\underline{r}$ and $\underline{r}'$ are said to be equivalent if $\Omega(\underline{r}) = \Omega(\underline{r}')$ for every property Ω. The equivalent points generated by the expression $\underline{r} + (L_1\underline{a}_1 + L_2\underline{a}_2 + L_3\underline{a}_3)$ where $\underline{r}$ is fixed and L_1, L_2, L_3 assume all possible integral values form what is termed a simple translation lattice. The vector $L_1\underline{a}_1+L_2\underline{a}_2+L_3\underline{a}_3$ is referred to as a translation vector.

The vector set $(\underline{a}_1, \underline{a}_2, \underline{a}_3)$ is not the only unique set which can be used to describe the medium. Any other set $\underline{a}_1'$, $\underline{a}_2'$, $\underline{a}_3'$ can also be chosen, subject to the condition that it satisfies the lattice postulate (2.1). However, if a set $\underline{a}_1$, $\underline{a}_2$, $\underline{a}_3$ has been chosen such that it is impossible to find any other set $\underline{a}_1'$, $\underline{a}_2'$, $\underline{a}_3'$ satisfying the condition

$$\underline{a}_1' \cdot (\underline{a}_2' \times \underline{a}_3') < \underline{a}_1 \cdot (\underline{a}_2 \times \underline{a}_3)$$

the former set defines a primitive unit cell of the lattice. A primitive unit cell is thus the smallest volume that represents the physical properties of the medium and obeys the lattice postulate. It is in general advantageous to choose the three vectors characterizing the medium such that the choice corresponds to one of the primitive unit cells. However, sometimes it is conventional to choose non-primitive unit cells in order to clearly reflect features of symmetry in the physical properties of the medium.

The diffraction information required in the structure investigation of a substance is obtained by recording the relative intensities of the x-rays scattered by the substance. A trial structure (i.e. the relative vector positions of all the atoms in the structure) is postulated, and the relative intensities predicted are compared with those measured. Good agreement between the measured and calculated values is an indication of the probable correctness of the postulated structure. Although there is no absolute way of deciding when 'good' agreement has been reached, one criterion is that the final structure must make sense chemically.

In the initial stages of the description of the scattering theory which follows, it will be assumed that

a) there is no absorption of either the incident or the scattered radiation inside the scatterer, and

b) each scattered wavelet travels through the scattering medium without being rescattered inside the medium.

This approximate treatment which neglects the effects of multiple reflection of the incident and scattered beams, is usually called the kinematical theory. Some of the necessary modifications in the results predicted by the theory when these assumptions are violated will be described in a later section.

Electrons are the basic units scattering x-rays in the crystal. If a bound electron is located in the path of an x-ray beam, it is forced into oscillation by the electromagnetic field of the x-rays impinging upon it. This acceleration causes the electron in turn to become a source of radiation, and in this way the electron is said to scatter the impinging radiation.

The scattering of x-rays by electron can be quantitatively treated by classical electromagnetic theory (18). When a randomly polarized beam of x-rays (i.e. one in which the electric vectors associated with the photons point in random directions in the plane perpendicular to the direction of propagation of the photons), with frequency much larger than any natural frequency of the bound electron, is incident on the electron with intensity I_o, the scattered intensity I_s is given by the expression

$$I_s \propto \frac{KI_o}{|\underline{r}|^2}\left(\frac{1}{2} + \frac{1}{2}\cos^2 2\theta\right)$$

where K is a constant which is a function of the mass and charge of the electron, 2θ is the deviation of the reflected beam from the incident beam direction, and $|\underline{r}|$ is the distance from the origin to the point at which the intensity is measured. The factor $(\frac{1}{2} + \frac{1}{2}\cos^2 2\theta)$ is called the 'polarization factor', and arises because a non-polarized incident x-ray beam is used in normal diffraction experiments. The experimentally measured intensity is multiplied by the inverse of this factor to make it comparable with the theoretical value expected when polarization effects are absent.

When we consider scattering by a number of electrons distributed in a volume whose dimensions are comparable with the x-ray wavelength, as in an atom, the phase differences between rays scattered from the different electrons in the volume have to be taken into account.

If $\underline{s}_o$ and $\underline{s}$ are unit vectors of magnitude $(1/\lambda)$, defining the incident and diffracted directions of the x-ray beam, and if $\underline{r}_1, \underline{r}_2 \ldots, \underline{r}_z$ are vectors defining the instantaneous positions of the z electrons of an atom whose nucleus is at the origin, the instantaneous amplitude of scattering at a point distant $\underline{R}$ from the atom where $|\underline{R}| >> |\underline{r}_j| (j = 1,2,\ldots z)$ is given by

$$E_{at} = E_e \Sigma_j \exp 2\pi i \underline{r}_j \cdot \underline{s}$$

where $\underline{S} = \underline{s} - \underline{s}_o$, and E_e is the amplitude of scattering by a single electron placed at the origin (p.92 of (19)). However, the electrons in an atom are changing positions so rapidly that it is quite impossible to measure the instantaneous amplitude and intensity of the scattered radiation. Accordingly we must deal with average rather than instantaneous values for these quantities. If $\sigma_1, \sigma_2, \ldots \sigma_z$, are distribution functions representing the various electrons such that $\sigma_j dv$ is the probability of finding the j^{th} electron in the volume element dv, it can be shown (p. 93, ibid) that the mean amplitude of scattering is given by

$$E_{at} = E_e \int .\rho(r) \exp 2\pi i \underline{r} \cdot \underline{s} \, dv \tag{2.2}$$

where $\rho(r) = \sum_j \sigma_j(r)$. $\rho(r)$ is the electron distribution function of the atom, and can be interpreted as resulting from the superposition of the distributions of the z individual electrons in the atom. The relative amplitude of scattering by an atom with respect to that by an electron placed at the origin, E_{at}/E_e, is defined as the atomic scattering factor, and denoted by f^o. From (2.2),

$$f^o = \int \rho(r) e^{2\pi i \underline{r} \cdot \underline{S}} \, dv. \tag{2.3}$$

When the electron distribution $\rho(\underline{r})$ has spherical symmetry, it is possible to integrate out the angular dependence and to express f^o in the simpler form (p. 94 of (19))

$$f^o(s) = \int_o^\infty 4\pi r^2 \; \rho(r) \; \frac{\sin|\underline{S}|\,|\underline{r}|}{|\underline{S}|\,|\underline{r}|} \, dr.$$

The electron density distribution function $\rho(r)$ has been calculated with considerable accuracy for most atoms. The atomic scattering factors, $f^o(s)$, can therefore be calculated using the above expression. The values of the scattering factors for the different atoms are tabulated in pp. 201-212 of the International Tables (20).

When any natural frequency of the bound electrons is near that of the incident x-ray wavelength, i.e. near an absorption edge of the atom, the scattering factor changes slightly both in magnitude and in phase (Ch. 4, (21)). This effect is known as 'anomalous scattering'. The resultant scattering factor can then be written as

$$f = f^{o} + \Delta f' + i\Delta f'' \qquad (2.4)$$

where f^{o} is the result from the usual assumption, $\Delta f'$ is the real part of the anomalous scattering correction, and the last term is related to the phase shift. Values of $\Delta f'$ and $\Delta f''$ are tabulated in pp. 213-216 of (20). New values of the scattering factor curves appear frequently in the literature as improved atomic wave functions become available. The references to the sources of the f-curves used in the present work have been given in the individual chapters.

Before calculating the intensity of scattering of x-rays by a crystal, we shall derive the effect of scattering by the contents of one unit cell. The term 'structure factor' is used to denote the amplitude of scattering by the electron density contained in one unit cell relative to the scattering by a single electron at the origin, and is represented by the symbol F. By analogy with eq. (2.3), F can be expressed as

$$F(\underline{S}) = \int \rho(r)\exp.2\pi i\ \underline{r}\cdot\underline{S}\ dv \qquad (2.5)$$

where $\rho(\underline{r})$ is the electron density distribution function characteristic of the medium. Usually it is a good approximation and simplifies the subsequent calculation to distribute the electrons between the various atomic nuclei contained in the unit cell. Let there be n atoms in the unit cell. The electron density $\rho(\underline{r})$ in the unit cell can then be considered as a superposition of the electron distribution functions for the various atoms, of the form $\rho_p(\underline{r}-\underline{r}_p)$, where $\rho_p(\underline{r}_p)$ corresponds to the maximum in the distribution for the p^{th} atom. i.e.

$$\rho(\underline{r}) = \sum_p \rho_p(\underline{r}-\underline{r}_p), p = 1,2,\ldots n \qquad (2.6)$$

Substitution of (2.6) in (2.5), and simplification using eq. (2.3), leads to

$$F = \sum_p f_p \exp 2\pi i \underline{r}_p \cdot \underline{S} \qquad (2.7)$$

where f_p is the scattering power of the p^{th} atom.

In an ideal crystal, if the origin is chosen at a corner of one unit cell the location of any other unit cell in the crystal is described by means of a lattice vector $A_L = L_1\underline{a}_1 + L_2\underline{a}_2 + L_3\underline{a}_3$ where L_1, L_2, L_3 are integral. The amplitude of scattering by all the unit cells in the crystal is given by

$$E_{x\ell} = F E_e \sum_{(L_1,L_2,L_3)} \exp 2\pi i \underline{S} \cdot (L_1\underline{a}_1+L_2\underline{a}_2+L_3\underline{a}_3).$$

If, for the sake of convenience, it is assumed that the crystal used has the form of a parallelepiped with N_1 unit cells along the $\underline{a}_1$ direction, N_2 unit cells along the $\underline{a}_2$ direction and N_3 along the $\underline{a}_3$ direction,

$$E_{x\ell} = FE_e \sum_{L_1=0}^{N_1-1} e^{2\pi i\underline{S}\cdot L_1\underline{a}_1} \sum_{L_2=0}^{N_2-1} e^{2\pi i\underline{S}\cdot L_2\underline{a}_2} \sum_{L_3=0}^{N_3-1} e^{2\pi i\underline{S}\cdot L_3\underline{a}_3}$$

This can be simplified to give the amplitude of scattering from the crystal relative to amplitude of scattering by a single electron,

$$\frac{E_{x\ell}}{E_e} = F \prod_j \left(\frac{e^{2\pi i N_j \underline{S}\cdot\underline{a}_j} -1}{e^{2\pi i\underline{S}\cdot\underline{a}_j} -1}\right) \qquad (j = 1,2,3)$$

The intensity ratio is obtained by multiplying the amplitude ratio by its complex conjugate.

$$\therefore \frac{I_{x\ell}}{I_e} = |F|^2 \prod_j \left(\frac{\sin^2 N_j \pi\underline{S}\cdot\underline{a}_j}{\sin^2 \pi\underline{S}\cdot\underline{a}_j}\right)$$

$$= |F|^2 \frac{\sin^2 N_1(\underline{S}\cdot\underline{a}_1)\pi}{\sin^2(\underline{S}\cdot\underline{a}_1)\pi} \times \frac{\sin^2 N_2(\underline{S}\cdot\underline{a}_2)\pi}{\sin^2(\underline{S}\cdot\underline{a}_2)\pi} \times \frac{\sin^2 N_3(\underline{S}\cdot\underline{a}_3)\pi}{\sin^2(\underline{S}\cdot\underline{a}_3)\pi} \qquad (2.8)$$

Here $\underline{S} = \underline{s}-\underline{s}_o$ where $\underline{s}_o$ and $\underline{s}$ are unit vectors of magnitude $(1/\lambda)$ representing the incident and diffracted directions of the x-ray beam. Eq. (2.8) gives the intensity of scattering from a crystal as a function of the scattering direction expressed in terms of the direction of incidence and the structure of the crystal (since the F term is involved). The intensity has maximum values when $\underline{a}_1\cdot\underline{S} = h$, $\underline{a}_2\cdot\underline{S} = k$, and

$\underline{a}_3 \cdot \underline{S} = \ell$, where h, k, ℓ are integers entirely independent of one another. For non-integral values of h, k or ℓ, it can be shown that the intensity is very nearly zero for large values of N_j, a condition readily satisfied even for crystals of the order of one micron in size (p. 4 of (21)). The three equations above are called Laue equations, and are simultaneously satisfied when $\underline{S}$ is expressed in the form

$$\underline{S} = h\underline{b}_1 + k\underline{b}_2 + \ell\underline{b}_3$$

where $\underline{b}_1$, $\underline{b}_2$, $\underline{b}_3$ are chosen so as to satisfy the conditions

$$\underline{a}_i \cdot \underline{b}_i = 1 \quad \text{and} \quad \underline{a}_i \cdot \underline{b}_j = 0 \quad (i \neq j). \qquad (2.9)$$

When the Laue equations are satisfied, eq. (2-8) reduces to

$$\frac{I_{x\ell}}{I_e} = |F|^2 N^2 \qquad (2.10)$$

where $N = N_1 N_2 N_3$ = total number of unit cells in the crystal.

Substitution of $\underline{r}_p = x_p\underline{a}_1 + y_p\underline{a}_2 + z_p\underline{a}_3$

and $\underline{S} = h\underline{b}_1 + k\underline{b}_2 + \ell\underline{b}_3$

in eq.(2.7) for F yields

$$F(hk\ell) = \sum_p f_p \exp 2\pi i(hx_p + ky_p + \ell z_p) \qquad (2.11)$$

Each set of triplets (hkℓ) associated with the vector $\underline{S}$ specifies a unique direction. Since h, k and ℓ can assume all possible integral values, the vectors $\underline{S}$(hkℓ) can be considered as lattice vectors of a translation lattice with the unit cell defined by the vectors $\underline{b}_1$, $\underline{b}_2$, $\underline{b}_3$. The ends of all the $\underline{S}$ vectors from a common origin lie on the points of this lattice, called the reciprocal lattice. The vectors $\underline{b}_1$, $\underline{b}_2$, $\underline{b}_3$ are called the reciprocal axes. Because of the relations $\underline{a}_i \cdot \underline{b}_i = 1$ and $\underline{a}_i \cdot \underline{b}_j = 0$, the reciprocal axes can be easily expressed in terms of the real axes and vice versa. The relations are summarized in pp. 11-14 of International Tables$^{(22)}$. In practice, a set of reciprocal axes is chosen from the diffraction pattern, and the corresponding crystal lattice axes $\underline{a}_1$, $\underline{a}_2$, $\underline{a}_3$ are calculated using these relations.

In eq. (2.11) f_p is the scattering factor for the p^{th} atom, and refers to scattering by the atom at rest. Actually, atoms in crystals always vibrate, with at least the zero point amplitude, and with increasing amplitude as the temperature increases. X-rays interact with the atomic electron density smeared out by this thermal motion because the period of the motion is negligible compared to the time required for the diffraction experiment. The effective electron density is smeared out about the equilibrium position, and can be represented by a Gaussian factor which is a function of the mean-squared amplitude $\overline{u^2}$ of the thermal motion. It can be shown (Appendix A of (23)) that the atomic scattering factor after modification for isotropic thermal motion of the atom is given by f_p', where

$$f_p' = f_p \exp(-\frac{B\sin^2\theta}{\lambda^2})$$

and $B = 8\pi^2\overline{u^2}$. B is called the isotropic temperature factor.

In practice, B is left as a variable parameter to be evaluated empirically. Since the atoms do not in general lie in an isotropic environment, thermal motion may be appreciably anisotropic, and the more complicated anisotropic form of temperature factor is often used. In this form the scattering factor is given (p. 205 of (23)) by

$$f_p' = f_p[\exp - (\beta_{11}h^2 + \beta_{22}k^2 + \beta_{33}\ell^2+2\beta_{12}hk+2\beta_{23}k\ell+2\beta_{13}h\ell)]$$

where the terms β_{ij} ($i = 1,2,3$; $j = 1,2,3$) describe the thermal ellipsoid of vibration of the i^{th} atom. The six parameters are included as parameters to be determined for each atom, except when the values of some of these are fixed by symmetry considerations$^{(24)}$. The expression for the structure factor, $F(hk\ell)$, given by eq. (2.10) is modified, on taking into account the thermal vibration of the atoms, to

$$F(hk\ell) = \sum_p f_p' \exp 2\pi i(hx_p+ky_p+\ell z_p). \qquad (2.12)$$

Two of the assumptions that have been made in the theory outlined above are a) there is no absorption of either the incident or the scattered beam inside the crystal, and b) the beam, once reflected, emerges through the crystal without being rescattered inside the medium of the crystal. In 'small' crystals of the order of a micron in size, the changes in relative intensities of the incident and diffracted beams when these two effects are taken into account are insignificant compared with normal experimental errors.

However, crystals used in practice in x-ray diffraction experiments are much larger than those implied by the assumptions of the above theory and errors arising from both these effects may become significant. Also, the assumption that the crystals are 'perfect' (i.e. have rigorous translational periodicity throughout the region of the crystal) is not realized in most crystals in practice. The intensities predicted by the theory for 'small' crystals can be corrected for absorption effects by methods described later in the section on data reduction. The imperfect nature of most real crystals encountered in practice results in changes both in the angular width of diffraction maxima and the intensities of the reflected beam compared to the theoretical predictions for a perfect crystal. These changes are understood easily in terms of the mosaic model for real crystals. This model treats a 'large' crystal (with dimensions comparable to those of crystals normally used in x-ray diffraction experiments) as formed of an aggregate of a large number of small blocks, about one micron in size, each block by itself being an ideal crystal, but the different blocks not being rigorously periodic but slightly misoriented with respect to each other. This model is called an 'ideally imperfect crystal', and is a satisfactory approximation for most crystals encountered in practice.

The diffraction maxima for the 'ideally imperfect crystal' are not given by sharply defined scattering directions as was the case in 'ideally perfect' crystals, but are distributed over a small angular region consisting of the scattering directions from the various 'blocks' of the mosaic crystal, which will differ slightly from each other depending on the extent of imperfection of the crystal. The width of the angular distribution is usually of the order of a few minutes in most crystals. The intensity of the diffracted beam from each 'block' is proportional to $|F_{(hk\ell)}|^2$ (eq. 2.8), since each 'block' can be considered a 'perfect' crystal. Since the different blocks are misoriented randomly with respect to each other over a small angular range, the diffracted beams from the different blocks are incoherent, and the intensity of the diffracted beam for each reflection from the whole crystal is given simply by the sum of the contributions from the different blocks, and therefore is proportional to $|F_{(hk\ell)}|^2$.

METHODS OF INTENSITY MEASUREMENT:

The experimental methods employed in estimating intensities are best illustrated by reference to the Ewald construction in reciprocal space and are discussed with great clarity in pp. 85-89 of (19)). The geometry employed in collecting data in the present work is described by the rotating crystal method, in which monochromatic radiation is used and the crystal is rotated in the beam in order to attain various angles of incidence. There are two principal methods of recording the intensities, the photographic method and the more direct quantum counter method. These are described in detail in Ch. 6 of (25). Either the peak intensity (corresponding to the maximum in the peak) or the integrated intensity (the intensity over the whole width of the peak) can be measured. Measurement of the integrated intensity more nearly describes the true situation of diffraction from normally encountered (ideally imperfect) crystals. For this reason, when film methods were used, integrated photographs were obtained for measuring intensities, except in the case of $Mg_3(VO_4)_2$ (Ch. 7), for which non-integrated photographs were obtained initially. However, in this latter case, the data collection was repeated and integrated intensities were measured using counter methods and it was this latter set of data that were used in refining the structure.

The principle of the integrating mechanism when film methods are used is described in detail in pp. 171-173 of (26). Among the counter methods used are the manually controlled Buerger x-ray diffractometer which is an extension of the Weissenberg method, and the four-circle automatic x-ray diffractometer. The principles of the former are elaborately described in pp. 118-122 of (25). The scanning technique used in the present work when the manual diffractometer was used in data collection was the 'stationary-counter-moving crystal' method, or the ω-scan(27). The experimental details are described in Ch. 3 of (28).

The data in the case of $Mg_3(VO_4)_2$ (Ch. 7) was collected using a General Electric XRD-6 four circle automatic diffractometer with a quarter χ-circle. The diagram of the instrument used appears in p. 126 of (25). The detailed principle of the method and the experimental procedure of aligning the crystal and proceeding to collect data are found in pp. 178-194 of (26). The 2θ scanning technique was employed, and the initial alignment was made at $\chi = 90°$ by centering a few ϕ-independent reflections. Some of the strongest reflections were measured both with and without a filter, and it was found that there was no need for correction for counter saturation in the present measurements.

<u>Space group determination</u>: Irrespective of which of the above methods is finally chosen for data collection, it is useful to obtain a few photographs recording peak intensities of reflections in a few sections of the reciprocal space. This provides an easy means of examining the quality, and assessing the symmetry, of the crystal. Except for a centre of symmetry in the intensity pattern which is an inherent property in all diffraction patterns when Friedel's Law (Appendix I) holds, presence of any other symmetry in the patterns is related to some symmetry in the arrangement of the N atoms in the unit cell. Symmetry reduces the number of independent atoms to be located in the unit cell, and thus

the number of parameters of the problem can be reduced substantially.

A crystal must belong to one of seven crystal systems listed in p. 11 of the International Tables$^{(22)}$. The particular system to which the crystal belongs can be recognized by an examination of the symmetry of the pattern, and the pattern can be indexed on the basis of a set of axes chosen so as to reflect the symmetry of the crystal system. In some cases it will be found that certain classes of reflections are not observed in the pattern (i.e. have unobservably low intensities). When these absences result from crystal symmetry, the general class of reflections with indices (hkℓ) will obey one of a set of conditions depending on the values of the sums (h+k), (k+ℓ), (h+ℓ), (h+k+ℓ) or (-h+k+ℓ). The limiting conditions and the accepted symbols used to denote them are listed in p. 53 of International Tables (22).

In addition to the systematic absences noted in the general class of reflections (hkℓ), certain special classes of reflections (such as h00, hk0, etc.) might show systematic absences . The symmetry elements implied by the various classes of absences are tabulated in p. 83 of (29), and the expected absences can be easily derived (pp. 29-30 of (30)) for a given symmetry element. Once all the information that can be obtained about the symmetry of the crystals from the systematic absences has been obtained, the crystal can be said to have one among a small subset of the 230 space groups defined and tabulated in The International Tables (22). In a few cases, there will be only one unique choice consistent with the set of observations of systematic absences. However, in many cases one encounters the situation that more than one space group in a given crystal system satisfies the same set of systematic absences, and there is thus an ambiguity in the choice of the correct space group. Packing considerations can sometimes provide the solution, as in the case of $Mg_3(AsO_4)_2$ (Ch. 5). A very reliable method, although not always applicable, for solving space group ambiguities is to use the effect of anomalous dispersion. The underlying principle is described in Appendix I. This method was used to confirm the correct space group for $Co_{24.2}As_9O_{48}$ (Ch. 4).

Data reduction: Once the space group has been determined and the intensities measured, certain corrections should be applied to the measured intensities so as to make them comparable with the conditions assumed in the theoretical derivation of the expected intensities. The polarization correction has already been indicated. Some of the other corrections required are the Lorentz correction, absorption corrections, and extinction corrections. The origins of these and the methods of correcting for these effects are explained in subsequent paragraphs.

The Lorentz correction is geometric in origin, and takes into account the different speeds with which reflections pass through the reflecting condition. The correction depends on the geometry of the method used for data collection, and the expressions for the different methods are summarized and tabulated in pp. 266-290 of (31).

The magnitude of absorption of the intensity of a particular reflection by the crystal is a function of the shape of the crystal and the relation of the incident and diffracted beams to this shape. The effect of absorption, integrated over the whole crystal, is exceedingly difficult to calculate, except for simple crystal shapes such as a sphere or a cylinder suitably oriented with respect to the incident beam. Thus in practice it is desirable to choose for intensity data collection a crystal which closely approximates a sphere or a cylinder. The corrections, called transmission factors A, are tabulated in pp. 295-298 and 302-305 of (31) for these two simple geometries of crystal shapes for various scattering angles and for various values of μR, where μ is the linear absorption coefficient for the radiation used in the medium of the crystal, and R the radius of the crystal. μ is given by $\rho \times \sum_i g_i (\mu/\rho)_i$ where ρ is the density of the crystal, the sum is over all kinds of atoms i, g_i is the weight fraction and $(\mu/\rho)_i$ the mass absorption coefficient of atom kind i. The value of the mass absorption coefficient for an element depends on the x-ray wavelength and is tabulated in pp. 162-165 and 175-192 of (20).

The intensity, I_{corr}, after correcting for these effects, can be written

$$I_{corr} = k \times I_{measured} \times (1/Lp) \times A$$

where L = Lorentz factor, p = polarization factor, A = transmission factor, and k is a scaling constant which depends on the volume of the unit cell and on the intensity and wavelength of the incident x-ray beam.

In addition to these, there is one other effect which can seriously affect the intensities of some reflections. This arises from violation of the assumption so far made that the incident beam, after being scattered by some volume element of the scatterer, emerges without being rescattered. The assumption will be true in an 'ideally imperfect' crystal, with each mosaic block being small enough to satisfy the assumption, and with the different mosaic blocks having appreciable variations in orientation so that there is no interaction between the scattered beams from the different blocks. Usually crystals used in experiments are imperfect but not 'ideally imperfect', and neither the assumption of 'small' mosaic blocks nor the assumption of 'appreciable differences in orientations' are rigorously satisfied. The changes in the diffracted beam intensities as a result of violation of the first assumption above are said to be caused by 'primary extinction effects' and those resulting from violation of the second assumption are termed 'secondary extinction effects'.

When the individual mosaic blocks are larger than those implied by the assumptions involved in deriving eq. (2.10), the diffracted beam intensity is less than that given by this equation as a result of attenuation of the beam caused by mutliple scattering, and can be represented by

$$I_{hk\ell} \propto |F_{hk\ell}|^n \text{ , where } n < 2,$$

the actual value of n being determined by the extent of the primary extinction effects. For most crystals, however, the mosaic blocks are small enough to justify the assumption that primary extinction is negligible, and therefore n is usually set equal to 2.

The more significant corrections required in the intensities predicted by the 'ideally imperfect' model when applied to real crystals are the result of the violation of the assumption that the different blocks in the crystal have appreciable variations in orientation so that there is no interaction between the scattered beams from the different blocks. The primary beam which is reflected from an interior block may have already passed through several other blocks at the correct orientation to diffract, so that the intensity of the beam is reduced, and the contribution from the interior blocks is less than assumed in the theory of scattering by an 'ideally imperfect' crystal. Correction of the observed intensities for secondary extinction effects depends on the extent of deviation of the crystal from an 'ideally imperfect' arrangement of the mosaic blocks, and is therefore difficult to estimate. The corrections are relatively more significant for very strong reflections, and are negligibly small for very weak reflections. Because of the difficulty in calculating the corrections, it has been customary to exclude from consideration in refinement (defined later) those reflections which appear to be most seriously affected by secondary extinction effects (indicated by considerably lower measured intensities compared to those predicted by the 'ideally imperfect' model).

The Patterson function: Eq. (2.5) can be written as

$$F(hk\ell)=\int_0^1\int_0^1\int_0^1 V\,\rho(x,y,z)\exp 2\pi i(hx+ky+\ell z)\,dxdydz \qquad (2.13)$$

$\rho(x,y,z)$ is the electron density distribution function in the crystal, and is given by the Fourier transform of $F(hk\ell)$.

$$\rho(x,y,z) = (1/V)\sum\sum\sum_{hk\ell} F(hk\ell)\exp -2\pi i(hx+ky+\ell z) \qquad (2.14)$$

$$= (1/V)\sum_{\underline{H}} F(\underline{H})\exp -2\pi i\,\underline{H}\cdot\underline{r} \qquad (2.15)$$

where

$$\underline{H} = h\underline{b}_1 + k\underline{b}_2 + \ell\underline{b}_3$$

and

$$\underline{r} = x\underline{a}_1 + y\underline{a}_2 + z\underline{a}_3.$$

Substitution of (2.11) in (2.15) gives

$$\rho(r) = (1/V) \sum_{H} \left(\sum_{n=1}^{N} f_n \exp 2\pi i \, \underline{H}\cdot\underline{r}_n \right) \exp -2\pi i \, \underline{H}\cdot\underline{r}$$

$$= \sum_{n=1}^{N} \left((1/V) \sum_{\underline{H}} f_n \exp -2\pi i \underline{H}\cdot(\underline{r}-\underline{r}_n) \right)$$

$$= \sum_{n=1}^{N} \rho(\underline{r}-\underline{r}_n) \qquad (2.16)$$

The result $\rho(\underline{r}) = \sum_{n=1}^{N} \rho(\underline{r}-\underline{r}_n)$ shows that the electron density $\rho(\underline{r})$ has been visualized as the sum of N distributions $\rho(\underline{r}-\underline{r}_n)$.

Since the phases of $F(hk\ell)$ are not known, $\rho(x,y,z)$ given by eq. (2.14) cannot be calculated. The structure can sometimes be derived from the function

$$P(\Delta\underline{r}) = V \iiint \rho(r)\rho(\underline{r}+\Delta\underline{r}) \, dv \qquad (2.17)$$

where the integration is over the complete unit cell. This function is called the Patterson function(32). The value of this function at a point $\Delta\underline{r}$ is the sum of the product of electron density at all points separated by the vector $\Delta\underline{r}$. A large value in the Patterson function at $\Delta\underline{r}$ means that there are points $(\underline{r}_i)$ and $(\underline{r}_i+\Delta\underline{r})$ which simultaneously have non-zero electron density. Thus the Patterson function results in a weighted collection of all the interatomic vectors of all the atoms in the unit cell.

Substitution of (2.16) in (2.17) and simplification gives

$$P(\Delta\underline{r}) = (1/V) \sum_{\underline{H}} F(\underline{H})F^*(\underline{H}) \exp 2\pi i\, \underline{H}\cdot\Delta\underline{r} \qquad (2.18)$$

where $F^*(\underline{H})$ is the complex conjugate of $F(\underline{H})$.

$$P(\Delta\underline{r})=(1/V) \sum_{H} \left(\left(\sum_{n=1}^{N} f_n \exp -2\pi i\, \underline{H}\cdot\underline{r}_n\right)\left(\sum_{m=1}^{N} f_m \exp 2\pi i\, \underline{H}\cdot\underline{r}_m\right)\times\exp 2\pi i \underline{H}\cdot\underline{r}\right)$$

$$= \sum_{\substack{n=1\\m=1}}^{N} \left((1/V) \sum_{\underline{H}} f_n f_m \exp 2\pi i\, \underline{H}\cdot\{\Delta\underline{r}-(\underline{r}_n-\underline{r}_m)\}\right)$$

$$= \sum_{\substack{n=1\\m=1}}^{N} P_{nm}\{\Delta\underline{r}-(\underline{r}_n-\underline{r}_m)\} \qquad (2.19)$$

Therefore the Patterson function, $P(\Delta\underline{r})$, has $nm(=N^2)$ contributions. Since the function (2.18) contains only the squares of the structure factors $|F(H)|^2$, which are directly proportional to the measured intensities, the computation of this function is straightforward. From (2.19), we see that the Patterson function contains as many peaks, N^2, as there are values of nm. Of these, N coincide at the origin, (those for which n=m), and $\frac{1}{2}N(N-1)$ are related to the remaining $\frac{1}{2}N(N-1)$ by a centre of symmetry. For every pair of atoms at $\underline{r}_n$ and $\underline{r}_m$, there is a peak at $(\underline{r}_n-\underline{r}_m)$. If the j^{th} atom $(j = 1,2,\ldots N)$ in the unit cell has z_j electrons, the N Patterson peaks at the origin will have approximate weights $z_j^2 (j = 1,2,\ldots N)$, and the remaining $N(N-1)$ peaks will have weights $z_i z_j (i\neq j)$.

It can be shown(33) that in most cases a complete labelling (identification) of the locations of the Patterson peaks is sufficient to determine the positions of the atoms themselves, and thus determine the structure. However, since the electron density associated with each atom is not located at a point but is distributed in a volume surrounding the nucleus, the Patterson function consists of collections of more or less broad and overlapping peaks, with the result that success in extracting all the required information is not guaranteed even for a moderate value of N. Usually only the vectors between the heaviest atoms (i.e. those having large number of electrons) are reasonably well enough resolved from the rest of the peaks, and thus a solution for the structure begins with their positions alone. Such a solution is not always unique, and the so-called 'trial-and-error' method (Ch. 6 of (30)) is used to decide the probable correctness or otherwise of the postulated positions. This involves calculating the magnitude of the structure factor, $F_c(hk\ell)$, given by equation (2.11), and comparing it with the observed value $F_o(hk\ell)$ for each reflection. It is usual to consider the overall agreement for all the T reflections by calculating the expression

$$R_w = \left\{ \frac{\sum_{i=1}^{T} w_i (|F_o| - |F_c|)_i^2}{\sum_{i=1}^{T} w_i |F_o|_i^2} \right\}^{\frac{1}{2}}$$

where w_i is the relative weight assigned to each reflection. The methods of choosing weights for the different reflections are described in App. II. R_w is called the weighted R factor. In the initial stages it is convenient to use unit weight for all observed reflections, and consider the factor R_1, given by

$$R_1 = \frac{\sum_{i=1}^{T} \left| |F_o| - |F_c| \right|_i}{\sum_{i=1}^{T} |F_o|_i}$$

as a measure of the correctness of the postulated structure. R_1 is also called the unweighted R factor, reliability index or discrepancy index.

The positions of the atoms in the model at any stage of structure determination can be improved (i.e. the R_1 and R_w-values minimized) by one of two methods commonly employed. These are a) the electron density difference synthesis and b) the least-squares refinement. The difference synthesis method was the earliest method used for refinement of the structure. The least-squares method of finding the best of parameters was first treated by Legendre, and the mathematics involved is described in App. II. Present day methods of refinement invariably involve use of the least-squares technique, supplemented by use of the difference synthesis method, described below.

For a partially determined structure, the $F_c(hk\ell)$ values, and the phases $\alpha_c(hk\ell)$, are calculated. For reflections for which there is fairly good agreement between the observed and calculated structure factor amplitudes $|F_o(hk\ell)|$ and $|F_c(hk\ell)|$, it is assumed that the phase of $F_o(hk\ell)$ is correctly given by that of $F_c(hk\ell)$. The Fourier series

$$\Delta\rho(x,y,z)=\frac{1}{V}\sum\sum\sum_{hk\ell}(|F_o(hk\ell)|-|F_c(hk\ell)|)e^{i\alpha_c(hk\ell)}e^{-2\pi i(hx+ky+\ell z)} \quad (2.20)$$

approximately represents a point-by-point subtraction of the trial electron density from the actual electron density, and is called the electron density difference synthesis. It should have a peak everywhere the trial model fails to provide sufficient electron density, and a negative region where it provides too much. As a first approximation, therefore, correctly placed atoms will not appear in the synthesis, incorrectly placed ones will be in holes, and missing ones will appear as peaks. Small shifts in incorrectly placed atoms can be estimated from the difference synthesis, and new atom positions can be assigned on the basis of the observed peaks. The success of the method depends on the degree to which the assumption about the phases is correct. In order to minimize errors arising from probable violations of this assumption, in computations of difference maps in the present work, those reflections for which $|F_c|<x|F_o|$ were not included, where x was assigned a value between 0.5 and 1.0 depending on the stage of the refinement. A more accurate treatment would involve use of all the data in an expression of the form

$$\rho_{obs}-\rho_{calc} = \frac{1}{V}\sum_j w_j(|F_o|-|F_c|)_j e^{-2\pi i(hx+ky+\ell z)}$$

where each contribution $(|F_o|-|F_c|)_j$ is assigned a weight w_j, which represents the probability of correctness of the associated phase. Various weighting schemes are possible to produce this result, and some of these are described in pp. 359-60 of (26).

Computations of the Patterson function, electron density and electron density difference maps, using expressions (2.18), (2.15) and (2.20) respectively, involve use of the complete 3-dimensional reflection data (summation over all integral values of h, k and ℓ). These are therefore called the 3-dimensional Patterson function, electron density and difference syntheses respectively. If the expression (2.15) for the 3-dimensional electron density $\rho(x,y,z)$ is integrated from $z = 0$ to $z = 1$, the result is given by

$$\rho(x,y) = \frac{1}{V} \sum_{hk}\sum F(hk0)\exp{-2\pi i(hx+ky)}. \tag{2.21}$$

$\rho(x,y)$ represents the projection of the electron density of the unit cell down the $\underline{a}_3$ axis on to the $\underline{a}_1\underline{a}_2$ plane. Analogous expressions can be derived for projections down the other axes, and similar expressions can be derived for Patterson syntheses projections and difference syntheses projections. Calculations of these projections involve fewer measurements of intensities than required for the 3-dimensional syntheses, since the former require only zero-layer data whereas the latter requires 3-dimensional data. The computation time is also reduced correspondingly. The choice between using projection syntheses or 3-dimensional syntheses at various stages of the structure determination is dictated by considerations of the available data, the information sought from these maps, and the economics of the computation time involved.

Once the positions of the atoms in the model have been corrected and new atom positions located using the difference syntheses, these positions are taken as parameters in a subsequent least squares refinement and the structure is refined till the best set of parameters are obtained. These refined parameters are then used to compute the difference synthesis. The cycle is generally continued until all the atomic positions are located, and the calculated shifts in the parameters of the structure are no longer significant in comparison to the errors (Appendix II) in the parameters. The structure is considered satisfactorily solved when there is reasonable agreement between the observed and calculated intensities, and the resulting structure consistent with chemical expectations (interatomic separations, coordination around atoms etc.).

Close-packed structures: Close-packing can be defined as a way of arranging equidimensional objects in space so that the available space is filled efficiently. A closest packing of like spheres is that arrangement of spheres which permits each sphere to be in intimate contact with the largest number of its neighbours. There is only one way of closest packing possible for a layer (i.e. with the centres of all the spheres in the same plane), and this corresponds to the arrangement in which each sphere is in contact with six spheres. In 3-dimensions, the closest packing corresponds to arrangements in which each sphere is in contact with 12 other spheres.

The number of closest packing arrangements in three dimensions, without imposing restrictions of periodicity requirements, is infinite (Ch. 7 of (31)). Therefore that arrangement of closest packed spheres in 3-dimensions which fills space most efficiently is not known. However, among the 3-dimensional closest packings, there are many that can be described in terms of closest packed layers stacked on one another. It is found that these arrangements fulfil periodicity requirements, and hence are of more direct interest in describing crystal structures. A closest packed layer is shown in fig. (2-1). We denote this as the 'A' layer. Each sphere has six voids in the same plane surrounding it. Half of these voids are designated 'β' and the remaining designated 'γ' in fig. (2.1). A closest packed layer translationally identical to the 'A' layer can be stacked on top of the 'A' layer either by locating the spheres of the second layer above the 'β' type voids or above the 'γ' type voids. The layer will be referred to as a 'B' layer in the former case and as a 'C' layer in the latter case. The two simplest closest packed arrangements which will be periodically repeated in space can then be symbolized by the sequence of layers ABABAB...

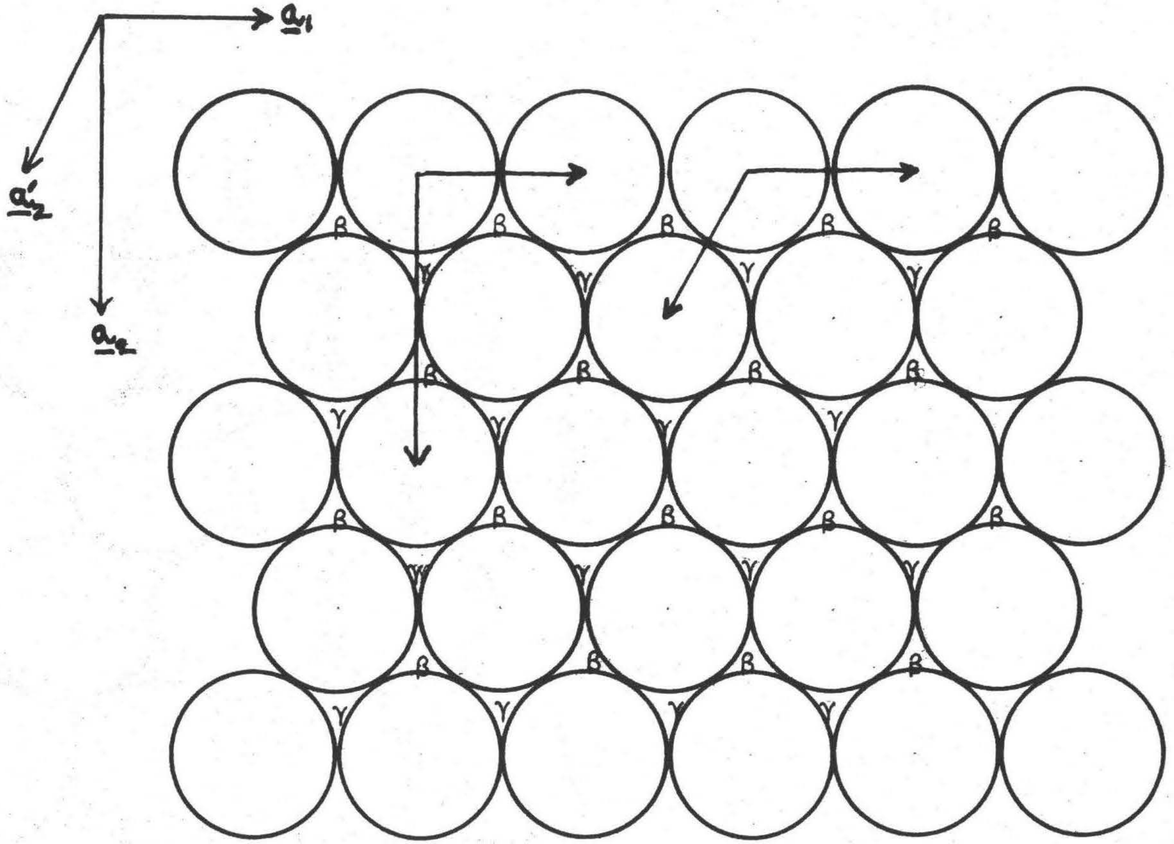

Figure (2.1). A closest packed layer

called hexagonal closest packing, or by the sequence ABCABCABC..., called cubic closest packing. In either case, each sphere is in contact with twelve others, a hexagon of six in the same plane, and two triangles of three above and three below. In hexagonal closest packing the upper triangle has the same orientation as the lower triangle, and in cubic closest packing it is rotated through 60°.

Other closest packed arrangements of this type can be described by the sequence ABACABAC..., ABCBACABCBAC..., etc. The different arrangements are distinguished by the number of layers required to complete the stacking sequence. This number of layers, n, is called the identity period of a closest packing. The direction normal to the stacked layers is called the stacking direction.

Each void in a closest packed layer is surrounded by a triangle of spheres (fig. 2-1). In 3-dimensional closest-packing two additional kinds of voids occur. If a triangular void in one layer has a sphere lying directly over it in the adjacent layer, there results a void in between the two layers, which has four spheres arranged at the corners of a tetrahedron. Such a void is called a tetrahedral void. The other possibility is that a triangular void in one layer has another triangular void lying directly above it in the next layer, but with the triangle associated with this second void rotated by 60° with respect to the triangle of the first void. The six spheres forming the two triangles lie at the corners of an octahedron, and the void enclosed by this arrangement is called an octahedral void. It can be shown (p. 65 of (34)) that there are as many octahedral voids as there are spheres in a closest packing,and twice as many tetrahedral voids. The radii of the spheres which can be inserted into the two kinds of voids can be shown to be 0.225 R and 0.414 R respectively, where R is the radius of the sphere representing the closest packed species. A sphere lying in a tetrahedral void is said to have tetrahedral coordination and the one in an octahedral void has an octahedral coordination. An alternate description of a closest packed arrangement can therefore be given in terms of packing of the coordination polyhedra surrounding the voids.

Often a crystalline substance can be considered to be a rather closely packed aggregate of atoms or ions, and it has been found that the structures of many crystals can be discussed in terms of the packing of rigid spheres. The description of a structure in terms of rigid spherical atoms or ions packed together in an ordered fashion is obviously far from reality. However, atoms and ions do have approximate spherical symmetry of electron distribution for those electrons not involved in bonding. It is customary to assign a 'radius' for each atom or ion such that the observed interatomic distances in crystals might be considered to correspond to the separation between the two atoms or ions nearest to each other. Since the observed bond distances are a function of many factors such as the coordination number around the species, and the nature and extent of the electrostatic forces between the different ions, the values for the radii are not unique. Values of atomic and ionic radii have been tabulated (1,35), and the consistency of these suffice for the purposes of our discussion.

The structures under consideration in this thesis have the common feature that they all have oxygen ions as the largest species in the structure. Thus, any closest packing model for these structures will be based on this species. If the radius of O^{-2} ions is assumed to be 1.40 Å(1), it can be shown(34) that the octahedral voids of a closest-packing of these ions can accommodate ions of radius 0.58 Å, and the tetrahedral voids can accommodate ions of radius 0.32 Å. The distance between consecutive layers of oxygen ions in the packing can be shown to be $(\sqrt{8/3} \times 1.4)$, or 2.3 Å. If n is the identity period of the closest packing, the repeat distance in the stacking direction is given by $(2.3 \times n)$ Å. If the stacking direction is chosen as one of the axes (say $\underline{a}_3$) to define the 3-dimensional packing, two convenient choices can be made in the plane of the stacking layers for the remaining two axes. One of these corresponds to choice of $\underline{a}_1$ and $\underline{a}_2$ (fig. 2-1), at 90° to each other, resulting in an orthogonal set of axes. The $\underline{a}_1$ direction will be a multiple of 2.8 Å (since the diameter of the oxygen ion is 2.8 Å), and the $\underline{a}_2$ direction can be shown to be a multiple of 4.8 Å. The other choice corresponds to $\underline{a}_1$ and $\underline{a}_2'$ directions, inclined at 120° to each other. In this case, both $\underline{a}_1$ and $\underline{a}_2'$ will be multiples of 2.8 Å. These will be the values if the packing corresponds to the ideal situation with no distortions in the packing. In general, depending on the electrostatic interactions in the crystal and the sizes of the ions occupying the voids, there will be distortions in the closest packing and therefore the actual lengths will be slightly different from these.

If considerations such as the sizes of the species in a compound, and the expected coordination characteristics of the cations, suggest the possibility that the compound might have a structure related to a closest packing arrangement, and if the unit cell dimensions chosen reinforce the possibility of a closest packed motif , it might be possible to choose a trial structure using these considerations. Recognition of the characteristic repeat distances in closest packed structures is also of value in understanding common structural features between apparently unrelated closest packed structures.

For purposes of comparison of related closest packed structures, it is easiest to consider these structures in terms of planes parallel to the closest packed layers (36), since the tetrahedral and octahedral voids in an ideal packing lie in such planes. If A and B represent two adjacent closest-packed layers of oxygen atoms, the region between the two layers can be divided into four equally spaced planes, numbered 0 to 3

in fig. (2-2). The tetrahedral voids lie in planes 1 and 3, and the octahedral voids in plane 2. A structure consisting of two layers per unit cell can be described in terms of eight planes, the planes numbered 2 and 6 containing octahedral voids, and the ones numbered 1, 3, 5 and 7 containing tetrahedral voids.
In general, an n-layer structure can be described in terms of 4n planes, the planes 4k, k=0,1,....,n-1, containing the closest packed ions, the planes 4k+2 containing octahedral ions, and the planes 2k+1 containing the tetrahedral ions.

The closest-packed structures described in this work have the common feature that they contain isolated XO_4(X=As or V) groups, i.e. no two XO_4 groups share a common oxygen atom. Some possible arrangements of isolated XO_4 groups in closest packed structures are illustrated in figs. (2-3) to (2-6). The O ions are represented by small filled circles, and the positions of the X ions are represented by joining these to the 4 O ions to which they are bonded. The layers of X and O ions are normal to the plane of the paper.

The arrangements of XO_4 groups shown in figs. (2-3) and (2-4) correspond to the case where all oxygen ions in two adjacent layers A and B are bonded to X ions lying in between A and B. As a consequence of the restriction that each oxygen ion is bonded to only one X ion, it can be seen from the figures that none of the tetrahedral positions lying on either side adjacent to the double layer AB can be occupied. Such arrangements have been designated as ...ONO... arrangements by Calvo(37) in

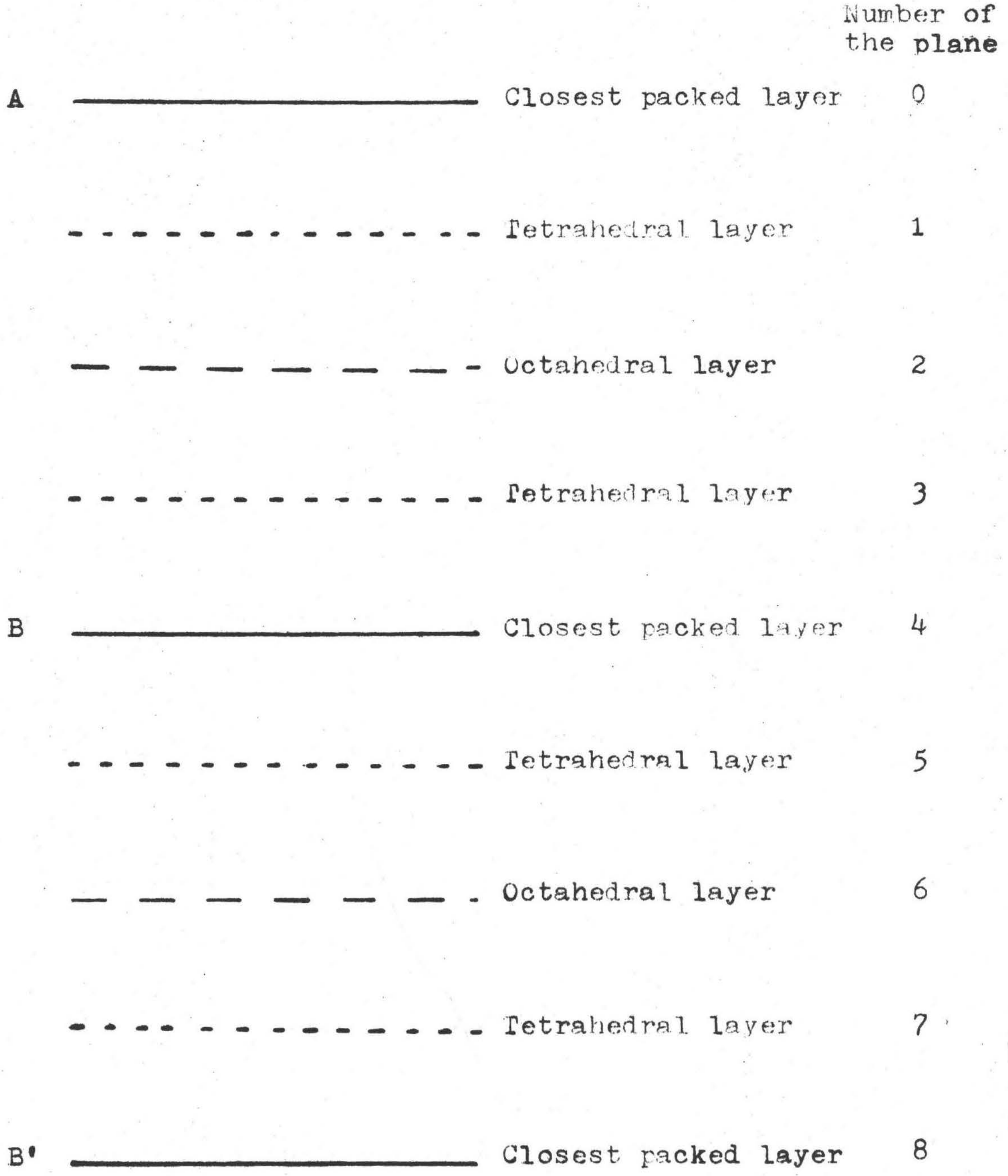

Figure (2-2).

Arrangement of octahedral and tetrahedral voids in closest packed structures.

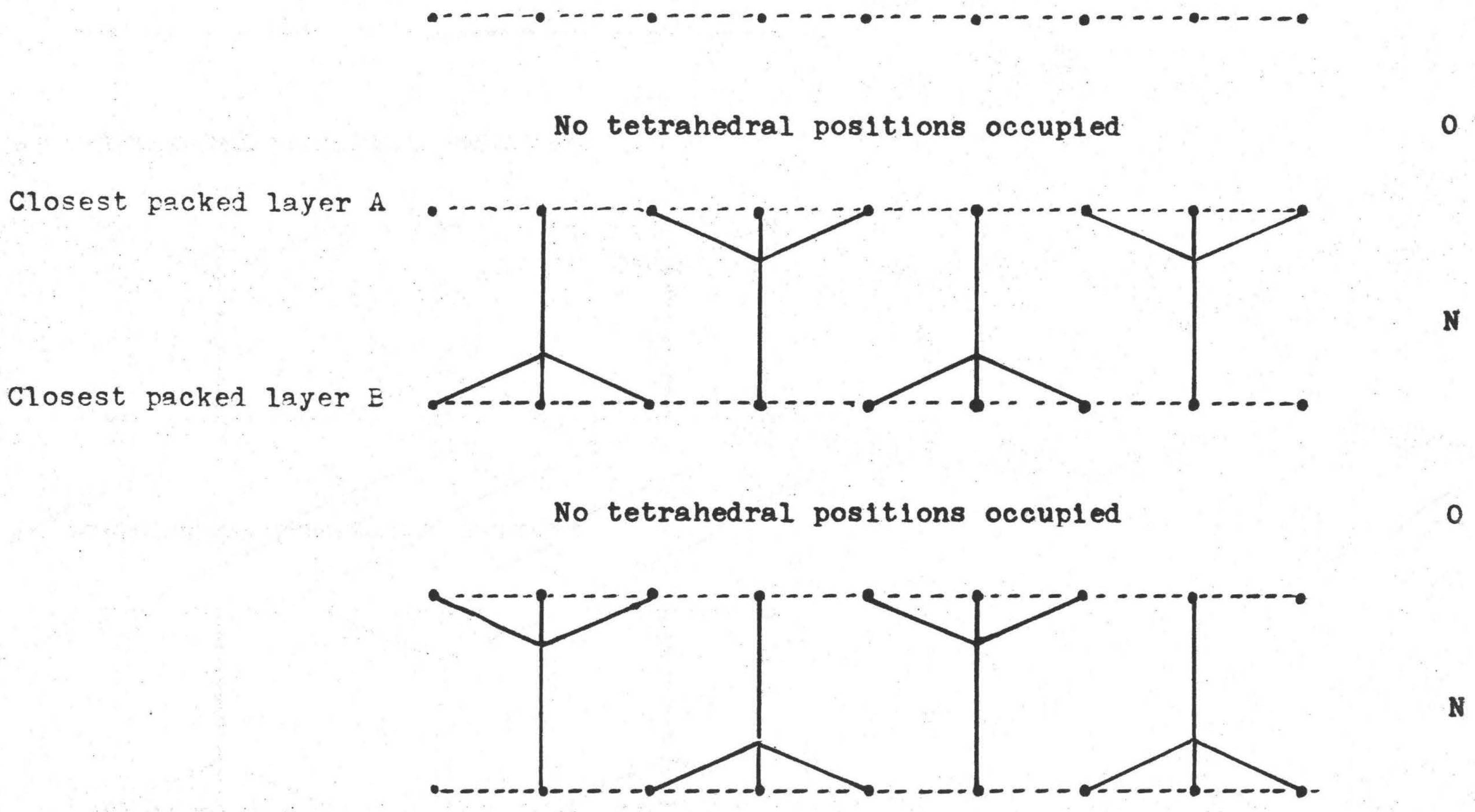

Figure (2-3). A non-polar ...ONO... arrangement.

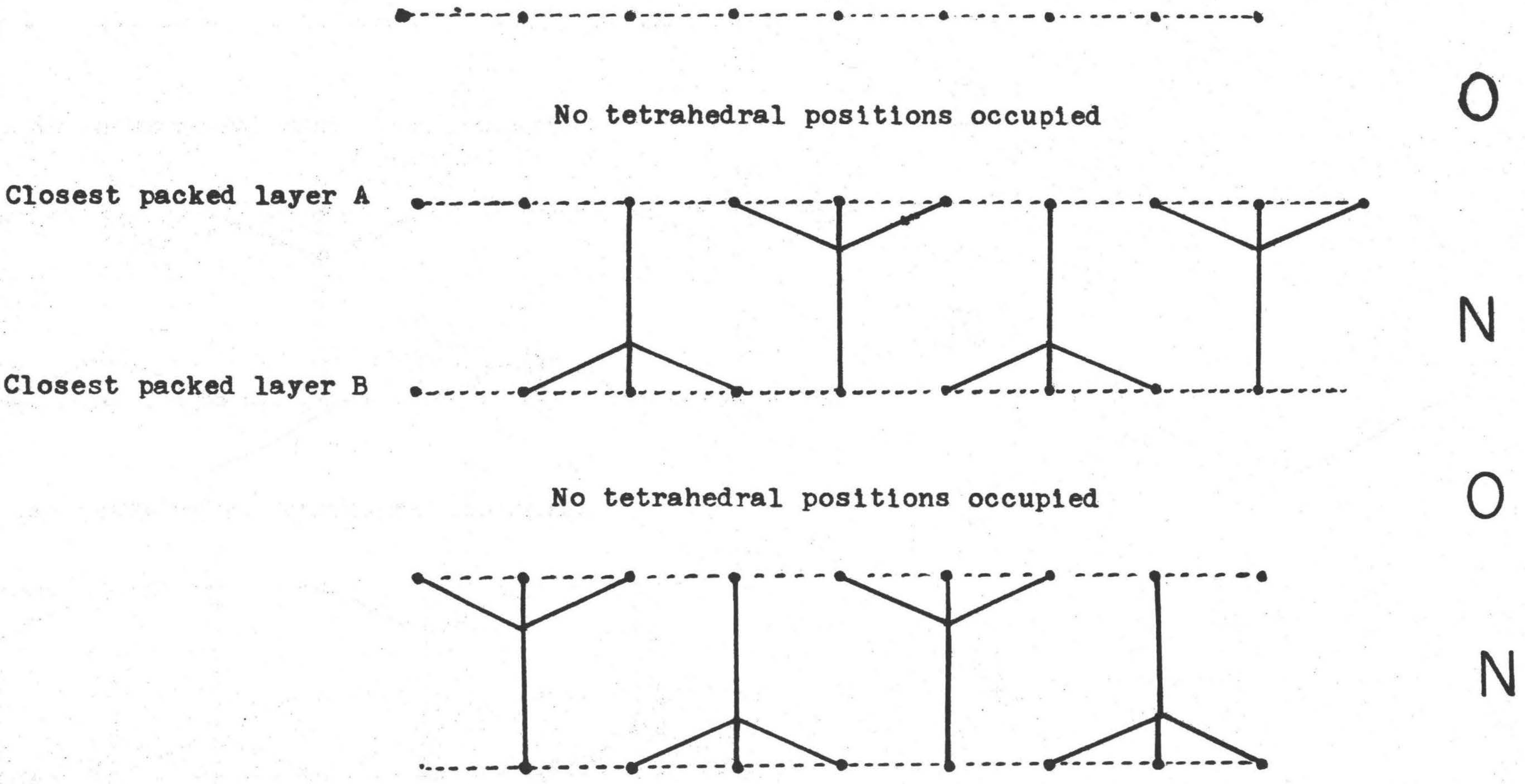

Figure (2-4). Another non-polar ...ONO... arrangement.

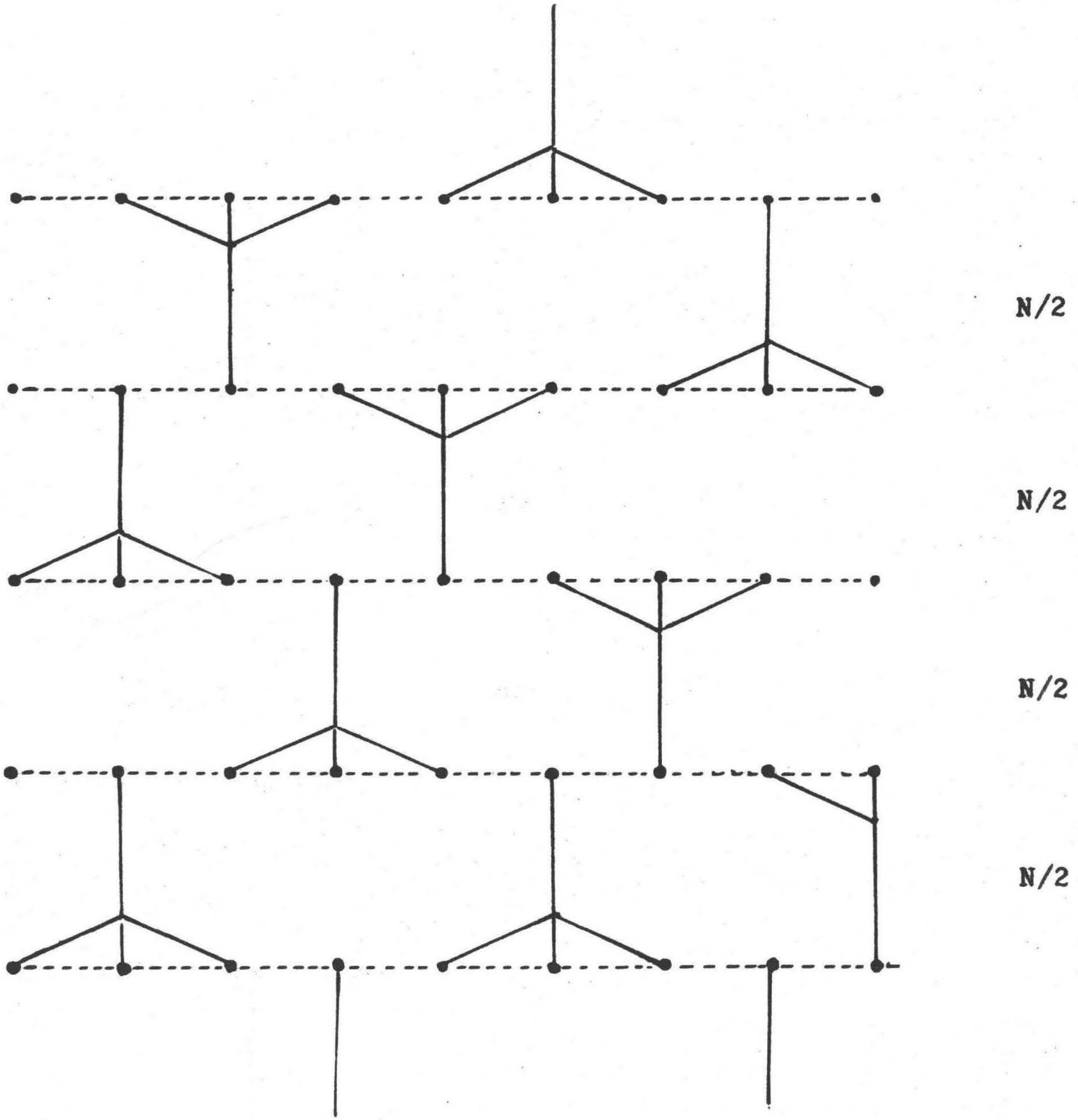

Figure (2-5). A non-polar ...N/2 N/2... arrangement.

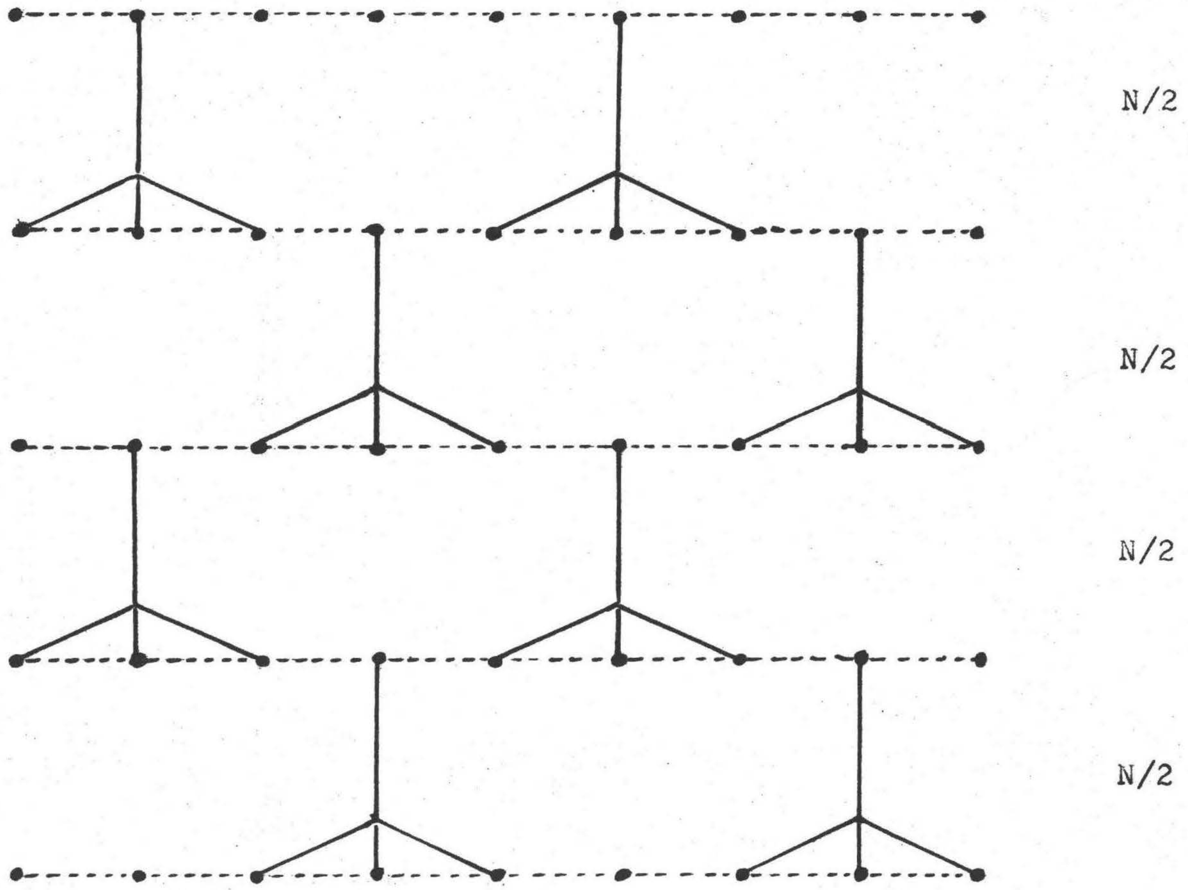

Figure (2-6). A polar ...N/2 N/2... arrangement.

a system of notation to describe the closest packed structures. Another simple arrangement corresponds to that shown in Fig. (2-5), and is designated as an ...N/2 N/2... arrangement. In each of the arrangements shown in figs. (2-3, 2-4 and 2-5), there are as many tetrahedra pointing upwards as there are pointing down. Such arrangements are referred to as 'non-polar' arrangements. Arrangements such as those shown in fig. (2-6) are called 'polar' arrangements, since all the tetrahedra in these are pointing in the same direction. In addition to the two simple arrangements described above, viz. the ...ONO... and the ...N/2 N/2... arrangements, many other arrangements of the type ...t, (1-t)... with t lying between O and N, can be conceived as possibilities that might be encountered in closest packed structures containing isolated XO_4 groups. The present discussion is restricted to the cases with $t=0$ and $t=\frac{1}{2}$, since all the closest packed structures studied in this work can be described in terms of one of these two possibilities.

Closest packed structures can also be described in terms of packing of coordination polyhedra of the tetrahedral and octahedral voids. In some cases this description has been found particularly useful in understanding the causes of distortions of these polyhedra from arrangements expected in ideal closest packed structures. Based on the observed packing arrangements in many closest packed structures, Pauling postulated a set of rules regarding packing of coordination polyhedra. These rules are described in detail in pp. 83-86 of (34). The one pertaining directly to our present discussion states:

> 'The cation polyhedra in a structure tend not to share edges, and in particular not faces, common to two polyhedra. If edges are shared, the shared edges are shortened.'

The reason that cations tend not to share polyhedral elements can be seen from fig. (2.7), which shows two unit cubes sharing a corner, an edge and a face. The distance separating the two positively charged cations at the centres of the cubes successively decreases from $\sqrt{3}$ to $\sqrt{2}$ to 1. Since the two positively charged cations repel each other, they naturally tend to be as far apart as possible. The higher the charge on the cation the greater this tendency becomes. It logically follows that if an edge is shared, the mutual repulsion between the two cations will result in a shortening of the shared edge, if the distance from the cation to the corners of its polyhedron is held constant. Generally it is found that tetrahedra share only corners, octahedra share

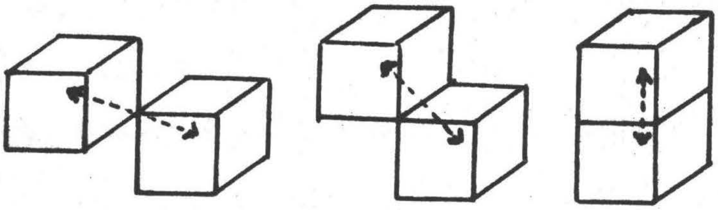

Figure (2-7).

corners and edges, and cubes share corners, edges and faces, though the number of structures in which cubes share faces is small.

The aforementioned concepts of describing closest packed structures will be used in subsequent chapters in discussing the structural features of the individual structures and in correlating the different closest packed structures that have been described in this thesis.

CHAPTER 3

CRYSTAL STRUCTURE OF $Co_3(AsO_4)_2$

Preparation and preliminary investigations: The compound was obtained by fusing hydrated cobalt orthoarsenate obtained from Alpha Inorganics, Inc. The hydrated compound was heated to about 1200°C in a platinum crucible and slowly cooled. The product contained crystals with two distinctly different colours. One type was reddish purple and the other was very dark purple in colour. The composition and structure of the dark purple crystal are discussed in the next chapter. A single crystal of the reddish purple type measuring approximately $0.1 \times 0.1 \times 0.2$ mm^3 was mounted with the long axis of the crystal parallel to the axis of rotation of the goniometer head. The zero- and first layer Weissenberg photographs with the crystal in this orientation were obtained. In addition a few zero-layer precession photographs were also obtained. These photographs indicated that the crystal possessed monoclinic symmetry. A set of reciprocal axes consistent with monoclinic symmetry were chosen, and the photographs were indexed on the basis of this choice. The systematic absences observed were : $h0\ell$ type reflections with $\ell = 2n+1$, and $0k0$ type reflections with $k = 2n+1$.

No other systematic absences were observed. The space-group corresponding to the set of axes chosen is uniquely determined as $P2_1/c$. The approximate unit cell dimensions were found to be $\underline{a}_1$ = 5.75 Å, $\underline{a}_2$ = 9.6Å, $\underline{a}_3$ = 10.26 Å, β = 93.5°. The space group symmetry and cell dimensions are analogous to those reported by Davis et al.(7) for $Ni_3(AsO_4)_2$, and thus the reddish purple crystal from the above reaction should correspond to $Co_3(AsO_4)_2$ based on the expected isomorphism(6).

Accurate unit cell parameters were determined by correcting the approximate parameters measured from the films for film shrinkage. The lengths of the $\underline{b}_2$ and $\underline{b}_3$ axes were obtained from a Weissenberg photograph calibrated with reflections from tetragonal TiO_2 crystal as standard. The parameters for TiO_2 were assumed to be $\underline{a}_1$ = 4.5959(5) Å and $\underline{a}_3$ = 2.9591(3) Å(38). Measurements of arc lengths for 12 reflections of $Co_3(AsO_4)_2$ were used and the $\theta_{0k\ell}$ values were derived (p. 119 of (26)). These were then used to find the best set of values for $\underline{b}_2$ and $\underline{b}_3$ by the method of least-squares. The value of $\underline{b}_1$ was derived from an hk0 precession photograph using the value of $\underline{b}_2$ and assuming isotropic film shrinkage. The angle β* was measured from an (h0ℓ) precession photograph. The real lattice parameters derived from these reciprocal parameters are $\underline{a}_1$ = 5.830(4) Å, $\underline{a}_2$ = 9.675(2) Å, $\underline{a}_3$ = 10.34(2) Å, β = 93.42(5)°.

A density determination on the material was not attempted since the product obtained was not pure $Co_3(AsO_4)_2$, but a mixture of $Co_3(AsO_4)_2$, $Co_{24.2}As_9O_{48}$ (Ch. 4), and possibly other products. However, since the similarity in the powder diffraction patterns of $Ni_3(AsO_4)_2$ and $Co_3(AsO_4)_2$(6) suggest that these are isostructural, and since the unit cell of $Ni_3(AsO_4)_2$ contains 4 molecules of $Ni_3(AsO_4)_2$(7), the analogous unit cell of $Co_3(AsO_4)_2$ is also assumed to contain 4 molecules.

Integrated precession photographs of the (hkn) zone reflections with n = 0, 1, 2, 3, and (hmℓ) zone reflections with m = 0, 1, 2, 3, 4, were obtained using MoKα radiation. The intensities were measured using a Joyce-Loebl microdensitometer. Reflections of the type (rkℓ) with r = 0, 1, 2, 3, 4 were measured using MoKα radiation, with a manually oriented scintillation counter mounted on a Weissenberg camera, and an ω-scan was used for the measurements.

The intensities were corrected for Lorentz and polarization effects and for absorption assuming cylindrical geometry for the crystal. The crystal used for intensity data collection had dimensions of approximately $0.1 \times 0.1 \times 0.3$ mm^3, and neglect of absorption would have led to average error of the order of 20% in intensities.

Patterson functions were computed using reflections of the (hk0), (0kℓ), and (h0ℓ) zones respectively. The solution of the Patterson function P_{VW} yielded trial y and z coordinates for three independent (i.e. non-symmetry related) cobalt atoms and two independent arsenic atoms in the structure. These were used to compute structure factors of the $(0k\ell)$ type reflections. The scattering factors used were those of Co^{+2}, As^{+4}, and O^- species tabulated by Thomas and Umeda(39). The scattering factors for cobalt and arsenic were corrected for dispersion for Mo radiation(20). A few cycles of least-squares refinement of the y and z coordinates of the five atoms, and the scale factor for the $(0k\ell)$ reflections, were carried out. Isotropic temperature factors B equal to 1.0 $\mathring{A}^2$ were used for all the atoms and held constant at this stage. The reliability index R_1 for the $(0k\ell)$ type reflections was 0.35.

Equivalent reflections between the different layers were used to scale all the data to a common scale. The scaled intensities in the different layers were averaged for each equivalent reflection, and the reflection assigned arbitrarily to one of the layers from which it arose. Three-dimensional Patterson sections at intervals of (5/60) along the x-direction were then computed using all the 2261 independent reflections that had been measured. The x-coordinates of the cobalt and arsenic atoms were determined from these maps. A few cycles of least-squares refinement were carried out using all the reflections, and the best set of values for the positional coordinates and individual isotropic thermal factors for the five atoms, and individual scale constants for the 14 layers of data used, were determined. Unit weights were used in the refinement at this stage. The approximate positions of the remaining atoms could be located from difference syntheses of the three principal axis projections and least-squares refinement, as outlined in Ch. 2.

At this stage, the weighting scheme was changed from unit weight for all the reflections, to the following scheme: $w = 0.136$ for $|F_o| < 50$, $w = (0.33|F_o|-8.0)^{-1}$ for $50<|F_o|<90$, and $w = (351.65 - 8.3|F_o| + 0.052|F_o|^2)^{-1}$ for $|F_o| >90$. These functions were determined from a plot of $|F_o|$ vs. $(|F_o|-|F_c|)^2$ such that the weights chosen make the expression $w(|F_o|-|F_c|)^2$ locally independent of $|F_o|$ (40). The isotropic temperature factors of all the atoms were converted to the anisotropic form and refinement of all the 118 parameters (14 scale factors, 39 positional and 78 thermal parameters) was carried out using the 2261 independent reflections until the shifts in all the parameters were less than one-third of the estimated standard deviations in the parameters. The final reliability index R_1 was 0.072, while the weighted R_w value was 0.082. The observed and calculated structure factor amplitudes are listed in Table (3-1). The final atomic positional and thermal parameters are given in Table (3-2). The more important bond distances and angles in the structure are collected in Table (3-3).

TABLE (3-1).

OBSERVED AND CALCULATED STRUCTURE FACTOR AMPLITUDES FOR $Co_3(AsO_4)_2$

UNOBSERVED REFLECTIONS ARE MARKED BY (L) AND UNRELIABLE REFLECTIONS BY (U)

K	ℓ		|FOBS|	|FCALC|
			H = 0	
0	2		22	18
0	4		11	13
0	6		34	35
0	8		23	22
0	10		31	26
0	12		174	178
0	14	L	9	11
0	16		10	13
0	18		10	11
0	20	L	10	5
1	2		31	33
1	3		92	101
1	4		36	38
1	5		112	131
1	6		111	122
1	7		151	165
1	8		58	58
1	9	L	7	7
1	10		59	60
1	11	L	8	2
1	12	L	8	3
1	13		15	20
1	14	L	9	6
1	15		59	55
1	16		10	14
2	-12		18	18
2	-8		14	10
2	0		24	22
2	1		74	71
2	2		65	74
2	3		96	115
2	4		68	71
2	5		50	52
2	6		29	29
2	7		48	49
2	9		45	45
2	10		36	36
2	11	L	8	8
2	13		46	45
2	14		32	34
2	15		65	62
2	17		33	29
3	-12	L	15	7
3	-10		14	12
3	-5		44	43
3	1		93	100
3	2		61	66
3	3		5	7
3	4		78	91
3	6		113	132
3	7		86	91
3	8		45	46
3	9		48	48
3	10		8	12
3	11	L	8	2
3	13		90	90
3	14		40	38
3	15	L	10	6
3	16		10	15
4	0		127	127
4	1		37	37
4	2		84	85
4	3		109	118
4	4		52	56
4	5		54	58
4	6		49	53
4	7		83	82
4	8		21	21
4	9		67	67
4	10		18	18
4	11		24	23
4	12		47	48
4	13		27	27
4	14	L	9	5
4	15		43	47
4	16	L	10	8
4	17	L	10	7
4	18		36	71
4	19		33	29
5	1		47	44
5	2		97	95
5	3	L	6	7
5	4		177	220
5	5		21	19
5	7		36	37
5	8		148	164
5	9		8	14
5	10		66	63
5	12		28	24
5	13	L	9	7
5	14		39	38
5	15		26	23
5	16		27	26
6	0		102	109
6	1		135	105
6	2	L	15	11
6	3		148	150
6	4		99	97
6	5		62	59
6	6		7	12
6	7		74	81
6	8		90	84
6	10	L	8	4
6	11		37	46
6	12		40	43
6	13	L	9	5
6	14	L	10	8
6	15		58	53
6	16		10	12
6	17		10	13
6	18		18	14
6	19		43	36
6	20		33	29
7	1		56	57
7	2		40	41
7	3		38	39
7	4		78	84
7	5	L	7	2
7	6		48	48
7	7		53	53
7	8		34	37
7	9		40	38
7	10		9	9
7	11		9	8
7	13		67	64
7	14	L	10	7
7	15	L	10	1
7	17	L	10	10
7	18		32	29
7	20	L	10	1
8	0		115	126
8	1	L	7	3
8	2		95	94
8	3		31	33
8	4		7	9
8	5		70	72
8	6		29	29
8	7		50	51
8	8	L	8	3
8	10		69	70
8	11		31	22
8	12		27	27
8	13	L	10	9
8	14		10	10
8	15		24	25
8	16	L	10	2
9	1		33	32
9	2		19	21
9	3	L	8	7
9	4		60	65
9	5		90	93
9	6		53	54
9	7		34	32
9	8		61	62
9	9	L	9	3
9	10		37	36
9	11		14	16
9	12		10	9
9	13	L	10	2
9	14	L	10	5
9	15	L	10	5
9	16	L	10	5
9	17		67	54
9	18	L	10	7
9	19	L	10	9
10	0		131	142
10	1		26	26
10	2		43	43
10	3		8	15
10	4		21	24
10	5		24	26
10	6	L	8	5
10	8		9	10
10	9		21	22
10	10		55	54
10	11		61	57
10	12		79	72
11	1		9	10
11	2		57	55
11	3		75	77
11	4		52	50
11	5		62	62
11	6		17	19
11	7		86	85
11	8	L	9	0
11	9		22	24
11	10		21	22
11	11	L	10	1
11	12		10	10
11	13		26	22
11	14		27	20
11	15		49	42
11	16		35	29
11	17		10	10
11	21	L	9	3
12	0		59	59
12	1		38	38
12	2	L	9	1
12	3		19	20
12	4		73	74
12	5		44	43
12	6	L	9	6
12	7		31	28
12	8		71	76
12	9		10	12
12	10	L	10	2
12	11		34	30
12	12		10	16
12	13		10	11
12	15		35	30
12	17		17	16
12	18	L	10	4
12	19	L	10	3
13	1		58	57
13	2		39	42
13	3	L	9	8
13	4		9	18
13	5		32	31
13	6		44	42
13	7	L	10	3
13	9	L	10	1
13	10	L	10	7
13	11		10	18
13	12		10	11
13	13		35	31
13	14		34	27
14	0		68	66
14	1		9	10
14	4	L	10	6
14	6	L	10	2
14	9		50	44
14	10	L	10	7
14	11		10	12
14	12		35	27
14	13		31	24
14	14	L	10	2
14	16	L	10	10
14	17	L	10	8
15	1		10	12
15	2		63	60
15	3		27	27
15	5	L	10	7
15	6		10	15
15	7		24	24
15	8		31	30
15	9		11	17
15	10		28	26
15	11		10	11
15	12	L	10	1
15	13	L	10	1
15	14		44	36
15	16	L	10	9
16	0		10	12
16	1		55	53
16	4		31	32
16	5		32	27
16	7		25	26
16	8		50	42
16	11		45	34
16	13		28	22
17	1		32	29
17	4		58	49
17	8		34	29
18	0	L	10	11
18	5		30	25
18	6	L	23	5
18	11		30	32
19	5		37	34
K	ℓ		H = 1	
0	-18		62	55
0	-16		43	41
0	-12		102	97
0	-10		39	40
0	-8		68	69
0	-6		151	155
0	-4		105	109
0	-2		92	87
0	0		49	47
0	2		83	81
0	4		53	53
0	6		52	52
0	8		41	38
0	10		77	76
0	12		101	99
0	14		44	42
0	18		61	55
1	-15	L	28	9
1	-14	L	21	3
1	-13		27	32
1	-12		24	26
1	-11		21	27
1	-10		101	98
1	-9		109	105
1	-8		59	57
1	-7	L	17	6
1	-6		65	63
1	-5		59	57
1	-4		63	63
1	-3	L	7	0
1	2		146	172
1	3		174	214
1	4		131	140
1	5		68	66
1	6		19	24
1	7		21	21
1	8		27	26
1	9	L	14	3
1	10		36	35
1	11		33	37
1	12		44	45
1	13		22	21
2	-18	L	31	10
2	-17	L	30	7
2	-16	L	29	11
2	-15		65	67
2	-14		25	29
2	-13		27	29
2	-12		29	29
2	-11	L	17	12
2	-10	L	22	19
2	-9		48	48
2	-8		43	47
2	-7		19	22
2	-6		69	66
2	-5	L	10	3
2	-4		58	57
2	-3	U	254	371
2	-2		68	71
2	-1		23	24
2	0		99	100
2	1		52	57
2	2	U	49	69
2	3	L	8	4
2	4		43	45
2	5		71	71
2	6		56	55
2	7	L	12	9
2	8		57	55
2	9		189	196
2	10		20	22
2	11	L	18	2
2	12		32	32
2	13	L	19	4
2	14	L	21	13
3	-17	L	31	23
3	-16	L	30	17
3	-15	L	29	5
3	-14	L	21	10
3	-13		61	58
3	-12	L	15	7
3	-11		98	91
3	-10		101	97
3	-9		36	38
3	-8		34	32
3	-7		102	102
3	-6		77	75
3	-5		54	56
3	-4	L	10	4
3	-3	L	9	2
3	-2		64	55
3	-1		115	119
3	0		68	68
3	1		190	230
3	2		112	113
3	3		91	90
3	4		140	142
3	5		169	177
3	6		25	25
3	7		82	83
3	8		29	31
3	9	L	14	9
3	10	L	14	9
3	11		39	41
3	12		62	57
3	13		45	42
4	-16	L	30	13
4	-15	L	29	1
4	-14		56	49
4	-13	L	27	18
4	-13		19	18
4	-12		13	14
4	-11		70	65
4	-10		59	57
4	-9		24	24
4	-8		49	46
4	-7		57	53
4	-6		124	123
4	-5		63	67
4	-4	L	16	15
4	-3		22	20
4	-2		80	80
4	-1		60	59
4	0		91	95
4	1		110	110
4	2		55	58
4	3	L	11	6
4	4		83	83
4	6		69	66
4	7		37	40
4	8		66	67
4	9	L	15	11
4	10		17	13
4	11		36	35
4	12		69	64
4	13		22	22
5	-20	L	31	16
5	-19	L	32	3
5	-18	L	31	9
5	-17	L	31	8
5	-16		83	80
5	-15	L	29	5
5	-14	L	28	17
5	-13	L	21	5
5	-12		40	41
5	-11	L	20	7
5	-10		47	47
5	-9	L	15	13
5	-8		22	27
5	-7		61	58
5	-6		42	44
5	-5		44	43
5	-4		121	135
5	-3	L	17	10
5	-2		51	50
5	-1		36	36
5	0		78	78
5	1		87	83
5	2		24	28
5	3		41	47
5	4		63	61
5	5		50	47
5	7		17	17
5	8	L	15	5
5	9	L	15	19
5	10		112	105
5	11		25	25
5	13		38	30
6	-17	L	31	8
6	-16	L	30	13
6	-14	L	29	12
6	-13		43	43
6	-12	L	20	15
6	-11		36	38
6	-10		76	69
6	-9		68	64
6	-8		37	40
6	-7	L	15	13
6	-6		93	82
6	-5		76	80
6	-4		25	29
6	-3		135	130
6	-2	L	15	14
6	-1		132	130
6	0		64	62
6	1	L	13	9
6	2		80	81
6	3		18	21
6	4		104	100
6	5		19	16
6	7		94	94
6	8	L	19	1
6	9		65	67
6	10		23	21
6	11		32	34
6	12		53	49
6	13	L	20	9
7	-13		42	39
7	-12	L	20	7
7	-11		86	80
7	-10	L	20	4
7	-8		86	79
7	-7		93	90
7	-6	L	18	5
7	-4	L	18	14
7	-3	L	17	6
7	-1		83	77
7	0		26	32
7	1		163	169
7	2		58	56
7	3		34	38
7	5		133	133
7	6		21	23
7	7		51	51
7	8		22	22
7	9		26	32
7	10	L	20	1
7	11		43	42
7	12	L	20	3
7	13		50	45
8	-12	L	26	12
8	-11		27	31
8	-10		33	37
8	-9	L	20	20
8	-8	L	20	10
8	-7	L	19	15
8	-6		95	93
8	-5		25	22
8	-3		146	133
8	-2		99	98
8	-1		36	37
8	0		62	60
8	1	L	15	8
8	2	L	15	7
8	3	L	15	2
8	4		21	29
8	5		22	23
8	8		88	88
8	9		89	38
8	10		20	20
8	11	L	20	6
8	12		63	57
8	13	L	19	8
9	-12	L	19	3
9	-11		20	17
9	-10		65	62
9	-9		51	50
9	-8		20	17
9	-7		80	77
9	-3	L	19	7
9	-2	L	19	5
9	-1		34	36
9	0		27	31
9	1		91	83
9	2		74	67
9	3		51	54
9	4		73	72
9	5		67	65
9	6	L	20	11
9	7		20	25
9	8	L	20	3
9	9	L	20	7
9	10		40	36
9	11		23	24
9	12		34	35
9	13		57	45
10	-11		36	37
10	-10	L	20	13
10	-9	L	20	10
10	-8		50	49
10	-7		33	36
10	-6		20	25
10	-5		20	21
10	-3		47	51
10	-2		64	55
10	-1		49	50
10	0	L	20	2
10	1		65	62
10	2		57	55
10	3	L	20	3
10	5		69	72
10	6	L	20	11
10	7		39	35
10	8		39	41
10	9		24	29
10	10		28	31
10	11	L	19	5
10	12		20	23
11	-11		18	26
11	-10	L	19	19
11	-9		50	51
11	-8		72	70
11	-7	L	20	5
11	-6	L	20	7
11	-3	L	20	13
11	-2		52	50

(Table (3-1) Continued)

			|FOBS|	|FCALC|
11	-1	L	20	9
11	0	L	20	7
11	1		79	40
11	2		67	63
11	3		80	79
11	6	L	20	5
11	7	L	20	6
11	8		29	35
11	9		20	21
11	10		20	29
11	11		22	28
12	-9	L	18	1
12	-8	L	19	1
12	-7	L	20	4
12	-6	L	20	7
12	-5		20	22
12	-4		21	23
12	-2		21	16
12	-1		37	42
12	1	L	23	11
12	2		24	22
12	3	L	21	6
12	4		26	30
12	5	L	20	3
12	6		29	38
12	7		36	45
12	8		19	23
12	9		79	81
12	10		20	23
13	-6		50	51
13	-4	L	20	1
13	-3	L	20	7
13	-2	L	20	11
13	0		44	46
13	1	L	20	7
13	2		54	56
13	3	L	20	9
13	5	L	20	18
13	6		19	26
13	7		35	39
13	8	L	17	1
15	5		30	31
16	5	L	31	6
17	5	L	31	23

K L H = 2

			|FOBS|	|FCALC|
0	-12		36	39
0	-10	L	20	1
0	-8		25	28
0	-6	U	263	389
0	-4	L	15	12
0	-2	L	10	7
0	0		62	50
0	2		42	44
0	4		26	22
0	6	U	295	401
0	8	L	19	7
0	10	L	20	14
0	12	L	19	12
1	-13		79	78
1	-12		35	39
1	-11		35	36
1	-10		21	16
1	-9		84	82
1	-8	L	19	3
1	-7		46	44
1	-6	U	18	2
1	-5		24	27
1	-4		74	71
1	-3		41	37
1	-2		71	63
1	-1		169	213
1	0		149	179
1	1		152	177
1	2		48	48
1	3		49	49
1	4		39	41
1	5		17	14
1	6	L	18	13
1	7	L	19	6
1	8	L	20	17
1	9		75	71
1	10		24	26
1	11		58	57
1	12		50	46
1	13		88	78
1	14		42	34
2	-13		34	32
2	-12		26	27
2	-11		40	45
2	-10		17	17
2	-9		103	106
2	-8		55	54
2	-7		86	86
2	-6		18	20
2	-5	L	12	5
2	-4		49	50
2	-3		31	30
2	-2		58	47
2	-1		47	47
2	0	L	14	8
2	1		56	56
2	2		47	47
2	3		55	61
2	4		54	56
2	5		26	27
2	6		25	26
2	7		57	57
2	8		47	46
2	9		93	81
2	10		17	14
2	11		37	33
2	12		20	23
3	-13		40	40
3	-12		59	55
3	-10	L	14	2
3	-9	L	13	5
3	-8		64	61
3	-7		119	129
3	-6	L	10	5
3	-3		46	45
3	-2		111	96
3	-1		114	114
3	0		139	164
3	1		74	73
3	2		85	98
3	3		39	41
3	4		28	28
3	5		43	43
3	7		81	84
3	8		53	52
3	9	L	13	0
3	10		16	16
3	11		15	9
3	12		62	62
3	13		43	43
3	14	L	17	10
4	-13		47	46
4	-12		56	55
4	-11		17	20
4	-10		13	17
4	-9		76	78
4	-8		29	28
4	-7		38	37
4	-6		83	80
4	-3		100	87
4	-2		41	40
4	-1		86	79
4	0		33	32
4	1		94	93
4	2		62	67
4	3		103	113
4	7		35	36
4	8		41	41
4	9		64	63
4	10		17	18
4	11		19	20
4	12		38	38
4	13		58	54
4	14	L	12	4
5	-2		243	253
5	-1		31	31
5	0		39	37
5	1		18	15
5	2		200	219
6	-3		62	61
6	-2		140	129
6	-1		76	70
6	0	L	17	10
6	1		92	89
6	2		99	106
6	3		114	117
7	-3		63	62
7	-2		65	63
7	-1		44	44
7	0		47	47
7	1		19	16
7	2		76	76
7	3		43	44
8	-2	L	19	2
8	-1		73	66
8	0	L	13	11
8	1		82	76
8	2	L	19	10
9	-2		80	81
9	-1		64	53
9	0		69	69
9	1		82	72
9	2		70	72
10	-2	L	20	4
10	-1		38	33
10	0	L	20	10
10	1		23	27
10	2		29	34
11	-2	L	21	17
11	-1		105	98
11	0		19	18
11	1		81	76
11	2		35	37
12	-2		90	83
12	-1		35	35
12	1		44	45
12	2		88	84

K L H = 3

			|FOBS|	|FCALC|
0	-22		21	13
0	-20		22	28
0	-18		53	64
0	-16		22	24
0	-14		45	43
0	-12		89	90
0	-10		76	73
0	-8		47	48
0	-6		115	105
0	-4		56	55
0	-2		62	61
0	0		90	92
0	2		73	79
0	4		83	88
0	6		83	83
0	8		48	47
0	10		27	28
0	12		44	48
1	-19		16	16
1	-18		16	15
1	-17	L	15	5
1	-16		33	36
1	-15		32	36
1	-14	L	14	12
1	-13		43	44
1	-12		44	46
1	-11		32	37
1	-10		65	68
1	-9	L	9	6
1	-8	L	9	3
1	-7		33	34
1	-6		36	36
1	-5		37	38
1	-4		149	153
1	-3		167	167
1	-2		65	64
1	-1		25	26
1	0		27	27
1	1		31	32
1	2		77	80
1	3	L	7	3
1	5		29	26
1	6		30	30
1	7		15	14
1	8		80	82
1	9		96	98
1	10		66	69
1	11		28	29
1	12		16	19
1	13		17	21
2	-20	L	16	14
2	-19		30	29
2	-18	L	16	13
2	-17		16	15
2	-16	L	15	7
2	-14		15	15
2	-13	L	11	1
2	-12		25	27
2	-11		10	10
2	-10		28	28
2	-9		142	137
2	-8		39	37
2	-7		16	13
2	-6		57	54
2	-5		14	12
2	-4		21	23
2	-3		69	64
2	-2		69	65
2	-1		66	64
2	0		62	61
2	1	L	7	2
2	2		66	69
2	3		221	293
2	4		36	34
2	5		23	23
2	6		61	61
2	7	L	9	2
2	8		29	28
2	9	L	17	7
2	10		26	27
2	11		34	37
2	12		27	28
2	13		19	18
2	15		71	79
3	-20	L	16	2
3	-19		21	22
3	-18	L	16	3
3	-17		34	34
3	-16		28	38
3	-15	L	15	7
3	-14	L	14	5
3	-13	L	12	5
3	-12		50	49
3	-11		24	26
3	-10		31	29
3	-9	L	10	1
3	-8		33	31
3	-7		99	96
3	-6		27	26
3	-5		146	150
3	-4		125	124
3	-3		78	68
3	-2		72	73
3	-1		98	138
3	0		52	53
3	1		54	54
3	2		17	18
3	4		25	25
3	5		80	78
3	6		60	57
3	7		109	116
3	8		43	44
3	9		37	40
3	10		77	79
3	11		73	76
3	12	L	11	1
3	13		34	39
3	14	L	16	6
4	-22	L	15	2
4	-21	L	16	4
4	-20		15	16
4	-19	L	16	7
4	-18		25	21
4	-17		39	38
4	-16		31	30
4	-15		25	23
4	-14		29	29
4	-13		16	17
4	-12		65	64
4	-11		47	44
4	-10		34	33
4	-9	L	10	2
4	-8		73	76
4	-7		31	29
4	-6		12	12
4	-5		93	93
4	-4		68	56
4	-3		20	17
4	-2		76	74
4	-1		72	66
4	0		137	141
4	1		72	68
4	2	L	17	8
4	3		16	16
4	4		30	30
4	5		45	44
4	6		61	59
4	7		57	56
4	8		20	19
4	9		14	15
4	10		55	54
4	11		48	50
4	12		20	23
4	13		17	21
4	14		30	37
5	-20		13	14
5	-19	L	16	4
5	-18		17	20
5	-17		13	8
5	-16		12	10
5	-15	L	15	7
5	-14		30	31
5	-13		14	12
5	-12		18	19
5	-11		20	18
5	-10		123	120
5	-9	L	10	7
5	-8		10	10
5	-7	L	9	2
5	-6		73	65
5	-5		33	29
5	-4		58	49
5	-3		42	32
5	-2	L	8	2
5	-1		59	59
5	0		67	61
5	1		43	46
5	2		75	75
5	3		22	16
5	4		77	75
5	5		32	29
5	6		46	43
5	7		57	59
5	9		21	22
5	10		40	41
5	11		11	16
5	12		33	37
5	13	L	12	2
6	-20	L	16	13
6	-19	L	16	11
6	-18	L	16	0
6	-17		41	40
6	-16		38	37
6	-15		42	42
6	-14	L	15	9
6	-13	L	15	3
6	-12		58	58
6	-11		24	25
6	-10		19	17
6	-9		28	31
6	-8	L	12	10
6	-7		85	80
6	-6		17	16
6	-5		31	27
6	-4		90	78
6	-3		60	57
6	-2		70	70
6	-1	L	8	3
6	0		90	91
6	1		103	98
6	2		18	17
6	3		103	108
6	4		21	16
6	5		82	80
6	6		41	41
6	8		32	35
6	9		34	32
6	10		66	65
6	11		21	21
6	12		25	31
6	13		38	43
7	-20	L	16	1
7	-19	L	16	15
7	-18	L	16	6
7	-17		28	31
7	-16	L	16	0
7	-15	L	16	5
7	-14		52	55
7	-13	L	15	12
7	-12	L	14	5
7	-11		33	33
7	-10	L	13	8
7	-9	L	11	8
7	-8		17	10
7	-7		66	61
7	-6		26	25
7	-5		133	126
7	-4	L	9	9
7	-3		36	32
7	-2		85	85
7	-1		101	104
7	0		9	10
7	1		40	38
7	2		24	22
7	3		37	36
7	4		18	19
7	5		69	65
7	6		21	20
7	7		105	111
7	8		48	46
7	9		17	19
7	10		15	18
7	11		65	67
7	12	L	12	6
7	13		25	26
8	-18		16	11
8	-17		16	18
8	-16		27	29
8	-15		16	18
8	-14	L	15	12
8	-13	L	15	12
8	-12		54	55
8	-11	L	14	1
8	-10	L	14	12
8	-9		71	71
8	-8		80	81
8	-7		32	28
8	-6	L	10	8
8	-5		35	34
8	-4		22	22
8	-3		26	23
8	-2		21	20
8	-1	L	9	5
8	0		80	86
8	1		31	32
8	2		67	66
8	3		108	113
8	4		57	57
8	5		25	20
8	6		57	55
8	7	L	11	2
8	8	L	11	7
8	10		33	35
8	11		16	18
8	12	L	12	10
8	13		24	29
8	14		48	51
8	15		48	41
9	-20	L	15	5
9	-19	L	16	4
9	-18	L	16	7
9	-17	L	16	4
9	-16		19	24
9	-15		33	37
9	-14	L	16	4
9	-13		40	41
9	-12		29	30
9	-11		23	21
9	-10		55	56
9	-9	L	14	8
9	-8		13	13
9	-7	L	11	6
9	-6	L	11	2
9	-5		35	36
9	-4		82	79
9	-3		58	57
9	-2		25	27
9	-1		84	88
9	0		28	30
9	1		48	45
9	2		37	37
9	5		30	30
9	6		33	33
9	7		59	60
9	8		36	38
9	9		37	39
9	10		44	46
9	11		29	28
10	-17	L	16	5
10	-16	L	16	5
10	-15	L	16	1
10	-14		24	23
10	-13		15	13
10	-12		24	24
10	-11	L	15	7
10	-10		32	32
10	-9	L	14	9
10	-8		51	49
10	-7		35	33
10	-6		21	24
10	-5		48	46
10	-4		23	26
10	-3	L	11	8
10	-2		52	55
10	-1		56	61
10	0		13	12
10	1		25	29
10	2		44	45
10	3		43	47
10	4		49	48
10	5		35	38
10	6	L	11	11
10	7		31	29
10	8		41	41
10	9	L	12	7
10	10		21	23
10	11		48	47
10	12		15	15
11	-16	L	16	3
11	-15		18	22
11	-14		41	42
11	-13		26	25
11	-12		15	10
11	-11		33	32
11	-10		26	27
11	-9		26	25
11	-8		15	17
11	-7		12	15
11	-6	L	12	4
11	-5		33	32
11	-4		30	28
11	-3		68	71
11	-2		74	70

(Table (3-1) continued)

			|FOBS|	|FCALC|
11	-1		24	24
11	0	L	19	4
11	1		20	24
11	2		57	53
11	3	L	11	4
11	4		40	43
11	5		19	20
11	6	L	12	2
11	7		12	14
11	8		54	53
11	9		49	48
11	10		20	22
11	11		28	27
11	12	L	16	1
11	14		17	16
12	-16	L	16	15
12	-15	L	16	4
12	-14		13	14
12	-13	L	16	4
12	-12	L	16	9
12	-11	L	16	1
12	-10		33	33
12	-9		65	68
12	-8		34	74
12	-7		39	40
12	-6		46	48
12	-5		24	25
12	-4		24	26
12	-3	L	14	10
12	-2	L	22	17
12	-1		22	17
12	0		17	15
12	1		31	31
12	2	L	14	11
12	3		98	101
12	4	L	12	1
12	5		21	23
12	6		12	10
12	7		15	19
12	8	L	15	9
12	10		24	25
12	11	L	13	7
12	12		39	30
12	13		31	30
12	15		42	42
13	-20	L	13	0
13	-19	L	14	6
13	-18	L	15	7
13	-17		23	24
13	-16		30	27
13	-15	L	16	10
13	-14	L	16	2
13	-13	L	16	10
13	-12		38	34
13	-11		26	28
13	-10	L	16	8
13	-9	L	16	8
13	-8	L	15	10
13	-7		32	33
13	-6		26	26
13	-5		31	30
13	-4		65	67
13	-3	L	12	2
13	-2		28	29
13	-1	L	12	6
13	0		35	36
13	1		48	51
13	2	L	14	9
13	3	L	12	2
13	4		12	17
13	5		52	53
13	6		49	50
13	7	L	15	3
13	8		30	33
13	9	L	16	4
13	10		44	43
13	11		16	18
13	12	L	16	10
13	15	L	16	3
14	-13		16	14
14	-12		29	25
14	-11		24	25
14	-10	L	16	11
14	-9		25	23
14	-8	L	16	4
14	-7	L	16	3
14	-6		15	12
14	-5		52	54
14	-4		24	24
14	-3	L	15	8
14	-2		40	40
14	-1		47	49
14	0		15	19
14	1	L	13	7
14	2		15	21
14	3		45	47
14	4		15	18
14	5	L	13	1
14	6		13	15
14	7		41	41
14	8		28	24
14	9	L	16	5
14	10		30	24
14	11		39	39
14	12	L	16	3
15	-15	L	16	6
15	-14	L	16	8
15	-13	L	16	5
15	-12		27	23
15	-11		16	15
15	-10		31	28
15	-8	L	16	7
15	-7		13	13
15	-6		13	14

			|FOBS|	|FCALC|
15	-5		25	25
15	-4		15	19
15	-3	L	15	2
15	-1		31	26
15	0		17	22
15	1		27	27
15	2		37	38
15	3	L	15	10
15	4		32	32
15	5		23	22
15	7		32	30
15	8	L	16	3
15	9	L	16	1
15	10	L	15	12
15	11	L	15	14
15	12	L	16	9
16	-15	L	15	9
16	-14	L	15	5
16	-13		25	19
16	-10		15	15
16	-9	L	16	5
16	-8		25	26
16	-7		20	21
16	-6		30	28
16	-5		16	16
16	-4		24	26
16	-3	L	16	4
16	-2		30	31
16	-1	L	16	13
16	0		12	19
16	1	L	15	14
16	2	L	16	1
16	3	L	16	1
16	4	L	16	7
16	5	L	16	18
16	6	L	16	19
16	7	L	15	12
16	8		24	25
16	10		21	19
16	11	L	16	11
17	-5		31	31
17	-4	L	16	7
17	-3	L	16	15
17	-2		32	34
17	-1		13	11
17	1		36	34
17	2	L	16	9
17	3	L	16	12
17	4	L	16	1
17	5		39	39
17	6	L	16	12
17	7	L	16	15
17	8		27	26
17	10	L	16	6
18	-9		15	18
18	-8		27	32
18	-7		26	23
18	-6	L	13	10
18	-5		30	30
18	-4	L	16	9
18	-3	L	13	3
18	-2		25	24
18	-1		25	24
18	1		16	17
18	2		32	34
18	3	L	16	14
18	4		35	31
18	5		16	17
18	6	L	16	5
18	7		15	21
18	8	L	15	4
19	-5		23	22
19	-4	L	16	6
19	-3		24	24
19	-1		31	34
19	1	L	15	15
19	2		16	18
19	3	L	22	6
19	4		21	19
19	5	L	16	6
19	7		35	31
19	8	L	15	10
20	-2	L	15	8
20	-1		20	19
20	2	L	15	16
20	3	L	15	5
20	4	L	15	15
20	5	L	15	0
20	8	L	14	6
21	2	L	15	5
21	3	L	15	2
21	4	L	14	8
21	5	L	14	2

K ℓ H = 4

0	-14	L	12	12
0	-12		103	112
0	-10		32	33
0	-8		19	15
0	-6		70	68
0	-4		23	21
0	-2		37	37
0	0	U	255	391
0	2	L	6	1
0	4	L	19	14
0	6		29	27
0	8		35	35
0	10		21	20
0	12		144	150
0	14	L	12	1
1	-17	L	13	12
1	-16		30	36
1	-15		42	46

			|FOBS|	|FCALC|
1	-14	L	12	5
1	-13		35	35
1	-12	L	11	3
1	-11		15	11
1	-10		47	50
1	-9	L	9	2
1	-8		35	34
1	-7		121	122
1	-6		91	88
1	-5		69	64
1	-4		12	9
1	-3		80	74
1	-2	L	13	1
1	-1		53	52
1	0	L	18	7
1	1		35	39
1	2		33	42
1	3		44	45
1	4		59	58
1	5		110	111
1	6		99	96
1	7		99	98
1	8		43	44
1	9	L	8	4
1	10		25	30
1	11	L	24	14
1	12	L	23	8
1	13	L	12	7
1	14	L	12	8
1	15		34	41
1	16	L	13	7
2	-17		23	23
2	-16	L	13	5
2	-15		44	47
2	-14		29	32
2	-13		43	46
2	-12		19	15
2	-11	L	11	3
2	-10		26	27
2	-9		82	82
2	-8		19	17
2	-7		42	41
2	-6		25	26
2	-5		55	49
2	-4		22	22
2	-3		117	110
2	-2		57	52
2	-1		86	85
2	0		26	24
2	1		26	28
2	2		36	38
2	3		16	13
2	4		18	14
2	5		30	29
2	6		16	13
2	7		37	37
2	8		19	15
2	9	L	19	9
2	10		29	30
2	11	L	19	4
2	12		20	20
2	13		26	29
2	15		43	42
2	16	L	13	4
3	-17	L	13	11
3	-16		23	25
3	-15	L	12	2
3	-14		20	28
3	-13		87	89
3	-12	L	16	10
3	-11	L	11	8
3	-10		16	17
3	-9		45	43
3	-8		14	15
3	-7		66	65
3	-6		88	82
3	-5	L	7	6
3	-4		30	28
3	-3		16	12
3	-2		57	55
3	-1		101	104
3	0	L	6	2
3	1		28	29
3	2		21	23
3	3		30	28
3	4		40	41
3	5		48	49
3	6		95	95
3	7		42	44
3	8		33	30
3	9		38	39
3	10	L	16	2
3	11	L	16	12
3	12	L	11	4
3	13		49	51
3	14		33	29
3	15	L	13	0
3	16	L	13	7
4	-16	L	13	5
4	-15		34	40
4	-14	L	12	5
4	-13		22	21
4	-12		13	9
4	-11		13	12
4	-10		9	8
4	-9		35	36
4	-8		21	19
4	-7		54	53
4	-6		66	65
4	-5		48	45
4	-4		31	29
4	-3		103	97
4	-2		51	51
4	-1		36	35

			|FOBS|	|FCALC|
4	0		109	93
4	1		26	25
4	2		70	69
4	3		59	58
4	4		21	20
4	5		38	37
4	6	L	8	1
4	7		71	72
4	8		30	33
4	9		64	64
4	10		22	21
4	11		24	24
4	12		57	57
4	15		27	28
4	16	L	13	5
5	-15		19	17
5	-14		26	28
5	-13		12	14
5	-12		11	11
5	-11	L	11	9
5	-10		65	62
5	-9		6	9
5	-8		132	125
5	-7		46	41
5	-6		11	13
5	-5		52	45
5	-4		122	105
5	-3		20	15
5	-2		48	43
5	-1		13	10
5	0	L	19	15
5	1		27	32
5	2		99	49
5	3	L	7	1
5	4		170	168
5	5		18	16
5	6		25	24
5	7	L	8	7
5	8		102	103
5	9		8	7
5	10		32	33
5	11		11	15
5	12		28	30
5	13	L	12	3
5	14		37	41
5	16		34	36
6	-15		36	42
6	-14		12	17
6	-13	L	12	2
6	-12		25	24
6	-11		67	66
6	-10	L	9	1
6	-9		6	13
6	-8		87	83
6	-7		62	57
6	-6		24	22
6	-5		66	61
6	-4		63	54
6	-3		144	133
6	-2		25	24
6	-1		48	46
6	0		76	71
6	1		88	86
6	2		12	8
6	3		69	63
6	4		83	79
6	5		20	20
6	7		60	63
6	8		62	59
6	9		52	52
6	10	L	9	2
6	11		58	54
6	12		40	41
6	13	L	12	7
6	14	L	13	3
6	15		38	37
7	-14	L	13	1
7	-13		69	68
7	-12	L	12	8
7	-11		15	15
7	-10	L	10	2
7	-9		48	45
7	-8		19	16
7	-7		39	37
7	-6		54	47
7	-5		34	30
7	-4		71	62
7	-3		24	20
7	-2		38	38
7	-1		89	82
7	0	L	8	3
7	1		16	14
7	2		8	14
7	3		42	41
7	4		66	62
7	5		23	21
7	6		31	31
7	7		28	26
7	8		42	41
7	9		23	24
7	10		19	19
7	11	L	12	11
7	12		12	16
7	13		34	36
7	14	L	13	7
7	15	L	13	1
7	16		26	28
8	-14	L	13	6
8	-13	L	13	8
8	-12	L	12	1
8	-11		30	31
8	-10		55	51
8	-9		26	26
8	-8		23	21

			|FOBS|	|FCALC|
8	-7		34	31
8	-6		33	31
8	-5		59	54
8	-4	L	8	2
8	-3		42	40
8	-2		59	57
8	-1	L	8	2
8	0		74	74
8	1		24	24
8	2		80	81
8	3	L	8	8
8	4	L	8	2
8	5		47	45
8	6	L	9	8
8	7		44	43
8	8	L	9	3
8	9	L	9	0
8	10		55	56
8	11		12	14
8	12		30	31
8	13	L	13	13
8	16	L	13	1
9	-19	L	12	9
9	-18	L	13	6
9	-14	L	13	2
9	-13	L	13	4
9	-12		17	16
9	-11	L	12	1
9	-10		34	35
9	-9	L	10	2
9	-8		41	41
9	-7		19	19
9	-6		45	43
9	-5		88	84
9	-4		25	24
9	-3	L	10	5
9	-2	L	8	3
9	-1		27	28
9	0		19	16
9	1		21	20
9	2		28	31
9	3		19	18
9	4		55	59
9	5		62	60
9	6		50	49
9	7		37	39
9	8		47	45
9	9	L	10	2
9	10		12	16
9	11		25	25
9	13	L	13	1
10	-15	L	13	8
10	-14	L	13	6
10	-12		51	53
10	-11		49	49
10	-10		41	42
10	-9		36	37
10	-8		9	12
10	-7		9	13
10	-6		18	18
10	-5	L	9	8
10	-4		37	35
10	-3		23	24
10	-2		22	26
10	-1	L	9	4
10	0		104	107
10	1		41	42
10	2		35	34
10	3		9	12
10	4	L	9	6
10	6		11	11
10	7		9	11
10	8		25	25
10	9	L	12	1
10	10		43	44
10	11		38	37
10	12		60	60
10	13	L	13	7
11	-17	L	13	4
11	-16		18	25
11	-14	L	13	9
11	-13		26	26
11	-12	L	13	1
11	-11	L	13	6
11	-9		22	21
11	-7		74	75
11	-6		30	28
11	-5		28	31
11	-4		53	49
11	-3		56	53
11	-2		42	43
11	-1		28	30
11	0	L	9	1
11	1	L	22	13
11	2		34	38
11	3		56	58
11	4		26	27
11	5		63	65
11	6		12	16
11	7		51	53
11	8		12	15
11	9		12	11
11	10		25	24
11	11	L	13	8
11	12	L	13	8
12	-16		13	12
12	-15		19	26
12	-14		17	21
12	-13		13	17
12	-12	L	13	5
12	-11		30	34
12	-10	L	13	3
12	-9		24	24
12	-8		45	48

(Table (3-1) concluded)

			|FOBS|	|FCALC|
12	-7		10	14
12	-6		10	10
12	-5		34	34
12	-4		53	54
12	-3		25	24
12	-2		17	18
12	-1		35	36
12	0		42	42
12	1		35	37
12	2	L	21	11
12	3	L	12	1
12	4		61	60
12	5		30	31
12	6	L	12	4
12	7		34	32
12	8		60	61
12	9	L	13	1
12	10	L	13	4
13	-13		23	25
13	-12		13	16
13	-7		12	8
13	-6		34	36
13	-5		33	34
13	-3		25	19
13	-2		30	28
13	-1		47	49
13	0	L	10	11
13	1		35	36
13	2		26	30
13	3	L	12	10
13	4		18	16
13	6		36	37
13	7		12	12
13	8		18	17
13	9	L	16	6
13	11		26	23
14	-9		39	40
14	-8		27	27
14	-2	L	12	6
14	-1		25	24
14	1	L	10	6
14	2	L	10	2
14	3		21	22
14	4		10	12
14	6	L	13	6
14	7		20	20
14	8	L	13	7
14	9		28	31
14	10	L	13	7
14	11	L	13	0
15	-8		31	32
15	-7		24	24
15	-6	L	13	4
15	-5		21	21
15	-4	L	13	5
15	-3		21	20
15	-2		42	47
15	-1	L	13	1
15	0		12	16
15	2		44	47
15	3		20	23
15	4		22	23
15	5	L	13	7
15	7	L	13	8
15	8		13	15
15	9		13	13
15	10		23	23
16	-11		24	24
16	-8		28	30
16	-7	L	13	11
16	-6	L	13	5
16	-5		20	27
16	-4		26	24
16	-3		22	20
16	-2	L	13	1
16	-1		39	41
16	1		39	39
16	2		11	14
16	4		29	30
16	5	L	13	11
16	6	L	13	1
16	7		33	30
16	8		37	37
16	9	L	13	11
16	12		14	10
17	-10	L	13	2
17	-9	L	13	10
17	-8		18	18
17	-7		13	12
17	-6		25	21
17	-5	L	13	9
17	-4		40	39
17	-3		20	20
17	-2	L	13	14
17	-1		27	28
17	1		19	20
17	4		42	37
17	5	L	13	3
17	8		30	26
18	-7		13	15
18	-6	L	13	1
18	-4		15	15
18	-3	L	13	6
18	-1	L	13	8
18	1		25	26
18	4	L	13	0
18	8	L	13	2
19	-9	L	12	5
19	-8		21	19
19	-7	L	12	9
19	-6	L	12	4
19	-5		35	36
19	-3	L	13	6
19	-2	L	13	9
19	-1	L	13	1
K	ℓ		H = 5	
0	-10		29	33
0	-8		43	46
0	-6		96	96
0	-4		88	85
0	-2		63	62
0	0		30	33
0	2		44	45
0	4		20	24
0	6	L	19	11
0	8		36	39
0	10		58	53
1	-12		23	26
1	-11	L	23	3
1	-10		70	65
1	-9		68	68
1	-8	L	24	8
1	-7		38	36
1	-6		41	44
1	-5		38	40
1	-4		87	85
1	-3	L	21	1
1	-2		21	18
1	-1	L	22	12
1	0		20	15
1	1		22	22
1	2		110	112
1	3		119	122
1	4		47	45
1	5		22	23
1	6	L	22	9
1	7	L	22	1
1	8		41	42
1	9	L	22	3
1	10	L	22	1
1	11		22	21
2	-13		28	32
2	-12		20	22
2	-11		19	20
2	-10	L	19	7
2	-9		50	48
2	-8		33	31
2	-7		17	15
2	-6		38	37
2	-5	L	17	7
2	-4		41	42
2	-3		173	172
2	-2		31	31
2	-1		19	15
2	0		59	57
2	1	L	16	4
2	2		20	23
2	3		40	41
2	4		38	37
2	5		50	52
2	6		38	36
2	7	L	17	5
2	8		38	39
2	9		145	138
2	10		19	12
2	11	L	13	11
2	12	L	17	11
3	-14	L	15	7
3	-13		47	45
3	-12	L	15	10
3	-11		60	58
3	-10		64	61
3	-9		23	22
3	-8		15	14
3	-7		22	24
3	-6		51	49
3	-5		23	21
3	-4		21	23
3	-3	L	14	6
3	-2		32	35
3	-1		92	90
3	0		35	32
3	1		124	126
3	2		80	80
3	3		55	53
3	4		66	64
3	5		82	83
3	6		14	14
3	7		31	32
3	8	L	15	8
3	9		15	14
3	10		15	13
3	11		41	42
3	12		40	37
3	13		50	46
4	-12		35	36
4	-11		55	54
4	-10		39	41
4	-9		21	22
4	-8		44	43
4	-7		28	30
4	-6		87	93
4	-5		60	60
4	-4		39	40
4	-3	L	11	3
4	-2		61	61
4	-1		34	34
4	0	L	10	4
4	1		74	75
4	2		23	21
4	3	L	11	3
4	4		60	60
4	5		49	47
4	6		76	76
4	7		37	39
4	8		18	19
4	9	L	12	8
4	10	L	12	4
4	11		23	21
5	-2		21	15
5	-1	L	22	9
5	0		66	63
5	1		39	41
5	2	L	21	19
6	-2	L	21	6
6	-1		85	81
6	0		19	11
6	1	L	22	5
6	2		46	46
7	-2		21	13
7	-1		65	65
7	0		27	28
7	1		122	118
7	2	L	21	16
8	-3		83	80
8	-2		73	71
8	-1		23	22
8	0	L	19	7
8	1		23	22
8	2	L	22	0
9	-2	L	22	14
9	-1	L	22	8
9	0	L	18	8
9	1		37	40
9	2		62	60
10	-2		55	54
10	-1		41	43
10	0		15	13
10	1		28	32
10	2		31	30
11	-2		21	22
11	-1	L	20	2
11	1		20	19
11	2		30	33
12	-3		81	77
K	ℓ		H = 6	
0	-8		19	24
0	-6		158	161
0	-4		19	21
0	-2		22	22
0	0		62	60
0	2		27	28
0	4		19	22
0	6		193	195
0	8	L	16	4
1	-11		22	19
1	-10		41	40
1	-9		55	53
1	-8	L	22	2
1	-7		47	49
1	-6	L	22	1
1	-5		26	26
1	-4		40	41
1	-3	L	22	9
1	-2		35	36
1	-1		112	107
1	0		97	92
1	1		64	61
1	2	L	22	13
1	3		31	27
1	4	L	22	3
1	5		26	32
1	6	L	22	8
1	7		22	26
1	8		21	18
1	9		35	34
1	10		31	30
2	-13		23	24
2	-12		18	20
2	-11		28	29
2	-10	L	19	5
2	-9		61	61
2	-8		36	36
2	-7		70	68
2	-6		19	18
2	-5	L	19	11
2	-4		20	22
2	-3		64	63
2	-2	L	17	8
2	-1		29	31
2	0	L	17	6
2	1		33	34
2	2	L	17	3
2	3		57	57
2	4		35	34
2	5		41	41
2	6		22	23
2	7		26	27
2	8		21	22
2	9		24	23
2	10	L	18	2
3	-13		14	14
3	-12		28	30
3	-11		21	20
3	-10		18	21
3	-9	L	15	2
3	-8		32	33
3	-7		97	94
3	-6	L	15	4
3	-5	L	15	2
3	-4	L	15	8
3	-3		44	43
3	-2		15	15
3	-1		52	54
3	0		79	74
3	1	L	15	4
3	2		21	21
3	3		24	26
3	4		21	24
3	5		46	45
3	6	L	15	4
3	7		29	29
3	8		23	25
3	9		15	15
3	10	L	16	5
3	11		16	15
3	12		46	44
3	13		25	20
4	-11		11	10
4	-10	L	12	3
4	-9		55	54
4	-8		21	21
4	-7		21	23
4	-6		23	23
4	-5		12	11
4	-4		32	35
4	-3		29	31
4	-2		12	9
4	-1		36	38
4	0		41	42
4	1		55	55
4	2		26	26
4	3		72	71
4	4		38	35
4	5		28	28
4	6		69	68
4	7		17	17
4	8		38	37
4	9		29	29
5	-2		133	128
5	-1		29	32
5	0		19	18
5	1		22	29
5	2		75	78
6	-2		81	76
6	-1		27	29
6	0		18	15
6	1		52	54
6	2		44	47
7	-2		29	29
7	-1		32	34
7	0		30	32
7	1	L	22	14
7	2		49	50
8	-2	L	22	12
8	-1		23	30
8	0		16	16
8	1		39	40
8	2	L	22	1
9	-2		42	41
9	-1		24	26
9	1		63	59
9	2		25	26
10	-2	L	21	17
10	-1		18	18
10	2		30	31
11	-2	L	19	2
11	2		34	35
K	ℓ		H = 7	
0	-6		83	81
0	-4		37	37
0	-2		20	22
0	0		54	52
0	2		61	62
0	4		54	49
1	-9	L	19	4
1	-8	L	20	7
1	-7		21	17
1	-6		27	27
1	-5	L	22	0
1	-4		73	71
1	-3		78	78
1	-2	L	22	7
1	-1	L	22	15
1	0		18	15
1	1		22	20
1	2		63	63
1	3	L	22	5
1	4		22	16
1	5	L	21	6
1	6	L	21	3
1	7	L	20	3
1	8		57	53
2	-11	L	16	3
2	-10		22	20
2	-9		50	50
2	-8		18	17
2	-7		19	17
2	-6		31	29
2	-5		18	21
2	-4	L	18	8
2	-2		26	29
2	-1		24	24
2	0		29	31
2	1	L	18	2
2	2		31	34
2	3		126	123
2	4		18	16
2	5		19	18
2	6		36	30
2	7		18	12
3	-12		23	26
3	-11		18	17
3	-10		23	24
3	-9	L	15	3
3	-8		15	15
3	-7		56	56
3	-6		15	14
3	-5		68	67
3	-4		62	62
3	-3		31	30
3	-2		24	23
3	-1		28	31
3	0		23	28
3	1		16	16
3	2	L	16	8
3	3	L	16	6
3	4		25	23
3	5		50	53
3	6		29	25
3	7		68	66
3	8		38	36
3	9		28	27
3	10		36	36
3	11		38	35
4	-8		39	38
4	-7		15	17
4	-6		37	37
4	-5		54	56
4	-4		27	29
4	-3		16	14
4	-2		45	44
4	-1		28	32
4	0		79	79
4	1		49	49
4	2		24	21
4	3	L	13	2
4	4		26	23
4	5		23	23
4	6	L	13	5
4	7		37	37
4	8	L	11	3
5	-2		22	22
5	-1		28	20
5	0		29	31
5	2		52	56
6	-2		30	33
6	-1		21	17
6	0		57	61
6	2	L	21	7
7	-2		69	64
7	-1		25	27
7	2	L	21	9
8	-2		21	20
8	-1	L	18	3
8	2		22	24
9	-2	L	19	3
10	-2		29	27

TABLE (3-2)

Atomic Positional and Thermal Parameters for $Co_3(AsO_4)_2$

(with estimated standard deviations in parentheses)

Atom	Coordinates			Thermal parameters $(X10^4)\mathring{A}^2$					
	x	y	z	U_{11}	U_{22}	U_{33}	U_{12}	U_{13}	U_{23}
Co(1)	-0.1129(2)	0.1352(1)	-0.4670(1)	162(7)	131(5)	146(5)	- 3(2)	8(2)	- 2(2)
Co(2)	-0.3502(2)	0.1401(1)	-0.2163(1)	176(7)	121(5)	140(5)	6(2)	7(2)	- 1(2)
Co(3)	0.3547(2)	0.1235(1)	0.0586(1)	168(7)	128(5)	134(5)	7(2)	5(2)	4(2)
As(1)	0.3675(2)	0.1549(1)	0.3809(1)	102(6)	90(4)	102(4)	- 6(2)	6(1)	- 5(1)
As(2)	-0.1283(2)	0.0523(1)	0.2032(1)	93(5)	89(3)	93(3)	- 2(2)	- 2(1)	1(1)
O(11)	0.3835(12)	0.2217(7)	0.2312(6)	137(35)	117(25)	127(35)	9(12)	- 2(12)	10(10)
O(12)	0.6035(14)	0.2389(8)	0.4534(6)	165(35)	177(30)	130(27)	- 8(14)	2(12)	- 4(12)
O(13)	0.1582(13)	0.2283(7)	0.4636(6)	179(37)	138(27)	129(27)	-26(13)	5(12)	-28(11)
O(14)	-0.3638(12)	0.0177(7)	0.6204(7)	103(34)	105(24)	185(30)	-25(12)	5(12)	-18(11)
O(21)	0.3723(12)	0.4867(7)	0.3777(6)	148(35)	150(26)	62(23)	1(12)	- 3(11)	15(10)
O(22)	-0.1365(12)	0.2255(6)	0.1909(6)	144(35)	66(22)	146(27)	11(11)	8(12)	2(10)
O(23)	0.1083(12)	-0.0104(8)	0.1325(7)	102(34)	163(29)	204(31)	25(13)	22(13)	23(13)
O(24)	0.1212(13)	0.5061(7)	0.1391(6)	237(40)	136(27)	67(23)	18(13)	- 6(12)	-12(10)

TABLE 3-3

Bonding geometry in $Co_3(AsO_4)_2^*$

Atoms	Coord. no. of oxygen atom	Bond Length (Å)	Atoms forming edge	Length of Edge (Å) (±.01 Å)	Angle subtended at the central cation by the edge (degrees (± 0.5°)	Edge shared with
$As(1)O_4$ group						
As(1)-O(12)	4	1.722(7)	O(11)-O(12)	2.56	97.5	Co(2)
-O(11)	3	1.685(6)	O(12)-O(13)	2.60	99.2	Co(3)
-O(13)	3	1.688(7)	O(11)-O($\overline{14}$)	2.78	112.2	
-O($\overline{14}$)	3	1.670(7)	O(11)-O(13)	2.81	112.6	
			O(13)-O($\overline{14}$)	2.83	114.6	
			O(12)-O($\overline{14}$)	2.92	119.1	
$As(2)O_4$ group						
As(2)-O($\overline{21}$')	4	1.728(7)	O(22)-O($\overline{24}$')	2.75	109.6	
-O(22)	3	1.681(6)	O(22)-O($\overline{21}$')	2.76	108.1	
-O(23)	3	1.710(7)	O(22)-O(23)	2.78	110.0	
-O($\overline{24}$')	3	1.689(6)	O(23)-O($\overline{24}$')	2.79	110.2	
			O($\overline{21}$')-O(23)	2.80	108.9	
			O($\overline{21}$')-O($\overline{24}$')	2.80	110.1	
$Co(1)O_6$ group						
Co(1)-O(12')	4	2.072(7)	O($\overline{24}$')-O(22)		173.4	
-O(13)	3	1.991(7)	O(12')-O(24')		165.4	
-O(14)	3	2.099(7)	O(13)-O(14)		171.6	
-O(22)	3	2.128(6)				
-O($\overline{24}$')	3	2.173(7)				
-O(24')	3	2.181(7)				

(continued next page)

TABLE 3-3 (continued)

Atoms	Coord.no. of oxygen atom	Bond Length (Å)	Atoms forming edge	Length of Edge (Å) (±.01 Å)	Angle subtended at the central cation by the edge (degrees (± 0.5°)	Edge shared with
			O(12')-O(14)	2.75	82.6	
			O(24')-O(14)	2.83	82.8	
			O(12')-O(22)	2.84	85.0	
			O($\overline{24}$')-O(13)	2.86	86.8	
			O(22)-O(14)	2.89	86.2	Co(2)
			O(24')-O(13)	2.92	88.8	
			O(12')-O($\overline{24}$')	2.96	88.5	
			O(22)-O(13)	3.03	94.5	
			O($\overline{24}$')-O(14)	3.11	93.4	
			O($\overline{24}$')-O(24')	3.13	92.0	Co(1)
			O(22)-O(24')	3.16	94.5	
			O(12')-O(13)	3.24	105.8	
<u>$Co(2)O_6$ group</u>						
Co(2)-O($\overline{21}$')	4	2.927(7)	O($\overline{21}$')-O(22')		171.8	
-O(12')	4	2.138(7)	O(11')-O($\overline{23}$)		169.8	
-O($\overline{23}$)	3	2.042(7)	O(12')-O(14)		170.2	
-O(14)	3	2.061(7)				
-O(22')	3	2.075(7)	O(11')-O(12')	2.56	74.5	As(1)
-O(11')	3	2.096(7)	O($\overline{21}$')-O(12')	2.83	79.4	Co(3)
			O(14)-O($\overline{23}$)	2.88	89.2	
			O(22')-O(14)	2.89	88.6	Co(1)
			O($\overline{21}$')-O(11')	2.98	85.5	
			O(11')-O(22')	3.04	86.4	
			O($\overline{21}$')-O($\overline{23}$)	3.04	88.8	Co(3)
			O(12')-O($\overline{23}$)	3.11	96.3	
			O(22')-O($\overline{23}$)	3.14	99.4	
			O($\overline{21}$')-O(14)	3.15	92.7	
			O(11')-O(14)	3.17	99.4	
			O(12')-O(22')	3.19	98.5	

(continued next page)

TABLE 3-3 (continued)

Atoms	Coord.no. of oxygen atom	Bond Length (Å)	Atoms forming edge	Length of Edge (Å) (±.01 Å)	Angle subtended at the central cation by the edge (degrees (± 0.5°)	Edge shared with
Co(3)O_6 group						
Co(3)-O(12')	4	2.287(8)	O(21')-O(11)		172.4	
-O(21')	4	2.161(6)	O($\overline{21}$')-O(13')		164.4	
-O($\overline{21}$')	4	2.143(7)	O(12')-O(23)		172.7	
-O(23)	3	2.111(8)				
-O(13')	3	2.048(7)	O(13')-O(12')	2.60	73.4	As(1)
-O(11)	3	2.021(6)	O(21')-O(12')	2.83	79.0	Co(2)
			O(21')-O(21)	2.87	83.6	Co(3)
			O(11)-O(23)	2.91	89.5	
			O(11)-O($\overline{21}$')	2.94	89.9	
			O(21')-O(13')	2.95	89.1	
			O(13')-O(11)	3.03	96.3	
			O(23)-O($\overline{21}$')	3.04	91.1	Co(2)
			O(21')-O(23)	3.14	94.6	
			O(12')-O($\overline{21}$')	3.18	91.6	
			O(12')-O(11)	3.24	97.3	
			O(13')-O(23)	3.26	103.3	

*Atom $\overline{n}$ is obtained from n by an inversion through the origin and n' by the c glide operation changing (x,y,z) to (x,½-y,½+z).

Description and Discussion of the Structure:

The structure consists of nearly closest packed layers of oxygen atoms lying parallel to the (010) plane, with the cobalt atoms distributed in octahedral voids and the arsenic atoms in tetrahedral voids. The stacking sequence corresponds to the ABAC... sequence with 4 layers per unit translation along the stacking direction. This is reflected in the $\underline{a}_2$ axis length of 9.675 Å, which is approximately equal to four times the expected distance of 2.3 Å between two adjacent closest packed layers of oxygen atoms, as explained in Ch. 2. The $\underline{a}_1$ axis length of 5.75 Å ($\sim 2 \times 2.8$ Å) and the $\underline{a}_3$ axis length of 10.26 Å ($\sim 4 \times 2.4$ Å) are also in agreement with those expected in closest packed structures. The 32 oxygen atoms in the unit cell are arranged in 16 pairs of two oxygen atoms each which nearly superimpose in projection down the $\underline{a}_1$ axis. This is seen in fig. (3-1) which shows the superimposed oxygen atoms by large split circles. The length of the $\underline{a}_1$ axis (5.75 Å) is thus nearly defined by the sum of two oxygen atom van der Waals contact distances. The β angle of 93.5° is close to the 90° angle expected in an ideally closest packed structure.

The four closest packed layers of oxygen atoms in the structure lie at levels $y \simeq 0, \frac{1}{4}, \frac{1}{2}$ and 3/4 respectively. The layers at $y \simeq 0$ and $\frac{1}{2}$ are related by the glide-plane at $y = \frac{1}{4}$, while the layers at $y = \frac{1}{4}$ and 3/4 are related by the centre of

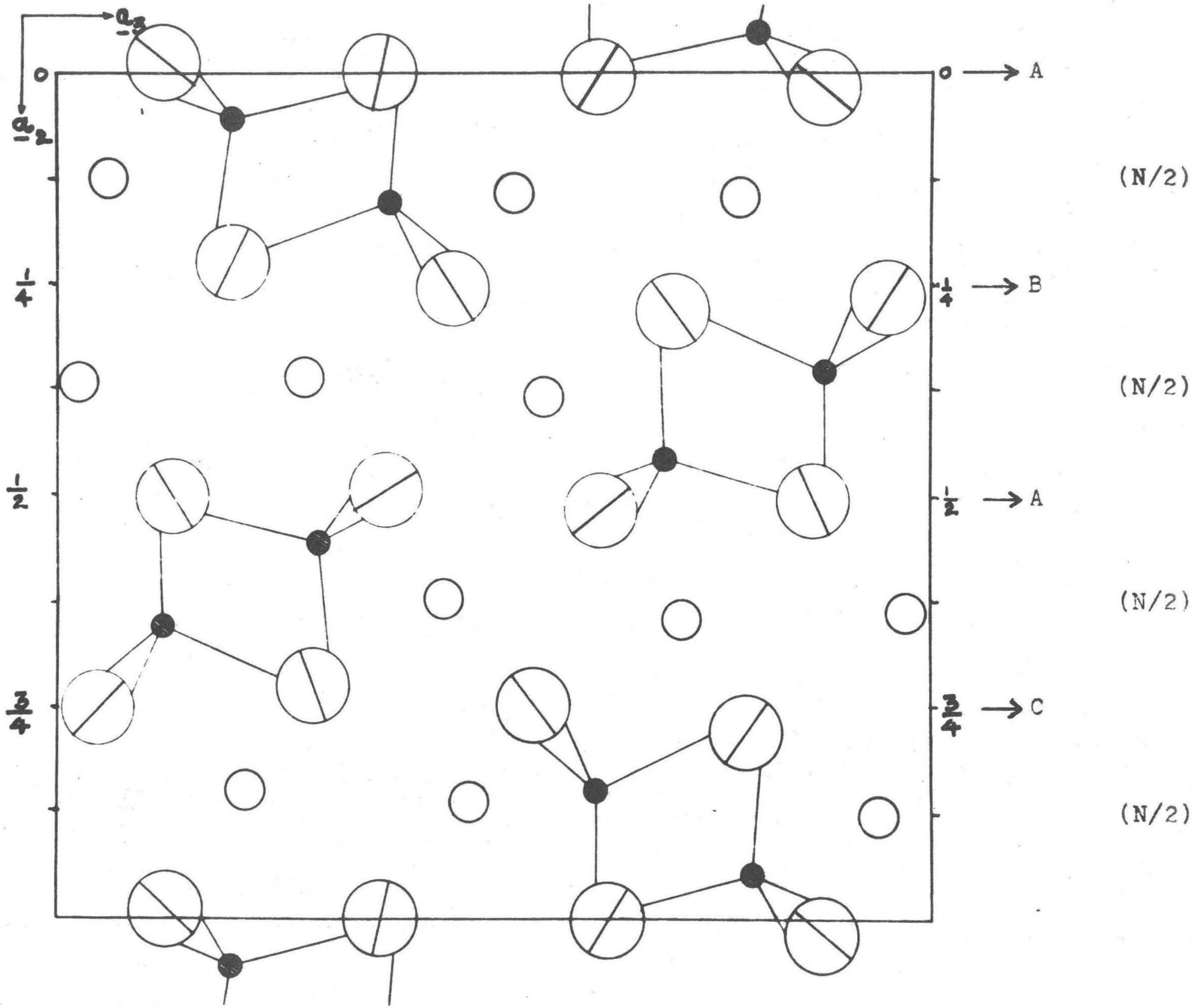

Figure (3-1). Structure of Co$_3$(AsO$_4$)$_2$ projected down the $\underline{a}_1$ axis.

symmetry at $(0,\frac{1}{2},0)$. The 12 cobalt atoms in the unit cell are arranged in the 4 octahedral layers (Ch. 2) at $y \simeq 1/8$, 3/8, 5/8 and 7/8 respectively, with 3 cobalt atoms per layer. The 8 arsenic atoms are located in tetrahedral positions in the 8 tetrahedral layers (Ch. 2) in the closest packing. The structure belongs to the N/2, N/2..... arrangement of (AsO_4) tetrahedra in the notation of Calvo(37). These features are illustrated in fig. (3.1).

There are three crystallographically independent cobalt atoms in the structure, each showing an irregular octahedral coordination of oxygen atoms. The average Co-O bond lengths are not significantly different, the values being 2.11(1) Å, 2.12(1) Å and 2.13(1) Å for Co(1), Co(2) and Co(3) respectively. However, the individual bond lengths in each CoO_6 group show significant differences between themselves (Table 3-3). There are two kinds of oxygen atom environments in the structure. The atoms O(12) and O(21) are strongly bonded to 4 cations whereas the other oxygen atoms are strongly bonded to only 3 cations. The coordination number of the oxygen atom involved in each Co-O and As-O bond is also listed in Table (3-3). The three longer Co-O bonds in the case of $Co(3)O_6$ involve oxygen atoms which are bonded to 4 cations whereas the 3 shorter bonds involve oxygen atoms bonded to 3 cations. This is in qualitative agreement with the expected influence of the different cation environments of the oxygen atoms on the individual Co-O bond lengths. However, there are significant differences in the lengths of the three longer Co-O bonds, all involving oxygen atoms with coordination number 4. The cause of these differences is not obvious. An analogous situation exists in the lengths of the three shorter Co-O bonds, all involving oxygen atoms with coordination number 3.

The two longer bonds in Co(2)O_6 group also involve oxygen atoms bonded to four cations, while the remaining four shorter bonds involve oxygen atoms with the smaller coordination, again in qualitative agreement with the expected influence of differences in anion coordination on the observed bond lengths. However, in the case of the Co(1)O_6 group a similar effect is not observed, and the Co(1)-O bond involving the 4-coordinated oxygen atom is not found to be the longest (Table 3-3).

While the three cobalt atoms have similar environments (six oxygen atoms octahedrally arranged at about 2.1 Å) as far as the first coordination sphere is concerned, the environments of the three are different when the differences in coordination of the individual oxygen atoms are taken into account. Thus Co(1) is bonded to 5 oxygen atoms with coordination number 3 and one with coordination number 4, Co(2) to four with the lower coordination and two with the higher coordination, and Co(3) to 3 with the lower and 3 with the higher coordinations.

The two crystallographically independent arsenic atoms in the structure, As(1) and As(2), have nearly tetrahedral coordination although the deviations from an ideal tetrahedral arrangement are significant. The average As(1)-O and As(2)-O bond lengths are 1.69(1) and 1.70(1) Å respectively, and thus are not significantly different from each other. The individual As(1)-O bond lengths are 1.670(7) Å, 1.685(6) Å, 1.688(7) Å and 1.722(7) Å (Table 3-3). The first three are not significantly different from each other, while the As(1)-O(12) bond is significantly longer. The elongation can be qualitatively explained on the basis of the difference in the environment of atom O(12) compared to those of the oxygen atoms involved in the other three bonds. A similar effect is found in the case of As(2), where the longest As(2)-O bond, 1.728(7) Å, involves oxygen atom $O(\overline{21})$ with coordination number 4, whereas the three shorter bonds involve oxygen atoms with coordination number 3.

The angles of the $As(1)O_4$ group show considerably greater deviation from ideal tetrahedral angles compared to those in the $As(2)O_4$ group. The angles in the former range from 97.5(5)° to 119.1(5)° whereas all the angles in the

As(2)O_4 group lie within 2° of the ideal values. Table (3-3) also lists the edges shared by these groups with other cations. The As(1)O_4 group shares two of its edges with two CoO_6 groups, whereas none of the edges of the As(2)O_4 group are shared with other polyhedra. Since sharing of polyhedral edges is expected to result in shortening of these shared edges, and consequently lead to a decrease in the angles subtended by these edges at the central atom (Ch.2), the angular distortions in the As(1)O_4 group might be attributed to these effects. The lengths of the shared edges and the angles subtended by these edges at As(1), listed in Table (3-3), support this explanation.

Features of the structure of $Co_3(AsO_4)_2$ in relation to the structures of other cobalt arsenates and other related structures will be dealt with in the concluding chapter.

CHAPTER 4

CRYSTAL STRUCTURE OF $Co_{24.2}As_9O_{48}$

This chapter deals with the structural and related studies on the dark purple crystals formed as a product of the reaction described in the first paragraph of the preceding chapter.

Preliminary investigations: A crystal was mounted with the long axis of the crystal parallel to the axis of rotation of the goniometer head. Preliminary photographs indicated that the diffraction pattern could be indexed on the basis of monoclinic symmetry for the crystal. A set of axes consistent with monoclinic symmetry were chosen, corresponding to approximate cell dimensions $\underline{a}_1 = 10.4$ Å, $\underline{a}_2 = 5.9$ Å, $\underline{a}_3 = 9.88$ Å, $\beta = 110°$. The systematic absence observed was: all $hk\ell$ type reflections with $h+k = 2n+1$. The space group possibilities consistent with this observation are C2, Cm and C2/m.

The density of the crystals was not determined since a sufficient amount of the crystals could not be selected from the reaction product. Initial information on the composition of the compound and the unit cell contents were obtained by making use of the similarity in the symmetry and cell dimensions of the title compound with those of the mineral aerugite(7). The similarity strongly suggested that the crystal under investigation was isostructural with aerugite. Davis et al.(7) have reported that the cell content in the case of aerugite corresponds to $Ni_{18}As_6O_{32}$. Therefore it was assumed in the initial stages of this study that the unit cell content in the present case is given approximately by the formula $Co_{18}As_6O_{32}$.

Davis et al.(7) have pointed out in the case of aerugite that the $\underline{a}_1$ axis is almost exactly $\sqrt{3}$ times the $\underline{a}_2$ axis. In the hexagonal or trigonal system, (in which the cell dimensions $\underline{a}_1$, $\underline{a}_2$, $\underline{a}_3$, α, β, γ have the symmetry restrictions $\underline{a}_1 = \underline{a}_2$, $\alpha = \beta = 90°$, $\gamma = 120°$), the $(-2\underline{a}_1-\underline{a}_2)$ direction is perpendicular to the $\underline{a}_2$ axis, and $|(-2\underline{a}_1-\underline{a}_2)| = \sqrt{3}|\underline{a}_2|$. Since the monoclinic cell axes $\underline{a}_1$ and $\underline{a}_2$ are related in a similar manner, the possibility that aerugite and the cobalt analog under investigation might possess higher symmetry than the monoclinic symmetry assigned to them in the preliminary investigations had to be considered. In addition, the $\underline{C}$ centering of the monoclinic cell implied that the crystals might in fact have rhombohedral symmetry.

Further examination of the diffraction patterns of the title compound confirmed that trigonal symmetry was the proper choice for this compound, and a unit cell with this symmetry and with approximate cell dimensions $\underline{a}_1 = \underline{a}_2 = 5.95$ Å,

$\underline{a}_3$ = 27.86 Å, were chosen. The patterns were reindexed on the basis of this new choice of axes, and the only systematic absence observed was: all hkℓ type reflections with $(-h+k+\ell)\neq 3n$. The space group possibilities consistent with these observations are R3, R$\bar{3}$, R32, R3m and R$\bar{3}$m. The Laue symmetry for the space groups R3 and R$\bar{3}$ is $\bar{3}$, and for the space groups R32, R3m and R$\bar{3}$m it is $\bar{3}$m(22). The hkl precession photograph showed the Laue symmetry to be $\bar{3}$m, and the space group possibilities are thus reduced to R32, R3m and R$\bar{3}$m. This conclusion is also confirmed by the fact that the space groups R3 and R$\bar{3}$ do not have subgroups with monoclinic symmetry (since they do not possess symmetry elements characteristic of the monoclinic space groups).

The solution of the ambiguity between the space groups R32, R3m and R$\bar{3}$m is more easily discussed in terms of the corresponding monoclinic subgroups C2, Cm and C2/m. The equivalent atom positions in the three space groups C2, Cm and C2/m, and the expected intensity equivalences in the diffraction pattern are listed below:

Space group	Equivalent Positions	Equivalent Reflections
C2	$x,y,z\ ;\ \bar{x},y,\bar{z}$	$hk\ell\ ;\ \bar{h}k\bar{\ell}$
Cm	$x,y,z\ ;\ x,\bar{y},z$	$hk\ell\ ;\ h\bar{k}\ell$
C2/m	$x,y,z\ ;\ x,\bar{y},z$	$hk\ell\ ;\ h\bar{k}\ell$
	$\bar{x},y,\bar{z}\ ;\ \bar{x},\bar{y},\bar{z}$	$\bar{h}k\bar{\ell}\ ;\ \bar{h}\bar{k}\bar{\ell}$

The equivalent positions are listed in International Tables(22), and the equivalent reflections are derived by writing the general structure factor equation in terms of the equivalent positions and collecting the coefficients of x, y, and z in the exponential in each term. Thus in the case of C2 with equivalent positions x, y, z and $\bar{x}, y, \bar{z}$,

$$F_{hk\ell} = \sum_n f_n \, e^{2\pi i[h(x)+k(y)+\ell(z)]} + \sum_n f_n \, e^{2\pi i[h(\bar{x})+k(y)+\ell(\bar{z})]}$$

$$= \sum_n f_n \, e^{2\pi i[x(h)+y(k)+z(\ell)]} + \sum_n f_n \, e^{2\pi i[x(\bar{h})+y(k)+z(\bar{\ell})]},$$

giving the equivalent positions as $(hk\ell)$ and $(\bar{h}k\bar{\ell})$. The equivalent reflections for other space groups are derived in a similar manner.

Since the cobalt atoms in the structure have a large contribution to the anomalous scattering of Cu radiation(20), a few photographs were taken using this radiation in an attempt to use the differences expected in the intensity equivalences to determine the correct space group. Oscillation photographs were obtained with the $\underline{a}_2$ axis as the rotation axis using Cu Kα radiation. Oscillation angles of about 40° were used and photographs were obtained to cover half of the reciprocal space. No significant differences were observed in the intensities of corresponding $hk\ell$ and $h\bar{k}\ell$ reflections in any of the photographs. This observation reduces the space group possibilities to Cm and C2/m.

The $hn\ell$ photographs with n = 0,1,2,3 and 4 were obtained using Cu Kα radiation, and the intensities of corresponding $hk\ell$ and $\bar{h}k\bar{\ell}$ reflections were compared. Again no differences were noticed in any given pair of reflections. This uniquely determines the space group for the crystal under investigation as C2/m in the monoclinic indexing. The corresponding space group with the trigonal indexing is R$\bar{3}$m.

Accurate cell dimensions for the crystal were obtained from precession photographs by calibration of the films with tetragonal TiO_2 crystal as standard. The procedure was similar to that described in the case of $Co_3(AsO_4)_2$(Ch.3). The $h0\ell$ reflections from the crystal under study and the hk -h+k) reflections from TiO_2 were recorded on the same film using the precession method. The shrinkage factor was derived from a comparison of the spacings measured from the film along the (110) direction of the TiO_2 pattern with the expected spacings based on the accurate parameters $\underline{a}_1$ = 4.5929(5) Å and $\underline{a}_3$ = 2.9591(3) Å assumed for TiO_2(37). Isotropic film shrinkage was assumed and the measured spacings of $\underline{b}_1$ and $\underline{b}_3$ axes of the title compound were corrected by the shrinkage factor derived for TiO_2. The average of 5 independent measurements were taken for $\underline{b}_1$ and 9 independent measurements for $\underline{b}_3$. The final values for the two parameters are $\underline{b}_1 = 0.1910(2)$ Å^{-1} and $\underline{b}_3 = 0.03564(6)$ Å^{-1}. The corresponding real lattice parameters are $\underline{a}_1 = \underline{a}_2 = 6.046(7)$ Å, $\underline{a}_3 = 28.06(5)$ Å.

Structure determination: It was convenient to index the diffraction patterns initially on the basis of the monoclinic cell. Consequently, preliminary attempts at finding a trial structure were carried out with this indexing, and the initial stages of the structure determination described below refer to the monoclinic designation.

Intensities of the $hn\ell$ reflections with $n = 0, 1, 2, 3$ and 4 were measured using Mo Kα radiation with a manually set scintillation counter mounted on a Weissenberg camera. An ω scan was used for the measurements. The procedure was the same as that used for $Co_3(AsO_4)_2$ (Ch. 3). The intensities were corrected for Lorentz and polarization effects. The crystal used had dimensions of approximately 0.01 × 0.01 × 0.015 cm^3 which leads to an average μR value of 1.0. The intensities were corrected for absorption using cylindrical geometry. Neglect of absorption would have led to an average error of the order of 20% in the intensities.

The three-dimensional Patterson function was computed at intervals of (5/60) along the $\underline{a}_2$ direction using 950 independent reflections that had been measured. On the basis of the assumed unit cell content given by $Co_{18}As_6O_{32}$, a total of 24 heavy atoms (18 cobalt atoms and 6 arsenic atoms) were to be located. The asymmetric unit of the Patterson map was found to have relatively large peaks at (u=0,w=0), (u=1/2, w=0) and (u=1/4, w=1/4) at sections v=0 and v=1/2, and at (u=0, w=1/4), (u=1/4, w=0) and (u=1/2,w=1/4) at sections v=1/4 and v=3/4. A trial structure with cobalt or arsenic atoms located at (x=0, z=0), (x=1/2, z=0) and (x=1/4,z=1/4) at levels y = 0 and y = 1/2, and at (x=0 , z=1/4), (x=1/4, z=0) and (x=1/2, z=1/4) at levels y=1/4 and y=3/4, was found to account qualitatively for all the large peaks in the Patterson map. This model also accounted for all the 24 cations expected in the monoclinic unit cell with C2/m symmetry.

On the basis of this trial structure, structure factors were calculated corresponding to all the data points which had been measured. No attempt was made to distinguish between arsenic and cobalt positions at this point. Since the scattering factors of Co^{+2} and As^{+5} species differ only by about 10% on the average, the scattering curve of Co^{+2} species (39) was used for all the 24 cations in the cell as a first approximation. Isotropic temperature factors $U = 0.01\ \mathring{A}^2$ were assigned to all the cations initially. A few cycles of least-squares refinement of the positional parameters of all the cations were carried out, along with individual scale constants for the five layers of data measured. A 3-dimensional electron density difference map was computed and this indicated that the atom at (x = 1/4, y = 1/2, z = 1/4) had been positioned incorrectly. However, a relatively strong peak was observed at (x = 0.3, y = 0.5, z = 0.4), and when a cation was located here, the R_1- value dropped from 0.46 to 0.30. The relatively good agreement indicated that the cations have been located at approximately their correct positions.

At this stage, the indices of the reflections and the coordinates of the atoms were transformed to correspond to the trigonal cell with $\underline{a}_1$ = 6.046 Å and $\underline{a}_3$ = 28.06 Å. The volume of the trigonal cell is 3/2 times that of the monoclinic cell, and the cell content of the trigonal cell should therefore correspond approximately to $Co_{27}As_9O_{48}$. The transformed positions of all the atoms were found to lie within 0.3 Å of special positions in the space group $R\bar{3}m$. These atoms were assigned to the corresponding special positions. This resulted in location of 4 independent cation sites with a total of 3 variable positional parameters in the trigonal unit cell with $R\bar{3}m$ symmetry. (The other 9 positional coordinates were fixed by symmetry requirements). Since there is a 3-fold axis in the $\underline{a}_3$ direction in $R\bar{3}m$ which of course is not present in C2/m, a number of reflections which had been indexed as independent reflections in C2/m were equivalent when transformed to $R\bar{3}m$. The scaled observed structure factor for each equivalent reflection was averaged, and the average value was taken as the new observed value. This process reduced the number of reflections from 950 in the monoclinic indexing to 625 in the trigonal indexing. The three variable positional parameters of the 4 independent cations were refined along with five layer scale factors using the 625 independent reflections. After a few cycles of refinement the minimum was reached with the value of R_1 at 0.27.

The position of all the oxygen atoms were located from a 3-dimensional electron density difference map. After a few cycles of refinement it was possible to use the individual cation-oxygen distances and the coordination of the cation to distinguish between arsenic and cobalt positions with reasonable certainty. Of the four cations in the asymmetric volume, one had a nearly tetrahedral coordination of oxygen atoms with an average cation-oxygen distance of about 1.7 Å. This position was assigned to an arsenic atom. The remaining three cations were in nearly octahedral positions. Two of these had average cation-oxygen distance of about 2.1 Å. The distances, as well as the coordination, compare well with the environment of divalent cobalt in other cobalt arsenates. These positions were thus identified as cobalt atom positions. These assignments account for 27 cobalt atoms and 6 arsenic atoms in the trigonal unit cell, with the expected cell content given by $Co_{27}As_9O_{48}$. The remaining cation site had an average cation-oxygen distance of about 1.85 Å. An arsenic atom was located in this site, and this accounted for 3 additional arsenic atoms in the unit cell.

Once the cobalt and arsenic positions had been identified, the appropriate scattering curves were used in the calculations. The scattering curves were obtained from the same sources as those used in the case of $Co_3(AsO_4)_2$ (Ch.3).

The unit cell content, $Co_{27}As_9O_{48}$, that has been assumed in the refinement upto this stage is only approximately correct, since it is based on the approximate composition of aerugite reported by Davis et al.$^{(7)}$. An attempt was made to derive the correct composition using the x-ray data by including the population parameters of the heavy atom sites as variables in the least-squares refinement. The thermal parameters of all the atoms were converted to anisotropic form the components as well. The weighting scheme was changed from unit weighting to a Cruickshank type weighting scheme of the form $w = (60.0 + 0.032|F_o| + 0.0077|F_o|^2)^{-1}$. The population parameters of neither of the two independent arsenic ions deviated significantly from the values required for complete occupancy of the site. Hence these values were reset to that required by the space group and kept fixed, and only the population parameters of the cobalt atom sites were included as parameters in the refinement. Refinement was terminated when the shifts in the parameters were less than the estimated standard errors in these parameters. The final unweighted R_1-

value was 0.091 and the R_w-value was 0.108. The final positional and thermal parameters are given in Table (4-1). The composition derived on the basis of the x-ray data is $Co_{24.2}As_9O_{48}$. The observed and calculated structure factors for the model are given in Table (4-2). The more important bond distances and angles in the structure are listed in Table (4-3).

Description of the structure:

The structure can be described in terms of a closest packed arrangement of oxygen atoms, with the cations occupying octahedral and tetrahedral voids in the packing. The stacking direction is parallel to the $\underline{a}_3$ axis. There are 12 closest packed layers per unit translation along the stacking direction, in agreement with the $\underline{a}_3$ axis length of 28.06 Å ($\sim$ 12 × 2.3 Å, where 2.3 Å is the expected distance between consecutive layers--Ch.2). The $\underline{a}_1$ and $\underline{a}_2$ axes, each of length 6.046 Å, and the interaxial angle of 120°, are also consistent with those expected in the closest packed arrangement of oxygen atoms. Fig. (4-1) shows the structure projected down the $\underline{a}_3$ axis, and it can be seen that the lengths of the $\underline{a}_1$ and $\underline{a}_2$ axes are nearly defined by twice the van der Waals contact distance of two oxygen atoms. The stacking sequence of the closest packed layers in the structure corresponds very nearly to the ABC...stacking, or the cubic closest packed arrangement.

Fig. (4-2) shows the structure projected down the $\underline{a}_2$ axis. The contents of only one-third of the cell are shown (in the range $\underline{z}$ = 0 to 1/3). The remaining atoms in the unit

TABLE 4-1

Atomic parameters for $Co_{24.2}As_9O_{48}$*

Atom	Site symmetry	Multiplicity	No.of atoms in unit cell	Fractional Coordinates			Thermal parameters ($\mathring{A}^2$) †					
				x	y	z	u_{11}	u_{22}	u_{33}	u_{12}	u_{13}	u_{23}
CO(1)	$\frac{2}{m}$	0.224(4)	8.1(2)	$\frac{1}{2}$	$\frac{1}{2}$	0	0.014(2)	0.011(1)	0.019(1)	$u_{11}/2$	-0.000(1)	$2u_{13}$
CO(2)	m	0.447(6)	16.1(2)	0.1655(5)	2x	0.08837(7)	0.014(1)	u_{11}	0.0180(8)	0.006(1)	-0.0003(8)	$-u_{13}$
As(1)	$\bar{3}m$	0.0833	3	0	0	0	0.009(1)	u_{11}	0.006(1)	$u_{11}/2$	0	0
As(2)	3m	0.1666	6	0.6666	0.3333	0.1412(1)	0.009(1)	u_{11}	0.137(9)	$u_{11}/2$	0	0
O(1)	m	0.5	18	0.144 (2)	2x	-0.0377(4)	0.015(8)	u_{11}	0.019(4)	0.010(4)	-0.001(3)	$-u_{13}$
O(2)	3m	0.1666	6	0.3333	0.6666	0.0411(7)	0.012(8)	u_{11}	0.014(7)	$u_{11}/2$	0	0
O(3)	3m	0.1666	6	0	0	0.1317(7)	0.009(7)	u_{11}	0.015(8)	$u_{11}/2$	0	0
O(4)	m	0.5	18	-0.487 (3)	-x	-0.1226(4)	0.016(7)	u_{11}	0.017(4)	0.006(4)	0.002(4)	$-u_{13}$

*Estimated standard deviations are in parentheses

†The thermal parameters have been obtained from $\beta_{ij} = 2\pi^2 \underline{b}_i \underline{b}_j u_{ij}$ where the β_{ij}'s appear as a thermal effect through $\exp[-(\beta_{11}h^2+2\beta_{12}hk + \ldots)]$ in the structure factor expression, and $\underline{b}_j$ are the reciprocal lattice vectors.

TABLE (4-2).

COMPARISON OF OBSERVED AND CALCULATED STRUCTURE FACTORS FOR $Co_{24.2}As_9O_{48}$.

UNOBSERVED REFLECTIONS ARE MARKED BY (*) AND UNRELIABLE REFLECTIONS BY ($)

H	L	|FOBS|	FCALC
		K = 0	
[illegible]	[illegible]	[illegible]	[illegible]
		K = 1	
[illegible]	[illegible]	[illegible]	[illegible]
		K = 2	
[illegible]	[illegible]	[illegible]	[illegible]
		K = 3	
[illegible]	[illegible]	[illegible]	[illegible]
		K = 4	
[illegible]	[illegible]	[illegible]	[illegible]
		K = 7	
[illegible]	[illegible]	[illegible]	[illegible]
		K = 8	
[illegible]	[illegible]	[illegible]	[illegible]

TABLE 4-3

Bonding geometry in $Co_{24.2}As_9O_{48}^*$

Atoms forming bond	Coordination no. of oxygen atom involved in the bond	Bond Length (Å)	Atoms forming edge	Length of edge (Å)	Angle subtended at central cation by the edge (degrees)	Edge Shared with
$As(1)O_6$ group:						
As(1)-O(1)a	5	1.84(1)	O(1)a-O(1)a'		180.0	
-O(1)a'	5	1.84(1)	O(1)b-O(1)b'		180.0	
-O(1)b	5	1.84(1)	O(1)c-O(1)c'		180.0	
-O(1)b'	5	1.84(1)				
-O(1)c	5	1.84(1)	O(1)a-O(1)b	2.60(2)	90.0	$Co(1)O_6$
-O(1)c'	5	1.84(1)	O(1)b-O(1)c	2.60(2)	90.0	$Co(1)O_6$
			O(1)c-O(1)a	2.60(2)	90.0	$Co(1)O_6$
			O(1)a'-O(1)b'	2.60(2)	90.0	$Co(1)O_6$
			O(1)b'-O(1)c'	2.60(2)	90.0	$Co(1)O_6$
			O(1)c'-O(1)a'	2.60(2)	90.0	$Co(1)O_6$
			O(1)a-O(1)b'	2.60(2)	90.0	$Co(2)O_6$
			O(1)b-O(1)c'	2.60(2)	90.0	$Co(2)O_6$
			O(1)c-O(1)a'	2.60(2)	90.0	$Co(2)O_6$
			O(1)a'-O(1)b	2.60(2)	90.0	$Co(2)O_6$
			O(1)b'-O(1)c	2.60(2)	90.0	$Co(2)O_6$
			O(1)c'-O(1)a	2.60(2)	90.0	$Co(2)O_6$
$As(2)O_4$ group:						
As(2)-O(3)d	4	1.70(2)	O(3)d-O(4)a	2.74(2)	108.0(4)	
-O(4)a	3	1.69(2)	O(3)d-O(4)b	2.74(2)	108.0(4)	
-O(4)b	3	1.69(2)	O(3)d-O(4)c	2.74(2)	108.0(4)	
-O(4)c	3	1.69(2)	O(4)a-O(4)b	2.79(2)	110.9(6)	
			O(4)b-O(4)c	2.79(2)	110.9(6)	
			O(4)c-O(4)a	2.79(2)	110.9(6)	

(continued next page).

TABLE 4-3 (continued)

Atoms forming bond	Coordination no. of oxygen atoms involved in the bond	Bond length (Å)	Atoms forming edge	Length of edge (Å)	Angle subtended at central cation by the edge (degrees)	Edge Shared with
Co(1)-O_6 group:						
Co(1)-O(2)a	6	2.09(1)	O(1)a-O(1)a'		180.0	
-O(2)a'	6	2.09(1)	O(1)b-O(1)b'		180.0	
-O(1)a	5	2.15(1)	O(2)a-O(2)a'		180.0	
-O(1)a'	5	2.15(1)				
-O(1)b	5	2.15(1)	O(1)a-O(1)b'	2.60(2)	74.1(4)	As(1)O_6
-O(1)b'	5	2.15(1)	O(1)a'-O(1)b	2.60(2)	74.1(4)	As(1)O_6
			O(1)a-O(1)b	3.44(2)	105.9(4)	-
			O(1)a'-O(1)b'	3.44(2)	105.9(4)	-
			O(1)a-O(2)a	2.97(2)	88.8(4)	Co(1)O_6
			O(1)a'-O(2)a'	2.97(2)	88.8(4)	Co(1)O_6
			O(1)b-O(2)a	2.97(2)	88.8(4)	Co(1)O_6
			O(1)b'-O(2)a'	2.97(2)	88.8(4)	Co(1)O_6
			O(1)a'-O(2)a	3.03(2)	91.2(4)	Co(2)O_6
			O(1)a-O(2)a'	3.03(2)	91.2(4)	Co(2)O_6
			O(1)b'-O(2)a	3.03(2)	91.2(4)	Co(2)O_6
			O(1)b-O(2)a'	3.03(2)	91.2(4)	Co(2)O_6
Co(2)O_6 group:						
Co(2)-O(2)a	6	2.20(1)	O(1)b'-O(4)c		164.2(4)	
-O(1)b'	5	2.16(1)	O(1)c'-O(4)a		164.2(4)	
-O(1)c'	5	2.16(1)	O(2)a-O(3)a		178.0(6)	
-O(3)a	4	2.12(1)				
-O(4)a	3	2.06(1)	O(1)b'-O(1)c'	2.60(2)	74.1(4)	As(1)O_6
-O(4)c	3	2.06(1)	O(2)a-O(4)a	2.96(2)	87.9(4)	Co(2)O_6
			O(2)a-O(4)c	2.96(2)	87.9(4)	Co(2)O_6

(continued next page)

TABLE 4-3 (continued)

Atoms forming bond	Coordination no. of oxygen atoms involved in the bond	Bond length (Å)	Atoms forming edge	Length of edge (Å)	Angle subtended at central cation by the edge (degrees)	Edge shared with
			O(1)b'-O(4)a	3.00(2)	90.6(4)	-
			O(1)c'-O(4)c	3.00(2)	90.6(4)	-
			O(1)b'-O(2)a	3.03(2)	88.1(5)	Co(1)O_6
			O(1)c'-O(2)a	3.03(2)	88.1(5)	Co(1)O_6
			O(3)a-O(4)a	3.04(2)	93.3(5)	-
			O(3)a-O(4)c	3.04(2)	93.3(5)	-
			O(1)b'-O(3)a	3.04(2)	90.4(5)	Co(2)O_6
			O(1)c'-O(3)a	3.04(2)	90.4(5)	Co(2)O_6
			O(4)a-O(4)c	3.26(2)	104.5(5)	-

---

[*] Symmetry transformations:

a: (x,y,z); b: (-y,x-y,z); c: (y-x,-x,z); d: $(\frac{2}{3}-x,\frac{1}{3}-y,\frac{1}{3}-z)$.

a':(-x,-y,-z); b' (y,y-x,-z); c': (x-y,x,-z).

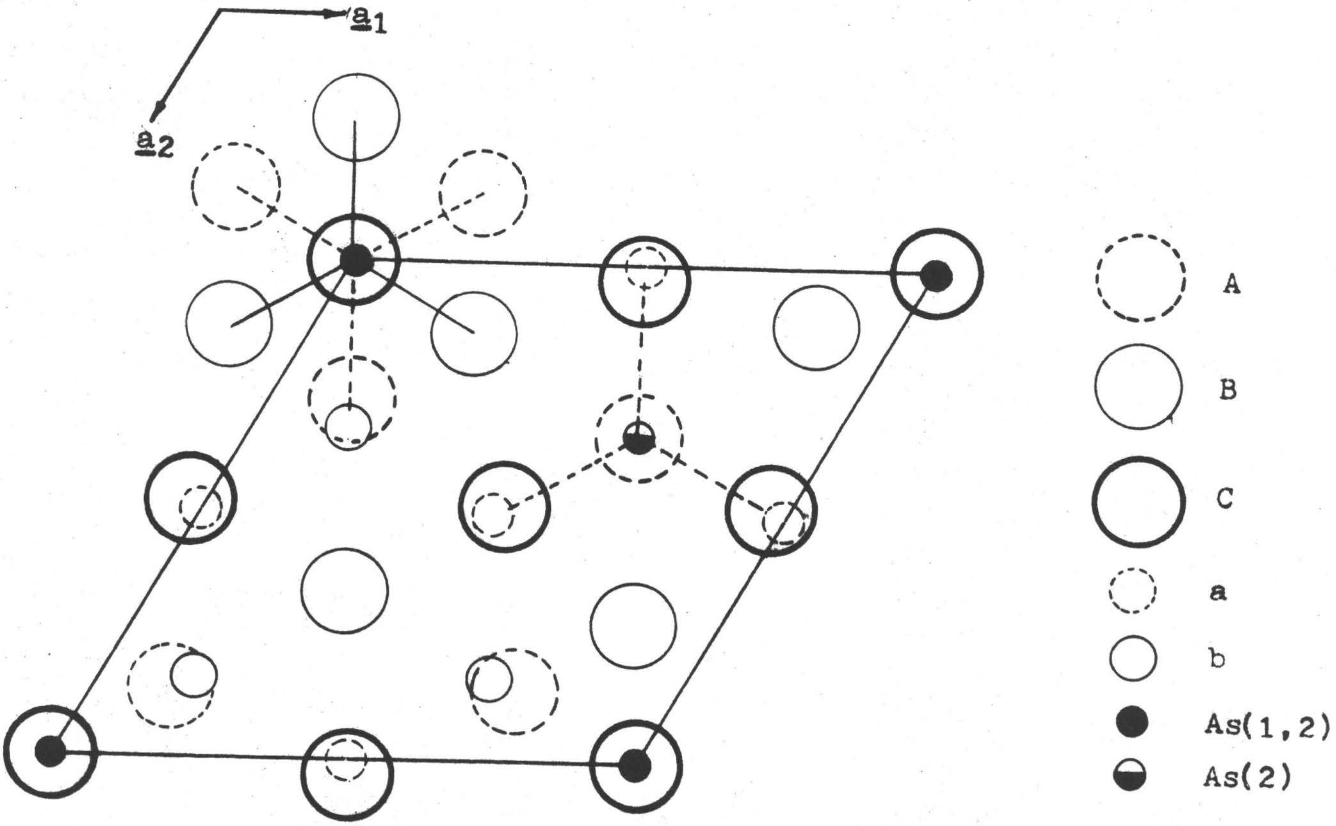

Figure (4-1).

The unit cell contents of $Co_{24.2}As_9O_{48}$ lying between $z = -0.04$ and $z = 0.29$ are shown in projection down the $\underline{a}_3$ axis. The large circles are oxygen atoms with A at $z = -0.04$ and $z = 0.21$, B at $z = 0.04$, and C at $z = 0.13$; the cobalt atoms are represented by the next larger circles with type a at $z = 0.00$ and $z = 0.24$, and type b at $z = 0.14$. The arsenic atom positions are shown by connecting these to the oxygen atoms to which they are bonded. An As(1) atom at $z = 0.00$ and an As(2) atom at $z = 0.19$ superimpose in projection.

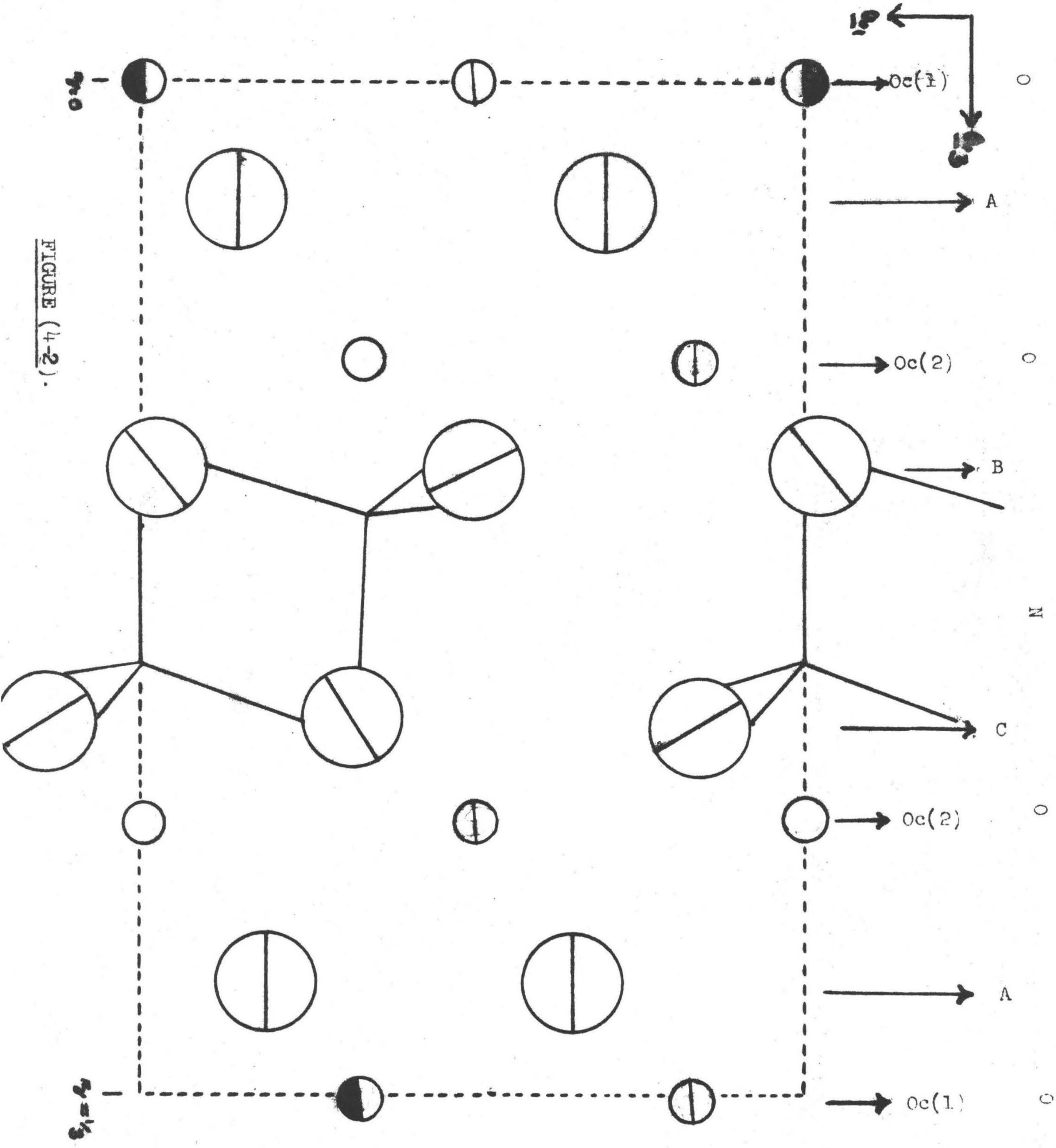

FIGURE (4-2).

cell are generated by the rhombohedral centering. The basic features of the structure can therefore be described by reference to fig. (4-2). As has been pointed out earlier, the structure consists of 12 nearly closest packed layers of oxygen atoms with the $\underline{a}_3$ direction as the stacking direction. The four layers in the unit shown in fig. (4-2) are marked A, B, C and A. When two atoms superimpose in projection, this has been indicated by split circles. The large circles in the diagram represent oxygen atoms, and the small circles represent octahedrally coordinated atoms. When the octahedrally coordinated atom is an arsenic atom, this has been represented by a filled circle, to distinguish it from an octahedrally coordinated cobalt atom, which is represented by an unfilled circle. The tetrahedrally coordinated atoms are shown by connecting these atom sites to the oxygen atoms to which they are bonded. The arrangement is such that either only the octahedral sites or only the tetrahedral sites are occupied between any two oxygen atom layers. In the notation of Calvo to describe closest packed structures (Ch. 2), the present structure will be grouped as an OONO... packing. The respective layers are shown in fig. (4-2) by these letters. Each layer containing the tetrahedral groups has 3 octahedral layers on either side of it ($\underline{\text{OOO}}\text{N}\underline{\text{OOO}}\text{N}\underline{\text{OOO}}$...). The octahedral layers are of two types. The first type, designated as Oc(1) in the figure, constitutes a layer in which all the available octahedral sites are filled (subject to the restriction that face-sharing between the octahedra is not favourable). There are four octahedrally coordinated atoms per layer of this type. The layer consists of sheets of edge-sharing octahedra with the octahedral sites lying in planes parallel to the $\underline{a}_1\underline{a}_2$ plane. Fig. (4-3) illustrates this feature of the structure. In the second type of octahedral layers, denoted as Oc(2) in fig. (4-2), only three out of the four available octahedral sites are occupied. The Oc(2) layers lie on either side of the tetrahedral layer, and the octahedral groups in these layers share corners with the As(2)O_4 groups in the tetrahedral layers.

There are two independent cobalt atoms, Co(1) and Co(2), in the structure. The Oc(2) type layer consists entirely of Co(2)O_6 groups, and the Oc(1) layer consists of Co(1)O_6 groups and As(1)O_6 groups. The Co(1)O_6 and Co(2)O_6 octahedra both deviate significantly from ideality (Table 4.3). The Co(1) atom lies at a site with 2/m symmetry. Two of the oxygen atoms of the Co(1)O_6 group, of type O(2), lie on the mirror plane. The other four oxygen atoms, O(1), are related to each other by the 2/m symmetry at the Co(1) site. The Co(1)-O(1) bond length is 2.15(1) Å and the Co(1)-O(2) bond length is 2.09(1) Å. The two Co(1)-O bonds are thus significantly different from each other. The O(2) atoms have strong bonds to six cobalt atoms, and the O(1) atoms are strongly bonded to four cobalt atoms and one arsenic atom. The environments of the two different kinds of oxygen

Figure (4-3)

The arrangement of edge sharing As(1)O_6 and Co(1)O_6 octahedra lying nearly parallel to the xy plane in $Co_{24.2}As_9O_{48}$. The smaller octahedra represent As(1)O_6 groups while the larger ones represent Co(1)O_6 groups. The oxygen atoms are at the corners of the octahedra.

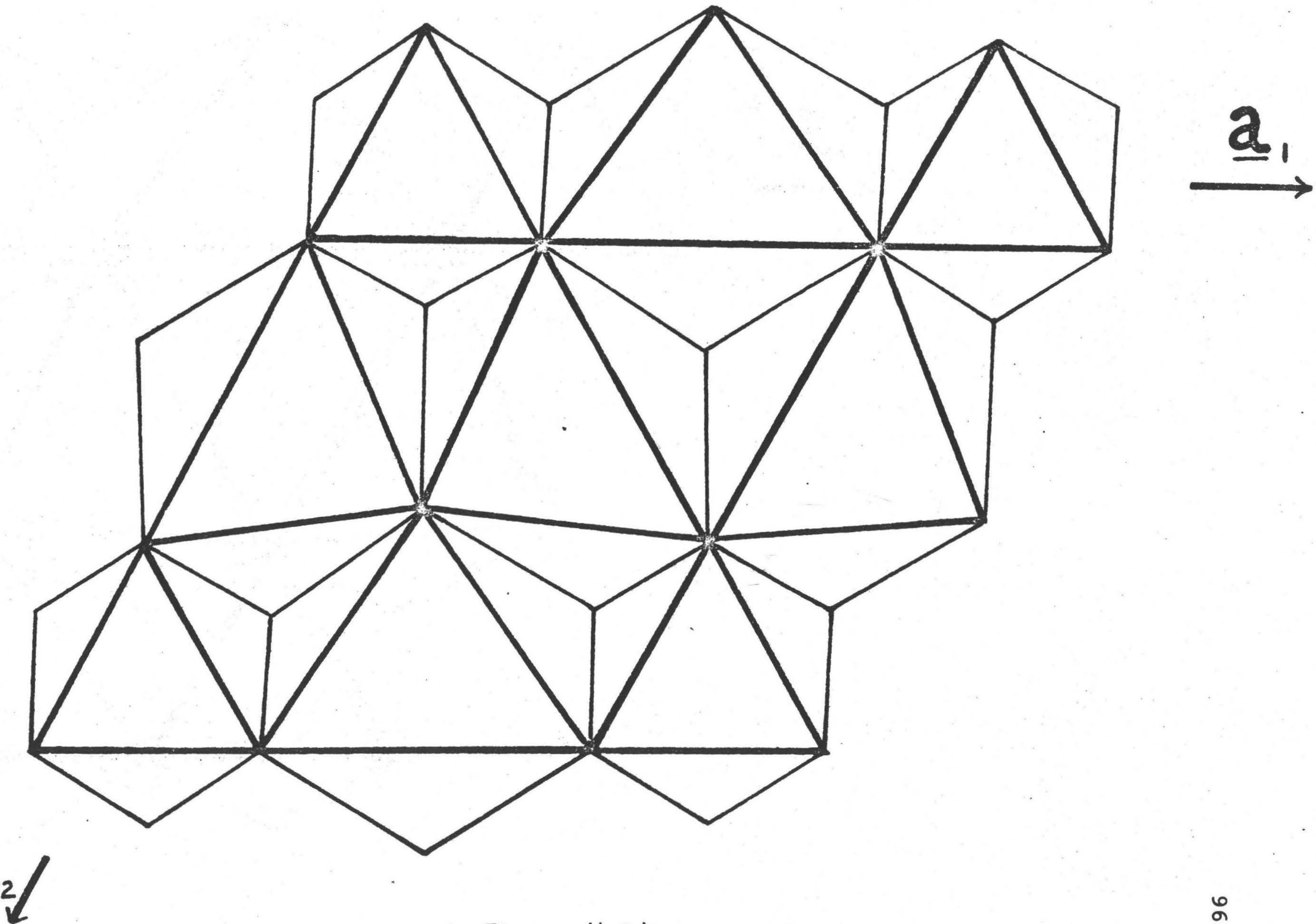

Figure (4-3).

atoms bonded to Co(1) differ not only in the number of the coordinated cations but also in the nature of the cations. The differences in the observed Co(1)-O(1) and Co(1)-O(2) bond lengths might be a consequence of these differences in the environments of the two kinds of oxygen atoms. The four angles subtended at Co(1) by the edges formed from any two adjacent equatorial oxygen atoms (O(1) atoms) deviate widely from the ideal octahedral angles, and are either 74.1(4)° or its supplement (Table 4-3). The other angles, subtended by edges formed from one of the two axial atoms (O(2)) and one of the equatorial atoms (O(1)), are close to the ideal octahedral angle, and are 88.8° or its supplement. The large deviation in the angles subtended by the four edges formed by the equatorial O(1) oxygen atoms can be traced to the relatively greater shortening of the edges shared between cobalt and arsenic octahedra as compared to those between two cobalt octahedra. A decrease in the length of the shared edge results in a decrease in the angle subtended by the edge at the centre of the polyhedron. The Co(1)O_6 group shares ten of its edges with the other surrounding octahedra. Of these, two are shared with two As(1)O_6 groups, and the others with Co(1)O_6 or Co(2)O_6 groups. The two edges shared with the arsenic polyhedra involve only the equatorial oxygen atoms O(1), whereas the other eight edges shared with the cobalt octahedra are formed from one equatorial (O(1)) and one axial

(O(2)) oxygen atom. The angle of 74.1° is subtended by the O(1)a-O(1)b' edge, and by the O(1)a'-O(1)b edge that is centrosymmetrically related to it. Both these edges are shared with As(1)O_6 groups. The supplementary angle of 105.93° is subtended by the O(1)a-O(1)b edge that is not shared with any other polyhedron, and by the centrosymetrically related edge O(1)a'-O(1)b'. The deviations in the angles in the Co(1)O_6 group are thus nicely explained by the greater coulombic repulsion between an arsenic ion and a cobalt ion, than between two cobalt ions.

The Co(2) atom lies on a mirror plane (site symmetry m), and has approximately octahedral coordination of oxygen atoms. Two of these oxygen atoms, O(2)a and O(3)a, (Table 4.3), lie on the mirror plane and subtend an angle of 178.0° at Co(2). The remaining four oxygen atoms, two O(1) and two O(4) atoms, lie in a plane perpendicular to the mirror plane. There are 4 independent Co(2)-O bond lengths (Table 4-3), and these are significantly different from each other. The observed differences are in qualitative agreement with the expected influence$^{(1)}$ of the coordination number of the oxygen atom (listed in the table) involved in each Co(2)-O bond. (However, it must be pointed out that the difference in the individual Co(1)-O bond lengths in the Co(1)O_6 group, 2.15(1) Å and 2.09(1) Å respectively, are not explained by a similar reasoning, since in this case the longer bond involves the oxygen atom O(1) bonded to 5 cations, and the shorter bond involves oxygen atom O(2) bonded to 6 cations).

The angles of the Co(2)O_6 group also show significant deviations from the ideal octahedral values (Table 4-3). The smallest angle, 74.1(4)°, is subtended by the O(1)b'-O(1)c' edge, which is shared with an arsenic polyhedron. This is also the only edge of the Co(2)O_6 group that is shared with an arsenic ion, the other six shared edges involving cobalt ions. The relatively large contraction in the angle subtended by this edge is thus understood in terms of the relatively strong repulsion between the Co^{+2} and As^{+5} ions at the centres of the polyhedra. The lengths of the shared edges listed in Table (4-3) support this speculation. In both the Co(1)O_6 and the Co(2)O_6 groups,the shortest edges are the ones that are shared with arsenic polyhedra, and subtend the smallest angles at the respective cobalt sites.

The large deviation from ideality of the angle of 104.5° subtended by the O(4)a-O(4)c edge can also be interpreted to be a consequence of the same reasons that were used to account for the small angle subtended by the O(1)b'-O(1)c' edge. This edge and the O(4)a-O(4)c edge lie approximately in a plane containing the Co(2) ion, and are related to each other by an approximate centre of symmetry at Co(2). The O(1)b'-O(1)c' edge is shared with an As^{+5} ion whereas the O(4)a-O(4)c edge is not shared with any other cation. As a result of the expected strong repulsion between the As^{+5} and

Co^{+2} ions sharing the former edge, the two cations, in particular the Co^{+2} ion for purposes of the present discussion, will tend to move away from the shared edge and towards the unshared edge. The net result is that the angle subtended by the unshared edge becomes larger, and that subtended by the shared edge smaller, than equal values expected in an ideal octahedral arrangement. The angles subtended by the other edges at Co(2) range from 87.9(4)° to 93.3(5)° (Table 4-3), and are relatively close to the ideal octahedral values. The angular distortion in the $Co(2)O_6$ group can thus be considered to be almost entirely caused by edge-sharing with an As^{5+} ion.

The average Co(1)-O and Co(2)-O bond lengths are both equal to 2.13(1) Å, and agree well with the average Co-O distances found in other compounds.

There are two independent arsenic atoms in the structure. One of these, As(1), lies in an octahedral site, and the other, As(2), in a tetrahedral site. The site symmetry of the As(1) atom is $\bar{3}m$. As(1) has an ideal octahedral arrangement of oxygen atoms around it with the As(1)-O(1) bond length of 1.84(1) Å. Each of the 12 edges of the $As(1)O_6$ group is shared with a CoO_6 group. All the shared edges are equal in length (2.60 Å), and are the shortest O-O distances in the structure. The As(1) atom lies in the octahedral layer of type Oc(1) described earlier, and forms part of the continuous sheet of edge-sharing octahedral groups.

The As(2) atom lies at a site with symmetry 3m, and has nearly tetrahedral coordination of oxygen atoms. Thus it is bonded to one O(3) oxygen atom lying on the 3-fold axis, and three O(4) oxygen atoms related to each other by the 3-fold axis. The As(2)-O(3) bond distance is 1.70(2) Å and the As(2)-O(4) length is 1.69(2) Å. The two types of bonds are thus not significantly different from each other. O(3) is bonded to three Co(2) and one As(2) atoms, and O(4) to only two Co(2) and one As(2) atoms. Based on observations in the other polyhedral groups discussed earlier, one would anticipate a noticeable difference in the two bond lengths as a result of the differences in the environments of the oxygen atoms involved in the two bonds. It is not clear why in the present case the environmental effect, if present, is not significant.

The O(3)-As(2)-O(4) angles are 108.0(4)°, and the O(4)-As(2)-O(4) angles are 110.9(6)°. The $As(2)O_4$ group is thus an almost regular tetrahedron, also indicated by the almost equal lengths for all the edges of this group (Table 4.3).

Discussion of the Structure:

a) Composition: An account of the investigations of Taylor and Heyding(6), Davis, Hey and Kingsbury(7), and Masson et al.(13) on the title compound and on the analogous nickel compound was presented in the introductory chapter. There it has been pointed out that the results of all these authors indicate the possibility that the title compound might have a non-stoichiometric composition. The unit cell content derived from the least-squares refinement of the present x-ray data is $Co_{24.2}As_9O_{48}$ with an estimated standard deviation of 0.4 on the number of cobalt atoms. Since the number of cobalt atoms is given as 24.2±0.4 by the present x-ray results, it is not possible to comment on whether the crystal under investigation has a truly stoichiometric composition represented by $Co_{24}As_9O_{48}$ (within one standard deviation), or $Co_{25}As_9O_{48}$ (within two standard deviations), or whether the composition is truly non-stoichiometric. Refinement of the structure with more accurate data (collected using automatic diffractometer methods etc.) might help determine the composition with greater accuracy, and answer the question regarding the stoichiometry or otherwise of the composition.

Davis et al.(7) have suggested the occurrence of a range of compositional stability for aerugite, the nickel analog of the present compound. The authors have discussed the composition of aerugite in terms of the contents of a unit cell with monoclinic symmetry, since this was erroneously considered to be the true symmetry of the crystal. Davis has since confirmed(41) that aerugite is isostructural with the title compound. Subsequent references to Davis et al.'s results on the composition of aerugite will therefore be based on the contents of a trigonal unit cell comparable to that chosen for the cobalt analog. These authors carried out chemical analyses on two different naturally occurring mineral samples of aerugite and two synthetic products of a reaction in which they attempted to prepare the stoichiometric compound $6NiO{\cdot}As_2O_5$. The compositions of the two mineral samples were determined to be $Ni_{23.65}(Co,Fe,Cu)_{0.78}As_{9.44}O_{48}$ and $Ni_{23.86}(Co,Fe,Cu)_{1.09}As_{9.23}O_{48}$, and those of the two synthetic samples were found to be $Ni_{25.69}As_{8.85}O_{48}$ and $Ni_{25.73}As_{8.97}O_{48}$. The spread in these values, and also the correlation of high values for nickel associated with low values for arsenic, led the authors to speculate that the structure may be stable over a wide range of compositions.

In view of the isostructural nature of aerugite and the cobalt analog under discussion, it is probable that a range of compositional stability occurs in this latter case as well. The composition $Co_{24.2}As_9O_{48}$ derived from the least-squares refinement of x-ray data collected from one single crystal gives only the composition of the material of this crystal, and further work is needed to test for the existence of other compositions in the neighbourhood of the presently derived composition, but with the same structure. If the suggested range of stability does exist, the structural basis for this is provided by the structure of $Co_{24.2}As_9O_{48}$. Since the cobalt sites in this structure are only partially occupied, in principle one can increase the occupancy of these sites up to the limit of 27 cobalt atoms (corresponding to full occupancy of both the cobalt sites), while partially emptying the arsenic sites in order to maintain overall charge neutrality of the compound, without significantly altering the structure.

b) Oxidation states of cobalt and arsenic: The starting compound $Co_3(AsO_4)_2 \cdot xH_2O$ in the present preparation loses water on heating to yield $Co_3(AsO_4)_2$. On further heating, this may be expected to decompose with loss of As_2O_5 to yield the stoichiometric compound $Co_6As_2O_{11}$, containing cobalt in divalent oxidation state and arsenic in pentavalent state. The product obtained in the present preparation has the composition $Co_{24.2}As_9O_{48}$, or $Co_{5.55}As_{2.06}O_{11}$, as derived from the refinement of the x-ray data. The derived composition requires that, for charge neutrality of the compound to be preserved, cobalt or arsenic or both must have undergone partial change in the oxidation state. The most stable oxidation states for cobalt are +2 and +3, and for arsenic, +5 and +3. The relative amounts of divalent and trivalent cobalt, and trivalent and pentavalent arsenic in $Co_{24.2}As_9O_{48}$ formed from $Co_3(AsO_4)_2$ will depend on the relative oxidation potentials of the redox couples

$$Co^{+2} \rightleftarrows Co^{+3} + e^- ,$$

$$As^{+3} \rightleftarrows As^{+5} + 2e^-,$$

$$\text{and } 2\,O^{-2} \rightleftarrows O_2 + 2e^-$$

under the conditions of formation of $Co_{24.2}As_9O_{48}$.

In the case of aerugite (the nickel analog), Davis et al.$^{(7)}$ detected the presence of trivalent arsenic by qualitative chemical tests, though attempts at a reliable quantitative determination were unsuccessful. In the case of $Co_{24.2}As_9O_{48}$ no chemical tests or other determinations such as magnetic measurements were carried out to establish whether cobalt or arsenic occur in variable oxidation states in this compound, since enough pure material was not available.

In principle, several possible combinations exist for the oxidation states of cobalt and arsenic in the present compound, depending on the extent of reduction of As^{+5} to As^{+3} and oxidation of Co^{+2} to Co^{+3}. The simplest of these corresponds to the case where no change in oxidation states of cobalt and arsenic have occurred compared to their +2 and +5 states respectively in the reactant. In this case, on the basis of the present structure (with no disorder between the cobalt and arsenic sites), the compound could have (consistent with charge neutrality requirements) the composition $Co_{(25.2+2.5\ x)}As_{(9-x)}O_{48}$, where x can have a value lying between 0.0 (corresponding to full occupancy of both the arsenic sites As(1) and As(2)), and 0.6 (corresponding to full occupancy of both the cobalt sites Co(1) and Co(2)). In the model proposed for the structure of the cobalt arsenate under discussion, it is assumed (on the basis of the least squares refinement) that both the arsenic sites are fully occupied (i.e. $x = 0$). The composition of the compound under the assumption of +2 oxidation state for cobalt and +5 state for arsenic will then be $Co_{25.5}As_9O_{48}$. The composition derived from the x-ray data is $Co_{24.2}As_9O_{48}$, with an e.s.d. of 0.4 on the number of cobalt atoms. The number of cobalt atoms in the derived composition differs by 3 e.s.d.'s from that in the expected composition $Co_{25.5}As_9O_{48}$. Thus the observed lower cobalt content seems to reflect the true situation in the present compound, and is probably not a result of unaccounted errors in the observations. This rules out the possibility that cobalt occurs only in divalent state and arsenic only in pentavalent state in the present compound.

Among the remaining possible combinations of oxidation states for cobalt and arsenic, all those which are consistent with overall charge neutrality of the composition $Co_{24.2}As_9O_{48}$ have the common feature that they all suggest presence of both divalent and trivalent cobalt in the compound. Thus, the present x-ray results, coupled with charge neutrality considerations, indicate that partial oxidation of divalent cobalt to the trivalent state has definitely occurred in the course of the preparation. However, these considerations do not assist in determining whether arsenic also exhibits variable oxidations states in this compound, or whether it is completely in the +5 or the +3 state. If the ratio of divalent to trivalent cobalt in the compound is determined, then it will be possible to distinguish between the above three possibilities of oxidation states of arsenic in the compound purely from charge balance considerations.

The observed Co-O bond lengths for both the Co(1) and Co(2) sites are in agreement with the values expected for high-spin Co^{+2} in octahedral coordination with oxygen atoms, and the observed As(1)-O and As(2)-O distances are in agreement with values reported for As^{+5} in comparable environments in other compounds. However, there is no literature available on As^{+3}-O distance either in tetrahedral or octahedral coordination with oxygen atoms, though it is known that As^{+3} prefers a triangular pyramidal coordination(42). Similarly no information seems to be available in the literature on accurate estimates of expected lengths of Co^{+2} (low spin)-O and Co^{+3}(high spin)-O bonds with the cobalt ion in octahedral coordination. Thus no definite conclusions could be drawn regarding the valence states of the cations in the different cation sites in the structure based on the observed bond lengths.

While some aspects of the crystallography of the cobalt arsenate under discussion have been established from the present x-ray work, answers to the crysto-chemical questions such as the valence states of the cations, composition, etc. raised by this study have to be sought from other experimental techniques such as magnetic susceptibility measurements, neutron scattering etc. An attempt to confirm independently the over-all composition of the compound using the electron microprobe analysis technique has been contemplated, but this has so far been hampered by instrumental failures. It will be valuable to determine the composition of the compound with greater accuracy by refinement of the structure using more accurate data (such as data collected using automatic diffractometer methods). In addition to the isostructural compounds $Co_{24.2}As_9O_{48}$ and the nickel analog aerugite, it is found that magnesium also forms an arsenate(16) giving a powder pattern closely resembling that of aerugite. While the cobalt and nickel compounds have the possibility that both the metal and arsenic in the compound can occur in more than one oxidation state, the magnesium compound differs in that it will be free of this complexity at least as far as magnesium is concerned. An accurate determination of the composition of the magnesium arsenate will give direct information on whether trivalent arsenic is present in this compound or not. An attempt to prepare the compound starting from MgO and As_2O_5 did not yield the desired product but instead resulted in a product containing crystals of magnesium orthoarsenate. A more detailed study of $Co_{24.2}As_9O_{48}$, aerugite, the isostructural magnesium arsenate, and other possible isostructural arsenates of other cations, will be valuable in obtaining a clearer understanding of the chemistry of these arsenates.

The structural relations of $Co_{24.2}As_9O_{48}$ to the other cobalt arsenates described in this thesis will be discussed in the concluding chapter.

CHAPTER 5

CRYSTAL STRUCTURES OF $Mg_3(AsO_4)_2$ AND THE TETRAGONAL PHASE OF $Co_3(AsO_4)_2$

Preparation and preliminary investigations: $Mg_3(AsO_4)_2$ was obtained by fusing hydrated magnesium orthoarsenate obtained from Alpha Inorganics Inc. in a silica crucible at about 1450°C. Single crystals for the investigation were obtained from the cooled melt.

Preliminary investigations indicated that the crystals had tetragonal symmetry. A set of axes consistent with the tetragonal system were chosen, and the approximate unit cell dimensions were $\underline{a}_1$ = 6.77 Å, $\underline{a}_3$ = 18.92 Å. The systematic absences observed were $hk\ell$ reflections with $(h+k+\ell) = 2n+1$ and $hh\ell$ reflections with $2h+\ell \neq 4n$. The space group possibilities are $I4_1md(C_{4v}^{11})$ and $I\bar{4}2d(D_{2d}^{12})$. The density was measured with a pycnometer$^{(43)}$, and the average of 4 determinations on the same sample led to the value 3.9(1) $g.cm^{-3}$. The calculated value assuming 6 molecules of $Mg_3(AsO_4)_2$ per unit cell is 4.03 $g.cm^{-3}$.

Crystals of the isostructural $Co_3(AsO_4)_2$ have been obtained from the product of one of the reactions in which the preparation of either the compound $6CoO.As_2O_5$ or $CoO.As_2O_5$ was attempted in a silica crucible starting from cobaltous carbonate, $2CoCO_3.3Co(OH)_2$ (Fisher Scientific Co.), and As_2O_5 (Mallinckrodt Analytical reagent). A crystal was chosen from the cooled melt of the product and preliminary investigations have clearly established that the magnesium and cobalt arsenates described above are isostructural. The hk0 and $hn\ell$ (n=0,1,2) precession photographs of the two crystals are superimposable, with some intensity differences expected as a consequence of the difference in scattering curves of cobalt and magnesium. The systematic extinctions in the two cases are the same, leading to the same space-group possibilities ($I4_1md$ or $I\bar{4}2d$) for both the compounds.

The following paragraphs describe the detailed structure investigation of $Mg_3(AsO_4)_2$ from single crystal data. A detailed investigation of the cobalt analog also seems necessary in spite of its being isostructural with $Mg_3(AsO_4)_2$, since another form of $Co_3(AsO_4)_2$ exists (Chapter 3), with monoclinic symmetry and space group $P2_1/c$, the analog of which is not known at present for $Mg_3(AsO_4)_2$. Unfortunately the crystals of the tetragonal form of cobalt orthoarsenate obtained from the reaction described above, while suitable for determining the cell dimensions and space group symmetry, were not suitable for collection of intensity data. The preparation of the compound is contemplated under conditions which might yield single crystals suitable for data collection.

Choice of space-group: The possible space-groups consistent with the observed extinctions are $I4_1md$ and $I\bar{4}2d$. There are 12 arsenic atoms in the unit cell. The general position in both the space-groups is 16-fold, and the arsenic atoms should therefore occupy 8-fold or 4-fold positions in either space group barring the possibility that the 12 arsenic atoms in the cell are distributed randomly in a 16-fold general position. In space group $I4_1md$, there are two sets of intersecting mirror planes, one parallel to the xz plane at levels $y = 0$ and $\frac{1}{2}$, and the other parallel to the yz plane at levels $x = 0$ and $\frac{1}{2}$. The 4-fold positions lie at sites of symmetry mm and the 8-fold positions at sites of symmetry m. It is not possible to place an arsenic atom either in the 8-fold special position or in a general position in space group $I4_1md$ without some of the oxygen atoms being separated by distances of the order of 1.7 Å (considerably smaller than their van der Waals contact distance of about 2.8 Å), or as the alternative, without these polyhedra sharing oxygen atoms. Sharing of oxygen atoms by arsenic polyhedra in this structure was considered unlikely since other known orthoarsenates, orthophosphates and orthovanadates contain isolated (AsO_4), (PO_4) or (VO_4) groups. This leaves the 4-fold positions with coordinates (o,o,z), and the symmetry-generated positions, as the only possible positions for arsenic atoms in this space group. The possible positions for arsenic, consistent with the Patterson function P_{uw}, are limited to (0,0,0), $(0,0,\frac{1}{4})$, $(0,0,\frac{1}{2})$ and $(0,0,\frac{3}{4})$. Since all these positions have site symmetry mm, all the oxygen atoms in the structure should be located on the mirror planes if the arsenic atoms have tetrahedral coordination of oxygen atoms. If sharing of oxygen atoms between arsenic polyhedra is to be avoided, it is possible to place arsenic atoms at only one of the two sets of positions ((0,0,0), $(0,0,\frac{1}{2})$), or ($(0,0,\frac{1}{4})$, $(0,0,\frac{3}{4})$), thus accounting for only 8 of the 12 arsenic atoms in the unit cell. These considerations suggested that the space group $I4_1md$ was not a suitable choice for $Mg_3(AsO_4)_2$. On this basis, the alternate space group $I\bar{4}2d$ was chosen as the correct space group and a solution to the structure attempted.

The above arguments are equally valid in the case of the isostructural tetragonal $Co_3(AsO_4)_2$, and the space group can thus be assigned as $I\bar{4}2d$ in this case as well.

The accurate unit cell parameters for $Mg_3(AsO_4)_2$ were obtained from measurements of arc lengths of 16 reflections from an uncalibrated powder photograph taken with Ni filtered Cu radiation, and least-square fitting the unit cell dimensions to the observed $\theta_{hk\ell}$ values. The reciprocal unit cell dimensions obtained from the least-squares refinement are $\underline{b}_1 = 0.1473(2)\text{Å}^{-1}$, $\underline{b}_3 = 0.0527(1)\text{Å}^{-1}$. The corresponding real lattice parameters are $\underline{a}_1 = 6.79(1)\text{Å}$ and $\underline{a}_3 = 18.98(4)\text{Å}$.

Intensities of the reflections $hn\ell$ ($n = 0,1,2,3$) were collected using an integrated precession camera and Mo Kα radiation,and measured using a Joyce-Loebl microdensitometer. The data were corrected for Lorentz and polarization effects, and the resulting structure factors were used for the structure solution. The mean dimensionsof the crystal used for data collection were approximately $0.2\times0.2\times0.4$ mm^3. However, the crystal had a very irregular shape, and hence absorption corrections were not applied. The value of μ is 125.37 cm^{-1} for $Mg_3(AsO_4)_2$, and it is suspected that the corrections could be significant. Equivalent reflections were averaged in the usual manner as described for $Co_3(AsO_4)_2$ (Ch. 3). The total number of independent reflections collected were 319, of which 19 were considered to be below the observable limit.

Structure solution: The unit cell content corresponds to $Mg_{18}As_{12}O_{48}$. The general position in the space group $I\bar{4}2d$ is 16-fold, and the special positions have 8-fold or 4-fold multiplities. The 12 arsenic atoms in the unit cell should be located in some of these special positions. An arsenic atom was initially located at the 4-fold position coinciding with the origin, the site symmetry $\bar{4}$ at this position being consistent with the normally encountered tetrahedral coordination of arsenic. For a tetrahedral arrangement of oxygen atoms around this arsenic, with expected As-O bond lengths of about 1.7 Å, the z-coordinate of the oxygen atom is fixed at z ≃ ±0.05. The only peaks lying within 2 Å of the origin in the P_{uv} Patterson projection were at (u=0, v=±0.2). These were identified as As-O interactions, and an oxygen atom was located at (0.0,0.2,0.05). The remaining eight arsenic atoms in the unit cell could then be located in either of the two 8-fold special positions (0,0,z) or $(x,\frac{1}{4},\frac{1}{8})$, both with local site symmetry C_2. (The position $(0,0,\frac{1}{2})$, which was the only 4-fold position available for occupancy at this stage, was not considered as a likely position for the arsenic atom, since locating an arsenic atom at this position would leave 4 remaining arsenic atoms to be located in the unit cell with no other 4-fold positions available for occupancy). The P_{uw} Patterson projection had relatively strong peaks at $(u=0,\ w=\frac{1}{4})$, $(u=0,\ w=\frac{1}{2})$, and $(u=0,\ w=\frac{3}{4})$. An arsenic atom at the 8-fold position $(0,0,\frac{1}{4})$ will be consistent with the Patterson peaks at $(u=0,\ w=\frac{1}{4})$ and $(u=0,\ w=\frac{3}{4})$. However, two of the oxygen atoms of the AsO_4 group at the origin were found to lie at about 2.1 Å from, and subtend the angle of about 90° at, the position $(0,0,\frac{1}{4})$. The As-O distance with arsenic in octahedral coordination of oxygen atoms is expected to be about 1.85 Å (Ch. 4), whereas the observed distance is in good agreement with the expected Mg-O distance for octahedrally coordinated Mg^{+2} (Ch. 7). Therefore the position $(0,0,\frac{1}{4})$ was considered as a likely position for magnesium rather than for arsenic, and a magnesium atom was located at this position. Use was made of the coordinates of the two oxygen atoms subtending a near-90° angle at this site and an approximately octahedral arrangement of oxygen atoms was generated about this site. At this stage all the 48 oxygen atoms in the unit cell had been approximately located.

The only prominent peaks unaccounted for in the Patterson projection maps at this stage suggested that an atom could be located at the 8-fold position $(\frac{2}{3},\frac{1}{4},\frac{1}{8})$ and one at the 8-fold position $(\frac{1}{4},\frac{1}{4},\frac{1}{8})$, consistent with packing considerations. The site $(\frac{2}{3},\frac{1}{4},\frac{1}{8})$ was found to have a nearly tetrahedral arrangement of oxygen atoms at distances about 1.7 Å from it. An arsenic atom was located at this position. The other site, $(\frac{1}{4},\frac{1}{4},\frac{1}{8})$, had an approximately octahedral arrangement of oxygen atoms at distances about 2.1 Å from it, and a magnesium atom was located at this position. At this stage all but 2 magnesium atoms in the unit cell had been located. Since the space group $I\bar{4}2d$ does not have any 2-fold special position, an a priori location of these 2 magnesium atoms in the unit cell was not possible.

The positions of all the atoms that had been located were refined along with 4 individual scale constants for the 4 layers of data measured, and individual isotropic thermal parameters for all the atoms. After a few cycles of refinement an electron density difference map was computed using the

$(h0\ell)$ type reflections. A large residual peak was found in the map at $(x=0, z=\frac{1}{2})$. This observation, together with packing considerations, suggested the position $(0,0,\frac{1}{2})$ and its symmetry-generated equivalent positions as the locations of the as yet unaccounted magnesium atoms in the unit cell. Since this is a 4-fold special position and since only 2 magnesium atoms had to be accounted for in the unit cell, the population parameter for the site was chosen as $\frac{1}{2}$. Refinement was continued including this position in the model. The isotropic temperature factors of all the atoms were converted to anisotropic factors and refined as well. A weighting scheme was chosen corresponding to $w = (30 + 0.117\ |F_{obs}|)^{-1}$ for $|F_{obs}| < 120.0$, and $w = ((|F_{obs}| - 114.0)/0.148)^{-1}$ for $|F_{obs}| > 120.0$. The 50 parameters (individual scale factors for the 4 layers, and the positional and anisotropic thermal parameters of all atoms) were refined until the minimum was reached at a value of 0.077 for both the unweighted (R_1) and weighted (R_w) values.

Since Robijn's work(8) indicated that the products in attempts to obtain magnesium orthoarsenate could have variable compositions, the population parameters of all the cations were refined at this stage. There were no significant changes in these parameters, and the largest change was less than 1.5σ. Thus the present x-ray data are consistent with assignment of the composition $Mg_3(AsO_4)_2$ for the crystal.

Table (5-1) gives the final positional and thermal parameters. The observed and calculated structure factor amplitudes are listed in Table (5-2). The more important bond distances and angles in the structure are collected in Table (5.3).

Description of the structure: There are two independent arsenic atoms, As(1) and As(2), in this structure. Both have tetrahedral coordination of oxygen atoms. As(1) is bonded to two 02 oxygen atoms and two 03 oxygen atoms, and As(2) is bonded to four 01 oxygen atoms. The mean arsenic-oxygen distances are 1.69(1) Å and 1.66(1) Å respectively in the two cases, which lie within two standard deviations of each other and therefore are not significantly different. The angles of the $As(1)O_4$ group vary from 100.9(8)° to 124.4(9)°, and those of the $As(2)O_4$ group are either 104.2(6)° or 120.7(6)° (Table 5-3). Thus both the AsO_4 groups deviate significantly from the ideal tetrahedral arrangement, though the $As(2)O_4$ group shows more angular distortion than the $As(1)O_4$ group. The $As(1)O_4$ group shares three of its edges with other polyhedra (one with an $Mg(1)O_6$ group and the other two with two $Mg(3)O_8$ groups), whereas none of the edges of the $As(2)O_4$ group are shared. The greater angular distortion in the $As(1)O_4$

Table (5-1)

Atomic parameters for $Mg_3(AsO_4)_2$

(Estimated standard deviations are in parentheses)

A: Positional parameters

Atom	Site Symmetry	Multiplicity	Fractional positional parameters		
			x	y	z
Mg(1)	2	1/2	0.243(1)	1/4	1/8
Mg(2)	2	1/2	0	0	0.2281(4)
Mg(3)	$\bar{4}$	1/8	0	0	1/2
As(1)	2	1/2	-0.3450(4)	1/4	1/8
As(2)	$\bar{4}$	1/4	0	0	0
01	1	1	0.054(2)	0.206(2)	0.0433(6)
02	1	1	0.495(2)	0.292(2)	0.1928(5)
03	1	1	0.230(2)	0.543(2)	0.1007(6)

Table (5-1) (continued)

B: Thermal parameters ($\mathring{A}^2$)

Atom	u_{11}	u_{22}	u_{33}	u_{12}	u_{13}	u_{23}
Mg(1)	0.004(3)	0.005(4)	0.010(3)	0	0	0.001(3)
Mg(2)	0.006(4)	0.005(4)	0.010(3)	-0.000(5)	0	0
Mg(3)	-0.00 (1)	u_{11}	0.011(8)	0	0	0
As(1)	0.003(1)	0.005(1)	0.010(1)	0	0	-0.001(1)
As(2)	0.001(2)	u_{11}	0.006(1)	0	0	0
O1	0.006(5)	0.001(6)	0.014(4)	-0.006(6)	-0.003(4)	0.003(4)
O2	0.007(4)	0.029(9)	0.006(4)	-0.002(8)	0.002(4)	-0.007(4)
O3	0.029(8)	0.001(5)	0.018(4)	0.003(9)	0.006(6)	0.000(4)

TABLE (5-2).

OBSERVED AND CALCULATED STRUCTURE FACTOR AMPLITUDES FOR $MG_3(ASO_4)_2$.

UNOBSERVED REFLECTIONS ARE INDICATED BY (*) AND UNRELIABLE REFLECTIONS BY ($).

K = 0

H	L		|FOBS|	|FCALC|
0	4		116	129
0	8		260	303
0	12		179	185
0	16		214	216
0	20		38	36
0	24		122	118
1	3		117	119
1	5		183	178
1	9		23	23
1	11		20	13
1	13		131	143
1	15		30	33
1	17	*	16	1
1	19		64	62
1	21		62	54
1	23	$	16	24
2	0	*	9	19
2	2		81	85
2	4	$	308	393
2	6		133	118
2	8		46	55
2	10		40	44
2	12		227	239
2	14		121	120
2	16		65	65
2	18		34	37
2	22		24	24
3	1		87	92
3	3		96	95
3	5		65	54
3	7		131	123
3	9		213	191
3	11		53	59
3	13		16	19
3	15		84	80
3	17		78	74
3	19		35	31
3	21		25	23
3	23		75	73
4	0		302	349
4	2		143	132
4	4		63	55
4	6		141	138
4	8		171	149
4	10		138	129
4	12	*	16	6
4	14		102	97
4	16		100	97
4	18		80	81
4	20		23	28
4	20		38	28
4	22		70	78
5	1		49	49
5	3		70	73
5	5		26	27
5	7		52	47
5	9		51	44
5	11	*	16	10
5	13		84	87
5	15		20	20
5	17		48	44
5	19		29	31
6	0		80	78
6	2		126	124
6	4		182	166
6	6		107	109
6	8		37	33
6	10		98	96
6	12		100	97
6	14		136	108
6	16		30	32
6	18		92	90
7	1		57	59
7	3		68	71
7	5		108	105
7	7		34	26
7	9		37	38
7	11		85	88
7	13		94	102
8	0		152	158
8	2		25	26
8	4	*	17	2
8	6		40	48
8	8		135	148
8	10		46	49
9	1		59	67

K = 1

H	L		|FOBS|	|FCALC|
0	25	*	17	16
1	6	$	143	173
1	10		110	109
1	14		108	111
1	18		114	101
1	22		95	102
2	1	$	150	189
2	3		104	116
2	5		53	59
2	7		83	99
2	9		136	154
2	11		100	97
2	13		77	70
2	15		92	90
2	17		125	123
2	19		41	41
2	21		48	48
2	23		57	61
3	0		10	17
3	2		57	54
3	4		83	84
3	6	$	79	54
3	8		97	96
3	10		97	95
3	12		65	56
3	14		95	97
3	16		78	73
3	18		95	97
3	20		74	70
3	22		69	69
3	24		39	37
4	1		38	40
4	3		97	101
4	5		141	152
4	7		56	50
4	9		85	81
4	11		23	29
4	13		124	122
4	15		44	38
4	17		57	53
4	19		69	69
4	21		65	60
4	23	$	19	26
5	0		158	182
5	2		73	58
5	4		127	136
5	6		88	76
5	8		113	114
5	10		87	78
5	12		117	116
5	14		92	94
5	16		89	79
5	18		74	72
5	20		60	64
5	22		79	84
5	24		60	62
6	1		93	85
6	3	*	15	10
6	5		56	54
6	7		47	43
6	9		105	104
6	11	*	16	19
6	13		27	33
6	15		38	40
6	17		73	76
6	19		18	20
6	21	*	16	13
7	0		51	48
7	2		41	42
7	4		68	64
7	6		57	48
7	8		77	72
7	10		78	78
7	12		67	60
7	14		70	71
7	16		63	62
7	18		68	70
7	20		57	63
8	1		51	49
8	3		75	69
8	5		85	76
8	7		54	56
8	9		35	39
8	11		70	65
8	13		81	81
8	15	$	31	38

K = 2

H	L		|FOBS|	|FCALC|
0	20		129	128
0	24		39	46
0	26		33	42
1	25		41	45
2	8	$	243	303
2	12		19	20
2	16		138	130
2	20		77	73
2	24		92	88
3	1		106	118
3	3		112	124
3	5		174	195
3	7		120	122
3	11		149	150
3	13		119	121
3	15		60	55
3	17		43	42
3	19		74	72
3	19		85	72
3	21		87	87
3	23		42	43
3	25		35	41
4	0		128	127
4	2		88	90
4	4		149	159
4	6		136	140
4	8		104	96
4	10		93	82
4	12		99	88
4	14		24	32
4	16		22	27
4	18		45	46
4	22		41	47
4	24		22	28
4	26		25	27
5	1		120	115
5	3		95	92
5	5		61	60
5	7		72	67
5	9		81	73
5	11		61	51
5	13		71	66
5	15		69	67
5	17		79	77
5	19		52	52
5	21		58	57
5	23		36	42
5	25		21	32
5	27		36	34
6	0		109	106
6	2		103	97
6	4		117	111
6	6		85	76
6	8		103	96
6	10		66	63
6	12		63	61
6	14		64	67
6	16		32	37
6	18		52	55
6	20	$	22	31
6	22		25	31
6	24		26	33
6	26		35	31
7	1		109	111
7	3		74	74
7	5		76	71
7	7		72	70
7	9		111	109
7	11		62	59
7	13		35	36
7	15		91	90
7	17		73	78
7	19		32	40
7	21	$	21	27
7	23		41	51
7	25		51	57
8	0		37	43
8	2	*	20	15
8	4		120	123
8	6	*	21	5
8	8		31	41
8	10		27	23
8	12		89	94
8	14	*	22	16
8	16	*	22	11
8	18	*	21	3
8	20		49	59
8	22	*	19	20

K = 3

H	L		|FOBS|	|FCALC|
0	25		77	73
1	26		48	52
3	10		97	98
3	14		103	101
3	18		114	110
3	22		67	67
4	7		102	113
4	9		127	141
4	11		58	51
4	13		50	43
4	15		75	69
4	17		98	88
4	19		46	45
4	21		24	22
4	23		69	69
4	25		61	64
5	0		95	98
5	2		120	137
5	4		68	66
5	6		113	112
5	8		50	47
5	10		122	122
5	12		54	57
5	14		123	118
5	16		19	24
5	18		107	101
5	20	*	17	17
5	22		96	95
6	1	*	13	12
6	3		92	86
6	5		111	111
6	7		40	38
6	9		48	48
6	11		81	76
6	13		89	83
6	15		46	42
6	17		17	23
6	19		55	53
6	21		77	72
6	23	*	14	9
7	0	*	15	8
7	2		97	95
7	4		21	26
7	6		93	91
7	8		16	22
7	10		72	74
7	12	*	17	5
7	14		78	77
7	16		19	22
7	18		79	84
8	1		90	89
8	3		56	60
8	5		23	27
8	7		83	79
8	9		89	87
8	11		49	52
8	13		31	33
8	15		61	64
8	17		67	69

Table (5-3)

Bond Distances and Angles in Mg$_3$As$_2$O$_8$

(Estimated standard deviations in parentheses)

	Distance(Å)	Angle (degrees)	
As(1)O$_4$ group			
As(1)-O2^{a}	1.71(1)	O2^{a}-As(1)-O2^{b}	100.9(8)
-O2^{b}	1.71(1)	O2^{a}-As(1)-O8^{c}	103.3(7)
-O3^{c}	1.67(1)	O2^{a}-As(1)-O3^{d}	111.4(7)
-O3^{d}	1.67(1)	O2^{b}-As(1)-O3^{c}	111.4(7)
		O2^{b}-As(1)-O3^{d}	103.3(7)
		O3^{c}-As(1)-O3^{d}	124.4(9)
As(2)O$_4$ group			
As(2)-O1^{a}	1.66(1)	O1^{a}-As(2)-O1^{d}	120.7(6)
-O1^{d}	1.66(1)	-As(2)-O1^{e}	104.2(6)
-O1^{e}	1.66(1)	-As(2)-O1^{f}	104.2(6)
-O1^{f}	1.66(1)	O1^{d}-As(2)-O1^{e}	104.2(6)
		As(2)-O1^{f}	104.2(6)
		O1^{e}-As(2)-O1^{f}	120.7(6)
Mg(1)O$_6$ group			
Mg(1)-O1^{a}	2.03(1)	O1^{a}-Mg(1)-O1^{b}	101.8(8)
-O1^{b}	2.03(1)	-Mg(1)-O2^{a}	166.7(8)
-O2^{a}	2.16(2)	-O2^{b}	91.5(3)
-O2^{b}	2.16(2)	-O3^{a}	86.9(6)
-O3^{a}	2.04(1)	-O3^{b}	90.1(6)
-O3^{b}	2.04(1)	O1^{b}-Mg(1)-O2^{a}	91.5(3)
		-O2^{b}	166.7(8)
		-O3^{a}	90.1(6)
		-O3^{b}	86.9(6)
		O2^{a}-Mg(1)-O2^{b}	75.2(7)
		-O3^{a}	92.2(7)
		-O3^{b}	91.5(7)
		O2^{b}-Mg(1)-O3^{a}	91.5(7)
		-O3^{b}	92.2(7)
		O3^{a}-Mg(1)-O3^{b}	175 (1)

continued ...

Table (continued)

Mg(2)O$_6$ group	Distance(Å)	Angle (degrees)	
Mg(2)-O2^{g}	2.06(1)	O2^{g}-Mg(2)-O1^{c}	92.2(6)
-O1^{c}	2.07(1)	-O2^{h}	86.6(7)
-O2^{h}	2.06(1)	-O3^{c}	90.3(5)
-O3^{c}	2.18(2)	-O1^{b}	104.3(6)
		OO3^{b}	172.7(6)
-O1^{b}	2.07(1)	O1^{c}-Mg(2)-O2^{h}	104.3(6)
-O3^{b}	2.18(2)	-O3^{c}	82.5(5)
		-O1^{b}	157.4(8)
		-O3^{b}	82.1(5)
		O2^{h}-Mg(2)-O3^{c}	172.7(6)
		-O1^{b}	92.2(6)
		-O3^{b}	90.3(5)
		O3^{c}-Mg(2)-O1^{b}	82.1(5)
		-O3^{b}	93.5(7)
		O1^{b}-Mg(2)-O3^{b}	82.5(5)

Mg(3)O$_8$ group	Distance	Angles (degrees)			
Mg(3)-O2^{i}	2.66(2)	O3^{i}-Mg(3)-O2^{j}	75.0(4)	O2^{k}-Mg(3)-O3^{h}	75.0(5)
-O2^{j}	2.26(2)	-O3^{g}	121.0(4)	-O2^{l}	122.6(4)
-O3^{g}	2.66(2)	-O2^{k}	161.7(4)	-O2^{m}	103.3(6)
-O2^{k}	2.26(2)	-O3^{h}	121.0(4)	-O3^{n}	75.0(4)
-O3^{h}	2.66(2)	-O2^{l}	75.0(4)	O3^{h}-Mg(3)-O2^{l}	64.5(5)
-O2^{l}	2.26(2)	-O2^{m}	64.5(5)	-O2^{m}	161.7(4)
-O2^{m}	2.26(2)	-O3^{n}	88.3(5)	-O3^{n}	121.0(4)
-O3^{n}	2.66(2)			O2^{l}-Mg(3)-O2^{m}	103.3(6)
		O2^{j}-Mg(3)-O3^{g}	161.7(4)	-O3^{n}	161.7(4)
		-O2^{k}	103.3(6)	O2^{m}-Mg(3)-O3^{n}	75.0(4)
		-O3^{h}	75.0(4)		
		-O2^{l}	103.3(6)		
		-O2^{m}	122.6(4)		
		-O3^{n}	64.5(5)		
		O3^{g}-Mg(3)-O2^{k}	64.5(5)		
		-O3^{h}	88.3(4)		
		-O2^{l}	75.0(5)		
		-O2^{m}	75.0(4)		
		-O3^{n}	121.0(5)		

continued ....

Table (continued)

Atom Transformations

a: x, y, z
b: x, 1/2-y, 1/4-z
c: -x, 1/2 + y, 1/4 - z
d: -x, -y, z
e: -y, x, -z
f: y, -x, -z
g: 1/2 + y, 1/2 - x, 1/2 - z
h: 1/2-y, 1/2 + x, 1/2 - z
i: 1/2 + x, 1/2 _ y, 1/2 + z
j: 1/2 + x, - y, 3/4 - z
k: y, 1/2 + x, 1/4 + z
l: -y, 1/2 - x, 1/4 + z
m: 1/2 - x, y, 3/4 - z
n: 1/2 - x, 1/2 - y, 1/2 + z

group might be a consequence of the electrostatic repulsion between the As^{+5} ion and the Mg^{+2} ions sharing common edges.

Two of the three independent magnesium atoms in the unit cell have octahedral coordination while the third magnesium atom is coordinated to 8 oxygen atoms in a distorted cubic arrangement. The average Mg(1)-O and Mg(2)-O distances with the magnesium in octahedral coordination are 2.08(1) Å and 2.10(1) Å respectively. These are not significantly different from each other and are in agreement with other octahedrally coordinated magnesium-oxygen distances. Both the $Mg(1)O_6$ and $Mg(2)O_6$ polyhedra deviate significantly from the ideal octahedral arrangement, and the distances range from 2.03(1) Å to 2.16(1) Å in the former and from 2.06(1) Å to 2.16(1) Å in the latter, while the angles range from 75.2(7)° to 101.8(8)° in the former and from 82.1(5)° to 104.3(6)° in the latter. The large distortions are expected as a consequence of five of the edges of $Mg(1)O_6$ group and four of $Mg(2)O_6$ group being shared with other polyhedra in the structure.

The $Mg(3)O_8$ group is a highly distorted cube, with 4 oxygen atoms at 2.26(2) Å away from the central Mg(3) atom, and the remaining four at 2.66(2) Å. (The Mg(3) atom is at a site of $\bar{4}$ symmetry). The angles subtended by the face-diagonal oxygen atoms at Mg(3) vary from 88.3(5)° to 122.6(4)°, and those subtended by the oxygen atoms forming edges of the cube vary from 64.5(5)° to 75.0(4)°, compared to 109.47° and

70.53° in an ideal cubic arrangement. The high distortion is consistent with sharing of all the 12 edges of the $Mg(3)O_8$ polyhedron, four of these being shared with four arsenic atoms, and the remaining eight with Mg(1) and Mg(2) atoms.

There is only one other structure reported in the literature with magnesium in eight-fold coordination, that of $Mg_2Al_2Si_3O_{12}$(45). The MgO_8 group in this structure also shows significant distortions from an ideal cubic arrangement, and has four Mg-O bonds of length 2.198(2) Å and the remaining four of 2.343(2) Å. The site symmetry of this magnesium atom is $\bar{4}$, as in the case of Mg(3) site in magnesium orthoarsenate. Six of the 12 edges of the MgO_8 group in $Mg_3Al_2Si_3O_{12}$ are shared with AlO_6 octahedra and SiO_4 tetrahedra.

The average Mg(3)-O distance of 2.46(2) Å in $Mg_3(AsO_4)_2$ is rather large compared to the distance of 2.270(2) Å in $Mg_3Al_2Si_3O_{12}$(45). Since the other cation-oxygen distances in the present structure are in agreement with the expected values, the large deviation in the Mg(3)-O distance is not easily explained.

Discussion: The powder pattern of the compound $3MgO.As_2O_5$ was reported by Travnicek et al.(16) in 1952, Ide et al.(17) in 1962, and by Robijn(8) in 1967. Robijn claimed to have indexed the powder pattern on the basis of a hexagonal cell with $\underline{a}_1$ = 10.5 Å, $\underline{a}_3$ = 19.1 Å. Unfortunately the tabulated d-values for magnesium orthoarsenate listed in his paper (Table II of

Ref. (8)), do not correspond to the diffraction spectrum presented in the same paper (Fig. 5B, ibid), and labelled as the 'diffraction spectrum of the magnesium arsenate of unknown composition', though at a later stage in the same reference the magnesium arsenate of unknown composition has been identified as magnesium orthoarsenate. Thus the reason for the disagreement between the spectrum and the table of d-values is not clear. Since the present single crystal study shows the symmetry to be tetragonal, at variance with Robijn's assignment of hexagonal symmetry, the d-spacings for magnesium orthoarsenate corresponding to the diffraction spectrum given in Robijn's paper were recalcualted. Since the diagram of the spectrum had been reduced from a photographic reproduction, it was possible to measure the intensities and 2θ values with fair accuracy by counting the number of grains from the figure under a binocular microscope. The values of both the d-spacings and intensities thus measured, while significantly different from the values listed in the table in the paper, agree very well with the powder patterns reported by Travnicek et al.(16), Ide et al.(17), and our own data from the single crystal study. These values are listed for comparison in Table (5-4). Thus it seems that the hexagonal cell assigned for $Mg_3(AsO_4)_2$ by Robijn is incorrect, and his compound is the same as the tetragonal $Mg_3(AsO_4)_2$ described here.

TABLE (5-4).

COMPARISON OF d- SPACINGS FOR $Mg_3(AsO_4)_2$.

Present work					Travnicek et al.		Ide et al.		Robijn	
h	k	l	$d^{\#}_{calc}$	I	d	I	d	I	d	I
0	0	4	4.74	2.6	4.74	18	4.76	32	4.70	29
1	0	3	4.63	10.7	4.58	34	4.63	48	4.53	65
1	1	2	4.28	12.2	4.24	36	4.29	43	4.20	43
									3.75	5
2	0	0	3.39	$u^{\dagger}$						
1	0	5	3.31	26.0	3.30	41	3.33	48	3.23	90
2	0	2	3.20	5.2	3.18	9	3.21	19	3.17	6
							3.13	19		
							3.06	8		
2	1	1	3.00	35.1	2.99	67	3.02	69	2.95	90
2	0	4	2.76	73.8	2.76	100	2.77	100	2.68	100
2	1	3	2.74	17.0			2.75	28		
1	1	6	2.64	16.0	2.63	28	2.65	32	2.60	46
0	1	7	2.52	$u^{\dagger}$			2.56	6		
2	2	0	2.40	5.0	2.37	19			2.36	24
0	0	8	2.37	13.2						
2	1	5	2.37	4.4						
0	2	6	2.31	13.9	2.31	11			2.30	15
3	0	1	2.25	6.0	2.24	4			2.24	7
3	1	0	2.146	0.1	2.13	4			2.13	5
2	2	4	2.141	3.6						
3	0	3	2.130	7.3						

Continued....

(TABLE (5-4) Continued)

Present work					Travnicek et al.		Ide et al.		Robijn	
h	k	ℓ	$d_{calc}^{\#}$	I	d	I	d	I	d	I
3	1	2	2.093	5.1	2.08	3			2.08	3
2	1	7	2.022	10.9	2.02	8			2.01	10
1	0	9	2.013	0.4						
3	1	4	1.95	10.8	1.95	8			1.95	10
2	0	8	1.944	1.7						
3	0	5	1.943	3.4						
3	2	1	1.873	18.9	1.87	12			1.87	13
3	2	3	1.804	21.0	1.80	11			1.80	22
3	1	6	1.776	9.8	1.77	5			1.76	5
1	1	10	1.764	9.4						
3	0	7	1.737	13.5	1.73	19			1.73	20
2	1	9	1.731	29.1						
0	4	0	1.697	35.5						
2	2	8	1.687	49.5	1.68	51			1.68	41
3	2	5	1.686	50.5						
0	1	11	1.667	0.3						
4	0	2	1.671	16.0						
2	0	10	1.656	1.3						
4	1	1	1.640	2.4						
4	0	4	1.598	3.1						
4	1	3	1.593	15.1					1.59	16
3	1	8	1.591	14.9						

#d_{calc} refers to the calculated d- spacings based on the unit cell dimensions determined in the present work.

†u refers to unobserved reflections.

The possibility that the compound might exist over a range of compositions has been suggested by Robijn$^{(8)}$ on the basis of a variation in the MgO contents as obtained in four separate determinations on the same $Mg_3(AsO_4)_2$ sample. The values for the molar ratio of MgO to As_2O_5 obtained were 3.06, 3.11, 3.06 and 3.45 respectively in the four determinations, compared to the theoretically expected value of 3.00 in the stoichiometric composition $3MgO.As_2O_5$. The errors in the determinations are not reported, and it is found that three of the four determinations agree to within 3% with each other and with the expected value for the stoichiometric compound. The present single crystal study indicates that the composition of the crystal that was used in data collection does not differ significantly from the stoichiometric composition. Only a systematic study of the compositions of a number of different samples of the magnesium orthoarsenates can clearly establish whether there is in fact a range of stable compositions for this compound. The situation is thus analogous to that in the case of $Co_{24.2}As_9O_{48}$ (Ch. 4). The present investigation, however, has established that there are features in the structure which justify the speculation that a range of stable compositions might exist for this compound with the same structure as that of $Mg_3(AsO_4)_2$ described here. Since the Mg(3) site in this structure is only half occupied, one can in principle introduce two more magnesium atoms in the unit cell by populating this site fully, while partially emptying the arsenic sites so that charge neutrality is maintained. If the suggested range of stable compositions does exist, one can speculate on the basis of the present structure that the magnesium-rich end of the stable range will have the composition $Mg_{20}As_{11.2}O_{48}$ (corresponding to complete occupancy of all three magnesium sites), and the arsenic-rich end will have the composition $Mg_{18}As_{12}O_{48}$ (corresponding to complete occupancy of both the arsenic sites).

The analogous isostructural cobalt arsenate provides the first case of Co^{+2} in eight-fold coordination. Since the ionic radii of Co^{+2} and Mg^{+2} are very nearly equal (octahedral radii of 0.74 and 0.72 Å respectively(1)), it is reasonable to expect the average Co-O bond distance in the distorted cubic coordination of oxygen atoms to be about 2.5 Å. In addition to the cobalt compound being of interest from the fact that this is the first case with eight-fold coordination for cobalt, a study of the magnetic properties of Co^{+2} in eight-fold coordination will also be of interest.

The common features and differences between the monoclinic form of $Co_3(AsO_4)_2$, (Ch.3) and the tetragonal form isostructural with the $Mg_3(AsO_4)_2$, will be dealt with in detail in the concluding chapter.

CHAPTER 6

CRYSTAL STRUCTURE OF COBALT DIARSENATE

Preparation and preliminary investigations: The cobalt diarsenate was prepared by precipitation from $Na_4As_2O_7$ and $CoC\ell_2$. The resulting $Co_2As_2O_7$ was filtered and after washing several times with distilled water to remove all traces of $NaC\ell$, the precipitate was heated to about 1150°C. (past the melting point) and slowly cooled.

The crystals obtained from the cooled melt were needle-shaped in appearance. A single crystal was mounted such that the longest dimension of the crystal paralleled the axis of the goniometer head. The rotation axis length as measured from a rotation photograph was about 5.1 Å. The zero-level Weissenberg photograph with this as the rotation axis was nearly superimposable with the $hk\ell$ photograph of $\beta\text{-}Mg_2As_2O_7$ (14). This has the thortveitite structure (46) with monoclinic symmetry. Since many of the phosphate analogs of thortveitite also had other polymorphic phases related to thortveitite, additional photographs of the present crystal were obtained to ascertain its detailed structural relation to thortveitite. It was found that while a set of axes comparable to those of thortveitite (46) could be chosen for the present crystal, the α^* and γ^* angles were slightly different from 90°, and the intensities showed significant violations of the requirements of monoclinic system, and thus the symmetry is triclinic.

A unit cell with axes nearly parallel to those of thortveitite(46) was chosen for $Co_2As_2O_7$, and the diffraction pattern was indexed. The only systematic absences observed were reflections with $(h+k) \neq 2n$. The space group possibilities consistent with these observations are C1 and $C\bar{1}$. The choice of a non-primitive C-centred unit cell was preferred over choice of a primitive unit cell with the conventional triclinic space group P1 or $P\bar{1}$, since the former choice would enable an easier comparison of the present structure with the thortveitite-type structures with space group C2/m of the monoclinic system.

The reciprocal unit cell dimensions of $Co_2As_2O_7$ were measured from uncalibrated (hk0) and (h0ℓ) precession photographs and an uncalibrated (0kℓ) Weissenberg photograph, all obtained with Mo Kα radiation. The real lattice parameters computed from the measured reciprocal dimensions are: a_1 = 6.60 Å, a_2 = 8.53 Å, a_3 = 4.75 Å, $\alpha = 90.5°$, $\beta = 103.1°$, $\gamma = 91.1°$. Since these values have been derived from measurements on uncalibrated films, it is not possible to assess the accuracy of these parameters. However, it may be pointed out that the lengths of the three axes are self-consistent to within about 0.01 Å, and the three interaxial angles to within about 0.1°.

The density was measured using the pycnometer method(43) and was found to be 5.0(1) g.cm.$^{-3}$. This is in good agreement with the calculated density of 4.91 g.cm.$^{-3}$ with 2 molecules of $Co_2As_2O_7$ per unit cell.

Intensity data of the type $hn\ell$ $(n = 0,1,2)$, and hkm $(m = 0,1)$ were obtained from integrated precession photographs obtained with Mo Kα radiation and measured using a Joyce-Loebl microdensitometer. It was not possible to collect further data since the crystal was lost at this stage. Repeated attempts at selecting further crystals from the above preparation yielded only double crystals misoriented by about 4°. While the diffraction patterns from the first crystal did have a few stray spots which could not be indexed on the basis of the unit cell with $C1$ or $C\bar{1}$ symmetry described above, thorough examination of the $hn\ell$ $(n = 0,1,2)$ patterns indicates that these stray spots must have arisen from randomly oriented crystallites adhering to the body of the single crystal. It is not clear why several attempts at choosing another single crystal from the sample were unsuccessful, as were attempts at preparing fresh undoubled crystals, though the first crystal chosen seems to have been suitable for intensity data collection. Thus only the 413 independent reflections collected from the first crystal were used, of which 93 were considered below the observable limit.

The intensities were corrected for Lorentz and polarization effects. The crystal used for data collection had approximate dimensions 0.1 × 0.1 × 0.2 mm^3, and could be assumed to be a cylinder for purposes of absorption correction. However, the orientation of the crystal with respect to the incident beam did not correspond to any of the simple cases(47) for which tabulated absorption correction values are already available. Therefore no absorption corrections were applied in the preliminary stages to the rather limited data collected in the present studies. The linear absorption coefficient for Mo Kα radiation in $Co_2As_2O_7$ is 201.7 cm^{-1}, and the data collected ranged in Bragg angles (θ) from about 5° to about 40°, and the absorption corrections are expected to be significant.

Structure Solution: Since the similarity in cell dimensions and intensity distribution in analogous photographs of $Co_2As_2O_7$ and $Mg_2As_2O_7$ indicated that the structure of the former will be similar to that of $Mg_2As_2O_7$, the refined parameters of the latter(14) were used as the trial structure for $Co_2As_2O_7$. The refinement was carried out initially assuming the centrosymmetric space group $C\bar{1}$ to be the correct one, though in later stages a few models were attempted in the lower symmetry space group also, in an attempt to choose the correct space group. Individual scale constants for the 5 layers of data collected, the positional parameters of all atoms (except those of oxygen atom O1 (Table 6-1a) fixed at (0,0,0) by symmetry), and individual isotropic thermal factors of all the atoms, were refined for a few cycles using the 413 reflections that had been measured. After a few cycles, the isotropic thermal parameters of all the atoms were converted to anisotropic factors and refined along with the positional parameters of the atoms. A weighting scheme was chosen such that $w = (11.6)^{-1}$ for $|F_{obs}| < 50.0$, and $w = (0.432 |F_{obs}| - 10.8)^{-1}$ for $F_{obs} \geq 50.0$. Refinement was continued until the shifts in the parameters were insignificant compared to the e.s.d.'s in these parameters. With a total of 56 parameters, the minimum was reached at the R_1-value of 0.077 and the weighted R_w-value of 0.078 for all reflections. While the agreement between observed and calculated structure factor amplitudes was quite good, the anisotropic thermal parameters of the bridging oxygen atom, 01, of the As-O-As linkage, located at the centre of symmetry, were anomalously large (Table 6-1b), suggesting that this oxygen atom is disordered, or as an alternative, that the true space group should be the lower symmetry group C1. In the latter case the bridging oxygen atom need not be restricted to the centre of symmetry. A few models with this oxygen atom displaced from the centre of symmetry in the directions suggested by the components of the anisotropic thermal factor for this atom were refined in space group C1, and these did not lead to better agreement than the $C\bar{1}$ model.

The final positional and thermal parameters resulting from refinement in the centrosymmetric space group $C\bar{1}$ are listed in Tables (6-1a) and (6-1b) respectively. The observed and calculated structure factors are compared in Table (6-2). The more important bond distances and angles in the structure are listed in Table (6-3). The positional coordinates and bond geometry in $Mg_2As_2O_7$ (14) are included in Tables (6-1a) and (6-3) respectively, for comparison.

Description of the structure:

The major structural features of $Co_2As_2O_7$ are similar to those of $Mg_2As_2O_7$ (14), and are reviewed here for comparison. The structure can be described as consisting of layers of oxygen atoms lying very nearly parallel to the $\underline{a}_1\underline{a}_2$ plane at intervals of $\frac{1}{2}\underline{a}3$ in the $\underline{a}_3$ direction, the atoms in any two adjacent layers being held together by either cobalt atoms or As-O-As groups alternately. The situation is illustrated in Fig. (6-1), where the structure is shown projected down the $\underline{a}_1$ axis. Bonding between two oxygen atom layers through the As-O-As groups results in double layers of oxygen atoms containing discrete As_2O_7 groups. Consecutive double layers are held together by cobalt atoms lying nearly in a plane parallel to the double layers and roughly half way between them.

The As_2O_7 group in the structure consists of corner-shared AsO_4 tetrahedra, with the bridging oxygen atom, 01, lying 1.66(1) Å from arsenic. The three terminal As-O bond lengths are 1.66(1), 1.66(2), and 1.70(2) Å. The average

Table (6-1a)[†]

Atomic positional parameters in $Co_2As_2O_7$ compared with those in $Mg_2As_2O_7$. (The latter are enclosed in [ ] brackets).

Atom	x	y	z
Co	0.4910(4)	0.1895(3)	0.5112(6)
[Mg]	[½]	[0.1881(5)]	[½]
As	0.2267(3)	-0.0001(3)	0.9060(4)
[As]	[0.2285(2)]	[0]	[0.9031(3)]
01	0	0	0
[01]	[0]	[0]	[0]
02	0.393 (2)	0.003 (2)	0.226 (3)
[02]	[0.400 (1)]	[0]	[0.221 (2)]
031	0.234 (2)	0.161 (2)	0.714 (3)
[03]	[0.231 (1)]	[0.165 (1)]	[0.716 (2)]
032	0.238 (3)	0.835 (2)	0.706 (5)
[03]	[0.231 (1)]	[0.835 (1)]	[0.716 (2)]

[†] Estimated standard deviations are in parentheses.

Table (6-1b)

Thermal parameters§ (in $\mathring{A}^2$) of atoms in $Co_2As_2O_7$

(Estimated standard deviations are in parentheses).

Atom	u_{11}	u_{22}	u_{33}	u_{12}	u_{13}	u_{23}
Co	0.027 (1)	0.016(2)	0.017 (1)	-0.003 (1)	-0.008 (1)	0.001(2)
As	0.0143(8)	0.026(1)	0.0122(9)	-0.0057(7)	-0.0025(5)	0.010(1)
01	0.05 (2)	0.33 (8)	0.20 (5)	0.01 (3)	0.06 (3)	0.19 (7)
02	0.029 (6)	0.012(7)	0.018 (6)	0.009 (5)	0.011 (5)	0.001(9)
031	0.035 (7)	0.019(8)	0.006 (5)	0.014 (6)	0.006 (5)	0.003(9)
032	0.07 (1)	0.04 (1)	0.04 (1)	-0.017 (9)	-0.02 (1)	0.01 (1)

---

§The values of u_{ij} have been obtained from the expression $\beta_{ij} = 2\pi^2 \underline{b}_i \underline{b}_j u_{ij}$ where the β_{ij}'s appear as a thermal effect through $\exp[-(\beta_{11}h^2+2\beta_{12}hk+\ldots)]$ in the structure factor expression, and $\underline{b}_i$ are the reciprocal lattice vectors.

TABLE (6-2).

OBSERVED AND CALCULATED STRUCTURE FACTOR AMPLITUDES FOR $Co_2As_2S_7$.

UNOBSERVED REFLECTIONS ARE INDICATED BY (*) AND UNRELIABLE REFLECTIONS BY ($).

H	L		|FOBS|	|FCALC|
				K = 0
[illegible]	[illegible]	[illegible]	[illegible]	[illegible]
				K = 1
[illegible]	[illegible]	[illegible]	[illegible]	[illegible]
				K = 2
[illegible]	[illegible]	[illegible]	[illegible]	[illegible]

H	K		|FOBS|	|FCALC|
[illegible]	[illegible]	[illegible]	[illegible]	[illegible]
				L = 0
[illegible]	[illegible]	[illegible]	[illegible]	[illegible]
				L = 1
[illegible]	[illegible]	[illegible]	[illegible]	[illegible]

Table (6-3)[†]

Bonding geometry in $Co_2As_2O_7$ compared with that in $Mg_2As_2O_7$

	Coordination no. of oxygen atom	$Co_2As_2O_7$	$Mg_2As_2O_7$[§]
As_2O_7 group:			
Distances			
As-01(a)	2	1.66(1)Å	1.671(1)Å
-02(a)	3	1.66(1)Å	1.653(5)Å
-031(a)	3	1.66(2)Å	1.661(7)Å
-032(a)	3	1.70(2)Å	1.661(7)Å
Angles			
01(a)-As-02(a)		101.7(6)	102.1(3)
01(a)-As-031(a)		106.0(5)	105.8(3)
01(a)-As-032(a)		108.7(8)	105.8(3)
031(a)-As-02(a)		114.3(7)	113.2(3)
031(a)-As-032(a)		116.9(9)	115.2(3)
032(a)-As-02(a)		113.7(9)	113.2(3)
MO_6 group (M=Co or Mg):			
Distances			
M-032(b)	3	2.07(2)	2.046(7)
-02(a)	3	2.07(1)	2.080(8)
-031(b')	3	2.08(1)	2.046(7)
-02(a')	3	2.12(1)	2.080(8)
-031(a)	3	2.14(2)	2.252(8)
-032(a')	3	2.27(2)	2.252(8)

Table (6-3) continued)

	Coordination no. of oxygen atom	$Co_2As_2O_7$	$Mg_2As_2O_7$
MO_6 group (M=Co or Mg): (continued)			
Angles			
O2(a)-M-O32(b)		145.8(9)	150.9(3)
O31(b')-M-O2(a')		156.5(7)	150.9(3)
O31(a)-M-O32(a')		168.3(8)	169.8(3)
O32(b)-M-O32(a')		69.0(8)	73.4(3)
O31(a)-M-O31(b')		75.5(5)	73.4(3)
O2(a)-M-O2(a')		78.5(5)	79.2(3)
O2(a)-M-O32(a')		77.7(6)	78.8(3)
O31(a)-M-O2(a')		82.7(6)	78.8(3)
O32(b)-M-O2(a')		92.9(7)	94.1(3)
O2(a)-M-O31(b')		93.5(5)	94.1(3)
O2(a')-M-O32(a')		88.4(7)	93.3(3)
O2(a)-M-O31(a)		93.2(6)	93.3(3)
O32(b)-M-O31(b')		105.2(7)	104.4(3)
O31(b')-M-O32(a')		111.9(7)	113.3(3)
O31(a)-M-O32(b)		118.8(8)	113.3(3)

[†] symmetry transformations:
a: (x,y,z); a': $(\bar{x},\bar{y},\bar{z})$; b: $(\frac{1}{2}+x, \frac{1}{2}+y, z)$; b' : $(\frac{1}{2}-x, \frac{1}{2}-y, -z)$

[§] In the case of $Mg_2As_2O_7$, the positions O31(a) and O32(a) in the present notation refer to symmetry-related positions of the same atom, [O3] in table (6-1a), and are related to each other by a mirror plane parallel to the yz plane and passing through the origin.

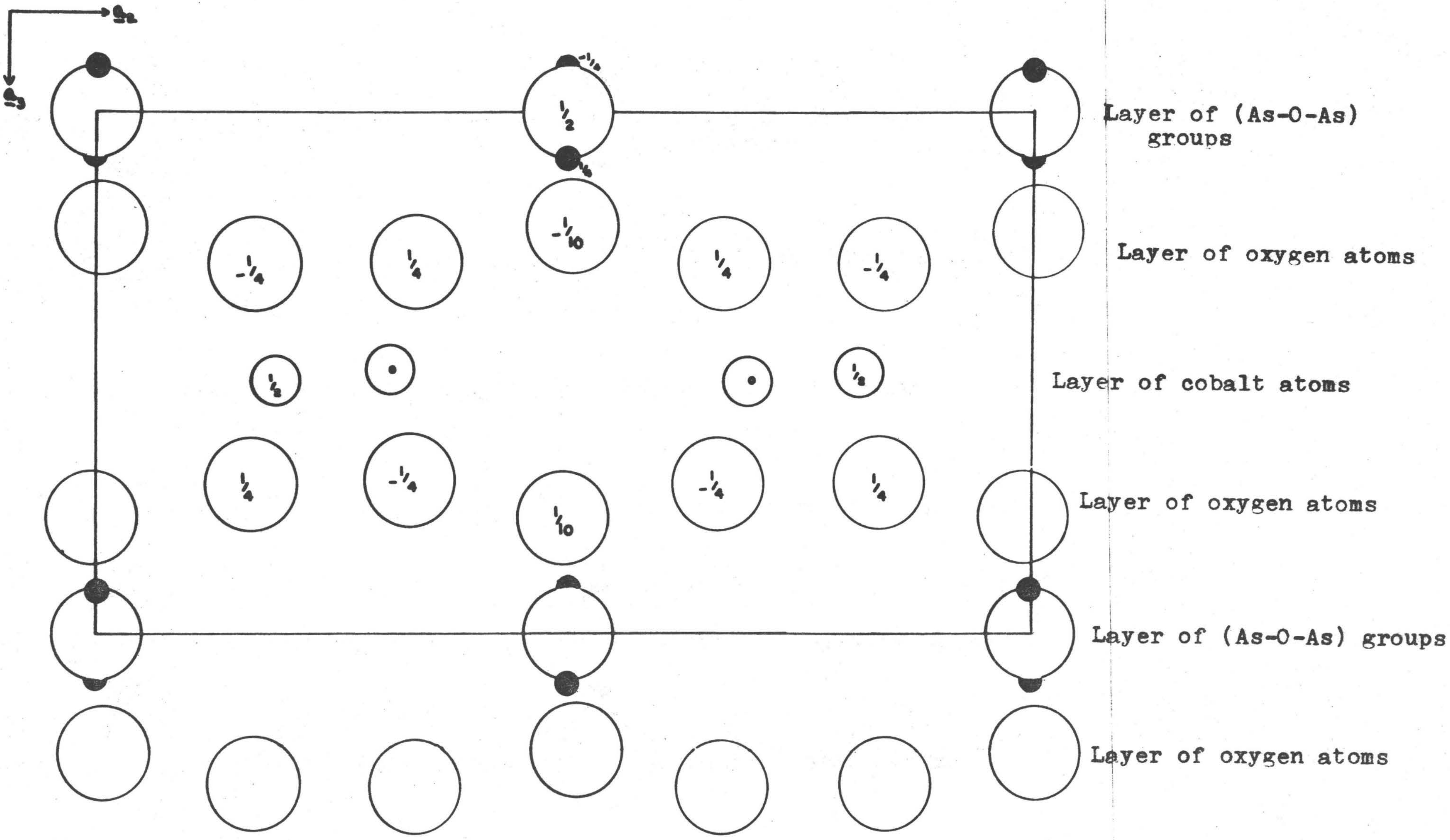

Figure (6-1). The structure of $Co_2As_2O_7$ projected down the $\underline{a}_1$ axis.

terminal As-O bond length is 1.67(2) Å, and is not significantly different from the bridging As-O bond length of 1.66(1) Å. It is expected(48,49) that the bridging X-O bond in the X_2O_7 group (X=P, As, V) should be significantly longer than the terminal X-O bonds, and is found to be the case in a number of pyrophosphates(50,51,52,53) having the thortveitite structure. The values of 1.66(1) and 1.67(2) Å for the As-O (bridging) and As-O (terminal) bonds respectively in $Co_2As_2O_7$ are uncorrected for thermal motion. In view of the large vibration of the bridging oxygen atom mainly in the $\underline{a}_2\underline{a}_3$ plane (very nearly perpendicular to the As-O-As vector), correction of the order of 0.15 Å could be applied to the bridging As-O bond length, compared to relatively insignificant corrections for the terminal As-O bond lengths. These corrections will place the bridging and terminal bond lengths in the present case more in line with the other members of the thortveitite series.

In previous determinations of the thortveitite-type structures of pyrophosphates(50,51,52,53), it has been noticed that the terminal O-P-O angles in the P_2O_7 group are larger than the ideal tetrahedral angle, whereas the O-P-O angles which involve the bridging oxygen atom are smaller, and the phosphorous atom appeared to be displaced from the centre of its tetrahedron towards the terminal oxygen atoms. The angles of the As_2O_7 group in $Co_2As_2O_7$ and $Mg_2As_2O_7$ (Table 6-3) are in agreement with this general feature found in thortveitite-type structures.

There is one crystallographically independent cobalt atom in the present structure, and this has a distorted octahedral coordination of oxygen atoms. The average Co-O bond length is 2.13(2) Å and is in good agreement with the values obtained in the other cobalt arsenates. The individual bonds vary from 2.07(2) Å to 2.27(2) Å, and the angles subtended by adjacent oxygen atoms at the cation range from 69.0(8)° to 118.8(8)°, whereas those subtended by oxygen atoms on opposite sides of the cation range from 145.8(9)° to 168.3(8)° and thus deviate substantially from the ideal angle of 180°. The octahedron around cobalt is thus very distorted. The cause of the distortion is understood through the alternate description of the structure as consisting of double layers of roughly close-packed oxygen atoms parallel to the $\underline{a}_1\underline{a}_2$ plane, with the Co^{+2} ions occupying octahedral voids in the double layer, adjacent double layers being held together by As-O-As groups lying between them. The bridging oxygen atom of the As-O-As group occupies an octahedral void between the double layers which it connects. Since in an ideal closest-packed arrangement of oxygen ions the species that can be accommodated in the octahedral void can have a maximum radius of 0.58 Å (Ch. 2), placing the bridging oxygen with the ionic radius of about 1.4 Å in the octahedral void causes a very large distortion of the closest-packed arrangement. This distortion is reflected in the large deviation from ideality in the angles of the CoO_6 group.

However, the variations in the individual Co-O bond lengths (Table 6-3) in the CoO_6 group are difficult to explain. Each of the six oxygen atoms involved in the six Co-O bonds has the same cation coordination (Table 6-3), and is strongly bonded to one arsenic and two cobalt atoms. There is thus no correlation between the observed Co-O bond length and the coordination number of the oxygen atom involved in the bond, contrary to expectations based on considerations of ionic radii(1). Baur(49) has investigated the packing systematics in a large number of borates, silicates, phosphates and sulphates, and has speculated that in structures containing more than one cation in different formal oxidation states, the distortions from ideality in the coordination polyhedron of the cation with the highest oxidation state (forming the strongest bonds to the anions) will predominantly influence the distortions in the coordination polyhedra of the cations with lower oxidation states (forming weaker bonds to the anions). On the basis of Baur's observations, in the present structure one might expect that the length of the Co-O bond involving a given oxygen atom should be correlated to the As-O bond length involving the same oxygen atom, and thus long Co-O bonds should correlate with short As-0 bonds, and vice versa. The mean Co-02, Co-031 and Co-032 distances in the present structure are 2.10(1), 2.11(1) and 2.17(2) Å, whereas the As-02, As-031 and As-032 distances are 1.66(1), 1.66(2) and 1.70(2) Å respectively, and no correlation is observed between short As-0 and long Co-0 bonds, and vice versa. Thus, the postulate that the distortions in the arrangement of the anions around the higher-valent cation predominantly influence the distortions around the lower-valent cations, does not account for the observed distortions in the CoO_6 group in the present structure.

Discussion: The final parameters of the structure listed in Tables (6-1a) and (6-1b) are from the refinement with the bridging oxygen atom 01 located at the centre of symmetry. While the anomalous thermal factors for this atom indicate disorder of this atom, there is no indication as to the nature of the disorder, which could be positional, vibrational or rotational. This feature is common to all thortveitite structures studied to date(54). However, only in the case of β-$Cu_2P_2O_7$ it has been possible to conclude that the disorder is positional(53), with the oxygen atom perhaps lying in a potential well with a double minimum. Suggestions have been made of a possible rotational disorder in $Mg_2As_2O_7$ with potential wells every 60°(14), even though the quality of the data in this case was not good enough to clearly distinguish between this and the other possibilities such as the one in β-$Cu_2P_2O_7$(53). In the thortveitite-type structures (with C2/m symmetry) a postulation of a double potential well restricts the oxygen atom to either a position on the 2-fold axis or on the mirror plane. In an analogous situation in the case of $Co_2As_2O_7$ the oxygen atom could occupy a general position and its centrosymmetrically related position with equal probability, since the restriction imposed by the 2/m symmetry at the origin in thortveitite structures is not present in $Co_2As_2O_7$, which has only $\bar{1}$ symmetry at the origin. In order to test whether the disorder in $Co_2As_2O_7$ corresponded to this situation, refinement of the structure in $C\bar{1}$ space group was carried out with the bridging oxygen atom being allowed to randomly occupy one of two equally probable positions related by the centre of symmetry at the origin. This model with anisotropic thermal parameters for all atoms including the bridging oxygen atom had 59 parameters and resulted in a minimum at the weighted R_w-value of 0.077. This represents an improvement in agreement at the 5% significance level(44) over the refinement with the oxygen atom restricted to the origin, which resulted in a minimum at the R_w-value of 0.078 with 56 parameters. The oxygen atom 01 in this double well potential model was found to be displaced by 0.43 Å from the origin, with the refined atomic coordinates at (x = -0.021(6), y = -0.03(1), z = -0.075(7)). However, the anisotropic thermal parameters of this oxygen atom were still anomalous, with a large component in the $\underline{a}_2$ direction, corresponding to an amplitude of vibration of about 0.5 Å. Thus while Hamilton's significance test(44) indicates an improvement (at the 5% significance level) in agreement for the double well potential model, the thermal parameters indicate that this model does not completely represent the true situation in the structure. Other models such as the rotational disorder model with potential wells every 60°(14) have not been tried. The nature of the disorder of the bridging oxygen atom in $Co_2As_2O_7$ is thus to be considered a still open question.

Isostructures of the mineral thortveitite, $(Sc,Y)_2Si_2O_7$, are found commonly among systems containing cations having radii less than about 1.0 Å and anions consisting of corner-shared tetrahedral groups. The diphosphates of magnesium(50), nickel(51), zinc(52), copper(53), manganese(55), and cobalt(56), the diarsenates of magnesium(14), zinc and cadmium(56), and the divanadates of manganese(57) and cadmium(54) are known to have this structure for one of their modifications, called the β-form, with space group C2/m, and cell dimensions close to those of thortveitite, $\underline{a}_1 = 6.54$ Å, $\underline{a}_2 = 8.59$ Å, $\underline{a}_3 = 4.67$ Å, $\beta = 102.5°$. Each of the diphosphates listed above, except that of manganese, has a lower temperature modification, called the α-form(58-62). While the α-forms of the different diphosphates are not all isostructural, they are closely related to the β-form, and thus to each other. The β-form has the characteristic feature that the P-O-P linkage of the (P_2O_7) group appears to be linear because of disorder of the bridging oxygen atom, indicated by the anomalously large temperature factor for this particular oxygen atom in all these structures. The lower-temperature α-modifications, on the other hand, have P-O-P bonds which deviate widely from linearity, the P-O-P angle being 157° in α-$Cu_2P_2O_7$(58), 144.1° in α-$Mg_2P_2O_7$(59), 142.6° in α-$Co_2P_2O_7$(60), 137° in α-$Ni_2P_2O_7$(61), and 139° and 148° for the two independent P atoms in α-$Zn_2P_2O_7$(62). The α-forms have also the common feature that the $\underline{a}_3$ axis is roughly double that in the β-form, with a c-glide plane replacing the mirror plane.

The number of diarsenate structures that have been investigated is relatively few and the available data are not enough to compare the diarsenate and diphosphate systems. Only the room temperature structure of $Mg_2As_2O_7$(14) has been investigated in detail, and this is found to have the thortveitite structure (β-form). Preliminary photographs of $Zn_2As_2O_7$ and $Cd_2As_2O_7$ indicate that they also exist in the β-form at room temperature(56). It will be of interest to investigate whether these have lower temperature modifications analagous to the α-form in diphosphates (characterized by a doubled $\underline{a}_3$ axis and substitution of the mirror plane in β-form by a glide plane in the α-form). Attempts so far made to search for the existence of phases other than the β-phase in the case of diarsenates of magnesium, cadmium and zinc have been unsuccessful(63).

However, in one of the attempts at duplicating the preparation of $Co_2As_2O_7$, crystals were obtained which were very similar to $Co_2As_2O_7$ but which gave rise to superlattice reflections at one-fifth of the spacings observed in $Co_2As_2O_7$ along the $(1\bar{1}1)$ direction. No attempt has so far been made to determine the detailed structure of this material, and since it was prepared by the same method as that used for preparation of $Co_2As_2O_7$, it will be of interest to determine its structure and investigate its detailed relationship to the structures of $Co_2As_2O_7$ and thortveitite.

The major features of the structure of $Co_2As_2O_7$ have been brought out by the present refinement using somewhat limited amount of data, which, in addition, have not been corrected for absorption effects, even though corrections for absorption are expected to be significant. The large errors in the bond lengths (of the order of 0.02 Å) are probably consequences of the limited data and neglect of abosrption corrections. Collection of more complete and more accurate data using automatic diffractometer methods, and refinement of the structure using these data after including any required correction for absorption effects, are contemplated.

CHAPTER 7

THE CRYSTAL STRUCTURE REFINEMENT OF $Mg_3(VO_4)_2$

Preparation and preliminary investigations: Hydrated $Mg_3(VO_4)_2$ obtained from Alpha Inorganics Inc. was used as the starting material, and crystals of $Mg_3(VO_4)_2$ were grown in a platinum crucible by slow cooling of a melt. Unit cell dimensions measured from preliminary photographs indicated that the compound was the same as that reported by Durif$^{(3)}$. The orthorhombic cell with approximate cell dimensions $\underline{a}_1 = 6.05$ Å, $\underline{a}_2 = 11.43$ Å, $\underline{a}_3 = 8.32$ Å, was $\underline{C}$-centred, with the extinction conditions $hk\ell$: $h+k$ = odd absent, $h0\ell$: ℓ = odd absent, and $hk0$: h odd absent and k odd absent. The space group possibilities consistent with these observations are Cmca(D_{2h}^{18}) and C2ca(C_{2v}^{17}). The former space group was chosen, since the isostructural $Ni_3(VO_4)_2$$^{(2)}$ has been reported to have this space group. Refinement of the present structure in this space group has led to satisfactory results, as will be seen later, thus confirming the choice.

Data of the type $nk\ell$ ($n = 0,1,2,3,4$) were measured by visual comparison from equi-inclination Weissenberg photographs taken with Mo Kα radiation. Intensities of the $h0\ell$, $hk0$ and hkk type reflections were measured with a Joyce-Loebl microdensitometer from integrated precession photographs obtained using Mo Kα radiation. The crystal used had dimensions approximately 0.15 × 0.15 × 0.20 mm^3. Absorption corrections were not applied since neglect of these corrections will cause maximum errors of less than about 15% in intensities.

Structure solution: The atomic coordinates reported for $Ni_3(VO_4)_2$ (2) were used as the starting parameters with magnesium in place of nickel. Scattering factor curves of Mg^{+2}, V^{+5}, (corrected for dispersion), and of O^-, were obtained from the International Tables for X-ray Crystallography (31). Individual scale factors were assigned for each layer and refined along with the positional parameters, and individual isotropic temperature factors. Unit weights were used in the initial stages. After a few cycles, when further refinements showed no significant improvement in the parameters, the isotropic thermal parameters were converted to anisotropic parameters and refined along with the other parameters using a Cruickshank type weighting scheme (40) of the form $w = (7.0 + 0.25\,|F_{obs}| + 0.01|F_{obs}|^2)^{-1}$. The minimum was reached at the R_1 value of 0.15 and the weighted R_w value of 0.17. A three-dimensional electron density difference map computed at this stage did not reveal any unaccounted structural features.

The reliability index of 0.15 is somewhat higher than anticipated. In addition, the temperature factors of all the atoms in the structure were non-positive definite, and the geometry of the VO_4 group was found to deviate significantly from an ideal tetrahedral arrangement. Three of the four V-O bonds involved oxygen atoms with coordination number 3 (two magnesium atoms and one vanadium atom) and had bond lengths 1.66(2) Å (twice) and 1.73(2) Å, while the remaining V-O bond involved an oxygen atom with coordination number 4 (three magnesium atoms and one vanadium atom) and had a bond length of 1.79(2)Å. Even though the estimated errors on the V-O bond lengths could be optimistic in view of the fact that many atoms lay on symmetry elements (Table 7-1), the differences in the individual V-O bond lengths appeared to be significant. It was not clear whether the observed large range (1.66(2) Å to 1.79(2) Å) for the V-O bond lengths was the true situation in the structure or whether the data was of poor quality, resulting in poor representation of the structure. Since no detailed structure of any other orthovanadate had been reported in the literature at the stage of this work, it was considered worthwhile to collect data of better quality to clarify this aspect of the geometry of the VO_4 group in the case of magnesium orthovanadate. Therefore a smaller crystal, with dimensions approximately $0.08 \times 0.08 \times 0.23$ mm^3, was mounted with the long axis of growth of the crystal parallel to the axis of the goniometer head, and was used to record the intensity of 1715 independent reflections on a quarter circle General Electric XRD6 automatic diffractometer using Mo Kα radiation. Least-square refinement of the dif-

Table 7-1

Atomic parameters for $Mg_3(VO_4)_2$*

Atom	Site Symmetry	Positional parameters			Thermal parameters†					
		x	y	z	u_{11}	u_{22}	u_{33}	u_{12}	u_{13}	u_{23}
Mg(1)	2/m	0	0	0	0.0052(7)	0.0074(7)	0.0032(7)	0	0	-0.0015(6)
Mg(2)	2	$\frac{1}{4}$	0.1359(1)	$\frac{1}{4}$	0.0037(4)	0.0044(4)	0.0062(5)	0	-0.0007(4)	-0.0008(4)
V	m	0	0.37990(5)	0.12091(7)	0.0031(1)	0.0022(1)	0.0033(1)	0	0	0.0000(2)
O(1)	m	0	0.2514(2)	0.2275(3)	0.0068(8)	0.0036(7)	0.0056(8)	0	0	0.0025(6)
O(2)	m	0	0.0038(2)	0.2447(3)	0.0054(8)	0.0034(7)	0.0037(8)	0	0	0.0001(7)
O(3)	1	0.2738(3)	0.1168(1)	0.9975(2)	0.0062(6)	0.0070(5)	0.0059(6)	-0.0012(5)	0.0014(5)	0.0003(5)

*Estimated standard deviations in parentheses

†Calculated from $\beta_{ij} = 2\pi^2 \underline{b}_i \underline{b}_j u_{ij}$ where the β_{ij}'s appear as a thermal effect through $\exp[-(\beta_{11}h^2 + 2\beta_{12}hk + ..)]$ in the structure factor expression, and $\underline{b}_i$ are the reciprocal lattice vectors.

fraction geometry of 17 reflections manually centred accurately on the GE diffractometer led to the lattice parameters $\underline{a}_1$= 6.053(3)Å, $\underline{a}_2$= 11.442(6)Å and $\underline{a}_3$= 8.330(6)Å. The program PICK2* was used for the above refinement as well as for calculating and punching angular settings for reflections up to 2θ values of 80° for use in the card-controlled diffractometer. Data beyond this limit were not collected since relatively few reflections near the upper angular limit had measurable intensities. A scanning rate through each reflection of 1° per minute was employed. Each reflection was scanned for a range starting from 1° below the α_1 peak to 1° above the α_2 peak. Background counts, each of 40 seconds duration, were made at fixed angles on either side of the peak. Ten reflections that were well distributed in reciprocal space were used as standards for checking of alignments, and were measured after about every 100 reflections. No significant alterations in the intensities of these standards were evident during the course of the measurements.

The intensities were corrected for the average background adjusting the counts to effective equal scan times. Standard

---

[*] A revision by D. M. Collins of Cornell University, of J. A. Iber's version of W. C. Hamilton's MODEl program, obtained through J. J. Park of this laboratory.

deviations were assigned for each intensity based on counting statistics (pp. 454--458 of (26)). Those reflections whose net intensity (after correcting for background) calculated to less than zero were considered unreliable and assigned zero weights in the refinement. Any reflection for which the calculated intensity was greater than zero but less than the standard deviation assigned on the basis of counting statistics, was considered unobserved, and its intensity was reset to be equal to the standard deviation assigned for that reflection. All the data were corrected for Lorentz and polarisation effects. The linear absorption coefficient is 37.5 cm^{-1} for $Mg_3(VO_4)_2$ for Mo $K\alpha$ radiation. No absorption corrections were applied, since this neglect will introduce extreme error of less than about 10% in the intensities, for the dimensions of the crystal used.

Refinement of the trial structure resulting from film measurements was carried out using the present data. Isotropic thermal factors were assigned for all atoms in the initial stages. $(1/\sigma^2)$ weighting was used. Five strong reflections which calculated to very large values of $|F_{hk\ell}|$ compared to the measured values and which were suspected to suffer from serious extinction effects were given zero weight in the refinement. When no further significant shifts were noted in the parameters, the temperature factors of all atoms were converted to anisotropic thermal factors and refined along with the other parameters. The minimum was reached at the R_1-value of 0.067

and the weighted R_w-value of 0.054. The final positional and thermal parameters are listed in Table (7-1). The observed and calculated structure factor amplitudes are compared in Table (7-2). The more important bond lengths and bond angles in the structure are given in Table (7-3).

Description of the Structure: The structure of $Mg_3(VO_4)_2$ can be described as consisting of cubic close-packing (ABC.... sequence) of oxygen atoms with magnesium ions in octahedral sites and V ions in tetrahedral sites. In this sense the structure is analogous to that of spinels(64), which also have a cubic close-packed arrangement of oxygen atoms, with the smaller ions distributed in octahedral and tetrahedral voids. The close-packing direction in $Mg_3(VO_4)_2$ is the ($\underline{a}_2$-$\underline{a}_3$) direction, of translational periodicity 14.14 Å, which compares well with the stacking direction ($\underline{a}_1$+$\underline{a}_2$+$\underline{a}_3$) in spinels, whose periodicity is close to 14.0 Å. Details of the relation between the two types of structures will be discussed in the concluding chapter.

The vanadium ion has tetrahedral coordination with mean V-O bond length of 1.725(2)Å, which compares well with the values reported in other structures. Thus the mean V-O bond lengths are 1.71(2)Å in $Zn_3(VO_4)_2$(65), 1.706(8)Å in YVO_4(66), 1.707(1)Å in $Ca_2(VO_4)Cl$(67), and 1.70(2), 1.71(2) and 1.69(2)Å for the three independent VO_4 tetrahedra in $Ca_3(VO_4)_2$(68).

The geometry of the VO_4 group in the present structure

TABLE (7-2).

Observed and Calculated Structure Factors for $Mg_3(VO_4)_2$

---

* Unobserved reflections are marked L, unreliable reflections E, and reflections for which the net counts calculated negative are marked U.

TABLE (7-2).

```
              |FOBS| FCALC
 K   L           H = 0
-2   0       57    51
 4   0     E138  -162
 6   0       12    14
 8   0     F209   267
12   0       71   -71
14   0       16    -6
16   0      104   107
18   0       30    28
20   0       28   -28
22   0       21   -21
24   0       44    49
 2   1       31    14
 4   1       25    22
 6   1       28   -26
 8   1       50   -49
12   1       36    35
14   1       27   -26
16   1       42   -42
18   1       21    21
20   1       24    25
22   1       22   -23
24   1       32   -31
 2   2       55    56
 4   2       80   -77
 6   2       15   -13
 8   2       16   -16
10   2       61    61
12   2       19   -20
14   2       24   -24
16   2        6    -3
18   2       37    37
20   2       19   -18
22   2       17   -18
24   2   L    4    -1
 2   3     E129   169
 4   3        2     0
 6   3     E119  -129
 8   3       12    12
10   3       91    93
12   3        4     3
14   3       55   -55
18   3       41    41
20   3       13    12
22   3       24   -23
24   3   U    0    -3
 2   4       30    28
 4   4       78    77
 6   4       55    52
 8   4       52    49
10   4       11   -10
12   4       57    57
14   4       42    42
16   4        4     3
18   4       20   -19
20   4       43    43
22   4       28    28
24   4        8    -7
 4   5        4     3
 6   5       90    92
10   5       68   -67
12   5   L    3     2
14   5       42    42
16   5        6    -7
18   5       32   -31
20   5        9    -7
22   5       18    17
24   5   L    4    -0
 2   6       29    26
 4   6   L    3     2
 8   6       20   -20
10   6       38    36
12   6   U    0    -1
14   6       19   -18
16   6        9    -9
18   6       24    24
20   6   U    0    -7
22   6       12   -14
24   6   L    4    -4
 2   7       23   -22
 6   7       25    26
 8   7       33    32
10   7       23   -23
12   7       26   -25
16   7       35    35
18   7       22   -22
20   7       22   -22
22   7       25    24
 2   8       32    31
 4   8       90   -95
 8   8     E127   141
10   8       32    30
12   8       57   -57
14   8   L    4    -3
16   8       76    77
18   8       29    29
20   8       27   -28
22   8       13   -14
 4   9       11    10
 6   9       12   -11
 8   9       23   -24
10   9       11    12
12   9       21    20
14   9       17   -16
16   9       26   -28
18   9       15    14
20   9       18    17

              |FOBS| FCALC
22   9       15   -15
 2  10   U    0    10
 4  10       15   -14
 6  10       14   -15
 8  10       15    13
12  10       18   -17
14  10       25   -25
16  10       13    11
18  10       22    23
20  10       14   -14
 2  11       74    76
 4  11   U    0     2
 6  11       66   -67
 8  11   U    0     0
10  11       58    57
12  11        8     9
14  11       41   -41
16  11   U    0    -3
18  11       35    34
20  11       13    14
 2  12       17    18
 4  12       29    29
 6  12       30    29
 8  12   L    4     2
10  12   L    4     2
12  12       23    28
14  12       29    29
16  12        5    -7
18  12   L    4    -6
 2  13       34   -33
 4  13        5     1
 6  13       30    29
 8  13   U    0    -5
10  13       27   -25
12  13   U    0     1
14  13       17    18
16  13        8    -5
18  13       12   -15
 2  14   U    0    -0
 4  14       15    15
 6  14        8   -10
 8  14        9    -8
10  14   L    4     5
12  14        8    10
14  14       12   -13
16  14   U    0    -4
 2  15       23   -21
 4  15        7    -5
 6  15       24    23
 8  15       14    14
10  15       20   -20
12  15       14   -13
14  15       23    22
 2  16       17    18
 4  16       48   -49
 6  16       10    10
 8  16       57    59
10  16       24    23
12  16       37   -37
 2  17   L    5     6
 4  17        7     4
 6  17        7    -7
 8  17        8    -9
10  17        7     6
 2  18   L    4    -1
 4  18       13   -13
 6  18       13   -12

 K   L           H = 1
 1   1       51   -43
 3   1     E100   108
 5   1      106   112
 7   1       18   -17
 9   1       41   -39
11   1       44    44
13   1       62    62
15   1   U    0    -3
17   1       31   -30
19   1       15    13
21   1       37    37
23   1   U    0     1
25   1       23   -23
 1   2   E   97  -107
 3   2       84   -85
 5   2       61    58
 7   2       92    93
 9   2       49   -49
11   2       63   -63
13   2       22    21
15   2       58    58
17   2       17   -17
19   2       43   -43
21   2        4     4
23   2       40    40
25   2   U    0    -3
 1   3       77    79
 3   3       18   -16
 5   3       26   -24
 7   3       54    53
11   3        6    -6
13   3       24   -23
15   3       21    21
17   3       37    36
19   3   L    4    -1
21   3       20   -20
23   3        7     6
 1   4       12    11
 3   4       28   -26

              |FOBS| FCALC
 5   4       24    21
 7   4   U    0    -2
11   4       12   -13
13   4       11    10
15   4        4     0
17   4   U    0     4
19   4        7    -8
21   4        4     5
23   4        7     0
25   4   L    3     4
 1   5       84    88
 3   5       15   -14
 5   5       27   -25
 7   5       66    67
11   5        6    -5
13   5       26   -27
17   5       44    43
19   5   U    0    -0
21   5       24   -24
23   5        8     8
 1   6       45    46
 3   6       83    85
 5   6       65   -65
 7   6       51   -51
 9   6       22    23
11   6       65    65
13   6       31   -31
15   6       40   -41
17   6        8     5
19   6       48    47
21   6       11   -12
23   6       31   -30
 1   7       23   -22
 7   7       11   -12
 9   7       25   -24
11   7       25    24
13   7       39    39
15   7   U    0    -4
17   7       23   -22
19   7        9     7
21   7       27    26
23   7   U    0    -0
 1   8       26    25
 3   8        5    -2
 5   8        5     6
 7   8       22   -21
 9   8       17    18
11   8   L    3     1
15   8       16   -15
17   8       12    11
19   8   U    0     2
21   8        6     6
23   8       10   -10
 1   9       25   -24
 3   9       57    59
 5   9       64    65
 7   9       11   -11
 9   9       30   -30
13   9       51    51
15   9        7    -2
17   9       28   -29
19   9       15    14
21   9       35    36
 1  10       52   -53
 3  10       33   -33
 5  10       22    22
 7  10       56    56
 9  10       34   -35
13  10        9     8
15  10       46    46
17  10       17   -18
19  10       29   -29
21  10   U    0    -1
 1  11       24    25
 3  11       10    -8
 5  11       12   -11
 7  11       18    17
 9  11       25    24
11  11        8    -6
13  11       13   -12
15  11        8     8
17  11       20    19
19  11   U    0    -3
 1  12        6    -1
 3  12       19   -20
 5  12       20    19
 7  12   U    0     4
 9  12   L    4     2
11  12       19   -18
13  12       15    13
15  12   L    4     6
17  12   L    4     5
19  12       12   -13
 1  13       43    43
 3  13       11   -11
 5  13       18   -18
 7  13       33    33
 9  13       42    41
11  13   U    0    -4
13  13       22   -22
15  13       19    20
17  13       33    33
 1  14       21    21
 3  14       38    38
 5  14       31   -31
 7  14       25   -26
 9  14       13    12
11  14       38    37
13  14       19   -19

              |FOBS| FCALC
15  14       25   -25
 1  15        7   -10
 3  15       13    13
 5  15       17    17
 7  15        7    -7
 9  15       15   -11
11  15        8     7
13  15       17    16
15  15   U    0    -4
 1  16       16    14
 3  16        6     6
 5  16   U    0    -3
 7  16       13   -15
 9  16       13    12
11  16        9     9
13  16        4     0
 1  17       15   -15
 3  17       31    32
 5  17       37    36
 7  17        7    -8
 9  17       21   -20
 1  18       21   -22
 3  18       19   -19
 5  18       14    13

 K   L           H = 2
 0   0       95   100
 2   0       44    43
-4   0     E112   125
 6   0   L    2     1
 8   0       77    78
10   0       51    51
12   0       27    22
14   0       20   -21
18   0       35    34
20   0   L    4    -3
22   0       21   -21
24   0       38    38
 2   1     E121   153
 4   1       12   -12
 6   1     E115  -125
 8   1        3     3
10   1       79    80
12   1       11   -11
14   1       55   -56
18   1       32    32
20   1        6    -1
22   1       24   -25
24   1       11   -12
 0   2       66   -64
 2   2       15    15
 4   2       38   -37
 6   2       60    59
 8   2       16   -14
10   2       18   -18
12   2       15   -15
14   2       43    43
16   2       12   -13
18   2       17   -18
20   2        5    -6
22   2       25    24
24   2       11   -12
 2   3       26    24
 4   3       29    28
 6   3       23   -21
 8   3       32   -30
10   3       26    28
12   3       43    43
14   3       22   -23
16   3       28   -28
18   3       26    27
20   3       35    36
22   3       19   -20
24   3       21   -20
 0   4     E125  -141
 2   4       29    29
 4   4     E185   277
 6   4       38    36
 8   4       90   -93
10   4        5     4
12   4     E128   137
14   4       30    28
16   4       42   -42
18   4       14   -14
20   4       65    65
22   4       28    27
24   4       16   -17
 2   5       15   -14
 4   5       22   -23
 6   5       12    13
 8   5       26    26
10   5       19   -20
12   5       38   -37
14   5       18    17
16   5       25    25
18   5       21   -21
20   5       32   -31
22   5       16    16
24   5       18    18
 0   6       23   -22
 2   6        6    -5
 4   6   L    2    -1
 6   6       40    39
12   6   U    0     2
14   6       35    36
16   6       19   -18
20   6   L    4     3
22   6       25    24

              |FOBS| FCALC
 4   7   L    3     4
 6   7       90    94
 8   7        4     3
10   7       66   -68
12   7        7     3
14   7       53    53
16   7       10    11
18   7       34   -33
20   7        9    -3
22   7       26    27
 0   8       47    47
 2   8       32    32
 4   8       29    26
 6   8        6     6
 8   8       43    44
10   8       39    39
12   8        9     4
14   8       11    -9
16   8       38    38
18   8       33    30
20   8        5    -7
22   8       14   -14
 2   9       58    59
 4   9        5    -5
 6   9       52   -52
 8   9   U    0     3
10   9       39    39
12   9        8    -8
14   9       31   -30
16   9        4    -1
18   9       19    19
20   9   L    4    -4
22   9       15   -15
 0  10       17    17
 2  10   L    3    -1
 4  10       16   -16
 6  10       15    14
 8  10       12    11
10  10       15   -14
12  10        9    -9
14  10       16    15
16  10        5     2
18  10       14   -14
20  10        6    -5
 4  11       11    12
 6  11       21   -22
 8  11       14   -14
10  11       26    25
12  11       25    26
14  11       23   -22
16  11       18   -18
18  11       23    24
20  11       26    27
 6  12       26    25
 8  12       56   -56
10  12        7     5
12  12       70    71
14  12       28    27
16  12       36   -35
18  12        4    -5
 2  13        7    -8
 4  13        7    -8
 8  13       10    10
10  13       11   -11
12  13       16   -18
14  13        9    10
16  13       14    13
18  13       11   -11
 0  14       12   -14
 2  14        6    -7
 4  14       19    19
 6  14        7     7
 8  14       14   -14
10  14       20   -19
12  14       17    17
14  14       15    15
16  14       13   -12
 2  15       51   -52
 4  15   U    0    -0
 6  15       47    49
 8  15        7     6
10  15       41   -40
12  15        7    -3
14  15       35    36
 0  16       19    19
 2  16       17    18
 4  16   L    4    -3
 6  16       11    -9
 8  16       21    19
10  16       23    23
12  16   L    4    -6
 2  17       17    17
 4  17        4    -2
 6  17       15   -16
 8  17   U    0     1
 0  18       14    15
 2  18   U    0    -5
 4  18        9    -7

 K   L           H = 3
 1   1        8    -7
 3   1       66    66
 5   1       67    67
 7   1        5    -4
 9   1       16   -17
11   1       35    35
13   1       43    44
15   1        5    -3

              |FOBS| FCALC
17   1       17   -19
19   1       14    14
23   1   L    4    -0
 1   2       83   -86
 3   2       73   -73
 5   2       51    51
 7   2       78    80
11   2       56   -58
13   2       17    20
15   2       54    54
17   2       17   -16
19   2       41   -41
21   2   L    4     4
23   2       37    38
 1   3       91    93
 3   3       35   -32
 5   3       45   -44
 9   3       71    71
11   3       10   -10
13   3       35   -35
15   3       19    19
17   3       45    44
21   3       28   -27
23   3        7     3
 1   4        9     8
 3   4       19   -19
 5   4       17    16
11   4       10   -11
13   4       10     9
15   4   U    0    -0
17   4        5     4
19   4        8    -7
21   4        6     5
23   4   U    0     0
 1   5       92    94
 3   5       28   -29
 7   5       59    60
 9   5       73    75
11   5        9    -9
13   5       36   -37
15   5       23    24
17   5       48    50
19   5   L    4     0
21   5       29   -30
23   5        8     6
 5   6       57   -57
 9   6       21    21
11   6       60    61
13   6       28   -29
15   6       39   -39
17   6        6     5
19   6       45    46
21   6       11   -11
23   6       28   -29
 1   7        9    -7
 3   7       33    33
 5   7       34    34
 7   7        4    -5
 9   7       11   -11
11   7       20    19
15   7   U    0    -4
17   7       14   -13
19   7        9     8
21   7       18    18
23   7        4    -2
 1   8       23    23
 3   8        3    -0
 5   8        4     4
 7   8       20   -21
 9   8       16    17
11   8   U    0     2
13   8        4     5
15   8       14   -15
17   8       10    10
19   8   L    4     2
21   8   L    4     6
 1   9       11   -12
 3   9       44    45
 5   9       48    49
 7   9   U    0    -5
 9   9       18   -18
11   9       29    29
13   9       38    39
17   9       20   -20
19   9       14    14
21   9       28    29
 1  10       48   -49
 3  10       30   -31
 5  10       20    21
 9  10       35   -33
11  10       33   -32
13  10        8     8
15  10       45    44
17  10       17   -18
19  10       27   -27
 1  11       32    31
 5  11       19   -20
 7  11       22    20
 9  11       32    31
11  11        7    -8
13  11       19   -21
15  11   L    4     7
17  11       24    25
19  11        4    -2
 1  12   U    0    -0
 3  12       19   -18
 5  12       18    17
 7  12   L    4     3
 9  12   U    0     3

              |FOBS| FCALC
11  12       14   -16
13  12       13    12
15  12   L    4     5
17  12        7     4
 1  13       46    48
 3  13       17   -17
 5  13       26   -26
 7  13       36    36
 9  13       48    47
11  13        6    -7
13  13       28   -28
15  13       19    19
17  13       37    38
 1  14       22    21
 3  14       37    37
 5  14       29   -29
 7  14       27   -26
 9  14        6    11
11  14       38    37
13  14       19   -18
15  14       25   -25
 1  15        8    -4
 3  15       10     8
 5  15   U    0     4
 7  15        8    -4
 9  15        5    -4
11  15   U    0     5
13  15        6     9
 1  16       15    15
 3  16        8     8
 5  16   L    4    -3
 7  16       13   -15
 9  16       15    12
 1  17        9    -9
 3  17       27    26
 5  17       29    29
 7  17   U    0    -4
 9  17       14   -13
 1  18       19   -21
 3  18       17   -18

 K   L           H = 4
 0   0     E194   287
 2   0       30    29
 4   0     E101  -110
 6   0       14    14
10   0       25    25
12   0       57   -57
14   0        5    -6
16   0       91    92
18   0       25    24
20   0       25   -25
22   0       18   -18
24   0       45    45
 2   1       18    16
 4   1       18    17
 8   1       36   -36
10   1       18    19
12   1       29    29
14   1       24   -24
16   1       37   -36
18   1       19    19
20   1       23    22
22   1       23   -22
24   1       28   -29
 2   2       35    34
 4   2       17   -16
 8   2       16   -17
10   2       44    43
12   2       12   -13
14   2       18   -18
16   2        4    -5
18   2       30    30
22   2       14   -15
24   2   L    4    -2
 2   3     E110   121
 4   3        3    -0
 8   3        7     8
10   3       73    74
12   3        5     3
14   3       47   -48
16   3   U    0     2
18   3       38    37
20   3       11    12
22   3       22   -21
24   3        5    -3
 0   4       56    54
 2   4       19    17
 6   4       42    41
 8   4       29    25
10   4       13   -11
12   4       52    53
14   4       37    37
16   4        6    -0
18   4       20   -19
20   4       41    41
22   4       27    27
 6   5       70    72
 8   5        9    -9
10   5       55   -56
12   5   L    3     0
14   5       36    37
16   5   L    4    -6
18   5       28   -28
20   5       10    -6
22   5       17    16
 0   6       30   -29
 2   6       19    19

              |FOBS| FCALC
 4   6       10     9
 6   6        5    -6
 8   6       20   -20
10   6       28    28
12   6   L    3    -0
14   6       13   -14
16   6       10   -10
18   6       19    19
20   6        5    -5
22   6       10   -11
 2   7       20   -22
 4   7       12   -11
 6   7       23    24
 8   7       26    27
10   7       21   -22
14   7       25    26
18   7       21   -21
20   7       21   -20
22   7       20    22
 0   8     E134   147
 2   8       23    24
 4   8       74   -76
 6   8       13    13
 8   8     E109   117
10   8       26    25
12   8       48   -49
14   8   L    4    -2
16   8       68    68
18   8       25    25
20   8       26   -25
 2   9        8     9
 4   9        8     9
 6   9       13   -11
10   9       13    12
12   9       17    17
16   9       26   -25
18   9       12    13
20   9       15    16
 0  10        9     9
 2  10        9     7
 4  10       11   -11
 8  10        9     9
10  10       20    19
12  10       12   -14
14  10       22   -21
16  10        9     9
18  10       19    19
20  10       11   -12
 2  11       64    66
 4  11        4     2
 6  11       58   -59
 8  11        7     0
10  11       51    52
12  11        8     9
14  11       38   -38
16  11        6    -3
18  11       32    32
 0  12        7     3
 2  12       15    15
 4  12       30    30
 8  12        4    -1
10  12        6     1
12  12       30    29
14  12       29    28
16  12       10    -8
18  12        9    -7
 2  13       30   -30
 4  13   U    0     1
 6  13       26    26
 8  13        5    -4
10  13       23   -23
16  13        7    -5
 0  14       13   -11
 2  14   U    0    -1
 4  14       15    15
 6  14        8    -8
 8  14        6    -9
10  14        5     3
12  14       11    10
14  14       12   -11
 2  15       21   -20
 4  15        6    -5
 6  15       22    21
 8  15       13    13
10  15       20   -19
12  15       11   -12
 0  16       61    61
 2  16       13    17
 4  16       43   -43
 6  16       10    10
 8  16       52    53
10  16       20    20
 2  17   U    0     5
 4  17        6     3
 6  17        7    -6

 K   L           H = 5
 1   1       43   -43
 3   1       81    85
 7   1       19   -20
 9   1       43   -44
11   1       36    36
13   1       59    60
15   1   L    4    -4
17   1       35   -36
19   1       12    10
21   1       40    39
23   1   L    4     3
```

Continued next page

TABLE (7-2) continued

			|FOBS|	FCALC
1	2		63	-64
5	2		40	41
9	2		36	-36
11	2		49	-50
13	2		16	17
15	2		49	49
17	2		12	-15
19	2		17	-18
21	2	U	0	1
23	2		35	34
3	3		6	-2
5	3		5	-5
7	3		29	30
9	3		32	32
11	3	U	0	-3
15	3		15	16
17	3		22	23
19	3		7	-3
21	3		11	-13
23	3		7	7
3	4		15	-15
5	4		14	13
7	4	U	0	-0
9	4		3	3
11	4		13	-11
13	4		9	8
15	4	L	3	0
17	4		7	4
19	4	U	0	-7
21	4	L	4	5
23	4	L	3	0
1	5		47	47
3	5	U	0	-4
5	5		9	-10
7	5		36	36
9	5		39	40
11	5		6	-3
13	5		15	-15
15	5		20	20
17	5		29	30
19	5		5	-1
21	5		17	-16
1	6		34	35
3	6		59	69
5	6		47	-47
7	6		33	-40
9	6		18	19
11	6		53	53
13	6		26	-26
15	6		34	-35
17	6		6	7
19	6		42	41
21	6		11	-11
1	7		24	-27
3	7		42	42
5	7		50	50
7	7		16	-15
9	7		32	-31
11	7		21	21
13	7		40	41
17	7		28	-27
19	7		5	5
21	7		29	29
1	8		18	17
3	8	L	3	-2
5	8		5	4
7	8		17	-16
9	8		13	14
11	8	L	3	0
13	8		5	5
15	8		15	-13
17	8		7	7
19	8	L	4	1
21	8	L	4	5
1	9		31	-30
3	9		53	53
7	9		16	-15
9	9		35	-36
11	9		30	31
15	9		6	-4
17	9		33	-32
19	9		14	17
1	10		43	-44
3	10		30	-29
5	10		19	19
7	10		48	48
9	10		30	-30
11	10		31	-31
13	10		7	7
15	10		43	42
17	10		16	-16
19	10		26	-27
1	11		11	13
3	11		5	-3
5	11		6	-3
7	11		12	11
9	11		11	12
11	11		8	-4
13	11		7	-5
17	11		17	11
1	12		7	-2
3	12		18	-19
5	12		16	17
7	12		6	5
9	12	U	0	1
11	12		19	-17
13	12		11	12
15	12	U	0	6
17	12	L	4	4

			|FOBS|	FCALC
1	13		31	30
3	13		8	-6
5	13		11	-10
7	13		25	25
9	13		31	30
11	13	L	4	-2
13	13		15	-14
15	13		14	17
1	14		19	18
3	14		33	33
5	14		26	-27
7	14		23	-22
9	14		9	10
11	14		32	32
13	14		16	-17
1	15		9	-14
3	15		15	15
5	15		18	20
7	15		11	-4
9	15		16	-16
11	15		7	7
1	16		13	12
3	16	U	0	5
5	16	U	0	-2
7	16		13	-12
9	16		7	10
1	17		17	-18
3	17		31	32
K	L			H = 6
0	0		66	67
2	0		26	25
4	0		32	28
6	0		5	-4
8	0		58	60
10	0		35	37
14	0		17	-19
16	0		46	49
18	0		31	30
20	0		7	-6
22	0		22	-21
2	1		82	86
4	1		5	-5
6	1		72	-75
8	1	L	3	0
10	1		54	55
14	1		43	-43
16	1		8	-6
18	1		76	27
20	1		4	-0
22	1		21	-22
0	2		5	4
2	2		9	9
4	2		30	-29
6	2		24	28
8	2	E	6	-0
10	2		6	-9
12	2		17	-16
14	2		26	26
16	2		10	-9
18	2		11	-11
20	2		10	-7
22	2		17	17
2	3		18	20
4	3		16	16
6	3		18	-19
8	3		20	-20
10	3		23	23
14	3		21	-20
16	3		22	-22
18	3		24	24
20	3		30	30
22	3		15	-17
0	4		74	-77
2	4		16	16
4	4	E	134	150
6	4		20	19
8	4		57	-59
10	4	L	3	3
12	4		95	97
14	4		22	20
16	4		32	-32
18	4		11	-10
20	4		53	54
22	4		22	20
2	5		13	-12
4	5		14	-13
6	5		13	13
8	5		16	17
12	5		26	-27
14	5	U	0	16
16	5		20	17
18	5		20	-19
20	5		27	-26
0	6		7	-5
2	6		5	3
4	6		4	-7
6	6		24	22
8	6		9	-9
10	6		11	-13
12	6	U	0	-1
14	6		23	23
16	6		13	-13
18	6		15	-16
20	6		5	1
2	7		72	-74
4	7	U	0	2
6	7		66	67

			|FOBS|	FCALC
8	7		4	3
10	7		52	-52
12	7		4	1
14	7		43	43
16	7		10	10
18	7		26	-21
20	7	U	0	-3
0	8		44	43
2	8		21	22
4	8		[illegible]	6
6	8	U	0	2
8	8		41	42
10	8		32	31
12	8	U	0	-3
14	8		11	-11
16	8		34	36
20	8		3	-1
2	9		43	43
4	9		4	-3
6	9		47	-43
8	9	L	4	0
10	9		32	31
12	9		6	-5
14	9		25	-25
16	9	U	0	-2
18	9		17	17
0	10		15	16
2	10	U	0	-1
4	10		18	-13
6	10		5	7
8	10		11	11
10	10		4	-3
12	10		11	-12
14	10	U	0	[illegible]
16	10		10	-3
2	11		23	22
4	11		11	3
6	11		20	-21
8	11		12	-11
10	11		24	23
12	11		21	21
14	11		19	-19
16	11		15	-16
0	12		56	-51
2	12		13	14
4	12		74	76
6	12		20	19
8	12		44	-43
10	12	U	0	5
12	12		56	57
14	12		21	21
16	12		28	-28
2	13		6	-8
4	13		9	8
8	13		11	8
10	13		8	-10
12	13		16	-15
14	13		9	8
0	14		5	-4
2	14		6	-6
4	14		14	17
6	14	U	0	4
8	14		10	-3
10	14		14	-15
12	14		12	11
2	15		44	-44
4	15	U	0	-0
6	15		46	42
8	15	L	4	5
0	16		20	21
2	16		15	16
4	16		4	-7
6	16		5	6
K	L			H = 7
3	1		30	30
5	1		31	31
7	1		4	-2
9	1		7	-7
11	1		21	21
13	1		24	25
15	1	L	4	-3
17	1		13	-11
19	1		12	11
21	1		18	13
3	2		44	-44
5	2		31	32
7	2		51	51
9	2		28	-30
11	2		41	-42
13	2		15	15
15	2		43	43
17	2		15	-13
19	2		34	-34
21	2	U	0	3
1	3		56	57
3	3		26	-26
5	3		36	-36
7	3		37	37
11	3		10	-11
13	3		35	-35
15	3		14	15
17	3		41	40
19	3		4	-0
21	3		27	-27
1	4		3	3
3	4		11	-9
5	4		8	-9

			|FOBS|	FCALC
7	4	L	3	-1
11	4		8	-8
13	4		8	6
15	4	U	0	-0
17	4		5	3
19	4		7	-6
21	4		4	5
1	5		60	62
3	5		27	-26
5	5		38	-38
9	5		57	59
11	5		11	-11
13	5		34	-37
15	5		20	19
17	5		46	45
19	5	U	0	-0
1	6		29	30
3	6		50	50
7	6		36	-36
9	6		17	16
11	6		47	48
13	6		23	-22
15	6		33	-33
17	6	U	0	4
19	6		38	38
5	7		16	16
7	7	U	0	-3
9	7		6	-4
11	7		12	12
13	7		14	14
15	7	U	0	-4
17	7		7	-5
19	7		8	7
1	8		17	17
3	8		5	1
5	8	U	0	1
7	8		18	-16
9	8		13	13
11	8	U	0	2
13	8	U	0	4
15	8		13	-13
17	8		9	9
19	8	L	3	3
1	9		6	-6
3	9		28	27
5	9		29	29
7	9		6	-3
9	9		10	-10
11	9		20	20
13	9		26	26
15	9		6	-1
17	9		13	-13
1	10		37	-37
3	10		23	-24
5	10		16	17
7	10		40	40
9	10		28	-27
11	10		25	-26
13	10		10	7
15	10		37	36
17	10		14	-15
1	11		29	28
3	11		18	-17
5	11		24	-23
7	11		19	17
9	11		31	30
11	11		8	-8
13	11		25	-23
15	11		7	6
1	12	U	0	0
3	12		13	-13
5	12		12	12
7	12	U	0	2
9	12	U	0	2
11	12		13	-12
13	12		8	10
1	13		43	43
3	13		19	-19
5	13		28	-27
7	13		32	32
9	13		43	44
11	13		7	-8
1	14		19	18
3	14		31	31
5	14		25	-25
7	14		21	-23
9	14		10	9
3	15	L	4	4
5	15		4	4
7	15		4	-2
1	16		13	13
K	L			H = 8
0	0	F	116	127
2	0		12	12
4	0		51	-54
6	0		8	7
8	0		99	103
10	0		14	14
12	0		35	-36
14	0		4	-4
16	0		65	65
18	0		14	16
20	0		17	-18
2	1		14	15
4	1		10	9
8	1		20	-21
10	1		15	16

			|FOBS|	FCALC
12	1		19	18
14	1		19	-20
16	1		27	-26
18	1		16	16
20	1		16	17
0	2		22	-22
2	2		15	14
4	2		5	-0
6	2		15	-16
10	2		21	21
12	2		3	-7
14	2		9	-4
16	2		5	-4
18	2		16	17
20	2		9	-10
2	3		64	65
4	3		4	0
6	3		57	-57
8	3		8	4
10	3		49	49
12	3	L	4	5
14	3		36	-35
16	3	U	0	0
18	3		23	23
20	3		11	10
0	4		11	7
2	4		6	7
6	4		26	25
8	4	U	0	1
10	4		16	-11
12	4		45	46
14	4		31	27
16	4		10	-7
18	4		20	-19
20	4		34	35
4	5	U	0	0
6	5		43	45
8	5		5	-4
10	5		38	-38
12	5		6	-2
14	5		27	27
16	5		4	-3
18	5		23	-22
0	6		26	-25
2	6		8	8
4	6		12	10
6	6		4	-2
8	6		21	-20
10	6		12	13
12	6		5	2
14	6		7	-7
16	6		13	-11
18	6		10	10
2	7		21	-20
4	7		7	-7
6	7		21	21
8	7		16	18
10	7		20	-20
12	7		15	-16
14	7		23	22
16	7		24	25
18	7		15	-17
0	8		87	89
2	8		14	14
4	8		46	-46
6	8		8	8
8	8		74	76
10	8		17	16
12	8		34	-34
14	8	U	0	-0
16	8		50	50
2	9		11	10
4	9		7	5
6	9		14	-11
8	9		14	-14
10	9		12	11
12	9		13	12
14	9		13	-13
16	9		19	-19
0	10	L	4	1
2	10		5	2
4	10		6	-6
6	10		8	-4
8	10		4	2
10	10		10	10
12	10		9	-8
14	10		13	-14
2	11		49	49
4	11	L	4	2
6	11		45	-44
8	11	L	4	-0
10	11		40	40
12	11		7	7
14	11		30	-30
0	12		9	-7
2	12		12	10
4	12		31	30
6	12		21	21
8	12		8	-9
10	12	U	0	-2
12	12		27	27
2	13		23	-23
4	13	U	6	0
6	13		21	21
8	13	U	0	-3
10	13		19	-17
0	14		14	-14
4	14		16	16

			|FOBS|	FCALC
6	14	L	4	-5
2	15		16	-17
K	L			H = 9
1	1		31	-31
3	1		44	43
5	1		52	52
7	1		16	-14
9	1		34	-36
11	1		24	24
13	1		45	46
15	1		6	-5
17	1		31	-32
19	1		10	8
1	2		37	-37
3	2		36	-36
5	2		26	26
7	2		41	42
9	2		25	-24
11	2		36	-36
15	2		38	38
17	2		12	-11
19	2		29	-30
1	3		18	18
3	3	L	3	-2
5	3	L	4	-3
7	3		14	15
9	3		17	16
11	3	L	4	-3
13	3		7	-6
15	3		9	11
17	3		12	14
1	4	U	0	0
3	4		3	-9
5	4		16	8
7	4		6	0
9	4	U	0	2
11	4		9	-8
13	4		6	6
15	4	U	0	1
17	4	L	4	2
1	5		24	24
3	5	L	4	-3
5	5		6	-6
7	5		20	20
9	5		22	23
11	5		7	-3
13	5		9	-9
15	5		14	13
17	5		18	19
1	6		24	24
3	6		40	39
5	6		32	-32
7	6		27	-27
9	6		16	14
11	6		37	39
13	6		19	-20
15	6		27	-27
17	6		5	4
1	7		23	-24
3	7		29	29
5	7		38	36
7	7		16	-15
9	7		28	-28
11	7		17	15
13	7		32	34
15	7	U	0	-5
1	8		9	11
3	8	U	0	-1
5	8	U	0	3
7	8		12	-11
9	8		11	9
11	8	U	0	0
13	8		5	4
15	8		9	-9
1	9		28	-27
3	9		40	39
5	9		47	46
7	9		17	-16
9	9		32	-32
11	9		24	24
13	9		41	42
1	10		33	-33
3	10		23	-23
5	10		16	15
7	10		38	37
9	10		24	-23
11	10		25	-25
13	10		6	5
1	11		8	6
3	11	L	4	-2
5	11		7	-1
7	11		7	6
9	11		7	5
11	11	L	4	-3
1	12		5	-3
3	12		14	-15
5	12		13	13
7	12		6	5
9	12	U	0	0
1	13		20	20
3	13	U	0	-3
5	13		9	-6
7	13		17	17
K	L			H = 10

			|FOBS|	FCALC
0	0		52	52
2	0		12	12
4	0	U	0	-2
6	0		7	-6
8	0		48	48
10	0		71	75
12	0		7	-7
14	0		15	-18
16	0		37	39
2	1		47	47
4	1	U	0	-1
6	1		43	-44
8	1	L	4	-1
10	1		36	35
12	1	L	4	-2
14	1		30	-30
16	1		6	-5
0	2		6	6
2	2		5	4
4	2		24	-24
6	2		13	11
8	2	L	4	2
12	2		17	-16
14	2		13	12
16	2		4	-3
2	3		17	12
4	3		8	9
6	3		18	-17
8	3		11	-11
10	3		21	20
12	3		20	20
14	3		17	-16
16	3		16	-16
0	4		38	-39
2	4		8	4
4	4		79	81
6	4		11	10
8	4		33	-33
10	4		5	2
12	4		61	61
14	4		11	11
16	4		21	-21
2	5		13	-13
4	5		7	-7
6	5		14	12
8	5		8	10
10	5		15	-15
12	5		19	-18
14	5		13	12
0	6	U	0	-1
2	6		6	0
4	6		11	-10
6	6		11	8
8	6		5	-4
10	6	U	0	-6
12	6		7	-6
14	6		11	11
2	7		47	-46
4	7	U	0	0
6	7		44	44
8	7	L	4	4
10	7		37	-36
12	7	U	0	-0
0	8		42	40
2	8		15	13
4	8		8	-8
6	8	L	4	-1
8	8		37	37
10	8		23	24
12	8		7	-10
2	9		29	27
4	9	U	0	-1
6	9		28	-27
8	9		6	-0
10	9		23	22
12	9	L	4	-3
0	10		16	15
2	10		6	-1
4	10		20	-17
6	10		4	1
8	10		10	12
10	10		7	-4
2	11		18	18
4	11		6	6
6	11		18	-17
8	11		9	-8
0	12		31	-32
2	12		9	10
4	12		48	49
K	L			H = 11
1	1	U	0	-4
3	1		16	16
5	1		17	17
7	1	L	4	-3
9	1		8	-6
11	1		13	12
13	1		15	16
15	1	U	0	-2
1	2		30	-30
3	2		27	-29
5	2		21	21
7	2		34	34
9	2		20	-20
11	2		30	-30
13	2		12	11
3	3		21	-20

			|FOBS|	FCALC
5	3		26	-27
7	3		22	23
9	3		36	36
11	3		10	-9
13	3		27	-27
3	4		7	-5
5	4		6	5
7	4	U	0	-0
9	4	U	0	2
11	4	L	4	-5
13	4		6	4
1	5		41	39
3	5		22	-21
5	5		27	-29
7	5		29	28
9	5		43	41
11	5		10	-10
13	5		24	-29
1	6		22	21
3	6		35	34
5	6		27	-27
7	6		25	-26
9	6		12	12
11	6		35	34
1	7	L	4	-2
3	7		5	4
5	7	L	4	9
7	7	U	0	-3
9	7		5	-3
11	7		4	7
1	8		12	12
3	8		8	1
5	8	L	4	0
7	8		9	-12
9	8		8	9
1	9		5	-5
3	9		17	17
5	9		20	19
7	9	L	4	-3
1	10		25	-26
3	10		17	-17
5	10		12	12
K	L			H = 12
0	0		65	66
2	0		8	5
4	0		26	-27
6	0		7	3
8	0		58	59
10	0		7	7
12	0		20	-20
2	1		14	14
4	1		8	5
6	1		14	-15
8	1		13	-12
10	1		13	13
0	2		19	-19
2	2		6	5
4	2		5	2
6	2	U	0	-0
8	2		17	-16
10	2		9	8
2	3		39	39
4	3	L	4	1
6	3		37	-35
8	3	U	0	0
10	3		31	32
0	4		11	-4
2	4	U	0	2
4	4		43	42
6	4		17	16
8	4		12	-10
10	4		11	-11
2	5		31	-31
4	5	U	0	-0
6	5		28	28
8	5	L	3	-1
0	6		24	-22
2	6	U	0	2
4	6		11	10
6	6	L	3	-0
8	6		19	-19
2	7		13	-16
4	7	L	4	-4
0	8		50	52
2	8		5	8
4	8		25	-26
K	L			H = 13
1	1		22	-21
3	1		27	26
5	1		32	32
7	1		13	-13
1	2		25	-24
3	2		24	-24
5	2		17	17
1	3		12	11
3	3		5	-4
5	3		9	-4
1	4	U	0	-3
3	4		8	-6
1	5		15	15

Table (7-3)

Bonding geometry in $Mg_3(VO_4)_2^{\S}$

Atoms involved in bond	Coord.no. of oxygen atoms	Bond length (±0.002Å)	Atoms forming edge or diagonal	Edge Length (±0.003Å)	Angle subtended by edge at central cation site (±0.1°)	Edge shared with
(VO_4) group:						
V-O(2)f	4	1.806	O(3)d-O(3)e	2.739	108.4	
-O(1)a	3	1.718	O(1)a-O(3)d	2.768	108.7	
-O(3)d	3	1.688	O(1)a-O(3)e	2.768	108.7	
-O(3)e	3	1.688	O(2)f-O(3)d	2.866	110.2	
			O(2)f-O(3)e	2.866	110.2	
			O(1)a-O(2)f	2.898	110.6	
$Mg(1)O_6$ group:						
Mg(1)-O(2)a	4	2.039	O(2)a-O(2)a'		180	
-O(2)a'	4	2.039	O(3)a-O(3)a'		180	
-O(3)a	3	2.129	O(3)b-O(3)b'		180	
-O(3)a'	3	2.129				
-O(3)b	3	2.129	O(3)b-O(3)a'	2.673	77.8	
-O(3)b'	3	2.129	O(3)b'-O(3)a	2.673	77.8	
			O(3)a-O(3)b	3.315	102.2	
			O(3)a'-O(3)b'	3.315	102.2	
			O(2)a-O(3)b	2.943	89.8	Mg(2)
			O(2)a'-O(3)b'	2.943	89.8	Mg(2)
			O(2)a-O(3)a	2.943	89.8	Mg(2)
			O(2)a'-O(3)a'	2.943	89.8	Mg(2)
			O(3)b-O(2)a'	2.954	90.2	
			O(3)b'-O(2)a	2.954	90.2	
			O(2)a-O(3)a'	2.954	90.2	
			O(2)a'-O(3)a	2.954	90.2	

(continued next page)

Table (7-3) (continued)

Atoms involved in bond	Coord.no. of oxygen atoms	Bond length (±0.002Å)	Atoms forming edge or diagonal	Edge length (±0.003Å)	Angle subtended by edge at central cation site (±0.1°)	Edge shared with
Mg(2)-O(2)a	4	2.139	O(2)a-O(1)c		174.4	
O(2)c	4	2.139	O(2)c-O(1)a		174.4	
O(3)a	3	2.119	O(3)a-O(3)g		168.2	
O(3)g	3	2.119				
O(1)a	3	2.018	O(1)c-O(2)c	2.836	86.0	Mg(2)
O(1)c	3	2.018	O(1)a-O(2)a	2.836	86.0	Mg(2)
			O(2)a-O(3)g	2.856	84.2	
			O(2)c-O(3)a	2.956	84.2	
			O(2)c-O(3)g	2.943	87.4	Mg(1)
			O(2)a-O(3)a	2.943	87.4	Mg(1)
			O(3)a-O(1)a	2.964	91.5	-
			O(1)c-O(3)g	2.964	91.5	-
			O(2)a-O(2)c	3.028	90.1	-
			O(1)a-O(1)c	3.050	98.2	-
			O(3)a-O(1)c	3.081	96.2	-
			O(1)a-O(3)g	3.081	96.2	-

[§] Symmetry transformation

$a = x, y, z$

$b = x, \bar{y}, \bar{z}$

$c = \frac{1}{2} + x, y, \frac{1}{2} - z$

$d = \frac{1}{2} + x, \frac{1}{2} - y, \bar{z}$

$e = \frac{1}{2} - x, \frac{1}{2} - y, \bar{z}$

$f = x, \frac{1}{2} + y, \frac{1}{2} - z$

$g = \frac{1}{2} - x, y, \frac{1}{2} - z.$

deviates significantly from an ideal tetrahedral arrangement. There are three independent V-O bonds (Table 7-3), the lengths of these being 1.806(2), 1.718(2) and 1.688(2)Å. There is only a small angular distortion in the VO_4 group, the angles subtended by the edges ranging between 108.4° to 110.6°. The deviation of the geometry of the VO_4 group from ideality in the present structure is thus mainly one of differences in the individual V-O bond lengths, in particular, the large value of the V-O(2) bond length (1.806(2)Å) compared to the mean V-O bond length of 1.725(2) Å. The large V-O(2) length is correlated with the fact that the oxygen atom O(2) is strongly bonded to 4 cations whereas the remaining oxygen atoms of the VO_4 group are bonded to only 3 cations. The deviation from ideality of the VO_4 group in the present structure can therefore be considered to result almost entirely from the position of the oxygen atom O(2) . The observed lengths of the edges of the VO_4 group, included in Table (7-3),also support this speculation. The edges involving the oxygen atom O(2) are considerably longer than the other edges, and can be considered to be a result of the displacement of this oxygen atom in a direction away from the plane of the other three oxygen atoms of the VO_4 group.

There are two independent magnesium atoms in the structure, both having octahedral coordination. The Mg(1) site has C_{2h} symmetry with four symmetry-related Mg(1)-O(3) bonds of length 2.129(2)Å and two Mg(1)-O(2) bonds of length 2.039(2)Å. The oxygen atom O(2) is strongly bonded to 4 cations whereas O(3) has strong bonds to only 3 cations. On the basis of the expected correlation between the individual cation-oxygen bond lengths in a cation polyhedron and the coordination number of the oxygen atom involved in the individual bond(1), one would expect the Mg(1)-O(3) bond to be shorter and stronger than the Mg(1)-O(2) bond. However, the Mg(1)-O bond involving the oxygen atom with the higher coordination is smaller in the $Mg(1)O_6$ group than the one involving the oxygen atom with the smaller coordination, and the difference in the two bond distances is not correlated with the coordination number of the oxygen atoms involved.

Baur(49) has suggested that in structures containing two cations M(1) and M(2) with different oxidation states n and m respectively ($n > m$), and coordinated to oxygen ions, the average M(1)-O(x) distance involving any oxygen atom, O(x), will predominantly influence the average M(2)-O(x) distance. On this basis, one would expect that in the present structure, the distances V-O(1), V-O(2) and V-O(3) will be correlated to the distances <Mg-O(1)>, <Mg-O(2)>, and <Mg-O(3)> respectively, and long V-O distances should correlate with short <Mg-O> distances and vice versa. The observed distances are 1.718(2), 1.806(2), and 1.688(2) Å for the vanadium-oxygen bonds involving oxygen atoms O(1), O(2) and O(3) respectively,and 2.018(2), 2.106(2), and 2.124(2) Å for the <Mg-O(1)>, <Mg-O(2)> and <Mg-O(3)> distances respectively. While the shortest V-O distance correlates with the longest <Mg-O> distance, the longest V-O distance does not show the expected correlation. Thus, Baur's(49) speculation regarding the relative influences of the differences in the oxidation states of the cations in determining the deviations in individual cation-oxygen distance from the mean, is not consistently supported by the observed bond lengths in the present structure. The reasons for the observed differences in the individual Mg(1)-O bond distances in the $Mg(1)O_6$ group in the present structure are therefore not clear. A similar situation exists in the isostructural $Zn_3(VO_4)_2$(65), with the Zn(1)-O(3) bond of 2.18(1) Å and Zn(1)-O(2) bond of 2.04(1) Å.

The angles subtended by the edges of the $Mg(1)O_6$ group at the Mg(1) site range from 78.8(1)° to 102.2(1)°. Thus the $Mg(1)O_6$ group shows considerable angular distortion from an ideal octahedron. The group shares four of its edges with other magnesium polyhedra. The oxygen atoms forming the edges, the edge lengths, and the angles subtended by these edges at Mg(1), are included in Table (7-3). On the basis of Pauling's postulates regarding sharing of polyhedral elements in structures (Ch. 2), it may be expected that the shared edges of the $Mg(1)O_6$ group should be shorter than the unshared edges, and that the angles subtended at the central cation site by the shared edges should be smaller than those subtended by the unshared edges. However, the data in Table (7-3) on the geometry of the Mg(1)O_6 group are in disagreement with these expectations. The two edges, formed by the atoms O(3)b and O(3)a', and by the centrosymmetrically related atoms, are not shared with any other cation in the structure, but these are the shortest edges of the Mg(1)O_6 group and subtend the smallest angles at the Mg(1) site. Therefore, the angular distortion in the Mg(1)O_6 group cannot be attributed to electrostatic repulsions between Mg(1) and other cations sharing common edges with the Mg(1)O_6 group, even though it has generally been possible to satisfactorily explain the angular distortions in XO_4 groups (X=As or V) in the structures described in previous chapters to these effects. Since no edge sharing occurs between the VO_4 group and the Mg(1)O_6 group in the present structure, it does not appear that the angular distortions in the Mg(1)O_6 group could have arisen from any distortions in the VO_4 group, contrary to the suggestion based on Baur's speculations(49). The Zn(1)O_6 group in $Zn_3(VO_4)_2$(65) presents a situation analogous to the Mg(1)O_6 group in the present structure.

The Mg(2) atom lies at a site with C2 symmetry and forms three independent Mg(2)-O bonds of lengths 2.018(2), 2.139(2), and 2.119(2) Å. The oxygen atom involved in each of these bonds, and the coordination number of the oxygen atom, are included in Table (7-3). Purely from considerations of influence of the differences in the environment of the oxygen atoms on the individual bond lengths, one would expect that the Mg(2)-O(2) bond should be weaker,(and longer), than the other two bonds. The observed Mg(2)-O(2) distance is in agreement with this expectation. However, the significant difference between the Mg(2)-O(1) and Mg(2)-O(3) bonds, 2.018(2) Å and 2.119(2) Å respectively, is not explained by the same considerations, since the oxygen atoms involved in these two bonds have the same cation coordination number. It has already been pointed out that the difference between the two distances is not explained by involving Baur's(49) postulated correlation between V-O and Mg-O distances.

The angles of the $Mg(2)O_6$ group range from 84.2(1)° to 96.2(1)°. The edge-lengths and the angles subtended by these are included in Table (7-3). The angular distortions in the $Mg(2)O_6$ group are relatively lower than in the $Mg(1)O_6$ group, even though both these groups share four of their edges with other polyhedra. The distortions in the $Mg(2)O_6$ group are also not consistently explained by invoking electrostatic repulsion between the cations sharing common edges as the principal cause of angular distortions in these groups. An analogous situation exists in the case of the $Zn(2)O_6$ group in $Zn_3(VO_4)_2$(65).

Discussion: It was pointed out earlier that the principal reasons that prompted collection of the more accurate diffractometer data for refinement of the structure $Mg_3(VO_4)_2$ were the somewhat poor agreement obtained with the visually measured data, and the suspiciously large differences in the individual V-O bond lengths in the structure refined with these data. Refinement with the better data obtained with the automatic diffractometer has confirmed that the deviations from ideality observed in the (VO_4) group from the earlier refinement are true features of the structure.

The large value of 1.806(2) Å for one of the V-O bonds compared to the average V-O bond length of 1.725(2) Å in the VO_4 group is a feature not unique for $Mg_3(VO_4)_2$. A similar situation is encountered in the isostructural $Zn_3(VO_4)_2$(65), where the average value is 1.73(1) Å, with one of the V-O bonds of length 1.80(1) Å. The largest bond in both cases involves the oxygen atom which is strongly bonded to four cations, compared to the shorter bonds which involve oxygen atoms strongly bonded to only three cations. The difference in the anion coordination number is probably related to the large observed difference in the two bond lengths. The sensitivity of the P-O bonds to their environment has been noted before(69), and Brown and Gibbs(70) have discussed a similar effect in silicate systems.

In the case of $Co_3(VO_4)_2$, one form isostructural with $Mg_3(VO_4)_2$ has been reported(5). Later work revealed the existence of two other forms of $Co_3(VO_4)_2$ (4), both with cubic symmetry and with structures related to that of spinel (64). Spinel with stoichiometry M_2BO_4 (M = octahedrally coordinated cation, B = tetrahedrally coordinated ion) can be converted in principle to $M_{3/2}BO_4$ (i.e. $M_3(BO_4)_2$) by removing one-fourth of the M cations either randomly or in an ordered manner. Provided that cubic symmetry for the crystal is to be maintained, there is only one way that each of these can be achieved. These correspond to the two forms of $Co_3(VO_4)_2$ for which isostructural analogs in $Mg_3(VO_4)_2$ are not presently known. Since Mg_2VO_4 is known to have the spinel structure (71), it will be of interest to attempt to prepare the forms of $Mg_3(VO_4)_2$ derived from Mg_2VO_4 in the above manner. However, Mg_2VO_4 has vanadium in the octahedral sites, whereas the forms of $Mg_3(VO_4)_2$ isostructural with the cubic forms of $Co_3(VO_4)_2$ will have vanadium in tetrahedral sites. In addition there is a change in oxidation state of vanadium from +4 in Mg_2VO_4 to +5 in $Mg_3(VO_4)_2$. It will be of interest to investigate the detailed structures of the spinel-like forms in order to understand the relation between these and the orthorhombic form, and also the nature of the phase transformation involved.

CHAPTER 8

CRYSTAL STRUCTURE OF $Co_{7.0}As_{3.6}O_{16}$

Preparation and preliminary investigations: The compound was obtained as a product of the reaction in which the preparation of $CoAs_2O_6$ was attempted. The compounds $2CoCO_3 \cdot 3Co(OH)_2$ (Fisher Scientific Co.) and As_2O_5 (Mallinckrodt Chemical Works) were mixed in proportions so as to yield $CoAs_2O_6$ on loss of CO_2 and H_2O, heated to fusion in an open vycor tube (to about 950°C), and slowly cooled. Preliminary photographs of single crystals extracted from this sample indicated that the crystals possessed orthorhombic symmetry. A unit cell consistent with orthorhombic symmetry and with approximate cell dimensions $\underline{a}_1 = 10.44$ Å, $\underline{a}_2 = 5.97$ Å, $\underline{a}_3 = 4.84$ Å, was chosen and the diffraction pattern indexed. The systematic absences observed were: $0k\ell$ reflections with $(k+\ell) \neq 2n$, and $hk0$ reflections with $h \neq 2n$. The space group possibilities consistent with these observations are $Pnma(D_{2h}^{16})$ and $Pn2_1a(C_{2v}^{9})$. The unit cell dimensions and the space group possibilities strongly suggested that the compound has an olivine-like structure(72). The density of the compound was not measured since the product of fusion appeared to contain more than one phase and it was difficult to isolate enough single crystals of the compound to carry out satisfactory density measurements.

Accurate unit cell dimensions were obtained from precession photographs calibrated with reflections from a standard TiO_2 crystal whose unit cell parameters were taken to be $\underline{a}_1$ = 4.5959 Å and $\underline{a}_3$ = 2.9591 Å(38). The cell dimensions for the crystal under investigation were found to be $\underline{a}_1$ = 10.48(1) Å, $\underline{a}_2$ = 5.97(1) Å, $\underline{a}_3$ = 4.86(1) Å.

The expected product of the reaction was $CoO{\cdot}As_2O_5$. However, the space group and cell dimensions of the crystal extracted from the reaction product did not agree with the hexagonal symmetry and unit cell dimensions assigned by Magneli(10) for $CoO{\cdot}As_2O_5$. This suggested that either the product of the reaction did not correspond to the expected product, $CoO{\cdot}As_2O_5$, or that it was a hitherto unreported polymorph of $CoO{\cdot}As_2O_5$.

Compounds with olivine-like structure but with varying stoichiometries are known. Thus, Mg_2SiO_4 (olivine)(72), $(Fe,Mn)PO_4$ (heterosite)(73), $(Fe,Mn,Ca)_3(PO_4)_2$ (sarcopside)(74) and $LiMnPO_4$ (lithiophilite)(75), all have olivine-like structures. Since the composition of the present crystal was not known in the initial stages, the composition $Co_3(AsO_4)_2$, analogous to that of sarcopside, was initially assumed for the crystal for purposes of formulating a trial structure; the occupancy factors of all the cation sites were included as variables in the final stages of the refinement in an attempt to derive the actual composition of the crystal on the basis of the x-ray data.

Mo Kα radiation was used for collection of intensity data. A crystal with approximate dimensions 0.15 × 0.06 × 0.45 mm^3 was used for data collection. Intensities of reflections of the type hkn, (n = 0,1,2) and mkℓ (m = 0,1,2,3,4) were measured using a Joyce-Loebl microdensitometer from integrated precession photographs. In addition, intensities of reflections of the type hsℓ, (s = 0,1,2,3,4), were measured using a manually set scintillation counter, and employing equi-inclination Weissenberg geometry and ω-scan.

The data were corrected for Lorentz and polarisation effects. Absorption corrections were applied only at the final stages of the refinement when the composition was ascertained. The total number of reflections collected using the precession method was 346, and that using Weissenberg geometry was 1095. The orientation of the crystal was such that cylindrical geometry with the axis of the cylinder normal to the x-ray beam could be assumed for purposes of absorption correction of the Weissenberg data, whereas the orientation of the crystal in the collection of the precession data did not correspond to one of the simpler cases for which tabulated absorption corrections are already available(47). However, since the number of reflections measured using the precession method corresponded to only about one-fourth of the total number of reflections measured, absorption corrections were not applied to the precession data in the present studies.

The extinction conditions lead to the space group possibilities Pnma or $Pn2_1a$, the latter lacking the centre of symmetry present in the former one. The centrosymmetric space group was chosen, since other olivine-like structures, (eg. $LiMnPO_4$(75), $NaMnPO_4$(76), Mg_2SiO_4(72)), have led to satisfactory agreement on refinement in this space group. No extensive attempts have been made to find a solution in the alternate lower symmetry space group, and therefore the lower symmetry space group is not entirely ruled out.

The number of independent reflections measured (after averaging common reflections which were measured in more than one layer) was 827, of which 258 were below the observable limit.

Structure solution:

The atomic coordinates of $LiMnPO_4$(75) were used as the initial parameters, with cobalt at Li and Mn sites, and arsenic at the P site. The composition $Co_3(AsO_4)_2$ (assumed at this stage by analogy with the composition of sarcopside(74)) was accounted for by assuming that the cobalt site at the origin (site symmetry $\bar{1}$) was only half occupied, whereas the remaining cobalt site (lying on a mirror plane), and also the arsenic and oxygen sites, were fully occupied.

Structure factors were calculated for 148 reflections, consisting of measurements from the $0k\ell$, $hk0$ and $h0\ell$ layers.

Individual scale constants for the 3 layers of data were refined along with the positional coordinates of the atoms and individual isotropic thermal factors. Unit weights were used in this refinement. After 2 cycles of refinement the R_1-value for the 148 reflections was 0.17. The relatively good agreement at this stage suggested that the trial structure was essentially correct.

The refinement was continued with all the 827 reflections. The isotropic temperature factors were converted to anisotropic temperature factors. The weighting scheme was changed from unit weights for all reflections, to a Cruickshank-type weighting scheme(40), of the form $w = (2.0+0.155\ |F_{obs}| + 0.002\ |F_{obs}|^2)^{-1}$. A total of 52 parameters consisting of 13 scale factors for the 13 layers of data measured, and the positional coordinates and anisotropic temperature factors of all the atoms, were refined. The minimum was reached at the R_1-value of 0.107 and the weighted R_w-value of 0.110 for all the reflections.

At this stage the occupancy factors of the cation sites were included as parameters in the refinement. Because of the expected strong correlation between the occupancy factor of a given atom site and the temperature factor of the corresponding atom, the occupancy factors were refined only in those cycles in which the temperature factors were kept fixed, and vice versa. The minimum for this refinement with 55 parameters was reached at the R_1-value of 0.073, and the weighted R_w-value of 0.085.

Table (8-1) lists the occupancy factors and positional parameters of the atoms resulting from this refinement. Calculation of the bond distances and angles in the structure shows that the two crystallographically independent cobalt atoms, Co(1) and Co(2), both have distorted octahedral environment of oxygen atoms. The mean Co(1)-O and Co(2)-O distances are 2.133(6) and 2.166(5) Å respectively. The arsenic atom has a nearly tetrahedral environment of oxygen atoms, with the mean As-O distance of 1.665(6) Å. The observed Co-O distances for both Co(1) and Co(2) compare well with the distances expected for octahedrally coordinated Co^{+2} ion with high-spin electronic configuration$^{(77)}$, and the observed As-O distances compares well with the distances observed for tetrahedrally coordinated As^{+5} ion. The composition derived from the least-squares refinement corresponds to $Co_{6.0}As_{3.15}O_{16}$, with estimated standard deviations of 0.1 and 0.06 on the number of cobalt atoms and arsenic atoms respectively.

Though the observed As-O and Co-O distances suggest that cobalt ion is in the divalent state with high-spin electron configuration and arsenic ion in pentavalent state in this compound, overall charge neutrality is not preserved in the derived composition when formal charges of +2 and +5 are assigned to cobalt and arsenic respectively in the compound. In fact, overall charge neutrality for the compound with the composition $Co_{6.0}As_{3.15}O_{16}$ requires that almost all the cobalt be present

TABLE (8-1)

Atomic parameters corresponding to minimum with all cation site occupancy factors varied.

(Estimated standard deviations in parentheses)

Atom	Site Symmetry	Occupancy factor	Positional parameters			Thermal parameters (x 10^4) $Å^2$					
			x	y	z	U_{11}	U_{22}	U_{33}	U_{12}	U_{13}	U_{23}
Co(1)	m	0.452(9)	0.27531(11)	1/4	0.9896(3)	87(4)	133(9)	124(5)		5(4)	
Co(2)	i	0.285(6)	0	0	0	88(5)	122(14)	105(5)	-43(7)	17(5)	-31(9)
As	m	0.397(8)	0.09449(11)	1/4	0.4283(3)	90(4)	190(9)	111(5)		9(3)	
O(1)	m	0.5	0.0964(6)	1/4	0.7692(15)	83(19)	232(48)	132(26)		8(19)	
O(2)	m	0.5	0.4485(6)	1/4	0.2033(15)	73(18)	220(47)	151(26)		20(19)	
O(3)	1	1	0.1686(5)	0.0337(11)	0.2783(12)	192(19)	177(30)	160(20)	26(23)	24(17)	14(22)

in the trivalent state, if it is assumed that arsenic has a formal oxidation state of +5 in this compound. However, the observed Co(1)-O and Co(2)-O bond distances, 2.133(5) Å and 2.166(5) Å respectively, do not agree with expected trivalent cobalt-oxygen distances. The expected Co^{+3}-O distance is about 1.92 Å if low-spin electron configuration is assumed for trivalent cobalt(77), and about 2.00 Å if high spin configuration is assumed(1). Thus the observed Co-O bond distances are in disagreement with the derived composition $Co_{6.0}As_{3.15}O_{16}$.

An electron density difference map computed at this stage did not indicate any unexplained structural features. Thus the cause of the disagreement between the valence states suggested for the cations by the observed bond distances on the one hand, and by the derived composition on the other, was not clear.

Therefore an attempt was made to determine the cause of the discrepancy and to correct the deficiency in the proposed model. The correlation matrix was computed and this revealed that the most probable cause of the anomalous results was the very strong correlation between the individual layer line scale factors and the occupancy factors of the cation sites, and between the occupancy factors of the three cation sites themselves. The coefficients in the correlation matrix corresponding to correlations of the former type ranged between -0.56 to -0.94, and those corresponding to correlations of the latter type were larger than 0.94. Such strong correlations between the occupancy factors of the three independent cation sites had not been anticipated in the course of the refinement.

The strong correlation that exists between the occupancy factors of the three independent cation sites suggests that the finer details of the crystal such as the exact composition, and accurate bond distances in the structure cannot be unequivocally determined purely from the least-squares refinement of the present x-ray data. In this sense, the situation is analogous to the case of $BaTiO_3$ (78).

In order to overcome these difficulties, the assumptions were made that cobalt in the compound has a formal oxidation state of +2, and arsenic has a formal oxidation state of +5. The assumptions are reasonable since the observed bond lengths in the structure are in agreement with these assumptions.

However all three cation sites (Co(1), Co(2), and As) in the structure cannot be simultaneously fully occupied under these circumstances. Thus occupancy disorder of at least some of the cation sites is inevitable in any model postulated under restrictions of these assumptions.

The charge neutrality condition for the contents of the unit cell containing 16 oxygen atoms in the present case, can be expressed by the relation

$$[(p \times 2) + (q \times 2) + (r \times 5)] \times 8 = 32 \qquad (8-1)$$

where p, q and r are the occupancy factors of the Co(1), Co(2) and As sites respectively. The factor 8 in this relation refers to the multiplicity of the general position in the space group Pnma.

Structure factors were calculated for all the reflections for the four models listed in Table (8-2), each with a different combination of occupancy factors for the three cation sites, and all satisfying the restricting condition represented by eq. (8-1). Each model was refined using an overall scale factor for all data, determined by the method of Hamilton et al.(79). In addition to the overall scale factor, the positional coordinates and individual isotropic temperature factors of all atoms were refined. The positional coordinates listed in Table (8-1) were used as the initial trial parameters. After two cycles of refinement, the R_1-value had dropped to less than 0.15 for all models (Table 8-2) except model 4, for which the R_1-value was 0.265. Therefore refinement of this last model was discontinued at this stage, while the other three models were refined till the minimum was reached in each case. The mean cation-oxygen bond lengths, the temperature factors of the cations, and the R_1-value corresponding to the minimum, as also the unit cell content assumed in each of these models, are compared in Table (8-2). The mean cation-oxygen distances in models 1, 2 and 3 are not significantly different. However, the values of the temperature factors of the three cations show significant differences between the three models. On the basis of the thermal

Table (8-2)

Comparison of the four models with cation site occupancy factors fixed

	Model 1	Model 2	Model 3	Model 4
Occupancy factor of Co(1) site	0.5	0.5	0.375	0.25
Occupancy factor of Co(2) site	0.5	0.25	0.375	0.5
Occupancy factor of (As) site	0.4	0.5	0.5	0.5
R_1-value corresponding to minimum	0.130	0.129	0.144	(0.265)†
<Co(1)-O> in Å	2.13(1)	2.14(1)	2.13(1)	2.14(1)
<Co(2)-O> in Å	2.16(1)	2.16(1)	2.17(1)	2.17(1)
<As-O> in Å	1.68(1)	1.66(1)	1.67(1)	1.65(1)
u(Co(1)) in Å2	0.0079(4)	0.0086(4)	0.0014(4)	-0.0075(7)
u(Co(2)) in $Å^2$	0.0212(7)	0.0021(5)	0.0134(7)	0.0103(9)
u(As) in $Å^2$	0.0073(5)	0.0135(5)	0.0145(6)	0.009 (1)
Unit cell content corresponding to the model assumed	$Co_8As_{3.2}O_{16}$	$Co_6As_4O_{16}$	$Co_6As_4O_{16}$	$Co_6As_4O_{16}$

†The convergence in this case was relatively slow, and refinement of this model was discontinued in favour of the other models after two cycles of refinement.

parameters observed for cobalt and arsenic in other structures (Ch. 3, 4, 6), values for u for these atoms in the present structure can be expected to be of the order of 0.01 $\mathring{A}^2$. The values of u(Co(1)) are closer to the expected value in models 1 and 2 than in model 3. This suggests that the value of 0.5 assumed for the occupancy factor of this site in models 1 and 2 is likely to be closer to the true occupancy factor in the structure, than the value of 0.375 assumed in model 3.

The values of the occupancy factors and the corresponding u(Co(2)) values in the three models suggest that the occupancy factor for this site should be intermediate between 0.5 and 0.25 assumed in models 1 and 2, and close to 0.375 assumed in model 3.

Similar comparison of u(As) and the corresponding occupancy factors of the As site in the three models suggests that the true occupancy factor for this site in the structure probably lies between 0.4 and 0.5 assumed in models 1 and 2 respectively.

Thus, the value for the occupancy factor of the Co(1) site in the correct model is likely to be close to that in models 1 and 2, and for the other two sites the values in the correct model are likely to lie between their respective values in models 1 and 2. In other words, the correct unit cell content is most probably somewhere intermediate between $Co_8As_{3.2}O_{16}$ and $Co_6As_4O_{16}$ assumed in models 1 and 2 respectively.

Further refinement of models 1 and 2 were undertaken separately with the objective of determining the true composition of the material of the crystal, and also the accurate positional and thermal parameters of the atoms in the structure. Since it was anticipated that independent refinements of the two models might lead to the same minimum, both the refinements were undertaken simultaneously.

The following approach was taken for the refinement of model 1. An appropriate weighting scheme was chosen from the plot of $|F_{obs}|$ vs. Δ^2, where $\Delta = \big| |F_{obs}| - |F_{calc}| \big|$. The weighting scheme chosen was: $w = (1/14)$ for $|F_{obs}| \leq 30.0$, and $w = (3.0\ |F_{obs}|$ $87.0)^{-1}$ for $F_{obs} > 30.0$. Initially, the values of the occupancy factors p, q and r (eq. 8-1) had been set to 0.5, 0.5 and 0.4 respectively in this model (Table 8-2). The parameter p was varied in the first cycle, and the value changed from 0.5 to 0.509(5). However, since the maximum value for p permitted by the space group symmetry is 0.5, the refinement of this parameter to a higher value is not physically meaningful. Therefore the value of p was reset to 0.5 and not varied in subsequent refinements. The charge neutrality condition (8-1) could therefore be rewritten as

$$[(q \times 2) + 1.0 + (r \times 5)] \times 8 = +32 \quad . \qquad (8\text{-}2)$$

The occupancy factor q was refined in the next step. There was a significant decrease in the value of q, and the new value was 0.473(5). The value of r was changed from the initial value of 0.4 to that given by eq. (8-2). With these new values of q and r fixed, the overall scale factor, the individual temperature factors, and the positional coordinates of all the atoms were refined for one cycle. At the end of this cycle, the parameter q was varied again, and the process was continued until the changes in the parameters were less than the estimated standard deviations in these parameters. The composition derived from the least-squares refinement corresponds to $Co_{7.0}As_{3.6}O_{16}$ to within 3 estimated standard deviations on both the number of cobalt and arsenic atoms ($1\sigma = 0.03$ in both cases). The mean Co(1)-O, Co(2)-O, and As-O bond distances are found to be 2.13(1), 2.16(1), and 1.67(1) Å respectively.

A parallel approach was made for the refinement of model 2. The weighting scheme used in this case was: $w = (3.0+|F_{obs}|+0.01|F_{obs}|^2)^{-1}$. The minimum in the refinement was reached at the R_1-value of 0.104 and the weighted R_w-value of 0.124. The composition derived from the least-squares refinement corresponds to $Co_{6.6}As_{3.8}O_{16}$ to within three estimated standard deviations both on the number of cobalt and arsenic atoms ($1\sigma = 0.03$ for both the number of cobalt and arsenic atoms in the unit cell). The mean Co(1)-O, Co(2)-O, and As-O bond distances are found to be 2.14(1), 2.17(1), and 1.66(1) Å respectively. The agreement between the observed and calculated structure factor amplitudes is poorer for this model than for model 1, considering that the number of parameters are identical in both the cases.

The atomic positional and thermal parameters resulting from the refinements of the two models, and the occupancy factors of the atom sites in each of these, are compared in Table (8-3). It is found that the positional parameters for all the atoms are the same in the two cases within one e.s.d. Thus the difference between the two models is in the unit cell contents in the two cases, and in the temperature factors of atoms Co(2) and As. From the present results, the assignment of the composition $Co_{7.0}As_{3.6}O_{16}$ resulting from refinement of model 1 is preferred, since this gives better agreement between the observed and calculated structure factor amplitudes. These are compared in Table (8-4) for model 1. The more important bond distances and angles in the structure are given in Table (8-5).

Description and discussion of the structure: Oxidation states of the cations: The model proposed has been derived on the assumption that cobalt occurs with a formal oxidation state of +2 and arsenic with +5 in this structure. The validity of the model therefore depends on the validity of this assumption. The observed Co-O and As-O distances are in agreement with the assignment of +2 and +5 oxidation states for cobalt and arsenic respectively. The relatively good agreement between the observed and calculated structure factor amplitudes indicated by the overall R_1-value of 0.101 suggests that the proposed model, and the derived composition based on this model, very nearly

Table (8-3)†

Comparison of atomic parameters corresponding to the minima in models 1 and 2

(The values of the parameters in model 2 are in [ ] brackets)

Atom	Occupancy factor	Positional parameters			Temperature factor u(Å^2)
		x	y	z	
Co(1)	0.5	0.2754(2)	0.25	-0.0100(4)	0.0082(2)
	[0.5]	[0.2754(2)]	[0.25]	[-0.0104(3)]	[0.0087(3)]
Co(2)	0.374(4)	0	0	0	0.0117(4)
	[0.329(3)]	[0]	[0]	[0]	[0.0086(4)]
As	0.451(4)	0.0945(1)	0.25	0.4286(3)	0.0102(3)
	[0.470(3)]	[0.0943(2)]	[0.25]	[0.4286(3)]	[0.0120(2)]
01	0.5	0.0975(8)	0.25	-0.229(2)	0.007(1)
	[0.5]	[0.0968(8)]	[0.25]	[-0.231(2)]	[0.008(1)]
02	0.5	0.4480(8)	0.25	0.204(2)	0.007(1)
	[0.5]	[0.4487(8)]	[0.25]	[0.203(2)]	[0.008(1)]
03	1.0	0.1676(6)	0.033(2)	0.279(1)	0.011(1)
	[1.0]	[0.1679(6)]	[0.035(2)]	[0.278(1)]	[0.012(1)]

---

† Estimated standard deviations are in parentheses

TABLE (8-4)

OBSERVED AND CALCULATED STRUCTURE FACTOR AMPLITUDES FOR $Co_{7.0}As_{3.6}O_{16}$.

Unobserved reflections are marked by (*) and unreliable reflections by ($).

Table (8-5) †

Bonding geometry in Co$_{7.0}$As$_{3.6}$O$_{16}$

(Estimated standard deviations are in parentheses)

Atoms forming bond	Coord.no. of oxygen atom	Bond Length (Å)	atoms forming edge or diagonal	Edge length (±0.01Å)	Angle subtended at the central cation site (degrees)	Edge Shared with
AsO$_4$ group						
As-O1a	4	1.664(9)	O3a -O3c'	2.58	101.5(4)	Co(1)O$_6$
-O2b	4	1.664(9)	O2b -O3a	2.64	104.8(3)	Co(2)O$_6$
-O3a	4	1.669(8)	O2b -O3c'	2.64	104.8(3)	Co(2)O$_6$
-O3c'	4	1.669(8)	O2b -O1a	2.79	113.8(5)	-
			O3a -O1a	2.82	115.2(3)	-
			O3c'-O1a	2.82	115.2(3)	-
Co(1)O$_6$ group						
Co(1)-O3d	4	2.065(8)	O3d -O3c'		159.8(3)	
-O3b'	4	2.065(8)	O3b'-O3a		159.8(3)	
-O1a	4	2.146(9)	O1a -O2a		179.9(2)	
-O2a	4	2.087(9)				
-O3a	4	2.217(8)				
-O3c'	4	2.217(8)				

(continued next page)

Table (8-5) (continued)

Atoms forming bond	Coord.no. of oxygen atom	Bond length (Å)	Atoms forming edge or diagonal	Edge length (±0.01Å)	Angle subtended at the central cation site (degrees)	Edge Shared with
$Co(1)O_6$ group (continued)						
			03a-03c'	2.59	71.3(3)	AsO_4
			01a -03a	2.88	82.6(3)	$Co(2)O_6$
			01a -03c'	2.88	82.6(3)	$Co(2)O_6$
			03b'-02a	2.93	89.8(2)	-
			03d -02a	2.93	89.8(2)	-
			03b'-01a	2.99	90.3(2)	-
			03d -01a	2.99	90.3(2)	-
			03b'-03c'	3.01	89.1(3)	-
			03d -03a	3.01	89.1(3)	-
			02a -03a	3.23	97.3(3)	-
			02a -03c'	3.23	97.3(3)	-
			03b'-03d	3.38	109.9(4)	-
$Co(2)O_6$ group:						
Co(2)-01a	4	2.122(6)				
-01a'	4	2.122(6)				
-02b	4	2.143(6)				
-02b'	4	2.143(6)	01a -01a'		180.0(4)	
-03a	4	2.228(7)	02b -02b'		180.0(4)	
-03a'	4	2.228(7)	03a -03a'		180.0(4)	

(continued next page)

Table (8-5) (continued)

Atoms forming bond	Coord.no. of oxygen atom	Bond length (Å)	Atoms forming edge or diagonal	Edge length (±0.01Å)	Angle subtended at the central cation site (degrees)	Edge shared with
			02b -03a	2.64	74.3(3)	AsO_4
			02b'-03a'	2.64	74.3(3)	AsO_4
			01a -03a	2.88	82.9(3)	$Co(1)O_6$
			01a'-03a'	2.88	82.9(3)	$Co(1)O_6$
			02b -01a	2.99	89.1(2)	$Co(2)O_6$
			02b'-01a'	2.99	89.1(2)	$Co(2)O_6$
			02b -01a'	3.04	90.9(2)	-
			02b'-01a	3.04	90.9(2)	-
			01a -03a'	3.26	97.1(3)	-
			01a'-03a	3.26	97.1(3)	-
			02b -03a'	3.48	105.7(3)	-
			02b'-03a	3.48	105.7(3)	-

---

§Symmetry transformations : a: (x,y,z); b: $(\frac{1}{2}+x, \frac{1}{2}-y, \frac{1}{2}-z)$ c: $(\bar{x}, \frac{1}{2}+y, \bar{z})$;
d: $(\frac{1}{2}-x, \bar{y}, \frac{1}{2}+z)$;
a': $(\bar{x},\bar{y},\bar{z})$; b': $(\frac{1}{2}-x, \frac{1}{2}+y, \frac{1}{2}+z)$; c': $(x, \frac{1}{2}-y, z)$;
d': $(\frac{1}{2}+x, y, \frac{1}{2}-z)$.

represent the true situation in the structure. Independent confirmation of the valence states of cobalt and arsenic, and of the composition of the compound, will be very valuable in verifying the present results. Attempts at independent confirmation of these results have been hampered by lack of enough pure material. Electron microprobe analysis for the cobalt and arsenic contents in the crystal have been attempted, but have not yielded satisfactory results because of instrumental failures.

The composition derived from the least-squares refinement of the present x-ray data corresponds to $Co_{7.0}As_{3.6}O_{16}$, with expected errors of about 0.1 on the number of cobalt and arsenic atoms. This composition corresponds very closely to the formulation $4CoO{\cdot}As_2O_5$. The similarity is easily recognized when this latter formulation is written in the equivalent form $Co_{7.11}As_{3.56}O_{16}$. However, the compound $4CoO{\cdot}As_2O_5$ or its nickel analog has not been identified in the studies of Taylor and Heyding(10), Masson(11), and Masson et al.(12). The present results suggest that a reinvestigation of the phase diagram of $CoO\text{-}As_2O_5$ and $NiO\text{-}As_2O_5$ systems is necessary. Compositions of the type $4MO.X_2O_5$ with (M=Ca,Sr,Ba or Cu) and (X=P,V, or As) have been reported(80,81), and by analogy one might expect similar stable compositions in the cases of cobalt and nickel as well under suitable conditions.

The major structural aspects of $Co_{7.0}As_{3.6}O_{16}$ are similar to those of olivine, Mg_2SiO_4(72). The structure consists of nearly hexagonally closest-packed oxygen atom layers (AB... sequence). The stacking direction is parallel to the $\underline{a}_3$ axis. The unit cell dimensions are consistent with those expected in structures based on closest-packing of oxygen atoms (Ch. 2).

The arsenic atom has a highly distorted tetrahedral environment of oxygen atoms. The three independent oxygen atoms 01, 02 and 03 in the structure have similar cation environments, and each is strongly bonded to one arsenic and three cobalt atoms. Thus the individual As-O bond distances in the AsO_4 group are not expected to differ significantly(1,49). The observed individual As-O distances in the structure are consistent with this expectation (Table 8-5).

The AsO_4 group shares two of its edges with two $Co(2)O_6$ groups and a third edge with a $Co(1)O_6$ group. The lengths of the edges of the AsO_4 group and the angles subtended by these edges at the As site are included in Table (8-5). It is found that the angles subtended by the shared edges are smaller than the ideal tetrahedral angle. Also, the shared edges are significantly shorter than the unshared edges. Thus the angular distortions in the AsO_4 group are correlated to the electrostatic repulsion between the cations at the centres of the polyhedral groups sharing edges (Ch. 2). It is interesting that the shortest edge, involving oxygen atoms 03a and 03c', is shared with $Co(1)O_6$ group, whereas the other two shared edges are slightly longer and are shared with $Co(2)O_6$ groups. The difference in the edge lengths is consistent with the lower average occupancy of the Co(2) site compared to the Co(1) site.

There are two crystallographically independent cobalt atoms, Co(1) and Co(2), in the structure. Both of these have distorted octahedral environments of oxygen atoms. The average Co(1)-O and Co(2)-O bond distances are 2.13(1) Å and 2.16(1) Å respectively, and are within 2 standard deviations of each other. The distances are comparable with Co^{+2}-O distances observed in other well refined structures containing divalent cobalt in octahedral coordination with oxygen atoms.

The individual Co(1)-O bonds and Co(2)-O bonds in the $Co(1)O_6$ and $Co(2)O_6$ groups respectively show significant variations between themselves, and range between 2.07(1) and 2.22(1) Å in the former, and between 2.12(1) and 2.23(1) Å in the latter. Since the first-neighbour environments of all the oxygen atoms are similar, it is not clear why there are such large differences in the individual bond lengths.

The angles subtended by the edges of the $Co(1)O_6$ group at Co(1) show wide variations, and range from 71.3(3)° to 109.9(4)°. The angular distortion of the $Co(1)O_6$ group may be interpreted as arising from sharing of some of the edges of this group with other polyhedral groups. In order to illustrate this, it is convenient to consider the Co(1)O_6 group as consisting of an equatorial plane of oxygen atoms O3a, O3c', O3b' and O3d, with the remaining two oxygen atoms O1a and O2a lying in axial positions on an axis nearly perpendicular to this plane. The edge (O3a-O3c') of the Co(1)O_6 group is shared with an AsO_4 group having the arsenic site approximately in the equatorial plane of oxygen atoms of the Co(1)O_6 group. The electrostatic repulsive forces between the Co^{+2} ion and As^{+5} ion involved in the edge-sharing will tend to displace both these ions away from each other. In particular, the Co^{+2} ion will move away from the shared edge, and towards the (O3b'-O3d) edge. In addition, if the Co-O and As-O distances are assumed to have fixed values, the electrostatic repulsion described above will lead to a shortening of the shared edge relative to its length when the repulsive forces are inoperative. The consequence of these effects will be

(a) a decrease in the length of the shared edge (O3a-O3c') compared to the lengths of the unshared edges;

(b) decrease in the angle subtended by this edge at Co(1) relative to the ideal octahedral angle of 90°;

and

(c) increase in the angle subtended by the (O3b'-O3d) edge at Co(1) compared to the ideal value of 90°.

The short length of 2.59(1) Å for the (O3a-O3c') edge, the small angle of 71.3(3)° subtended by this edge at Co(1), and the large value of 109.9(4)° subtended by the (O3b'-O3d) edge at Co(1), (Table 8-5), are all in accord with these expectations.

The two next shortest edges of the Co(1)O_6 group are the (O1a-O3a) and (O1a-O3c') edges, each of length 2.88(1) Å. Each of these edges is shared with a different Co(2)O_6 group, and subtends an angle of 82.6(3)° at Co(1). The short lengths of these edges and the deviations from ideality in the angles subtended by these at the Co(1) site may both be attributed to the repulsion between the Co(1) and Co(2) ions sharing the common edge. However, if this is the cause of the significant decrease from 90° in the angles subtended by these shared edges at Co(1), then one would anticipate that the angles subtended by the opposite edges (O3b'-O2a) and (O3d-O2a) respectively at Co(1) should both be significantly larger than 90°. This is not found to be the case, and both these angles are 89.8(2)°. Thus, the electrostatic repulsion between the Co(2) ions sharing common edges does not seem to be the significant factor contributing to the angular distortion in the Co(1)O_6 group. However, it seems possible to attribute the angular distortions in the Co(1)O_6 group to the electrostatic repulsions between Co(1)$^{+2}$ and As^{+5} ions sharing common edges in the structure. Thus, each of the edges which subtends an angle significantly different from 90° at Co(1) involves an oxygen atom which is expected to have suffered significant displacement from its ideal position in a regular octahedral arrangement, as a result of edge-sharing between an As^{+5} and a $Co(1)^{+2}$ ion. Thus, it appears that the angular distortions in the $Co(1)O_6$ group arise almost entirely because of sharing of common edges between arsenic and cobalt ions, and that edge-sharing between two cobalt ions does not contribute significantly to the observed distortions.

The $Co(2)^{+2}$ ion lies at a site of $\bar{1}$ symmetry. The $Co(2)O_6$ group shares six of its edges with other polyhedral groups in the structure. The edge lengths and the angles subtended by the edges of the $Co(2)O_6$ group at Co(2) are included in Table (8-5). The (02b-03a) edge and the (02b'-03a') edge are each shared with a different AsO_4 group. The angle of 74.3(3)° subtended by each of these edges at Co(2), the angle of 105.7(3)° subtended at Co(2) by the (02b-03a') and by the (02b'-03a) edges, and the short length of 2.64(1) Å for the (02b-03a) and (02b'-03a') edges, can all be considered to be consequences of the expected strong repulsion between the $Co(2)^{+2}$ ion and the As^{+5} ions sharing common edges.

However, the other angular distortions in the $Co(2)O_6$ group are not explained by the destabilising effects that might be expected to arise as a consequence of sharing of some of the other edges of the $Co(2)O_6$ group with other CoO_6 groups. Thus, while the angles subtended at Co(2) by the edges shared in common between the $Co(2)O_6$ group and a $Co(1)O_6$ group is

82.9(3)° (Table 8-5), those subtended by edges shared in common between two Co(2)O_6 groups do not differ significantly from the ideal octahedral angle of 90°, and are equal to 89.1(2)°. The situation is analogous to that encountered in the case of the Co(1)O_6 group. The edges shared in common between two cobalt ions and subtending angles significantly different from the ideal octahedral angle of 90° at Co(2), are formed of two oxygen atoms one of which is expected to have undergone significant displacement from its ideal position in a regular octahedral arrangement, as a result of edge-sharing between an As^{+5} ion and the $Co(2)^{+2}$ ion of the Co(2)O_6 group.

The common features of the structure of $Co_{7.0}As_{3.6}O_{16}$ to the other cobalt arsenates and related structures described in this thesis will be discussed in the concluding chapter.

CHAPTER 9

CONCLUSION

The details of the space group and cell dimensions of the structures described in the previous chapters are collected in Table (9-1). The cell dimensions of the tetragonal form of cobalt orthoarsenate (No. 5 in the table) were measured from an uncalibrated ($h0\ell$) precession photograph of a polycrystalline specimen, and hence no estimate of the accuracy of the cell dimensions is given. No structural investigation was undertaken for this compound, and for the purposes of the present discussion it is assumed that this compound is completely isomorphous with $Mg_3(AsO_4)_2$ (Ch. 5) in its structural features such as the packing and the coordination numbers of the cations in the structure.

Structural relationships between the different cobalt arsenates:

Of the five cobalt arsenates investigated, the first three are related structurally in the sense that these can be described in terms of closest packing of oxygen atoms, with the smaller cations in the structure occupying octahedral and tetrahedral voids in the packing. The unit cell dimensions in the three cases are consistent with the values expected in structures containing closest packing of oxygen atoms (Ch. 2), and the agreement is indicated in brackets following the axes lengths.

Table (9-1)

No.	Compound	Unit cell dimensions	Vol. per oxygen atom in the unit cell ($Å^3$)	Stacking sequence	Identity period	Reference
1	$Co_3(AsO_4)_2$	Monoclinic ($P2_1/c$) $\underline{a}_1$=5.83Å(∼2×2.8Å) $\underline{a}_2$=9.68Å(∼4×2.3Å) $\underline{a}_3$=10.34Å(∼4×2.4Å) β = 93.42°	18.2	ABAC...	4	Ch. 3
2	$Co_{7.09}As_{3.6}O_{16}$	Orthorhombic (Pnma) $\underline{a}_1$=10.48Å(∼4×2.4Å) $\underline{a}_2$=5.97Å(∼2×2.8Å) $\underline{a}_3$=4.86Å(∼2×2.3Å)	19.0	AB...	2	Ch. 8
3	$Co_{24.2}As_9O_{48}$	Trigonal ($R\bar{3}m$) $\underline{a}_1$=6.05Å(∼2×2.8Å) $\underline{a}_3$=28.06Å(∼12×2.3Å)	18.5	ABC...	12	Ch.4

(continued next page)

Table (9-1) (continued)

No.	Compound	Unit cell dimensions	Vol. per oxygen atom in the unit cell (Å^3)	Stacking sequence	Identity period	Reference
4	$Co_2As_2O_7$	Triclinic ($C\bar{1}$) $\underline{a}_1$=6.60 Å, $\underline{a}_2$=8.53 Å, $\underline{a}_3$=4.75 Å α = 90.5°, β =103.1°, γ =91.1°	18.6	AB...	2	Ch. 6
5	$Co_3(AsO_4)_2$	Tetragonal ($I\bar{4}2d$) $\underline{a}_1 \simeq$ 6.9 Å $\underline{a}_3 \simeq$ 19.3 Å	∿19.1			Ch. 5
6	$Mg_3(AsO_4)_2$	Tetragonal ($I\bar{4}2d$) $\underline{a}_1$ = 6.79 Å $\underline{a}_3$ = 18.98 Å	18.2			Ch. 5
7	$Mg_3(VO_4)_2$	Orthorhombic (Cmca) $\underline{a}_1$ = 6.053 Å $\underline{a}_2$ = 11.442 Å $\underline{a}_3$ = 8.330 Å	18.0	ABC...	6	Ch. 7

The similarity is further brought out by comparison of the volume per oxygen atom in the unit cell, given in col. 4 of Table (9-1). The major differences between these structures are in the identity period of the stacking (i.e. the number of layers normal to the stacking direction per unit translation in the stacking direction), and in the ratio of cobalt to arsenic content in the compounds. $Co_3(AsO_4)_2$, $Co_{7.0}As_{3.6}O_{16}$ and $Co_2As_2O_7$ have also the common feature that in these compounds the cobalt atoms occupy only octahedral voids and the arsenic atoms occupy only tetrahedral voids. $Co_{24.2}As_9O_{48}$ and tetragonal $Co_3(AsO_4)_2$ differ from the others and between themselves in this aspect of their structures. In $Co_{24.2}As_9O_{48}$, all the cobalt atoms have octahedral coordination, and two-thirds of the arsenic atoms have tetrahedral coordination while the remaining are octahedrally coordinated. In tetragonal $Co_3(AsO_4)_2$, while all the arsenic atoms in the structure are tetrahedrally coordinated, two of the eighteen cobalt atoms in the unit cell have a distorted cubic coordination, while the remaining are octahedrally coordinated.

$Co_2As_2O_7$ differs from the others in that pairs of AsO_4 groups share corners (resulting in As_2O_7 units) in $Co_2As_2O_7$, whereas the other cobalt arsenates contain discrete AsO_4 groups, and in addition discrete AsO_6 groups in the case of $Co_{24.2}As_9O_{48}$.

The average Co-O and As-O bond distances for octahedrally coordinated cobalt and tetrahedrally coordinated arsenic in the different cobalt arsenates studied in the present work are compared in Table (9-2). The average bond distances do not differ significantly at the 99.9% confidence limit in the cases compared.

Structural relationships between the two forms of $Co_3(AsO_4)_2$:

Two forms of $Co_3(AsO_4)_2$ have been identified. The structure of the monoclinic form has been investigated in detail (Ch. 3). The tetragonal form is isostructural with $Mg_3(AsO_4)_2$ (Ch. 5), as is revealed from a comparison between the intensities and symmetry of the diffraction patterns of the two compounds. The crystal-chemical relationship between the two forms of $Co_3(AsO_4)_2$ is not obvious, since the monoclinic form is based on a closest packing of oxygen atoms, whereas the tetragonal form is not based on a closest packing motif. The former contains all the cobalt in octahedral sites, while in the latter, two of the eighteen cobalt atoms have a highly distorted cubic coordination, and the remaining have octahedral coordination. Both the forms contain isolated AsO_4 tetrahedra, with each oxygen atom bonded to only one arsenic atom. The average volume per oxygen atom is 18.2 $\mathring{A}^3$ in the monoclinic form, and about 19.1 $\mathring{A}^3$ in the tetragonal form. The closely comparable values suggest that the packing efficiencies are similar in both cases.

The number of polyhedral elements of different types shared in the two forms per volume unit containing 16 oxygen

Table (9-2)[§]

Mean cation-oxygen bond distances in CoO_6 and AsO_4 groups in cobalt arsenates

Compound	Group	<Co-O> (Å)	group	<As-O> (Å)	Reference
$Co_3(AsO_4)_2$	Co(1)O_6	2.11(1)	As(1)O_4	1.69(1)	Ch. 3
	Co(2)O_6	2.12(1)	As(2)O_4	1.70(1)	
	Co(3)O_6	2.13(1)			
$Co_{24.2}As_9O_{48}$	Co(1)O_6	2.13(1)	As(2)O_4	1.69(2)	Ch.4
	Co(2)O_6	2.13(1)			
$Co_2As_2O_7$	CoO_6	2.13(2)	(As_2O_7)[†]	1.69(2)	Ch. 6
$Co_7As_{3.6}O_{16}$	Co(1)O_6	2.16(1)	AsO_4	1.67(2)	Ch. 8
	Co(2)O_6	2.13(1)			

[§] Estimated standard deviations in parantheses

[†] Consists of two centrosymmetrically related AsO_4 groups sharing a common oxygen atom.

atoms are compared in Cols. 2 and 3 of Table (9-3). There are on the average 5 1/3 more edges shared between the different CoO_6 groups in the tetragonal form than in the monoclinic form, while there are four less corners shared between the different CoO_6 groups in the tetragonal compared to the monoclinic form. Also, there are on the average 1 1/3 more edges and 1 1/3 less corners shared between CoO_6 and AsO_4 groups in the tetragonal compared to the monoclinic form. Since polyhedral edge-sharing is less favoured than corner-sharing according to Pauling's postulates regarding sharing of polyhedral elements (Ch. 2), the monoclinic form should be the more stable one. The two forms were obtained in two different preparations, and no attempt has been made to interconvert one form into the other. Questions regarding the relative stabilities of the two forms at finite temperatures can be only answered by detailed consideration of the differences in the energies between the two forms.

Structural relations of $Mg_3(VO_4)_2$ to spinel-like $Co_3(VO_4)_2$:

$Mg_3(VO_4)_2$, whose structure is described in Ch. 7, is based on a closest-packed arrangement of oxygen atoms, even though the choice of axes consistent with the orthorhombic symmetry and space group Cmca does not easily reveal this feature. The structure can be described as consisting of cubic closest packing of oxygen atoms, with the stacking

Table (9-3)

Polyhedral elements shared per volume unit containing 16 oxygen atoms

(1)	(2)	(3)	(4)	(5)
	Tetragonal $Co_3(AsO_4)_2$	Monoclinic $Co_3(AsO_4)_2$	Cubic $Co_3(VO_4)_2$	Orthorhombic $Co_3(VO_4)_2$
Shared corners: M-M†	12	16	24	0
M-X†	$26\,^{2}/_{3}$	28	36	36
X-X	0	0	0	0
Shared edges: M-M	$21\,^{1}/_{3}$	16	30	24
M-X	$5\,^{1}/_{3}$	4	0	0
X-X	0	0	0	0

†M refers to the octahedrally coordinated cation and X to the tetrahedrally coordinated cation.

direction lying parallel to the ($\underline{a}_2$-$\underline{a}_3$) direction, with translational periodicity of 14.14 Å (∿ 6 × 2.3 Å), corresponding to the period of stacking equal to 6. The volume per oxygen atom in the unit cell is equal to 18.0 $Å^3$ (Table 9-1), which is comparable to those in the different closest packed cobalt arsenates, and to that in the cubic closest packed series of oxides isostructural with spinel, Mg_2AlO_4(64).

$Co_3(VO_4)_2$, which has an orthorhombic form(5) isostructural with $Mg_3(VO_4)_2$, has also been reported(4) to have two lower temperature modifications with structures closely related to that of normal spinels. One of these two cubic forms has been isolated (referred to hereafter as Form I), and a trial structure has been proposed for this on the basis of intensity data measured from its powder diffraction pattern. The other low temperature form (referred to hereafter as form II) has not been isolated, but its existence has been reported on the basis of differential thermal analysis. The space group $P4_132$ or $P4_332$ proposed for the low temperature form I is a subgroup of the higher symmetry space group Fd3m of spinels. The trial structure proposed for this form corresponds to an ordered emptying of four of the sixteen octahedral cobalt sites from a hypothetical 'normal spinel' with stoichiometry Co_2VO_4. (The actual structure of Co_2VO_4 itself is an 'inverse spinel' arrangement(82), with eight of the sixteen cobalt atoms in tetrahedral positions). A phase transformation has been observed(4) from form I to the higher temperature orthorhombic form (through the intermediate form II). Therefore it should be possible to relate the structure of the orthorhombic form of $Co_3(VO_4)_2$, and therefore of the isostructural $Mg_3(VO_4)_2$, to tht of the low temperature forms of $Co_3(VO_4)_2$, and thus to that of spinel itself.

Crystallographic data have been reported only for the low temperature form I and for the orthorhombic form$^{(4)}$. A unit cell comparable to that of the orthorhombic form can be chosen for the cubic form I, with the axes $\underline{a}_1'$, $\underline{a}_2'$, $\underline{a}_3'$ of this transformed cell being related to the cubic unit cell axes $\underline{a}_1$, $\underline{a}_2$, $\underline{a}_3$ by

$$\underline{a}_1' = (\underline{a}_3 - \underline{a}_2)/2; \quad \underline{a}_2' = (\underline{a}_2 + \underline{a}_3); \quad \underline{a}_3' = \underline{a}_1.$$

Fig. (9-1) shows the structure of the low temperature form I in projection down the $\underline{a}_1'$ axis of the transformed cell, and fig. (9-2) shows the structure of the high tempeature form projected down the corresponding axis of the orthorhombic cell. It found that the oxygen atom frameworks in the two structures are essentially unchanged. Both the structures are based on cubic closest-packing of oxygen atoms, with the closest packing direction corresponding to $[0\bar{1}1]$ in the diagrams. The closest packed layers perpendicular to this direction are labelled A, B and C in the figures. It is seen from the figures that the VO_4 group in both the structures are packed according to the NONO... packing defined in Ch. 2. There are two types of N layers

Figure legends

Figures (9-1) and (9-2): The large circles represent oxygen atoms, and the small circles refer to magnesium atoms. The oxygen atoms superimpose in pairs in projection, and this has been represented by split circles. When two cobalt atoms superimpose in projection, this has been indicated by half-filled circles. The vanadium positions are indicated by joining these to the positions of the oxygen atoms to which these are bonded. The fractional x-coordinates of the atoms are indicated adjacent to the atom positions.

Figures (9-3) and (9-4): Only the cobalt positions in the structures are shown. The notation used in Figures (9-1) and (9-2) for representing cobalt atom positions is followed.

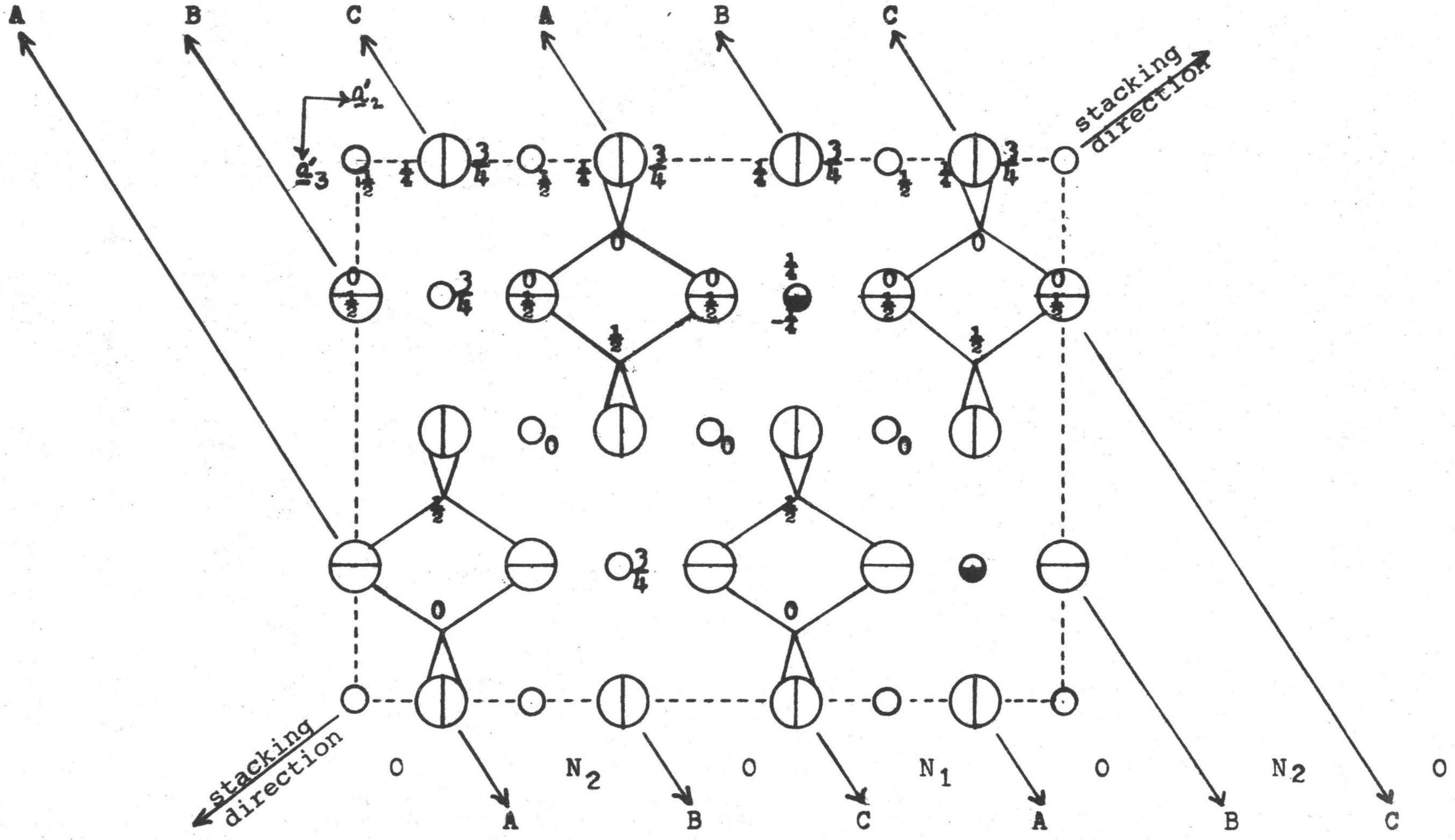

Figure (9-1). Structure of the low temperature form I of $Co_3(VO_4)_2$ projected down the $\underline{a}'_1$ axis of the transformed cell (see text).

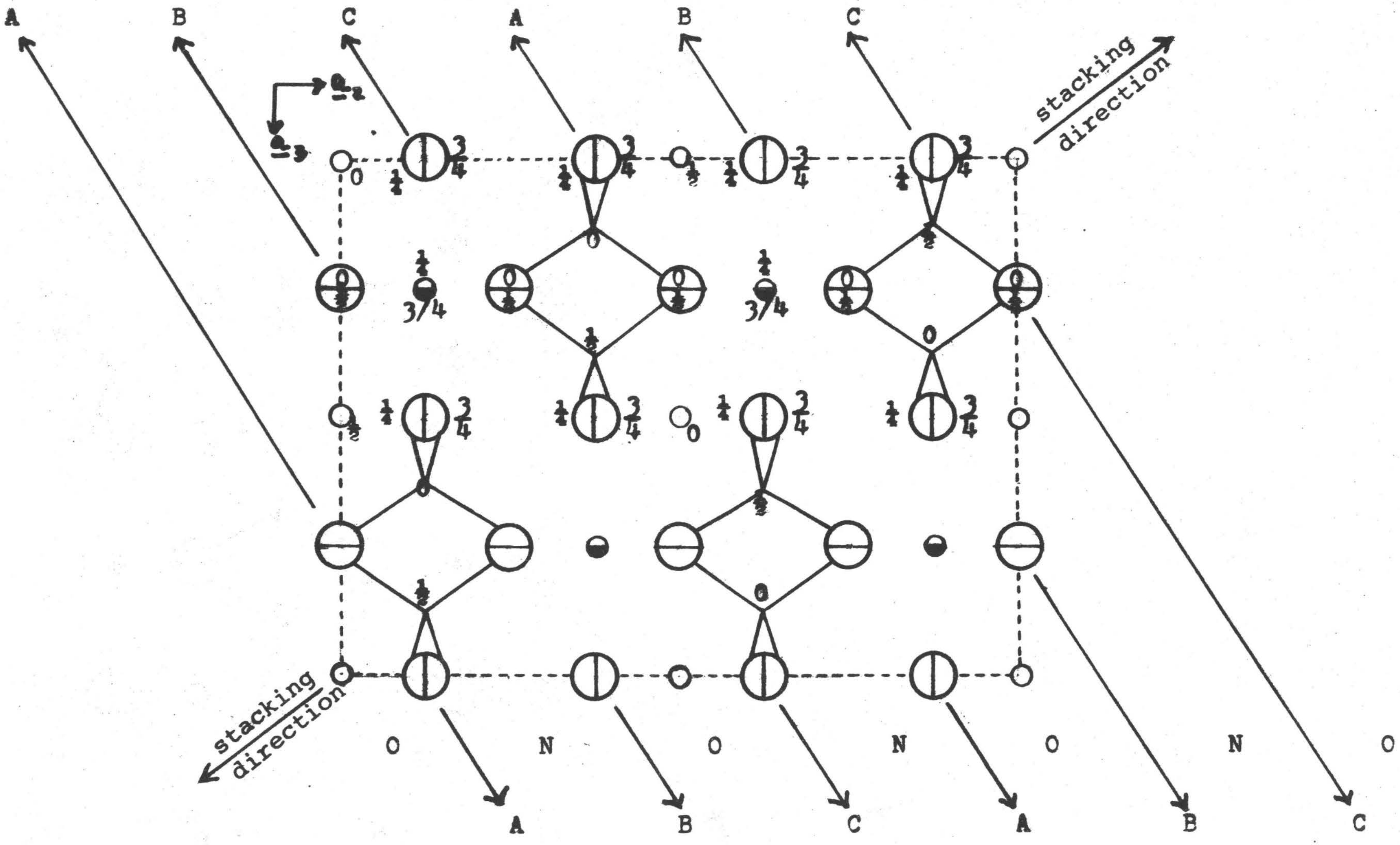

Figure (9-2). Structure of $Mg_3(VO_4)_2$ projected down the $\underline{a}_1$ axis. (This is also the structure of the high temperature form of $Co_3(VO_4)_2$, with Co in Mg positions).

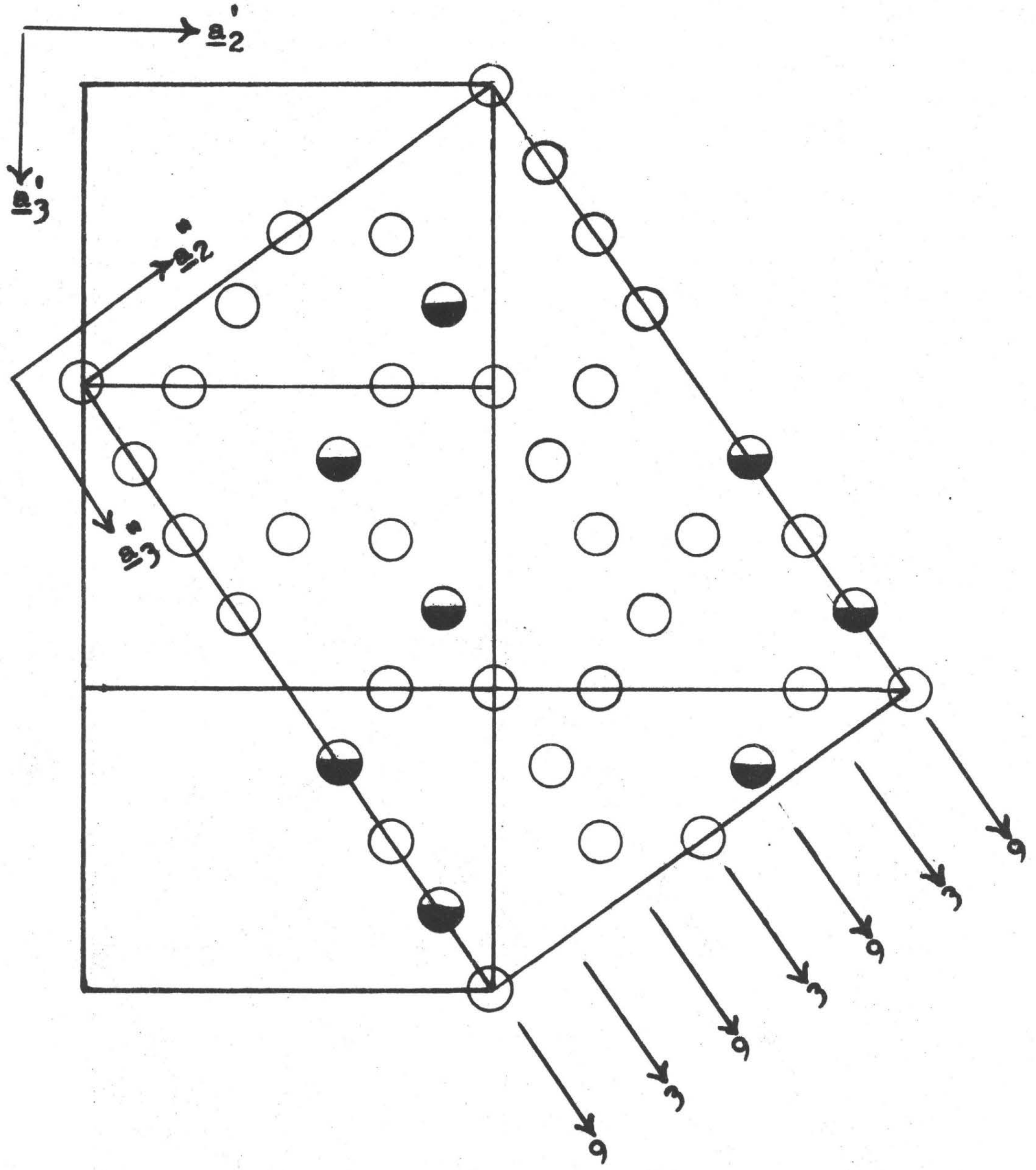

Figure (9-3).

Arrangement of cobalt atoms in layers ∥ to the closest packed oxygen atom layers in the cubic form I of $Co_3(VO_4)_2$.

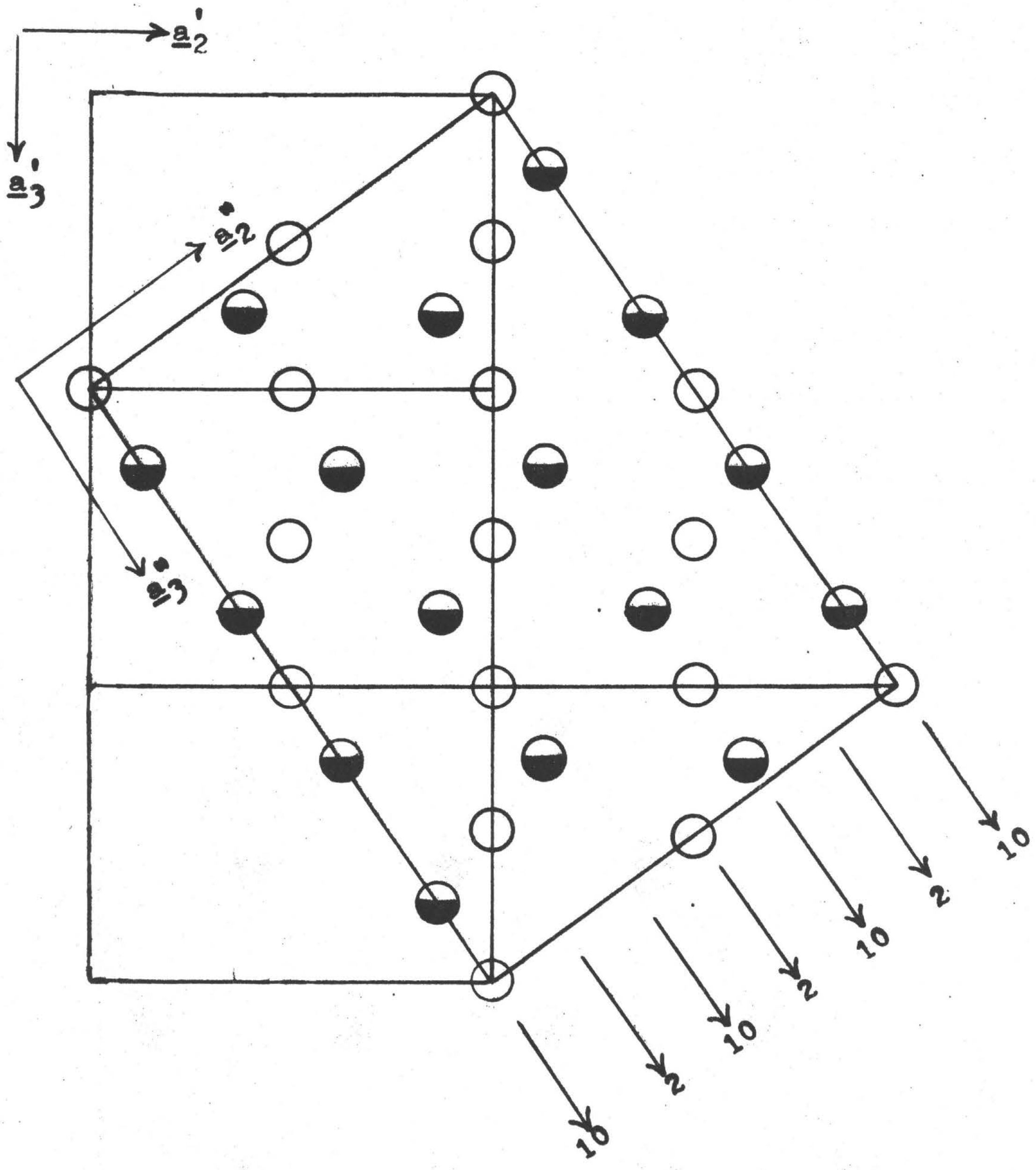

Figure (9-4).

Arrangement of cobalt atoms approximately in planes ∥ to the closest packed oxygen atom layers in the orthorhombic form of $Co_3(VO_4)_2$.

in each structure, and these are denoted as N_1 and N_2 in the figures. The arrangement of VO_4 groups in the N_1 layer is same in the low and high temperature forms. However, the vanadium atoms in the N_2 layers in the two structures are displaced with respect to each other by half a unit cell in the $\underline{a}_1$ direction. Thus the relative arrangements of VO_4 groups in consecutive N layers is different in the two structures.

Consideration of only the first-near neighbour interactions suggests that the two arrangements are equally favourable energetically, since in both cases each vanadium has 4 oxygen atoms tetrahedrally coordinated, each oxygen atom is bonded to only one vanadium atom, and each oxygen atom is surrounded by 12 other oxygen atoms. Because of the difference in the relative arrangements of tetrahedra in the two structures, the octahedral positions that are occupied in the two structures are different (remembering that face-sharing between polyhedra is not favoured).

The difference in the relative arrangements of the occupied octahedral positions in the two structures is illustrated by the description of the structures in terms of layers of closest-packed atoms, with the octahedrally coordinated ions lying in planes parallel to the closest-packed layers (described in Ch. 2). Choice of a set of axes $\underline{a}_1''$, $\underline{a}_2''$, $\underline{a}_3''$, related to the orthorhombic axes $\underline{a}_1'$, $\underline{a}_2'$, $\underline{a}_3'$ (figs. 9-3 and 9-4) by the transformations

$$\underline{a}_1'' = \underline{a}_1' \;;\quad \underline{a}_2'' = (\underline{a}_2' - \underline{a}_3') \;;\quad \underline{a}_3'' = (\underline{a}_2' + 2\underline{a}_3')$$

and with periodicities $\underline{a}_1'' \simeq 6$ Å, $\underline{a}_2'' \simeq 14$ Å, $\underline{a}_3'' \simeq 20$ Å, is convenient for this description. In this cell, $\underline{a}_2''$ is the stacking direction and there are six closest packed layers per unit cell (also suggested by the periodicity of ∿ 14 Å (≃ 6 × 2.3 Å, where 2.3 Å is the expected separation between successive layers)). The volume of the cell is 3 times that of the orthorhombic cell, and thus the unit cell content of the transformed cell is $Co_{36}V_{24}O_{96}$. The arrangements of the cobalt atoms in the two structures are shown in projection down the $\underline{a}_1''$ axis of the transformed cell in figures (9-3) and (9-4). The 36 cobalt atoms in the low temperature form are found to be distributed in the six octahedral layers in the sequence (9,3,9,3,9,3), while the 36 cobalt atoms in the corresponding layers in the high temperature form are distributed in the sequence (10,2,10,2,10,2). Thus in addition to the difference that the vanadium atoms in alternate layers are displaced relative to each other in the low and high temperature forms, the arrangement of the cobalt atoms is also different in the two forms. This results in a difference in sharing of the polyhedral elements in the two structures. Comparison of the number of polyhedral elements of different types shared in the low and high temperature forms of $Co_3(VO_4)_2$ (Cols. 4 and 5 of Table 9-3) shows that the low temperature form I contains 24 more shared corners and six more shared edges of the Co-Co type than the orthorhombic form. Based on Pauling's postulates regarding sharing of polyhedral elements (Ch. 2), the orthorhombic form is expected to be the more stable form.

The mechanism of the transformation from the low temperature form to the high temperature form is not evident from a comparison of the structures of the two forms. Isostructural orthorhombic forms of the orthovanadates of magnesium, cobalt, nickel and zinc are known(2,3,5). However, the low temperature cubic form is reported only for cobalt. Attempts to prepare the isostructural cubic $Ni_3(VO_4)_2$ have been unsuccessful(4). In view of the comparable sizes of Mg^{+2}, Co^{+2}, Ni^{+2} and Zn^{+2} ions it will be of interest to investigate whether stable low temperature cubic forms isostructural with that of cobalt are formed by magnesium and zinc.

General structural relations between compounds with stoichiometry $M_3(XO_4)_2$ (M = Ni, Mg, Cu, Co, Zn, Fe or Mn: X = As, V or P):

One of the aims of the present study was to investigate in detail a few structures of arsenates and vanadates of cations of comparable sizes, and to use the information obtained from these studies to predict the structure type assumed by the arsenates and vanadates of other similar cations in cases where structural information is lacking. The available structural information on the orthoarsenates and orthovanadates of cations with radii lying close to that of Co^{+2} are listed in Table (9-4). In view of the often assumed isomorphism between analogous phosphates, arsenates and vanadates(9), the data on the phosphate systems is also included in the table.

None of the arsenate structures so far determined are isostructural with the orthovanadates of the cations of comparable radii. Of course, neither the arsenates nor the vanadates of these cations have been investigated in enough detail to identify all the stable phases. Of the structures studied, the only orthoarsenates that have some structural relation with the orthovanadates are those of the monoclinic forms of $Co_3(AsO_4)_2$ and $Ni_3(AsO_4)_2$. These arsenates and the orthovanadates of cobalt, nickel, magnesium and zinc all consist of closest packed arrangement of oxygen ions, with the cations in octahedral and tetrahedral positions. The stoichiometry of all these can be represented by $M_3(XO_4)_2$, where M is the octahedrally coordinated cation, and X the tetrahedrally coordinated cation. The number of tetrahedral and octahedral positions occupied in a unit containing the same number of oxygen atoms is the same in all the cases. However, the orthoarsenates of cobalt and nickel consist of hexagonal closest packing (ABAC..sequence) of oxygen atoms, whereas the orthovanadates have cubic closest packing (ABC... sequence). In the notation of Calvo(37) to describe the closest-packed structures (described in Ch. 2), the former

Table (9-4)

Structure types of $M_3(XO_4)_2$ with (x=As,V or P), and M a divalent cation with radius comparable to that of Co^{+2}

(References are in parentheses)

M=	Ni	Mg	Cu	Co	Zn	Fe	Mn
$M_3(AsO_4)_2$	Monoclinic Type 1§ (7)	Tetragonal Type 2 (Ch. 5)	Monoclinic Type 3 (83)	Monoclinic Type 1 (Ch.3) Tetragonal Type 2 (Ch. 5)			Monoclinic Type 3 (84)
$M_3(VO_4)_2$	Orthorhombic Type 4 (2)	Orthorhombic Type 4 (Ch. 7)		Orthorhombic Type 4 (65) Cubic Type 5 (4)	Orthorhombic Type 4 (65)		
$M_3(PO_4)_2$		Monoclinic Type 6 (85)		Monoclinic Type 6 (86)	Monoclinic Type 7 (87) Monoclinic Type 8 (88)	Monoclinic Type 3 (89)	Monoclinic Type 3 (89) Monoclinic Type 9 (28)

Table (9-4) (continued)

§ Type 1: $Co_3(AsO_4)_2$: $\underline{a}_1$ = 5.830(4) Å, $\underline{a}_2$ = 9.675(2) Å, $\underline{a}_3$ = 10.34(2) Å, β = 93.42(5)°; $P2_1/c$

Type 2: $Mg_3(AsO_4)_2$: $\underline{a}_1$ = 6.79(1) Å , $\underline{a}_3$ = 18.98(4) Å ; $I\bar{4}2d$.

Type 3: $Mn_3(AsO_4)_2$: $\underline{a}_1$ = 9.2(1) Å, $\underline{a}_2$ = 11.6(1) Å, $\underline{a}_3$ = 6.5(1) Å, β = 98.5(5)°, $P2_1/c$.

Type 4: $Mg_3(VO_4)_2$: $\underline{a}_1$ = 6.053(3) Å, $\underline{a}_2$ = 11.442(6) Å, $\underline{a}_3$ = 8.330(6) Å; Cmca

Type 5: $Co_3(VO_4)_2$: $\underline{a}_1$ = 8.324(5) Å; $P4_132$ or $P4_332$

Type 6: $Mg_3(PO_4)_2$: $\underline{a}_1$ = 5.06(1) Å, $\underline{a}_2$ = 8.235(5) Å, $\underline{a}_3$ = 8.788(5) Å, β=120.42(5)°; $P2_1/c$

Type 7: α-$Zn_3(PO_4)_2$: $\underline{a}_1$ = 8.14(2) Å, $\underline{a}_2$ = 5.63(1) Å, $\underline{a}_3$ = 15.04(4) Å, β=105.1(2)°; C2/c

Type 8: β-$Zn_3(PO_4)_2$: $\underline{a}_1$ = 9.393(3) Å, $\underline{a}_2$ = 9.170(6) Å, $\underline{a}_3$ = 8.686(3) Å, β = 125.7(1)°; $P2_1/c$

Type 9: β'-$Mn_3(PO_4)_2$: $\underline{a}_1$ = 8.94(3) Å, $\underline{a}_2$ = 10.04(2) Å, $\underline{a}_3$ = 24.14(12) Å, β = 120.8(1)°; $P2_1/c$

structures belong to the N/2 N/2... arrangement of the tetrahedral groups, while the latter belong to the NONO... sequence. Thus, even though the structures of the orthoarsenates and orthovanadates of cobalt and nickel are similar in that they all consist of closest-packing of oxygen atoms, they are not isostructural as suggested by packing considerations.

A somewhat similar situation has been dealt with by Kamb(90) in an attempt to explain the occurrence of some compounds of general stoichiometry M_2XO_4 with olivine structure (consisting of hexagonal closest packing of oxygen atoms), and others with the spinel structure (consisting of cubic closest packing). From analysis of a large number of observed structures of both types, he finds that the distortions in the closest packing in olivine structures are such that the tetrahedral void is smaller,and the octahedral void larger, than that in ideal packing. In spinels, the opposite situation is found to be the case. Conversely, a compound of stoichiometry M_2XO_4 can be expected to have the olivine structure if the radius of M is larger and X smaller, than those expected in ideal closest packing of oxygen atoms, and the spinel structure can be expected if the radius of M is smaller and X larger, than those in the ideal packing. Kamb expressed these conditions in terms of the ratio of the average (M-O/X-O) bond lengths, and, for cases with the charge on the X ion equal to +5, analysis of the available data indicated that, when this ratio was greater than about 1.22, the olivine structure with a hexagonal closest packing was assumed by the compound, and when the ratio was less than this value, the spinel structure with cubic closest packing was found.

The observed smaller-than-ideal size of the tetrahedral void in olivine and larger-than-ideal size in spinel, and the reverse in the case of the octahedral void, have been traced by Kamb as direct consequences of shortening of shared edges in these structures (Ch.2). Thus, the basic feature that determines the structure choice between olivine and spinel for M_2XO_4 compounds has been attributed by Kamb to the electrostatic repulsion between the cations sharing common edges.

Kamb's treatment deals only with M_2XO_4 compounds, and the choice between olivine and spinel structures for them. However, if the structure type assumed by a crystal is mainly determined by the electrostatic forces between the cations sharing polyhedral elements in the structure, it should be possible to extend Kamb's approach to other structure types in addition to olivine and spinel types, and to stoichiometries other than M_2XO_4 as well.

The ratios of (M-O/X-O) bond distances in the refined closest packed structures that may be expected to be isostructural with $Co_3(AsO_4)_2$ on the basis of packing considerations are given below:

Compound	$\frac{M-O}{X-O}$	Packing sequence of XO_4 groups	Ref.
$Mg_3(VO_4)_2$	1.21	NONO...	Ch. 7
$Zn_3(VO_4)_2$	1.23	NONO...	(65)
$Co_3(AsO_4)_2$	1.25	$\frac{N}{2}\,\frac{N}{2}\cdots$	Ch. 3

The structures of $Ni_3(AsO_4)_2$(N/2 N/2 ... sequence (7)), $Co_3(VO_4)_2$ (NONO... sequence (4)), and $Ni_3(VO_4)_2$ (NONO ... sequence (2)), are not included since these structures have not been fully refined, and while the structure type is known in these cases, the actual (M-O/X-O) ratio is not known. On the basis of the three structures which have been fully refined, one can suggest that the boundary (M-O/X-O) ratio between closest-packed structures with the NONO... sequence of (XO_4) groups, and those with the N/2 N/2... sequence, is about 1.24. The structures of $Cu_3(VO_4)_2$, $Fe_3(VO_4)_2$, $Zn_3(AsO_4)_2$, $Fe_3(AsO_4)_2$, and $Mn_3(VO_4)_2$ are not presently known, and it will be of interest to investigate whether these form closest-packed structures as suggested by packing considerations, and whether their structure-types conform to the NONO... or the N/2 N/2... sequence depending on the boundary value of 1.24 for the (M-O/X-O) ratio in these compounds.

Distortions in polyhedral groups and prediction of bond lengths and bond angles expected in a crystal whose structure type is known:

In the structures that have been described in the previous chapters, it has invariably been possible to rationalise the difference in individual bond distances in XO_4 groups (X = As or V) on the basis of considerations of differences in coordination number of the individual oxygen atom involved in each bond$^{(1)}$. However, it was found that the differences in individual M-O bond distances in MO_6 groups (M = Co or Mg) could not in general be consistently rationalised on these same considerations.

Baur$^{(49)}$ has arrived at a similar conclusion on the basis of a different empirical approach (to be described in a later paragraph) using structural data available in the literature on borates, silicates, phosphates and sulphates of monovalent and divalent cations. He has found that, in structures containing two cations A and B, with formal charges n and m ($n>m$) respectively, and both bonded to a common oxygen atom O_n, the observed A-O_n distance has a relatively good correlation to the environment of O_n, whereas the correlation between the B-O_n distance and the environment of O_n is much poorer.

Baur's method of relating the individual cation-oxygen bond lenths in cation polyhedra to the environments of the oxygen atom involved in each bond consists of deriving linear relations of the form

$$d(A\text{-}O_n) = m\ p(O_n) + b \qquad (9\text{-}1)$$

where $d(A\text{-}O_n)$ is the bond length between the cation A and oxygen atom O_n, $p(O_n)$ is a function of the environment of the oxygen atom O_n, and m and b are constant to be derived empirically for a given cation A in a given coordination. $p(O_n)$ in eq. (9-1) is the sum of the contributions to the strength of the electrostatic bond from oxygen atom O_n to the r cations to which it is bonded, and has been defined by Pauling$^{(91)}$ as

$$p(O_n) = \sum_{i=1}^{r} S_i = \sum_{i=1}^{r} \frac{Z_i}{(CN)_i}$$

where Z_i is the formal charge on cation i, and $(CN)_i$ is the coordination number around cation i.

Baur derived linear relations between $d(A\text{-}O_n)$ and $p(O_n)$ values for a number of cations, by a least-squares fit of a large set of observed $d(A\text{-}O_n)$--$p(O_n)$ values obtained from known structures, and pointed out that the relations thus derived can then be used to predict $A\text{-}O_n$ bond lengths in other structures where the $p(O_n)$ values are known (i.e., where the basic structure type is known) but the actual $A\text{-}O_n$ bond lengths are unknown (i.e., the finer details of the structure such as the individual A-O bond lengths are unknown). He has illustrated the use of the method by verifying that the predicted P-O bond lengths in the PO_4 group in $MgHPO_4 \cdot 3H_2O$

agree to within 0.02 Å with the observed bond lengths in the structure.

The data on As-O bond lengths in AsO_4 groups in the structures investigated in the present work were used along with the data from Ca_2AsO_4Cl (67), $Cd_3(AsO_4)_2$ (92), $Mg_2As_2O_7$ (14), and $Cu_3(AsO_4)_2$ (83), to derive the slope and intercept of the relation of the form (9-1) for AsO_4 groups. 39 sets of (As-O)--p(O) values, nineteen of which were obtained from the present work, were used in deriving the relation, given by

$$d(As\text{-}O_n) = 0.10 \quad p(O_n) + 1.49 \quad . \qquad (9\text{-}2)$$

The values of $d(As\text{-}O_n)$ and $p(O_n)$ used in deriving the relation (9-2) are plotted in fig. (9-5). The mean deviation between the observed bond lengths and the d(As-O) values predicted by eq. (9-2) for the 39 observations is 0.02 Å. Only in three out of the 39 cases did the deviation exceed 0.03 Å. It appears that relation (9-2) can be used to predict As-O bond lengths to the accuracy of about 0.02 Å in AsO_4 groups in a crystal whose structure type, but not the detailed bonding geometry, is known.

A linear relation between $d(V\text{-}O_n)$ and $p(O_n)$ was derived using 19 sets of d(V-O)--p(O) values obtained from $Mg_3(VO_4)_2$ (Ch. 7), $Zn_3(VO_4)_2$ (65), Ca_2VO_4Cl (67), $Cd_2V_2O_7$ (69), YVO_4 (66), and $Ca_2V_2O_7\cdot 2H_2O$ (93), and is given by

$$d(V\text{-}O_n) = 0.15\ p(O_n) + 1.43 \ . \qquad (9\text{-}3)$$

The values of the slope and intercept in eq. (9-3) should be considered tentative, since only 19 sets of d(V-O)--p(O) values

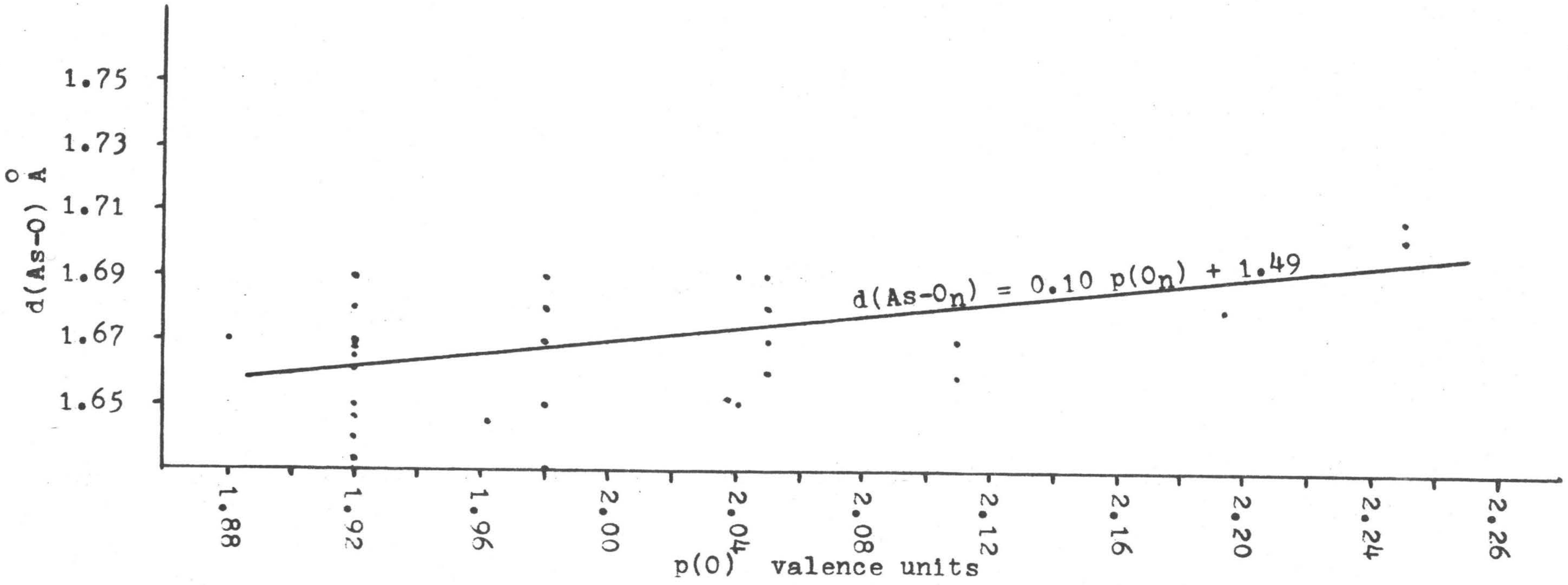

Figure (9-5). d(As-O)--p(O) plot for AsO_4 groups.

have been used in deriving the relation. No attempt has been made to include more data that might be available in the literature. Relation (9-3) results in an average deviation of 0.02 Å between observed and predicted d(V-O) values for the 19 sets of data used.

It seems possible to predict certain trends in the relative sensitivities of the P-O, As-O and V-O bond lengths to changes in oxygen environments by comparing the relationship derived for d(P-O)--p(O) derived by Baur$^{(49)}$, and those for d(As-O)--p(O) and d(V-O)--p(O) derived in the present work (eq. 9-2 and 9-3). The relationships are

$$d(\mathrm{As{-}O}) = 0.10\ p(\mathrm{O}) + 1.49 \quad \ldots \quad (9\text{-}2)$$

$$d(\mathrm{V{-}O}) = 0.15\ p(\mathrm{O}) + 1.43 \quad \ldots \quad (9\text{-}3)$$

$$d(\mathrm{P{-}O}) = 0.11\ p(\mathrm{O}) + 1.32 \quad \ldots \quad (\mathrm{Baur})$$

The slopes of the d(P-O)--p(O) and d(As-O)--p(O) dependences are comparable, whereas the slope of the d(V-O)--p(O) dependence is larger. Eq. (9-3) predicts that an increase in the p(O) value of an oxygen atom in a VO_4 group by 0.33 (corresponding to an increase in the coordination of the oxygen atom by an octahedrally coordinated divalent cation) should correspond to an increase of 0.05 Å in the V-O bond length; in the analogous case in an AsO_4 group, eq. (9-2) predicts an increase of 0.03 Å in the As-O bond length. Thus, equations (9-2) and (9-3) together imply that vanadium-oxygen distances in VO_4 groups should be more sensitive to the coordination around the oxygen atoms bonded to vanadium, than arsenic-oxygen distances should be to changes in coordination of the oxygen atoms bonded to arsenic.

In the VO_4 group in $Mg_3(VO_4)_2$ (Ch. 7), there are two types of oxygen atoms,differing in their p(O) values by 0.33, and the observed difference in the V-O distance involving these two types of oxygen atoms is 0.108 Å; in the two AsO_4 groups in $Co_3(AsO_4)_2$ (Ch. 3), the observed increase in As-O distances corresponding to an increase of 0.33 in the p(O) value are 0.041 Å and 0.035 Å respectively. The observed increase in the V-O bond length corresponding to an increase in p(O) value is significantly higher than the observed increase in the As-O bond length for the same increase in p(O) value, and this is in qualitative agreement with the difference in slopes between the d(V-O)--p(O) dependence and the d(As-O)--p(O) dependence (eq. 9-2 and 9-3 respectively).

However, the actual magnitude of the increase in V-O distance predicted by eq. (9-3) for an increase in the p(O) value of 0.33 is only 0.05 Å, but the observed increase in the V-O distance in the (VO_4) group in $Mg_3(VO_4)_2$ is 0.108 Å, almost twice the predicted value. The large difference in this case between the predicted and observed values could have arisen from many factors. It has already been pointed out that the relation (9-3) has been derived from very limited data. Inclusion of more data in deriving the d(V-O)--p(O) relationship might lead to better agreement between the observed and predicted values. Quite apart from this, equations of the form (9-1) are based on the assumption of a linear relation between $d(A\text{-}O_n)$ and $p(O_n)$. However, Baur$^{(49)}$ points out that linear relations were assumed simply because there was no conclusive evidence of a non-linear relationship, and that with more and better data, it might be necessary to resort to higher degree curves in order to successfully predict the bond lengths.

Also, Baur does not consider possible differences in contribution to the electrostatic bond strength from chemically different cations with the same charge and coordination number. Thus, the individual As-O bond distances in AsO_4 groups in the β-form of $Mg_2As_2O_7$, $Mn_2As_2O_7$ and $Zn_2As_2O_7$$^{(14)}$, and in $Co_2As_2O_7$ (Ch. 6), are predicted by eq. (9-2) to be identical, though the As-O distances in the different structures should bear some relationship to the force with which the electrons of the O^{-2} ion can be drawn towards the nuclei of the different divalent cations. Also, Baur's treatment assumes that each of the i cations, all with the same formal charge Z and with the same coordination number, but lying at different distances $r_1, r_2, \ldots\ldots, r_i$, from the oxygen ion O_n to which they are bonded, make equal contributions to the electrostatic bond strength of the oxygen ion O_n. This assumption is contrary to the expectations based on the electrostatic model, which would suggest an inverse-square law dependence for the attractive force between the anion and each of the cations.

Because of the uncertainty of a definite linear relationship between d(A-O_n) and p(O_n) expressed by Baur, and because of the implicit assumptions that are involved in Baur's method on the basis of which equations (9-2) and (9-3) have been derived, the accuracy with which the As-O and V-O bond distances can be predicted from a knowledge of the p(O) values using these equations might not be significantly better than about 0.02 Å.

Angular distortions in cation polyhedra:

Baur$^{(49)}$ attempted to account for angular distortions from ideality in the cation polyhedra in terms of a correlation with the 'distance distortion' and under the assumption that to a first approximation the anion framework in the structure is rigid. Baur derived an empirical relation between the 'averaged angle' subtended at the central cation by any two pairs of edges of a polyhedral group, and the averaged distances of the anions forming these edges from the central cation, and observed good correlation between the averaged angles and the averaged distances in the cases of BO_3, PO_4, SiO_4 and SO_4 groups.

No attempt has been made in the present work to verify whether correlations of the type claimed by Baur do exist in the arsenate and vanadate systems. However, the distortions observed in the AsO_4 and VO_4 groups in the structures investigated in the present work indicate that there are significant distortions in the anion framework, and that there is an almost perfect qualitative correlation between the distortions in the anion framework and the angular distortions in the cation polyhedra, contrary to Baur's assumption. Table (9-5) lists the geometries of several AsO_4 groups, two VO_4 groups, one PO_4 group and one CrO_4 group. The data in the table have been obtained from the structures described in the previous chapters, and from the structures of Ca_2XO_4Cl (X = As,V,Cr or P)$^{(67)}$ and $Cd_3(AsO_4)_2$$^{(92)}$. In all the cases considered, it is found that the smallest angles of the polyhedral group are always associated with the shortest edges. Thus the present anlysis indicates that any satisfactory attempt at accounting for angular distortions in polyhedral groups should take into consideration the correlation between edge-lengths and the angles subtended by the edges. The edge-lengths themselves are strongly correlated with whether or not these are shared with other polyhedral groups. Thus, shared edges in the XO_4 groups investigated (Table 9-5) have been found without exception to be shorter than the unshared edges. In effect, it has invariably been possible to qualitatively account for the observed angular deviations from an ideal tetrahedral arrangement in the XO_4 groups listed in Table (9-5) in terms of the electrostatic repulsion between the X ion and the other cations at the centres of the polyhedra

Table (9-5)†

Observed correlation between edge-lengths in (XO_4) groups and the angles subtended by the edges at X.

	Atoms forming edge	Edge length (Å)	Angle subtended by edge at central cation (degrees)	Edge shared with
AsO_4 group in Ca_2AsO_4Cl (67)				
	02 -02'	2.672	105.5	Ca(1)
	01 -02'	2.678	105.3	Ca(2)
	01'-02	2.678	105.3	Ca(2)
	01 -01'	2.720	107.2	Ca(1)
	01 -02	2.873	117.1	-
	01'-02'	2.873	117.1	-
VO_4 group in Ca_2VO_4Cl (67)				
	02 -02'	2.713	105.6	Ca(1)
	01 -02'	2.724	105.9	Ca(2)
	01'-02	2.724	105.9	Ca(2)
	01 -01'	2.751	107.0	Ca(1)
	01 -02	2.902	116.4	-
	01'-02'	2.902	116.4	-
PO_4 group in Ca_2PO_4Cl (67)				
	02 -02'	2.477	107.7	Ca(1)
	01 -02'	2.481	107.3	Ca(2)
	01'-02	2.481	107.3	Ca(2)
	01 -01'	2.495	105.7	Ca(1)
	01 -02	2.578	113.6	-
	01'-02'	2.578	113.6	-
CrO_4 group in Ca_2CrO_4Cl (67)				
	02 -02'	2.670	104.4	Ca(1)
	01 -02'	2.694	104.8	Ca(2)
	01'-02	2.694	104.8	Ca(2)
	01 -01'	2.719	105.3	Ca(1)
	01 -02	2.931	119.2	-
	01'-02'	2.931	119.2	-

(continued next page)

Table (9-5) (continued)

	Atoms forming edge	Edge length (Å)	Angle subtended by edge at central cation (degrees)	Edge shared with
$As(1)O_4$ group in $Cd_3(AsO_4)$ (92)	03 -01	2.62	101.3	-
	02 -03	2.73	107.8	-
	02 -04	2.74	107.9	-
	03 -04	2.79	111.1	-
	02 -01	2.82	111.8	-
	01 -04	2.89	116.6	-
$As(2)O_4$ group in $Cd_3(AsO_4)_2$ (97)	06 -07	2.61	100.8	Cd(1)
	07 -08	2.78	110.1	-
	05 -06	2.79	110.7	-
	05 -08	2.79	110.3	-
	06 -08	2.82	112.1	-
	05 -07	2.82	112.7	-
$As(1)O_4$ group in $Co_3(AsO_4)_2$ - (Table 3-3 of Ch. 3)	O(11)-O(12)	2.56	97.5	Co(2)
	O(12)-O(13)	2.60	99.2	Co(3)
	O(11)-O($\overline{14}$)	2.78	112.2	-
	O(11)-O(13)	2.81	112.6	-
	O(13)-O($\overline{14}$)	2.83	114.6	-
	O(12)-O($\overline{14}$)	2.92	119.1	-
$As(2)O_4$ group in $Co_3(AsO_4)_2$ - (Table 3-3 of Ch. 3)	O(22)-O($\overline{24}$')	2.75	109.6	-
	O(22)-O($\overline{21}$')	2.76	108.1	-
	O(22)-O(23)	2.78	110.0	-
	O(23)-O($\overline{24}$')	2.79	110.2	-
	O($\overline{21}$')-O(23)	2.80	108.9	-
	O($\overline{21}$')-O($\overline{24}$')	2.80	110.1	-

(continued next page

Table (9-5) (continued)

	Atoms forming edge	Edge length (Å)	Angle subtended by edge at central cation (degrees)	Edge shared with
As(2)O_4 group in $Co_{24.2}As_9O_{48}$ - (Table 4-3 of Ch. 4)	O(3)d-O(4)a	2.74	108.0	-
	O(3)d-O(4)b	2.74	108.0	-
	O(3)d-O(4)c	2.74	108.0	-
	O(4)a-O(4)b	2.79	110.9	-
	O(4)b-O(4)c	2.79	110.9	-
	O(4)c-O(4)a	2.79	110.9	-
As(1)O_4 group in $Mg_3(AsO_4)_2$ - (Table 5-3 of Ch. 5)	$O2^a - O2^b$	2.64	100.9	Mg(1)
	$O2^a - O3^c$	2.65	103.3	Mg(3)
	$O2^b - O3^d$	2.65	103.3	Mg(3)
	$O2^a - O3^d$	2.79	111.4	-
	$O2^b - O3^c$	2.79	111.4	-
	$O3^c - O3^d$	2.95	124.4	-
As(2)O_4 group in $Mg_3(AsO_4)_2$ - (Table 5-3 of Ch. 5)	$O1^a - O1^e$	2.62	104.2	-
	$O1^a - O1^f$	2.62	104.2	-
	$O1^d - O1^e$	2.62	104.2	-
	$O1^d - O1^f$	2.62	104.2	-
	$O1^a - O1^d$	2.89	120.7	-
	$O1^e - O1^f$	2.89	120.7	-
(VO_4) group in $Mg_3(VO_4)_2$ - (Table 7-3 of Ch. 7)	O(3)d-O(3)e	2.739	108.4	-
	O(1)a-O(3)d	2.768	108.7	-
	O(1)a-O(3)e	2.768	108.7	-
	O(2)f-O(3)d	2.866	110.2	-
	O(2)f-O(3)e	2.866	110.2	-
	O(1)a-O(2)f	2.898	110.6	-
AsO_4 group in $Co_{7.0}As_{3.6}O_{16}$ - (Table 8-5 of Ch. 8)	O3a-O3c'	2.58	101.5	Co(1)
	O2a-O3a	2.64	104.8	Co(2)
	O2b-O3c'	2.64	104.8	Co(2)
	O2b-O1a	2.79	113.8	
	O3a-O1a	2.82	115.2	
	O3c'-O1a	2.82	115.2	

[†] The notations used for denoting the atom positions are those used in the references.

sharing common edges with the XO_4 groups. In only two cases ($As(2)O_4$ group in $Mg_3(AsO_4)_2$ and $As(1)O_4$ group in $Cd_3(AsO_4)_2$) out of the cases investigated, it was not possible to correlate the observed angular distortions in the XO_4 group to the electrostatic repulsion between cations sharing common edges, since the two groups do not share any of their edges with other cations but still show significant angular distortions.

The $CoO-As_2O_5$ system:

In addition to the five phases of cobalt arsenates listed in Table (9-1) for which structural details have been presented in the previous chapters, at least five other phases have been prepared. One of these is the metaarsenate, $CoO \cdot As_2O_5$, for which a trial structure has been reported by Magneli(10) based on powder data. Attempts to prepare single crystals of the metaarsenate in the course of this work were unsuccessful. Since this phase is unique among the cobalt arsenates in that it is said to have all the arsenic atoms and all the cobalt atoms in octahedral coordination, a refinement of this structure based on accurate single crystal data is considered desirable.

A stable composition with stoichiometry $CoAs_4O_{11}$ has been reported by Mason et al.(13) on the basis of fractional pyrolysis studies on the compound $CoO \cdot 2As_2O_5 \cdot 5H_2O$. No attempt was made in the present work, or has been reported elsewhere in the literature, to reproduce the preparation.

The other three phases of the $CoO-As_2O_5$ system that have been isolated are all monoclinic. One of these, having a diffraction pattern similar to that of $Co_2As_2O_7$, but showing in addition superstructure reflections at 1/5th the spacing along $(1\bar{1}1)$, has already been described in Ch. 6. The methods of preparation and the approximate cell dimensions of the other two forms are collected in Table (9-6). However, it is not possible to speculate on the probable compositions of these compounds on the basis of the compositions and molar ratio of the reactants used in the preparation, since, as has been pointed out in Ch. 4, complications such as the oxidation of cobalt, reduction of arsenic and loss of As_2O_5 from the system, might occur in the course of the reactions, and the extent to which these occur will determine the final compositions. The compositions of the crystals of the three monoclinic forms described above should be considered unknown until further work establishes their true compositions.

Some success has been achieved in the present study towards understanding the crystal chemistry of a few of the ten compositions of the $CoO-As_2O_5$ system thus far identified. However, the need for further and more thorough investigation of this system, in particular the chemical aspects of the mixed valence states for the cations in these compounds, and a reinvestigation of the complete phase diagram of the system, have also become more obvious as a result of the present work.

Table (9-6)

Data on two phases of the CoO-As_2O_5 system with presently undetermined compositions

Method of Preparation	Space group and cell dimensions of crystal selected from reaction product	Volume of unit cell
$2CoCO_3 \cdot 3Co(OH)_2 + As_2O_5$ in ratios to yield $6CoO \cdot As_2O_5$ on loss of H_2O and CO_2 $\xrightarrow[\text{Pt crucible}]{\sim 1200°}$	Ic or I2/c $\underline{a}_1 \simeq 10.8$ Å $\underline{a}_2 \simeq 12.7$ Å $\underline{a}_3 \simeq 6.8$ Å $\beta \simeq 95°$	~ 929 Å^3
Same as that used for preparation of $Co_2As_2O_7$ described in Ch. 6	C2,Cm or C2/m $\underline{a}_1 \simeq 6.7$ Å $\underline{a}_2 \simeq 15.4$ Å $\underline{a}_3 \simeq 10.1$ Å $\beta \simeq 105.5°$	~ 1004 Å^3

APPENDIX I

ANOMALOUS DISPERSION APPLIED TO SPACE GROUP DETERMINATION IN $Co_{24.2}As_9O_{48}$

It has been pointed out in Ch. 2 that the scattering factor of atom j can be written as

$$f_j = f_j^o + \Delta f_j' + i\Delta f_j'' \quad (f_j^o,\ \Delta f_j' \text{ and } \Delta f_j'' \text{ are real})$$

where f_j^o is the contribution assuming that the frequency ω of the incident radiation is large in comparison with any natural absorption frequency ω_{kn} of the scattering atom. The correction terms $\Delta f_j'$ and $\Delta f_j''$ are introduced (pp. 136-7 of (21)) to take into account the fact that the assumption $\omega_{kn} >> \omega$ is not always true. In cases where $\omega_{kn} \simeq \omega$, i.e. when the frequency of the incident radiation is just above or below that of the absorption frequency, there is anomalous scattering of the radiation in the material of the scatterer, and thus the scattering factor depends markedly on the frequency of the radiation under these conditions.

It can be shown(94) that when $\Delta f'' = 0$ for all atoms in a unit cell, the intensities of pairs of reflections with indices $(hk\ell)$ and $(\bar{h}\bar{k}\bar{\ell})$ will be equal. However, when $\Delta f'' \neq 0$ for one or more atoms in a unit cell , the equivalence $I(hk\ell) = I(\bar{h}\bar{k}\bar{\ell})$ will hold only when N/2 of the total of N atoms in a unit cell are related to the remaining N/2 by a centre of symmetry. The statement of equivalence of the intensities of pairs of reflections with indices $(hk\ell)$ and $(\bar{h}\bar{k}\bar{\ell})$

is called Friedel's Law, and will be true in all crystals when $\Delta f''$ for all atoms in the unit cell are zero, but will not hold for non-centrosymmetric space groups when one or more atoms in the unit cell scatter the radiation used anomalously.

Therefore, by appropriate choice of radiation to fulfil the condition $\omega_{kn} \simeq \omega$, the contribution of the term $\Delta f''$ to the scattering factor f_j of the j^{th} atom can be made large, and then if it is found that $I(hk\ell) = I(\bar{h}\bar{k}\bar{\ell})$ for all $(hk\ell)$, the crystal has a centre of symmetry, and if it is found that $I(hk\ell) \neq I(\bar{h}\bar{k}\bar{\ell})$, the crystal lacks a centre of symmetry. In a non-centrosymmetric crystal, the method can be extended to test for other symmetry elements as well.

In Ch. 4, it was pointed out that the intensity equivalences expected on the basis of the symmetry elements of the space-groups C2, Cm and C2/m (which are indistinguishable on the basis of systematic absences), are

$$\begin{array}{lll} \text{C2:} & I(hk\ell) = I(\bar{h}k\bar{\ell}) & \\ \text{Cm:} & I(hk\ell) = I(h\bar{k}\ell) & \text{(A)} \\ \text{C2/m:}\ I(hk\ell) = & I(\bar{h}k\bar{\ell}) = I(h\bar{k}\ell) = I(\bar{h}\bar{k}\bar{\ell}) & \end{array}$$

respectively. If, in addition, Friedel's Law holds, additional intensity equivalences will be observed in C2 and Cm, making these later space groups indistinguishable from C2/m by using the differences in intensity equivalences (A). However, by proper choice of radiation so as to permit experimentally significant anomalous scattering effects, it is possible to distinguish between the three space-group possibilities C2, Cm and C2/m using the differences in intensity equivalences. This procedure was used in making the choice of the correct space group for $Co_{24.2}As_9O_{48}$ (Ch. 4).

APPENDIX II

METHOD OF LEAST SQUARES IN REFINEMENT OF STRUCTURE PARAMETERS

The method of least squares consists of finding the values of a set of variables which best satisfy a set of somewhat inconsistent observations. This problem was first treated by Legendre, who proposed that the most acceptable values of the variables were such as to make the sum of the squares of the errors a minimum(95). Thus, if $\Delta_i (i = 1, 2, \ldots, n)$ are the errors in the n observations, w_i the weight, and m_j $(j = 1, 2, \ldots r$ and $n > r)$ the initially chosen value of the j^{th} parameter, then the least squares method consists of choosing shifts Δm_j in m_j so that

$$D = \sum_{i=1}^{n} w_i \Delta_i^2$$

is a minimum.

The refinement of a structure consists of making small variations in a set of initially chosen parameters (positional, thermal and occupancy) of the atoms in the unit cell so that the set of calculated structure factor amplitudes, $|F_c(hk\ell)|$, gives the 'best' fit to the set of observed values, $|F_o(hk\ell)|$. In x-ray diffraction, we take Δ_i to be the difference between the observed and calculated structure factor amplitudes for the i^{th} reflection, and thus require that

$$D = \sum_{i=1}^{n} w_i (|F_o|-k|F_c|)_i^2 \qquad (1)$$

be a minimum . In (1), the summation is over all the measured reflections, and F_c is a function of the r parameters $p_j (j = 1, 2, \ldots, r)$ of the structure. k is the scaling constant between $|F_o|$ and $|F_c|$ and has been described in Chapter 2.

Minimisation is achieved by taking the derivative of D with respect to each of the r parameters $p_j (j = 1,2,\ldots,r)$ and equating each to zero. One gets

$$\sum_{i=1}^{n} w_i [(|F_o|)_i - k|F_c(p_1,p_2,\ldots,p_r)|_i] \frac{\delta}{\delta_{pj}} (|kF_c(p_1,p_2,\ldots,p_r)|)_i = 0 \qquad (2)$$

$$j = 1,2,\ldots r \text{ .}$$

These r equations for the r-parameter problem are called the 'normal equations' for the problem. If the observables, $F_c(hk\ell)$, are linear functions of p_j, then the r equations are linear equations in the r unknowns, and one obtains a unique solution of the r parameters. In our case the F_c's are non-linear in p_j, but are known functions of p_j. Thus, if an approximate set p_j' of the parameters is known, one can expand F_c to the first order of Δp_j in a Taylor series,

$$|kF_c(p_1,p_2,\ldots,p_r)| = |kF_c(p_1',p_2',\ldots,p_r')| + \sum_{j=1}^{r} \frac{\delta}{\delta p_j}(|kF_c(p_1,p_2,\ldots p_r)|)\Delta p_j \qquad (3)$$

Substituting (3) in (2),

$$\sum_{i=1}^{n} [(\Delta F_c)_i - \sum_{t=1}^{r} \frac{\delta}{\delta p_t}(|kF_c(p_1',p_2',\ldots,p_r')|)_i \, \Delta p_t]$$

$$\times \frac{\delta}{\delta p_j} (|kF_c(p_1,p_2,\ldots,p_r)|)_i = 0 \text{ ; } j = 1,2,\ldots r \qquad (4)$$

where

$$(\Delta F_c)_i = (|F_o|_i - |kF_c(p_1',p_2',\ldots,p_r')|_i) \quad .$$

Expansion and rearrangement lead to the set of equations:

$$\sum_{i=1}^{n} w_i (\Delta F_c)_i \frac{\delta}{\delta p_j} (|kF_c|)_i =$$

$$\sum_{i=1}^{n} w_i \frac{\delta}{\delta p_j} (|KF_c|)_i \left(\sum_{t=1}^{r} \frac{\delta}{\delta p_t} (|kF_c|)_i \right) \Delta p_j; \qquad j = 1,2,\ldots r. \qquad (5)$$

This is a system of r linear equations, of the form

$$v_j = a_{j1}\,\Delta p_1 + a_{j2}\,\Delta p_2 + \ldots\ldots + a_{jr}\,\Delta p_r; \; j = 1,2,\ldots.r \qquad (6)$$

where

$$v_j = \sum_{i=1}^{n} w_i (\Delta F_c)_i \frac{\delta}{\delta p_j} (|kF_c|)_i$$

and

$$a_{jt} = \sum_{i=1}^{n} w_i \frac{\delta}{\delta p_j} (|kF_c|)_i \frac{\delta}{\delta p_t} (|kF_c|)_i$$

The set of r linear equations can be solved for the r unknowns, Δp_j, and thus new values $p_j = p_j' + \Delta p_j$ can be obtained for the r parameters. These new values yield better fits between the set of observed and calculated structure factor amplitudes than the initial set. One uses these new values p_j in the next step as the starting values, and improves upon these values by finding a new set of Δp_j in the next cycle of least squares refinement. The process is continued until the minimisation condition (1) is achieved .

The standard deviation $\sigma(\Delta p_j)$ in Δp_j (which is the same as the standard deviation in the parameter p_j), is obtained from

$$\sigma^2_{p_j} = \sum_{i=1}^{n} \left(\frac{\delta(\Delta p_j)}{\delta|F_c|_i}\right)^2 \sigma^2_F$$

where

$$\sigma^2_F = \sum_{i=1}^{n} \frac{w_i(\Delta F)^2_i}{n-r}$$

n and r being the number of observations and the number of parameters respectively.

The standard deviations in the bond lengths and bond angles derived from the atomic parameters are dependent on the standard deviations in these latter parameters. The formulae for estimating the standard deviations in the bond length and bond angles are described in Ch. 18 of (26).

w_i in relation (1) refers to the weight assigned to the measurement of the i^{th} reflection. In practice, absolute estimates of the weights are not known in advance, and relative estimates must be made. In making these, account must be taken both of the accuracy of the $(|F_o|)_i$ and of the appropriateness of the calculated model on which the $(|F_c|)_i$ are based.

The proper weight to be assigned an observation is equal to the reciprocal of the variance of that observation; i.e.,

$$w_i = (1/\sigma^2_i)$$

where σ_i is the standard deviation. A common method of estimating σ is by making repeated measurements of the same quantity.

It is not feasible in structure determinations involving large numbers of reflections to measure each one a sufficient number of times to obtain reliable estimates of σ. Instead, estimates may be based on single measurements of intensities of a large number of reflections in a small range of intensity, and deviations in the measured values in this range from the expected intensities for the 'correct' model can be taken to be a measure of the accuracy of the measurements of intensities in this range.

This is the principle on which weighting functions have been chosen for refinement of the structures described in earlier chapters. A plot of the mean $|\Delta F|$ vs. mean $|F_o|$ for groups of reflections of similar magnitudes was used, and expressions for $w = \frac{1}{|\Delta F|^2}$ were derived as functions of $|F_o|$.

One of the commonly used functional forms for w is that suggested by Cruickshank(46), and corresponds to $w_i = (a+b|F_o|_i + c(|F_o|_i^2)^{-1}$, where w_i is the weight assigned the ith reflection, and a, b, c are constants which can be chosen from the plot of mean $|\Delta F|$ vs. mean $|F_o|$.

BIBLIOGRAPHY

(1) R. D. Shannon, C. T. Prewitt; Acta Crystallogr., B25, 925 (1969).

(2) A. Durif, E. F. Bertaut; J. Phys. Radium, 20, 54 S (1959).

(3) A. Durif, Anal. Chem., 31(10), 1741 (1959).

(4) J. C. Joubert, A. Durif; Bull. Soc. Fr. Mineral. Cristallogr., 87, 47 (1964).

(5) C. Brisi; Ric. Sci., 30, 1339 (1960) ; (see also Structure Reports, 24, 446).

(6) J. B. Taylor, R. D. Heyding; Can. J. Chem., 36, 597 (1958).

(7) R. J. Davis, M. H. Hey, A.W.G. Kingsbury; Mineral. Mag., 35, 72 (1965).

(8) P. Robijn; Ind. Chim. Belge, 32 (Spec. No.) (Part 2), 601 (1967).

(9) M. T. Pope, B. W. Dale; Quart. Rev. Chem. Soc., 22(4), (1968).

(10) A. Magneli; Ark. Kemi , Mineral. Geol., Bd. 17B, No. 5, (1941).

(11) K. H. Jost, H. Worzala, E. Thilo; Acta Crystallogr., 21(5), 808 (1966).

(12) H. Guerin; C.R. Acad. Sci., Ser. C., 201, 1133 (1935).

(13) J. Masson, B. Charles-Messance, M. Bastick, H. Guerin; C. R. Acad. Sci., Ser. C, 250, 859 (1960).

(14) C. Calvo, K. Neelakantan; Can. J. Chem., 48, 890 (1970).

(15) H. Guerin, J. Masson; C.R. Acad. Sci., Ser. C, 241, 415 (1955).

(16) M. Travnicek, F. A. Kroger, Th. P.J. Botden, P. Zalm; Physica, 18(1), 33 (1952).

(17) H. Ide, N. Kawai, S. Yamazaki; Denki Kagaku, 30(4), 233 (1962).

(18) W. Panofsky, M. Phillips; "Classical Electricity and Magnetism", Addison-Wesley, Reading, Mass., (1962).

(19) W. H. Zachariasen; "Theory of x-ray diffraction in crystals", Dover Publications, Inc., New York (1967).

(20) International Tables for x-ray Crystallography, vol. III, Kynoch Press, Birmingham (1962).

(21) R. W.James; "The Crystalline State", Vol. II, ed. by L. Bragg, "The optical principles of the diffraction of x-rays", Cornell University Press, New York (1965).

(22) International Tables for x-ray Crystallography, Vol. I, Kynoch Press, Birmingham (1952).

(23) G. B. Carpenter; "Principles of crystal structure determination", W. A. Benjamin, Inc., New York (1969).

(24) W. J. A. M. Peterse, J. H. Palm, Acta Crystallogr., 20, 147 (1966).

(25) M. J. Buerger; "Crystal structure analysis"; John Wiley and Sons, New York (1960).

(26) G.H. Stout, L. H. Jensen; "X-ray structure determination - A practical guide"; Macmillan Co., New York (1968).

(27) L. E. Alexander, G. E. Smith; Acta Crystallogr., 15, 983 (1962).

(28) J. S. Stephens; Ph.D. Thesis, McMaster University (1967).

(29) M. J. Buerger; "X-ray crystallography", John Wiley and Sons, New York (1966).

(30) H. Lipson, W. Cochran; "The Crystalline State", vol. 3, ed. by L. Bragg, "The determination of crystal structures", G. Bell and Sons, London (1966).

(31) International Tables for x-ray Crystallography, Vol. II, Kynock Press, Birmingham (1952).

(32) A. L. Patterson; Phys. Rev., 46, 372 (1934).

(33) M. J. Buerger; "Vector Space", John Wiley and Sons, New York (1959).

(34) L.V. Azaroff; "Introduction to Solids", McGraw-Hill Book Co., Inc., New York (1960).

(35) J. C. Slater; "Quantum Theory of Molecules and Solids " Vol. 2, McGraw-Hill Book Co., New York (1965).

(36) S. Ho, B. E. Douglas; J. Chem. Educ., 46(4), 207 (1969).

(37) C. Calvo; Can. J. Chem., (To be published).

(38) D. T. Cromer, K. Herrington; J. Amer. Chem. Soc., 77, 4708 (1955).

(39) L. H. Thomas, K. Umeda; J. Chem. Phys.,26, 293 (1957).

(40) D.W.J. Cruickshank, D. E. Pilling, A. Bujosa, F. M. Lovell, M. R. Truter; in "Computing Methods and the phase problem in x-ray crystal analysis", ed. by R. Pepinsky, J. M. Robertson, and J. C. Speakman, Pergamon Press, New York (1961).

(41) R.J. Davis; private communication.

(42) Z. Galdecki, E. Jozefowicz; Lodz. Tow. Nauk., Acta Chim., 9, 4 (1964).

(43) "Physical Methods of Organic Chemistry", ed. by A. Weissberger, Vol. I, part 1, Interscience Publishers, New York (1949).

(44) W. C. Hamilton; Acta Crystallogr., 18, 502 (1965).

(45) G. V. Gibbs, J. V. Smith; Amer. Mineral., 50, 2023 (1965).

(46) D.W.J. Cruickshank, H. Lynton, G. A. Barclay; Acta Crystallogr., 15, 491 (1962).

(47) M. J. Buerger; "The precession method", John Wiley and Sons, Inc., U.S.A. (1964).

(48) D.W.J. Cruickshank; J. Chem. Soc., 5486 (1961).

(49) W. H. Baur; Trans. Amer. Crystallogr. Ass., 6, 129 (1970).

(50) C.Calvo; Can. J. Chem., 43, 1139 (1965).

(51) A. Pietraszko, K. Łukaszewicz; Bull. Acad. Pol. Sci., Ser. Sci. Chim., 16(4), 183 (1968).

(52) C. Calvo; Can. J. Chem., 43, 1147 (1965).

(53) B. E. Robertson, C. Calvo; Can. J. Chem., 46, 605 (1968).

(54) P.K.L. Au, C. Calvo; Can. J. Chem., 45, 2297 (1967).

(55) K. Łukaszewicz, R. Smajkiewicz; Rocz. Chem., 35, 741 (1961).

(56) C. Calvo, private communication.

(57) E. Dorm, B. Marinder; Acta Chem. Scand., 21, 590 (1967).

(58) B. E. Robertson, C. Calvo; Acta Crystallogr., 22, 665 (1967).

(59) C. Calvo, Acta Crystallogr., 23, 289 (1967).

(60) N. Krishnamachari, C. Calvo; To be published.

(61) K. Łukaszewicz; Bull. Acad. Pol. Sci., Ser. Sci. Chim., 15(2), 47 (1967).

(62) B. E. Robertson, C. Calvo; J. Solid State Chem., 1, 120 (1970).

(63) C. Calvo, private communication.

(64) Strukturbericht, Band 1, p. 350.

(65) R. Gopal, C. Calvo; To be published.

(66) J. A. Baglio, G. Gashurov; Acta Crystallogr., B24, 292 (1968).

(67) E. Banks, M. Greenblatt, B. Post; Inorg. Chem., 9(10), (1970).

(68) R. Gopal, C. Calvo; To be published.

(69) C. Calvo, P.K.L. Au; Can. J. Chem., 47, 3409 (1969).

(70) G. E. Brown, G. V. Gibbs; Amer. Mineral., 54, 1528 (1969).

(71) "Structure Reports", Vol. 11, p. 500.

(72) N. V. Belov, E. N. Belova, N. H. Andrianova, P. F. Smirnova; Dokl. Akad. Nauk. S.S.S.R., 81, 399 (1951); See also Structure Reports, Vol. 15, p. 306.

(73) C. O. Bjorling, A. Westgren; Geol. Foeren. Stockholm Foerh., 60, 67 (1938); See also Strukturbericht, Band 6, p. 107.

(74) M. E. Mrose, D. E. Appleman; Programs and Abstracts, Amer. Crystallogr. Ass. Ann. Meet., July 3-Aug. 4, 1961; p. 18.

(75) S. Geller, J. L. Durand; Acta Crystallogr., 13, 325 (1960).

(76) A. Bystrom; Ark. Kemi, Mineral. Geol., 17B(4) (1943).

(77) O. Knop, K.I.G. Reid, Sutarno, Y. Nakagawa; Can. J. Chem., 46, 3463 (1968).

(78) S. Geller; Acta Crystallogr., 14, 1026 (1961).

(79) W. C. Hamilton, J. S. Rollett, R. A.Sparks; Acta Crystallogr., 18, 129 (1965).

(80) H. Bauer, W. Balz; Z. Anorg. Allg. Chem., 340, 225 (1965).

(81) H. Guerin, R. Mas; C. R. Acad. Sci., Ser. C, 227, 973 (1948).

(82) N. N. Greenwood; "Ionic crystals, lattice defects and non-stoichiometry", Butterworth and Co. (Publishers) Ltd., London (1968) , p. 96.

(83) S. J.Poulson, C. Calvo; Can. J. Chem., 46, 917 (1968).

(84) N. Krishnamachari, C. Calvo; (unpublished results).

(85) A. G. Nord, P. Kierkegaard; private communication.

(86) J. A. Sarver; Trans. Brit. Ceram. Soc., 65, 191 (1966).

(87) C. Calvo; Can. J. Chem; 43, 436 (1965).

(88) J. S. Stephens, C. Calvo; Can. J. Chem. 45, 2303 (1967).

(89) C. Calvo; Amer. Mineral.,53, 742 (1968).

(90) B. Kamb; Amer. Mineral.,53, 1439 (1968).

(91) L. Pauling, "The Nature of the Chemical Bond"; (3rd Ed.); Cornell Univ. Press, Ithaca, (1960).

(92) G. Engel; private communication.

(93) H. T. Evans, Jr., private communication.

(94) Y. Okaya, R. Pepinsky; in "Computing Methods and the phase problem in x-ray crystal analysis", ed. by R. Pepinsky, J. M. Robertson, and J. C. Speakman, Pergamon Press, New York (1961).

(95) E. T. Whittaker, G. Robinson; "The Calculus of Observations", 4th Ed., Blackie and Son, Glasgow (1944).